

The influence of climate and prey availability on flatfishes on the Newfoundland Grand Banks

By

© Matthew D. Robertson

A thesis submitted to the

School of Graduate Studies in partial

fulfillment of the requirements

for the degree of

Doctorate of Philosophy – Fisheries Science

Memorial University of Newfoundland

May 2, 2023

St. John's, Newfoundland, Canada

Abstract

Fishing and environmental variability interactively affect fish population dynamics, where fishing can increase population variability in response to environmental change. Therefore, developing fisheries management strategies that account for these interactions is necessary for managing recovering populations in a changing climate. Using a combination of ecological and population dynamics approaches, this thesis investigated the interactive effects of overfishing and environmental variability on yellowtail flounder (*Limanda ferruginea*) and American plaice (*Hippoglossoides platessoides*) populations on the Newfoundland Grand Banks, Canada. These populations were selected given their different recovery patterns following population collapse in the early 1990s, despite sharing similar life history characteristics, inhabiting similar environments, and having been managed under the same fishing moratoria. Specifically, the yellowtail flounder population recovered in four years, while the American plaice population has yet to recover 30 years after collapse. By coupling spatiotemporal models of bottom water temperature and population distributions, I revealed that variability in spatial population distribution was influenced by a combination of density-dependent processes and spatiotemporal variability in temperatures. By developing a novel statistical method to integrate stomach contents and bottom trawl research data to estimate prey dynamics I also showed that northern sand lance (*Ammodytes dubius*), an important forage fish prey species for American plaice, has exhibited oscillatory dynamics over time, which may affect the productivity of their predators. Furthermore, expanding on indications that American plaice population dynamics may be influenced by natural mortality, results from a metapopulation dynamics model identified that natural mortality was not a

primary driver of juvenile dynamics following population collapse. Finally, through the development of a modeling framework to underscore the importance of incorporating various population and ecosystem processes in population dynamics models, I revealed that American plaice population dynamics were strongly affected by variability in recruitment and adult natural mortality over time and that both stocks were influenced by an integrated regional climate index. Overall, by coupling ecological and population dynamics research, this thesis adds to the growing base of research that indicates that understanding how fishing and the environment interact is necessary to produce ecosystem-informed management advice to identify appropriate rebuilding strategies for collapsed populations.

General Summary

Fishing and environmental variability interactively affect how fish populations change over time. Therefore, accounting for these interactions in the development of fisheries management strategies to recover populations after they have undergone overfishing is necessary. Using a combination of approaches, this thesis investigated the interactive effects of overfishing and environmental variability on yellowtail flounder (*Limanda ferruginea*) and American plaice (*Hippoglossoides platessoides*) populations on the Newfoundland Grand Banks, Canada. Despite inhabiting similar environments and having the same fisheries management measures imposed following population collapse in the early 1990s, the yellowtail flounder population recovered rapidly while the American plaice population has yet to recover 30 years after collapse. Using statistical models that accounted for changes across space and time, I identified that the locations inhabited by these populations changed over time in response to changes in their population size and bottom water temperatures. Meanwhile, through the development of a novel statistical method to combine data sources to estimate how prey fish populations change through time, I identified that northern sand lance (*Ammodytes dubius*), an important prey species for American plaice, has fluctuated over time in ways that may have influenced their predators. Furthermore, although past studies indicated that the lack of recovery for the American plaice population may be strongly influenced by sources of mortality external to the fishery (i.e., natural mortality), I identified that natural mortality was not a primary driver of changes for juvenile American plaice following population collapse. Finally, I developed a modeling framework to identify the importance of accounting for different aspects of the population and ecosystem when estimating how

populations change over time. This framework identified that variability in the size of the American plaice population were strongly affected by changes in adult natural mortality over time and that both populations were influenced by regional climate. Overall, this thesis adds to the growing base of research describing how fishing and the environment interact, which is necessary to produce fisheries management advice to identify appropriate rebuilding strategies for collapsed populations.

Acknowledgments

First, I would like to thank my supervisor Dr. Fan Zhang for allowing me to develop a thesis that matched my interests and being there to talk through the research as it developed. I would also like to thank my supervisor of the past two years, Dr. Tyler Eddy for being willing to take me on as a student as you were just starting a lab. Both of your supportive and positive outlooks made this work possible. Furthermore, I would like to thank my supervisory committee Drs. Noel Cadigan, Paul Regular, and Mariano Koen-Alonso for their support, patience, and expertise.

Research presented in this thesis was supported by the Vanier Canada Graduate Scholarship from the National Sciences and Engineering Research Council of Canada (NSERC), the Ocean Frontier Institute through an award from the Canada First Research Excellence Fund, and the Ocean Choice International Industry Research Chair program at the Marine Institute of Memorial University of Newfoundland. The Centre for Fisheries Ecosystems Research was initiated through support by the Government of Newfoundland and Labrador.

Living in Newfoundland over the last five years has been a wonderful experience thanks to many friends and colleagues. We endured the harsh weather of the North Atlantic coupled with a global pandemic together and had fun doing it. I am thankful for the many conversations that we had that not only influenced the research described in this thesis but that have also continued to shape me as a person.

Lastly, and most importantly, I want to thank my family: Minke, for always wagging your tail when you see me and forcing me to go on walks even in the worst weather. Tanya, for starting this long and sometimes challenging journey of completing a Ph.D. together; I am so glad that I have had you here to support me. My parents and sister, whose unconditional love and support have truly made this work possible. All the time spent on the water with you during my childhood built a foundation for my interest in asking the types of questions that I have spent this thesis attempting to answer.

Publication Permissions Chapter 2

Matthew Robertson

From: Shrutika Konde <srep@nature.com>
Sent: November 25, 2022 2:10 AM
To: Matthew Robertson
Subject: Re: Permission for publication inclusion in thesis_Robertson

Dear Dr. Matthew,

Thank you very much for your message.

Since this is your own manuscript which is published in Scientific Reports, you do not require any permission to use the data from this manuscript in your dissertation. You can mention this manuscript with publication details and cite it in your dissertation

We value your association with Scientific Reports. Feel free to ask us if you have any doubts

Thank you and stay safe.

Best regards,
Shrutika Konde
Editorial Support at [Scientific Reports](#)

On Thu, 24 Nov at 5:49 PM , Matthew Robertson <matthew.robertson@mi.mun.ca> wrote:

[External - Use Caution]

Hello,

I am emailing today to request permission to include a manuscript that I published as lead author in Scientific Reports in 2021 in my PhD thesis. The publication citation is: Robertson, M.D., Gao, J., Regular, P.M. et al. Lagged recovery of fish spatial distributions following a cold-water perturbation. Sci Rep 11, 9513 (2021). <https://doi.org/10.1038/s41598-021-89066-x>.

I have attached a form describing this request in more detail that needs to be signed by a member of the Scientific Reports team if permission is granted.

Please let me know if there is any more information needed to complete this request.

Thank you for your time and assistance.

Best regards,
Matthew Robertson

This email is governed by the Terms and Conditions found in our [Disclaimer](#).

Publication Permissions Chapter 3

WILEY

Q Search Wiley for what you're looking for

[Research Libraries](#) ▾ [Publishing Services](#) ▾ [Education Resources](#) ▾ [Professional Development](#) ▾

If you publish your thesis or dissertation through a commercial publisher in the future, you will need to reapply for commercial reuse licenses. The legal rights granted for content reuse in non-commercial publications, such as a thesis or dissertation, are different from the rights required by commercial publishers to legally republish third-party content.

Do I need to request permission to use my own work as my dissertation?

If you are the author of a published Wiley article, you have the right to reuse the full text of your published article as part of your thesis or dissertation. In this situation, you do not need to request permission from Wiley for this use.

If your institution still requires a reuse license in this case, follow the steps below to request your license via RightsLink.

Request permission from Wiley

To request a reuse license, our partner RightsLink is a great place to start. You can request thesis and dissertation permissions through **RightsLink Marketplace**.

You can also find a link to a RightsLink permissions request form at the point of content on Wiley Online Library. Watch the video below to see how.

Publication Permissions Chapter 4



SCHOOL OF
GRADUATE STUDIES

Request to Include Copyright Material

Adobe Reader, minimum version 8, is required to complete this form. Download the latest version at <http://get.adobe.com/reader>. (1) Save the form by clicking on the diskette icon on the upper left side of the screen; (2) Ensure that you are saving the file in PDF format; (3) Specify where you would like to save the file, e.g. Desktop; (4) Review the [How to create and insert a digital signature](#) webpage for step by step instructions; (5) Fill in the required data and save the file; (6) Send the completed form to the copyright holder.

Student Contact Information

Last name: Robertson **First name:** Matthew D.
Academic Unit: Centre for Fisheries Ecosystems Research **Degree:** PhD
Email Address: matthew.robertson@mi.mun.ca **Telephone No.:** (734)660-1068

Copyright Material Request

I, Matthew D. Robertson, request that you permit the inclusion of the described material in the thesis/report/practicum listed below and grant an irrevocable, non-exclusive licence to Memorial University of Newfoundland and to Library and Archives Canada to reproduce, lend or sell the material described below as part of my thesis/report/practicum. The title of the thesis/report/practicum is:

The influence of climate and prey availability on flatfishes on the Newfoundland Grand Bank

to be submitted in partial fulfilment of the requirements for the degree of PhD at Memorial University of Newfoundland.

Description of the Material to be Included

Robertson, M.D., Regular, P.M., and Cadigan, N. 2022. Limited temporal variability in natural mortality for juvenile American plaice on the Grand Bank of Newfoundland. J. Northw. Atl. Fish. Sci., 53: 47–56. <https://doi.org/10.2960/J.v53.m738>

Permission of Copyright Holder

I, Alexis Pacey, (Name - type) do do not grant permission for the indicated use of the material described above.

Company/Organization: Northwest Atlantic Fisheries Organization (NA)
Position Title: Senior Publications/Web Manager
Address: 1601 Lower Water St. Suite 401
Halifax, NS B3J 3P6

Signature: Alexis Pacey Digitally signed by Alexis Pacey
Date: 2022.11.24 15:10:05 -04'00' **Date:** 24 November 2022

Note: Signature required on each additional attachment

Memorial University protects privacy and maintains the confidentiality of personal information. The information requested in this form is collected under the general authority of the Memorial University Act ([RSNL1990CHAPTERM-7](#)). It is required for administrative purposes of the School of Graduate Studies. If you have any questions about the collection and use of this information please contact the School of Graduate Studies at 709.864.2445 or sqs@mun.ca.

Updated September 2020

Table of Contents

Abstract	i
General Summary	iii
Acknowledgments	v
Publication Permissions Chapter 2	vii
Publication Permissions Chapter 3	viii
Publication Permissions Chapter 4	ix
List of Tables	xiii
List of Figures	xiv
List of Appendices	xviii
Co-authorship statement	xix
Publications Arising	xx
Code Accessibility	xxii
1 Introduction	23
2 Lagged recovery of fish spatial distributions following a cold-water perturbation	30
Abstract	31
2.1 Introduction	32
2.2 Materials and Methods	34
2.2.1 Spatiotemporal temperature interpolation.....	34
2.2.2 Spatiotemporal model	35
2.2.3 Testing for density-dependent habitat selection	38
2.2.4 Correlation analysis for recovery response	40
2.3 Results	41
2.3.1 Bottom water temperature interpolation	41
2.3.2 VAST Estimates.....	41
2.3.3 Density-dependent habitat selection	42
2.3.4 Distribution – temperature correlation.....	44
2.4 Discussion	45
2.5 List of Figures	54

3 Accounting for a non-linear functional response when estimating prey dynamics using predator diet data	58
Abstract.....	59
3.1 Introduction	60
3.2 Materials and Methods	62
3.2.1 Non-Linear Functional response Prey dynamics Model (NLFPM).....	62
3.2.2 Simulation.....	66
3.2.3 Case Study	70
3.3 Results	72
3.3.1 Simulation.....	72
3.3.2 Case Study	73
3.4 Discussion.....	74
3.4.1 Model Advantages	75
3.4.2 Model Assumptions and Future Directions	77
3.4.3 Case-Study	79
3.5 List of Tables.....	83
3.6 List of Figures.....	84
4 Limited temporal variability in natural mortality for juvenile American plaice on the Newfoundland Grand Banks.....	92
Abstract.....	93
4.1 Introduction	94
4.2 Materials and Methods	96
4.2.1 Metapopulation dynamics process model.....	96
4.2.2 Observation model	97
4.2.3 Data.....	99
4.2.4 Model fitting	99
4.3 Results	100
4.4 Discussion.....	101
4.5 List of Tables.....	108
4.6 List of Figures	109
5 Testing models of increasing complexity to develop ecosystem-informed fisheries advice.....	114

Abstract	115
5.1 Introduction	116
5.2 Materials and Methods	119
5.2.1 Modeling Approach	119
5.2.2 Single-Species Dynamics.....	120
5.2.3 Environmental Drivers.....	122
5.2.4 Competition.....	126
5.2.5 Estimation	127
5.2.6 Recovery simulations.....	128
5.3 Results	129
5.3.1 Single-species models.....	129
5.3.2 Environmental Drivers.....	130
5.3.3 Competition.....	132
5.3.4 Best-performing models.....	132
5.3.5 Recovery simulations.....	133
5.4 Discussion	134
5.4.1 Yellowtail flounder	135
5.4.2 American plaice	136
5.4.3 Competition.....	139
5.4.4 Management implications.....	140
5.5 List of Tables.....	144
5.6 List of Figures	146
6 General Conclusions	153
6.1 Thesis Overview.....	153
6.2 Implications for Regional Fisheries Management	154
6.3 Implications for Rebuilding Fisheries	158
Bibliography	164
Appendices	191

List of Tables

Table 3.1 Functional response shape parameter estimates and associated 95% confidence intervals.	83
Table 3.2 Model outputs for all three models run. Δ represents difference and NLL represents the negative log-likelihood (NLL) from the NLFPM.	83
Table 4.1 Model names, descriptions and comparisons using AIC and BIC. + represents effects that were included, while a blank space indicates that the effect was not included. n_0 represents cohort effects, τ represents survey year effects, and δc represents M deviations. The subscript d indicates that the effect was only allowed to vary by Division rather than by survey (i.e., season and Division), the subscript s represents when an effect varied by survey, and the subscript c represented when an effect varied by cohort. k is the number of parameters, nll is the negative log-likelihood and the Δ columns represent the difference in the number of criterion points from the model with the lowest respective criterion points. The bolded row (M5) indicates the model that I determined to have the best fit.	108
Table 5.1 Model comparisons for different formulations of both single-species models. nll represents the negative log-likelihood, k represents the number of parameters, Δ represents the difference in model criterion score from the model with the lowest model criterion score. The bolded row indicates the model with the lowest AIC and BIC.	144
Table 5.2 Model comparisons for different formulations of the two best null models. nll represents the negative log-likelihood, k represents the number of parameters, Δ represents the difference in model criterion score from the model with the lowest model criterion score. The bolded row indicates the model with the lowest AIC and BIC.	144
Table 5.3 Model comparisons for the multispecies formulations. $Ampl$ is an abbreviation for American plaice and $Ytfl$ is an abbreviation of yellowtail flounder. The column headers represent the process (Rec. or M) for a given species that was estimated to have a relationship with a covariate. Text within the $Ampl$, Rec, $Ampl M$, and $Ytfl$ Rec. columns indicates the covariate modeled to explain a particular process, where SSB refers to the other species spawning stock biomass while Rec. refers to the other species recruitment. nll represents the negative log-likelihood, k represents the number of parameters, Δ represents the difference in model criterion score from the model with the lowest model criterion score. The bolded row indicates the model with the lowest AIC and BIC.	145

List of Figures

Figure 2.1 Conceptual diagram of spatial distribution recovery and non-recovery. The curved lines represent how an organism's spatial distribution will change with an environmental driver where, a) is a distribution that recovers when the environmental driver returns to previous conditions and b) is a distribution that does not recover when the environmental driver returns to previous conditions. The S-shape in b) represents an unstable equilibrium between distributional states, where a distribution above the dashed line will be driven to the upper asymptote and distributions below the dashed line will be driven the lower asymptote (similar to the concept of hysteresis in ecosystem states; Scheffer et al. 2001). The colored circles on the lines represent three snapshots in time ($t_1 - t_3$) that are meant to represent the same environmental driver conditions between panels a) and b), and the dotted grey arrows represent the transition between each snapshot. The circles within boxes represent the snapshots of the spatial states for the organism's distribution.54

Figure 2.2 Bathymetry and dominant currents of the Grand Banks region/North Atlantic Fisheries Organization (NAFO) divisions 3LNO. Bathymetric contours shown for 100 (dotted lines), 200 (dashed lines), and 1000 m (solid lines). Approximate pathways for the Labrador Current represented by black arrows and the Gulf Stream represented by white arrows. Inset in the bottom left shows the position of the study area (red rectangle) in reference to the rest of the Atlantic Ocean.....55

Figure 2.3 The estimate of the slope (exponent) between local and total biomass (b_k) from the knot specific exponential models comparing yellowtail flounder local density based on total biomass across the fifty knots in the VAST. Red circles represent a $b_k > 1$ which indicate large local biomass changes with total biomass changes (i.e., marginal habitat), white circles represent a $b_k = 1$, and blue circles represent a $b_k < 1$ which indicate that local biomass is stable with changes in total biomass (i.e., ideal habitat).56

Figure 2.4 Diagram of spatial distribution recovery results, format based on Figure 2.2. Line drawings for a-b) represent the theoretical pattern that matches the observations for each species. t_1 and t_3 represent snapshots in time with equal temperature, while t_4 represents a snapshot with a higher temperature. Maps for a-b) represent snapshots that define each spatial state, where the maps for a) represent the residuals (blue = negative, red = positive) of the density-dependent model for yellowtail flounder (see Appendix A Fig. A16) and maps for b) represent the spatial distribution (blue = low density, red = high density) of American plaice from the Vector Autoregressive Spatiotemporal model [VAST] (see Appendix A Fig. A8). Finally, c-d) is the correlation analysis of spatial distributions (y-axis) and bottom water temperature distributions (x-axis) over time (yellow = high correlation, red = negative correlation) along with the mean annual temperature trend on the Grand Banks shown beneath the correlation plots (dashed grey

lines represent the minimum [1991] and maximum [2011] mean temperatures; dotted red line represents the mean temperature over the entire time-series). Positive correlation in panels c-d) indicates that areas with high density occur in areas with warmer temperatures and negative correlation indicates that areas with high density occur in areas with cold temperatures.57

Figure 3.1 Overview diagram for the simulation. The Operating Models panel portrays prey and predator abundance over time (Eqn. 3.7-3.8), the functional response (Eqn. 3.4), and the number of predators that have consumed prey (Eqn. 3.10). The Observation Models panel portrays comparisons between the true dynamics and a trawl index estimated based on the random draws from a binomial distribution and a stomach contents index estimated from a Poisson distribution. The Estimation Models panel portrays functional response curves from the LFPM and NLFPM as well as an estimate of prey dynamics from a model with only trawl data. The Evaluation Models panel portrays the calculations of precision, mean squared error, and bias between the Estimation Models and the true prey dynamics.84

Figure 3.2 The different functional response shapes used in the simulation.85

Figure 3.3 MSE between estimated relative index of prey abundance and the scaled true prey abundance from all simulations. Grey points represent the MSE from each simulation and the dashed red line represents zero. The grey points were jittered on the x-axis to improve visualization. The boxplots were created using the default settings in the ggplot2 package in R (Wickham 2009), where the boxes represent the 25th – 75th percentiles, the horizontal line represents the median, the vertical lines represent 1.5 * the interquartile range, and black points represent any data outside 1.5 * the interquartile range.86

Figure 3.4 Bias between estimated relative index of prey abundance and the scaled true prey abundance from all simulations.86

Figure 3.5 Difference in AIC between the NLFPM and LFPM for both operating models. Negative values indicate that the LFPM had a larger AIC than the NLFPM.87

Figure 3.6 Estimates for the shape parameter values in the functional response from the simulation. The dashed red line indicates the true parameter value for each shape. The panels on the far right represent the true shape of the functional response (red lines), the shapes given by all estimated shape parameter values (grey lines), and the median shape parameter values (dark blue lines).88

Figure 3.7 Percent difference in annual standard deviation estimates for the prey abundance index between the NLFPM and a model with no stomach contents data for both operating models. Percent difference was based on the mean of the standard

deviation estimates from the model with no stomach contents data. Negative values indicate a smaller standard deviation for a particular year in the NLFPM.	89
Figure 3.8 Estimated functional responses (lines) and 95% confidence interval (shaded grey polygon) for both predator species when modeled separately and together.	90
Figure 3.9 Estimated sand lance relative abundance index and 95% confidence interval (shaded grey polygon) from models that used each predator's data separately and one that modeled American plaice and Atlantic cod data together.	91
Figure 4.1 Map of NAFO Divisions 3LNO (a) and estimates of recent spawning stock biomass (b) and fishing mortality (c) from the most recent run of the stock assessment model (Wheeland et al. 2021). Light grey lines in panel a represent bathymetric contours at 100, 200, 400, and 1000 m depth. Spawning stock biomass estimates are in the 1,000's of tons and estimates of fishing mortality are the average estimates for ages 9-14.	109
Figure 4.2 Time-series of cohort effect deviations estimated for each survey index using model M5. The black lines represent the point-estimates while the shaded grey area represents the 95% confidence intervals.	110
Figure 4.3 Spatial correlations of the cohort effects between the six survey indices from model M5. The size and darkness of the circles indicate the magnitude of the correlations. The stars indicate significance, where more stars represent lower p -values (1 star = $P < 0.05$, 3 stars = $P < 0.01$).	111
Figure 4.4 Dendrogram of a dissimilarity matrix of the spatial correlations of cohort effects in model M5.	112
Figure 4.5 Time-series of annual natural mortality rate deviations from model M5. The black line represents the point-estimates and the shaded grey area represents 95% confidence intervals.	113
Figure 5.1 Mean historical distribution (1985-1989) of NAFO Divisions 3LNO yellowtail flounder and American plaice overlaid on spring bottom water temperatures from the same time-period. Circle size represents biomass density (kg km^{-2}) estimates for each stock estimated using VAST models in Robertson et al., (2021). Bottom water temperature was estimated using universal kriging while accounting for depth of the bottom trawl surveys. The temperature scale was limited to have a maximum value of 6 for visualization purposes despite some temperatures exceeding this range.	146
Figure 5.2 Conceptual diagram of the process of extending and comparing population dynamics models of increasing complexity.	147

Figure 5.3 Model comparisons between spawning stock biomass (American plaice) or biomass (yellowtail flounder) from the current stock assessment (grey lines) to the single-species model (purple lines; YTFL1 & AMPL1 from Table 5.1), and the single-species model with M deviations (orange lines; AMPL2 & YTFL2 from Table 5.1). 148

Figure 5.4 Comparison of deviation parameters (recruitment and M) between the best performing non-extended models (orange lines; AMPL2, YTFL1) and the best performing extended models (grey lines; AMPLE6, YTFLE1). 95% confidence interval for estimates from best performing extended models are shown as grey polygons. 149

Figure 5.5 Estimates of the effects (black lines) and 95% confidence intervals (grey polygons) of environmental covariates for AMPLE6 and YTFLE1. The red dashed line in the American plaice panel represents 1, which would indicate no effect on M since the effect is multiplicative..... 150

Figure 5.6 Comparison of SSB/biomass estimates and fishing mortality between the best performing non-extended models (grey lines; AMPL2, YTFL1) and the best performing extended models (orange lines; AMPLE6, YTFLE1). 95% confidence interval for estimates from best performing extended models are shown as orange polygons. Estimates of SSB are shown for American plaice while yellowtail flounder estimates are for biomass. Fishing mortality estimates for American plaice are averaged from ages 9-14 years. 151

Figure 5.7 Simulations of how population dynamics would have differed if their environmental drivers followed different trajectories from 1992 onwards. The polygons represent the 20-80% (orange) and 10-90% quantiles (grey) of dynamics from 1,000 simulations. The different trajectories are based on the starting value of the random walk for the environmental covariates in each simulation. Since environmental covariates were scaled, -1 was used for lower values (left panels), 0 was used for average values (middle panels), and 1 was used higher values (right panels). 152

List of Appendices

A. Appendix for Chapter 2.....	191
Appendix A Bibliography	218
B. Appendix for Chapter 3.....	219
B1. Density value range	219
B2. Homogenously distributed sand lance.....	223
B3. Ontogenetic Diet Shift.....	233
B4. Additional supplemental information.....	236
Appendix B Bibliography	248
C. Appendix for Chapter 4.....	249
D. Appendix for Chapter 5.....	262
D1. Yellowtail flounder models.....	262
D1.1 Model description.....	262
D1.2 Model outputs.....	267
Appendix D1 Bibliography	273
D2. American plaice models.....	274
D2.1 Model description.....	274
D2.2 Model Output.....	279
Appendix D2 Bibliography	306
D3. Ecosystem data.....	307

Co-authorship statement

The research presented in this thesis was conducted by Matthew D. Robertson under the guidance of his supervisors Drs. Fan Zhang and Tyler Eddy, and supervisory committee members Drs. Noel Cadigan, Paul Regular, and Mariano Koen-Alonso. Matthew D. Robertson was responsible for initial development of research ideas and led all planning and implementation of data analyses for all chapters and is lead author on all manuscripts. Dr. Fan Zhang (Marine Institute & Shanghai Ocean University) co-authored Chapters 2, 3, & 5, provided advice on data analyses, reviewed manuscript drafts, and provided initial financial support. Dr. Tyler Eddy (Marine Institute) co-authored Chapter 5, provided advice on data analyses, and reviewed manuscript drafts. Dr. Noel Cadigan (Marine Institute) co-authored Chapters 3 – 5, provided advice on data analyses, and reviewed manuscript drafts. Dr. Paul Regular (Fisheries & Oceans Canada) co-authored Chapters 2 – 5, provided research vessel survey data, and reviewed manuscript drafts. Dr. Mariano Koen-Alonso (Fisheries & Oceans Canada) co-authored Chapters 3 & 5, provided predator stomach contents data, and reviewed manuscript drafts. Dr. Jin Gao (Marine Institute) co-authored Chapter 2, provided data analysis advice, and reviewed the manuscript draft. Dr. M. Joanne Morgan (Fisheries & Oceans Canada) co-authored chapter 2 and reviewed the manuscript draft. Dr. David Bélanger and Dr. Frédéric Cyr (Fisheries & Oceans Canada) both co-authored Chapter 5, provided data, and reviewed the manuscript draft.

Publications Arising

The following publications were produced through this dissertation:

Chapter 2:

Robertson, M.D., Gao, J., Regular, P.M., Morgan, M.J., & Zhang, F. (2021). Lagged recovery of fish spatial distributions following a cold-water perturbation. *Scientific Reports*. 11, 9513. <https://doi.org/10.1038/s41598-021-89066-x>

Chapter 3:

Robertson, M.D., Koen-Alonso, M., Regular, P.M., Cadigan, N., & Zhang, F. (2022). Accounting for a non-linear functional response when estimating prey dynamics using predator diet data. *Methods in Ecology and Evolution*, 13(4), 880-893 <https://doi.org/10.1111/2041-210X.13795>

Chapter 4:

Robertson, M.D., Regular, P.M., & Cadigan, N. (2022). Limited temporal variability in natural mortality for juvenile American plaice on the Grand Bank of Newfoundland. *Journal of Northwest Atlantic Fisheries Science*. 53, 47-56 <https://doi.org/10.2960/J.v53.m73>

Chapter 5:

Robertson, M.D., Cadigan, N., Regular, P.M., Koen-Alonso, M., Zhang, F., & Eddy, T. Sequentially testing models of increasing complexity to develop ecosystem-informed fisheries advice. *Fish & Fisheries*. In Prep.

In addition to my thesis chapters, I have contributed to several publications during my Ph.D. These include:

Collaborations within the Centre for Fisheries Ecosystems Research:

Duplisea, D.E., Eddy, T.D., Robertson, M.D., Ruiz-Díaz, R., Solberg, A. & Zhang, F. The ghosts of overfishing past that haunt the effectiveness of present day fisheries management. *Fish and Fisheries*. In Prep.

Eddy, T.D., Duplisea, D., Robertson, M.D., Ruiz-Díaz, R., Solberg, C.A., & Zhang, F. Barriers to implementation of dynamic approaches in fisheries management. *FACETS*. In Press.

Cadigan, N., Robertson, M.D., Nirmalkanna, K., & Zheng, N. (2022) The complex relationship between weight and length of cod off southern Newfoundland. *Canadian Journal of Fisheries Aquatic Sciences*. 79(11), 1798-1819. <https://doi.org/10.1139/cjfas-2021-0325>

Duplisea, D.E., Eddy, T.D., Robertson, M.D., Ruiz-Díaz, R., Solberg, A. & Zhang, F. (2021). Report on Ocean Frontier Institute Workshop on Fisheries Management Reference Points in Highly Dynamic Ecosystems. *EcoEvoRxiv*. <http://dx.doi.org/10.32942/OSF.IO/3WV8Y>

Zheng, N., Robertson, M.D., Cadigan, N., Zhang, F., Morgan, M.J., & Wheeland, L. 2020. Spatiotemporal variation in maturation: A case study in American plaice (*Hippoglossoides platessoides*) on the Grand Bank off Newfoundland. *Canadian Journal of Fisheries Aquatic Sciences*, 77(10), 1688-1699. <https://doi.org/10.1139/cjfas-2020-0017>

Collaborations with Fisheries and Oceans Canada:

Regular, P.M., Buren, A.D., Dwyer, K.S., Cadigan, N.G., Gregory, R.S., Koen-Alonso, M., Rideout, R. M., Robertson, G.J., Robertson, M.D., Stenson, G.B., Wheeland, L. J., & Zhang, F. (2022). Indexing starvation mortality to assess its role in the population regulation of northern cod. *Fisheries Research*, 247, 106180. <https://doi.org/10.1016/j.fishres.2021.106180>

Collaborations with Louisiana State University:

Midway, S.R., Brum, J., & Robertson, M.D. (2023). Show and tell: Approaches for effective figures. *Limnology and Oceanography Letters*. 8, 213-219. <https://doi.org/10.1002/lol2.10288>

Midway, S.R., Robertson, M.D., Flinn, S., & Kaller, M.D. (2020). Comparing multiple comparisons. *PeerJ*, 8, e10387. <https://doi.org/10.7717/peerj.10387>

McCormick, A., Robertson, M.D., Brasso, R., & S.R. Midway. 2020. Mercury concentrations in store-bought shrimp. *Food Science and Nutrition* 8, 3731-3737 <https://doi.org/10.1002/fsn3.1659>

And collaborations through paid contracts:

Robertson, M.D., Midway, S.R., Embke, H. S., Kaz, A.L., Lang, M., Paukert, C., Sievert, N. A., & Lynch, A. J. Estimating Recreational Fisheries Catch and Effort Throughout the United States. *Fisheries Management and Ecology*. In Revision.

Code Accessibility

The code used for some of the chapters has been made available online:

Chapter 2:

Code and walkthrough of analyses: <https://doi.org/10.5281/zenodo.6567495>

Chapter 3:

Code and walkthrough of analyses: <https://doi.org/10.5281/zenodo.5570311>

R package for Non-linear Functional response Prey dynamics Model (NLFPM):
<https://doi.org/10.5281/zenodo.5617236>

1 Introduction

Global overfishing drove the collapse of many of the world's fisheries in the second half of the 20th century (Hilborn et al. 2020). These collapses spurred effort by many fisheries management organizations to reduce overfishing and allow for rebuilding of populations to previous levels of abundance/biomass (Caddy and Agnew 2005). Although there is evidence that reducing fishing pressure has promoted population rebuilding, there have been dramatic differences in the magnitude and time required to rebuild (Hutchings 2000; Worm et al. 2009; Lotze et al. 2011; Neubauer et al. 2013), indicating that current management policies for rebuilding may be insufficient (Khan and Neis 2010). The mechanisms that affect the magnitude and timeline for rebuilding can include a wide range of biological, ecological, social, economic, and institutional factors (Garcia et al. 2018). Therefore, part of the current challenge of identifying appropriate rebuilding strategies for collapsed fish stocks is caused by fisheries management's continued focus on single species population dynamics.

Population dynamics models attempt to understand how populations vary over time, generally based on estimates of births, growth, natural mortality, and fishing mortality (Haddon 2001). Simplistic versions of these models (e.g., biomass dynamic models) assume that populations change based on some intrinsic rate of population growth, carrying capacity, and fisheries removals (Hilborn and Walters 1992b). Meanwhile, more modern models (e.g., state-space, age-structured models) attempt to explicitly model processes like births, growth, and mortality (Cadigan 2015; Aeberhard et al. 2018; Stock and Miller 2021). Despite the existence of a wide variety of population

dynamics models used to provide tactical fisheries management advice (i.e., stock assessment models), these models often assume that vital rates (e.g., growth, natural mortality) and population productivity do not change over time and space. Meanwhile, there is a growing body of evidence that population productivity is non-stationary (i.e., changes in the mean or variance of a process over time) and that changes can be driven by the combined effects of overfishing and environmental variability (Szuwalski et al. 2015; Szuwalski and Hollowed 2016; Zhang et al. 2021b). This is problematic because our understanding about stock productivity ultimately influences estimates of stock status (Punt et al. 2014; Collie et al. 2021).

Fishing populations can directly impact species vital rates and can affect how a population interacts with its environment. Vital rates vary over time and space in response to bottom-up (Smith et al. 2011; Petrik et al. 2019; Regular et al. 2022) and top-down processes (Tyrrell et al. 2008; Baum and Worm 2009), where fishing acts as a top-down process. Harvesting fish populations directly reduces population size and can modify population spatial structure (Rose et al. 2000; Ciannelli et al. 2013). Furthermore, by selectively harvesting large, old individuals, fishing has been well documented to directly impact population age structure, growth rates, and maturity (Berkeley et al. 2004; Hsieh et al. 2010; Heino et al. 2015; Charbonneau et al. 2022). Fishing can also affect population vital rates and productivity by modifying community structure and dynamics (Garrison and Link 2002; Blanchard et al. 2005; Collie et al. 2013). For example, fishing induced reductions in prey populations can affect the growth and mortality of predators that rely on them (Smith et al. 2011). By directly modifying population size, vital rates,

spatial distribution, and genetic diversity, overharvested populations are more likely to be negatively affected by environmental variability.

Environmental variability tends to have a smaller effect on fish populations when those populations are large, occur over widespread areas, and have greater genetic diversity (Planque et al. 2010; Shelton and Mangel 2011; Schindler et al. 2015; Thorson et al. 2018). This is known as the portfolio concept, where the variability of an aggregate system (e.g., stock complex) depends on the diversity and covariation among its component parts (e.g., single stock). For example, the population size of a regional stock complex of Pacific salmon (*Onchorychus* spp.) has been shown to be substantially less variable in size over time than populations at smaller scales (Schindler et al. 2010; Krkošek and Drake 2014). Some of this reduced variability in population size over time has been linked to differences in age-structure, where individuals spend different lengths of time at sea, therefore reducing the probability that all individuals within a cohort will encounter adverse environmental conditions. Overall, accounting for overharvesting induced changes in the diversity of population components and how those changes alter the effects of environmental variability on population dynamics (i.e., the covariation of those components) will produce more appropriate management strategies for recovering populations in a changing climate.

Ecosystem-based fisheries management (EBFM) describes a holistic approach to fisheries management that accounts for interactions between the physical, chemical, biological, sociological, and economic components of the ecosystem (Pikitch et al. 2004; Link and Browman 2014). This approach has been taken up by fisheries management

organizations globally (FAO 2003) but has continued to struggle to operationalize broad, ecosystem advice into tactical fisheries management (Skern-Mauritzen et al., 2016; Pepin et al., 2022; but see Marshall, Jensen, Koehn, Levin, & Essington, 2019). This difficulty can often be linked back to two primary questions: how do we disentangle the effects of different ecosystem interactions on population productivity?; and how do we know if those effects warrant modifications to assessments and management (Link et al. 2021)? Although a significant amount of research has been conducted towards understanding ecosystem interactions in the Northwest Atlantic, there has been limited implementation of ecosystem approaches on the commercially important Newfoundland Grand Banks ecosystem (Link et al. 2011a; Koen-Alonso et al. 2019).

There were numerous population collapses and a dramatic shift in the biological community on the Newfoundland Grand Banks in the 1990s. The Grand Banks are a series of shallow (<200 m) underwater plateaus off the east coast of Newfoundland where the environment is defined by the confluence of the Labrador current and the Gulf stream (Lozier et al. 1995; Urrego-Blanco and Sheng 2012; Colbourne et al. 2018). Where the Labrador current supplies cold, nutrient rich water from the north and Gulf stream supplies warm water from the south. This ecosystem was historically productive, once maintaining one of the world's largest fisheries, the fishery for northern cod (*Gadus morhua*) (Myers et al. 1997; Schrank 2005). In the 1990s, several groundfish populations, including northern cod, collapsed and the community shifted from being dominated by groundfish to being dominated by shellfish (Dempsey, Koen-Alonso, Gentleman, & Pepin, 2017). This shift occurred following a prolonged period of intense fishing pressure

and when local water temperatures reached a historical low, generating questions about the primary drivers for population collapse and the community shift (Dempsey, Gentleman, Pepin, & Koen-Alonso, 2018). Fishing moratoria and rebuilding plans were established for several groundfish populations following the collapse, yet despite these management actions some populations have yet to recover nearly 30 years later (DFO 2020).

Two often overlooked groundfish populations (in comparison to northern cod) that collapsed in the 1990s are Northwest Atlantic Fisheries Organization (NAFO) Divisions 3LNO American plaice (*Hippoglossoides platessoides*) and yellowtail flounder (*Limanda ferruginea*). Both species of flatfish inhabit similar environments on the Grand Banks, have similar life history characteristics (e.g., maximum age ~25 years, maximum size ~60 cm), consume similar benthic (e.g., amphipods, crustaceans) and forage fish prey (e.g., sand lance and capelin; Gonzalez et al. 2006), and were captured as part of international bottom trawl fisheries that also targeted Atlantic cod (*Gadus morhua*) with catches that peaked in the late 1960s – early 1970s (~95,000 t for American plaice, ~40,000 t for yellowtail flounder; Parsons, Rideout, & Rogers, 2021; Wheeland et al., 2021). Although both populations collapsed to a similar level of biomass in the early 1990s (~20,000 t; Brodie et al. 2010), the magnitude of collapse was much larger for American plaice (population biomass ~300,000 t in the 1970s) than yellowtail flounder (population biomass ~50,000 t in the 1970s). Furthermore, there is evidence that the collapse of American plaice was coupled with fishing induced modifications to life history traits (Morgan and Colbourne 1999; Barot et al. 2005; Zheng et al. 2020b), while our

understanding about shifts in yellowtail flounder life history are limited based on aging difficulties (but see Walsh and Morgan 1999). Following their collapses in the early 1990s, both populations had directed fishing moratoria put in place in 1994. Yellowtail flounder presumably responded to their fishing moratorium rapidly, with the directed fishing moratorium being lifted in 1998 and the population recovering to previous levels of biomass in less than 10 years (Brodie et al. 2010). Meanwhile, American plaice still maintains a directed fishing moratorium to this day with little sign of recovery and is primarily captured as bycatch in the yellowtail flounder fishery (<15% of total catch limit; Morgan et al. 2011; Wheeland et al. 2021). Overall, although slower recovery trajectories are expected for stocks that experience larger magnitude declines (Hutchings and Reynolds 2004), the mechanisms that yielded the dramatic difference in recovery trajectories for two species with similar life history characteristics, inhabiting the same environment, and that were subject to the same fisheries management interventions have yet to be determined.

The overall aim of this thesis is to investigate the interactive effects of overfishing and environmental variability on fish population recovery. To accomplish this, I focus on the differing recovery trajectories of the NAFO Divisions 3LNO yellowtail flounder and American plaice populations. Specifically, the thesis is divided into six chapters (including this introductory chapter) that explore potential population dynamic and ecosystem mechanisms that may have differentially impacted these populations and to weigh the evidence for the impact of these drivers on population recovery following collapse. Chapter Two focuses on understanding whether the spatial distributions of these

populations have changed over time and whether shifts in their spatial distributions can be attributed to density-dependent processes or changes in bottom water temperatures. Chapter Three develops a methodology for estimating prey abundance by combining bottom trawl survey and stomach content data to identify how a key prey population for American plaice has changed over time. Chapter Four applies a juvenile population dynamics model to address whether American plaice juvenile natural mortality has varied since the population collapse. Chapter Five involves the development of models of increasing complexity for both yellowtail flounder and American plaice to identify the most important population processes that have assisted or hindered recovery and whether those processes appear to have been affected by ecosystem mechanisms. Finally, Chapter Six synthesizes the findings from the four data chapters to place them into context regarding how this research has demonstrated the interactive effects of overfishing and environmental variability on fish population recovery.

2 Lagged recovery of fish spatial distributions following a cold-water perturbation

Authors: Robertson, M.D.¹, Gao, J.¹, Regular, P.M.², Morgan, M.J.², & Zhang, F.¹

Author Affiliations

1. Centre for Fisheries Ecosystems Research, Fisheries and Marine Institute of Memorial University of Newfoundland, P.O. Box 4920, St. John's, NL, A1C 5R3, Canada
2. Fisheries and Oceans Canada, Northwest Atlantic Fisheries Centre, P.O. Box 5667, 80 East White Hills Rd., St. John's, NL A1C 5X1, Canada.

A version of this chapter was published in Scientific Reports:

Robertson, M.D., Gao, J., Regular, P.M., Morgan, M.J., & Zhang, F. (2021). Lagged recovery of fish spatial distributions following a cold-water perturbation. Scientific Reports. 11, 9513. <https://doi.org/10.1038/s41598-021-89066-x>

Abstract

Anomalous local temperature and extreme events (e.g., heat-waves) can cause rapid change and gradual recovery of local environmental conditions. However, few studies have tested whether species distribution can recover following returning environmental conditions. Here, I tested for change and recovery of the spatial distributions of two flatfish populations, American plaice (*Hippoglossoides platessoides*) and yellowtail flounder (*Limanda ferruginea*), in response to consecutive decreasing and increasing water temperature on the Newfoundland Grand Banks, Canada from 1985 to 2018. Using a Vector Autoregressive Spatiotemporal model, I found the distributions of both species shifted southwards following a period when anomalous cold water covered the northern sections of the Grand Banks. After accounting for density-dependent effects, I observed that yellowtail flounder re-distributed northwards when water temperature returned and exceeded levels recorded before the cold period, while the spatial distribution of American plaice has not recovered. My study demonstrates nonlinear effects of an environmental factor on species distribution, implying the possibility of irreversible (or hard-to-reverse) changes of species distribution following a rapid change and gradual recovery of environmental conditions.

2.1 Introduction

Climate change can affect the range of physiologically suitable habitats of species, leading to shifts in their spatial distributions across terrestrial, freshwater, and marine ecosystems (Chen et al. 2011; Poloczanska et al. 2013; Lenoir and Svenning 2015). For example, there is increasing evidence of unidirectional, often poleward, shifts of marine organisms in response to changes in the distribution of their thermal habitat (Dulvy et al. 2008; Cheung et al. 2009; Poloczanska et al. 2013). Shifts in the distribution of thermal habitat can influence species spatial distribution via direct effects on animal physiology and phenology (Pörtner 2001; Chuine 2010; Sunday et al. 2012), and indirect effects on biotic interactions (Gilman et al. 2010). For instance, when temperature exceeds a mobile organisms' physiological threshold, the organism will move towards habitat with tolerable thermal conditions (Fey et al. 2019). Although many studies focus on unidirectional shifts in species distributions due to environmental change at regional or global scales (Lenoir and Svenning 2015), organisms generally experience and respond to the local environment which may not show monotonic variations (Burrows et al. 2011; Pinsky et al. 2013). As a result, species distributions may exhibit more complex dynamics in response to fluctuating environmental conditions.

Anomalous local temperature and extreme events in particular can cause rapid changes in species distributions (Harley and Paine 2009; Wernberg et al. 2015; Ummenhofer and Meehl 2017). For example, a marine heat wave accelerated the poleward shift in the spatial distribution of a temperate marine fish (*Silago schomburgkii*) in Western Australia (Smith et al. 2019). Following anomalous events, environmental

conditions typically show a gradual return to previous levels. However, few studies have tested whether species distribution can recover following returning environmental conditions (Fig. 2.1; i.e., whether species distribution responds linearly to environmental factors). This is especially important to natural resource management because irreversible (or hard-to-reverse) changes in species distributions may lead to spatial mismatch with management/conservation areas, increasing the risks of local overexploitation or underutilization of natural resources (Kerr et al. 2017). Furthermore, understanding distributional change and recovery following fluctuating environmental conditions is important for predicting species response to climate change beyond the current focus on unidirectional trends (Ummenhofer and Meehl 2017).

In this study, I aim to test for change and recovery of the spatial distributions of two flatfish populations, American plaice (*Hippoglossoides platessoides*) and yellowtail flounder (*Limanda ferruginea*), in response to consecutive decreasing and increasing temperatures on the Newfoundland Grand Banks, Canada. The Grand Banks is an underwater plateau located at the confluence of the Labrador current and Gulf stream in the northwestern Atlantic ocean (Fig. 2.2). This ecosystem once maintained one of the world's most productive and valuable commercial fisheries (Davies and Rangeley 2010), however, in the mid-1990's, the biological community shifted from groundfish-dominated to being dominated by lower trophic level fishes and invertebrates (Dempsey et al. 2017), which was associated with prolonged intensive fishing and a period of anomalously cold ocean temperature (Dempsey et al. 2018). Ocean temperature affects population distribution via density-independent effects and fishing mainly affects

population distribution via density-dependent processes (i.e., changes in total population size; Garrison & Link, 2002; Hsieh et al., 2010). For example, density-dependent processes are expected to drive population distributions to expand towards marginal habitats when population density increases and contract towards core habitats when population density declines (Matthysen 2005; Borregaard and Rahbek 2010; Thorson et al. 2016). Therefore, to test for the change and recovery of spatial distributions in response to changing water temperature, I will 1) derive spatiotemporal variations of bottom water temperature on the Grand Banks, 2) model the spatiotemporal changes in yellowtail flounder and American plaice distributions, 3) account for density-dependent effects of population size on spatial distribution, and 4) test for a change and recovery of population distribution following a change and recovery in bottom water temperature.

2.2 Materials and Methods

2.2.1 Spatiotemporal temperature interpolation

I examined annual stratified random, bottom trawl surveys, conducted in the spring (April-June) by the Canadian Department of Fisheries and Oceans (DFO), on the Newfoundland Grand Banks in Northwest Atlantic Fisheries Organization (NAFO) divisions 3LNO from 1977 – 2018 (Doubleday 1981; Healey et al. 2012). I excluded data from 1981, 1983, and 1984 due to poor spatial survey coverage (i.e., the survey did not cover one or more of the NAFO divisions). I used ordinary kriging to estimate annual temperatures throughout the Grand Banks with the automap package (Hiemstra 2015) in R (see Appendix A Figs. A1-A5). To accomplish this, I fit a variogram to the annual raw temperature data (200-400 samples yr⁻¹) and then predicted temperatures across the Grand Banks using the weighted least squares method to fit a spherical model to the sample

variogram with a nugget effect, considering all observations for the kriging neighborhood (Oliver and Webster 2015). This simple kriging approach was deemed appropriate since estimates did not differ significantly from models with alternative assumptions about spatial correlation or with depth included as a covariate. I sampled the annual temperature estimates using the same knot locations used in the Vector Autoregressive Spatiotemporal (VAST) model (see Section 2.2.2) to allow direct spatial comparisons between fish biomass density and bottom-water temperature. Finally, I estimated a mean annual time-series of bottom-water temperature from the same knot locations described above to permit temporal comparisons between shifts in spatial distribution and bottom-water temperature.

2.2.2 Spatiotemporal model

I used fish biomass data from the aforementioned DFO research vessel surveys from 1985 – 2018 to model fish distribution changes over time. I excluded data collected prior to 1985 due to incomplete survey coverage and differences in gear (i.e., Yankee survey trawl was used prior to 1983 and cannot be directly compared to the Engel or Campelen trawls used afterwards due to differences in catchability; Wheeland et al. 2021). These data were modeled using VAST, a modeling platform to assess how the distribution of species/communities have changed over time (Thorson 2019a). VAST is capable of predicting biomass density across locations s , and time intervals t for multiple categories c (here, c is species; Thorson 2019b). VAST model predictions are made across a pre-specified number of locations (here, 50 locations, referred to as knots) within a Gaussian Markov Random Field, such that a prediction at any location is equal to its

value at the nearest location. I used the minimum number of knots that produced similar results to what was observed in the raw data and models with higher numbers of knots, to minimize the risk of overfitting the model. A variety of recent research has shown that VAST is capable of providing sound spatiotemporal advice to fisheries management, specifically for estimating indices of abundance, distribution shifts, and range expansion/contraction (Thorson et al. 2015b; Thorson 2019a).

The parameterization used here involves a delta model to separately model encounter probability p and biomass density via positive catch rates r :

$$\Pr(b_i = B) = \begin{cases} 1 - p_i & \text{if } B=0 \\ p_i \times \text{Gamma}(B; \log(r_i), \sigma_b^2(c)) & \text{if } B>0 \end{cases} \quad (2.1)$$

where b_i is the sampled biomass for each sample i . I specifically used a Poisson-link delta model which is proposed to be more biologically interpretable than the conventional delta model because it correlates predicted encounter probability and positive catch rates based on a joint dependence on group biomass density (Thorson 2017). Encounter probability p_i assumes that individuals are randomly distributed in the sampling area and the probability of encountering at least one fish is modeled as

$$p_i = 1 - \exp(-\alpha_i \times \exp(p_1(i))) \quad (2.2)$$

where α_i is an offset for the area swept by the bottom trawl and p_1 is an encounter probability linear predictor that is described below. Positive catch rate r_i is then defined as

$$r_i = \frac{\alpha_i \times \exp(p_1(i))}{p_i} \times \exp(p_2(i)) \quad (2.3)$$

where p_2 is a positive catch rate linear predictor that is described below.

Both the encounter probability and positive catch rates were estimated spatiotemporally using separate linear predictors, where encounter probability is modeled using a logit-link and

$$p_1(i) = \text{logit}[p(s_i, c_i, t_i)] = \gamma_p(c_i t_i) + \omega_p(s_i c_i) + \varepsilon_p(s_i c_i t_i) \quad (2.4)$$

where s is the location, and t is the time of the sample. $\gamma_p(c_i t_i)$ is an intercept for temporal encounter probability for each category, $\omega_p(s_i c_i)$ estimates spatial variation in encounter probability for each category, and $\varepsilon_p(s_i c_i t_i)$ represents the spatiotemporal variation in each category. Positive catch rates are modeled almost identically but with a log-linked predictor:

$$p_2(i) = \log[r(s_i, c_i, t_i)] = \gamma_r(c_i t_i) + \omega_r(s_i c_i) + \varepsilon_r(s_i c_i t_i) \quad (2.5)$$

where the three parameters estimate the temporal, spatial, and spatiotemporal variability respectively, for each category for the positive catch rates. For both linear predictors, the temporal intercepts and spatial parameters were treated as fixed effects, and the spatiotemporal parameters were treated as autoregressive random effects. Model convergence was evaluated by ensuring that the gradient of the approximated marginal log-likelihood for all fixed effects was $<10^{-6}$ and that the Hessian matrix was positive definite at the maximum-likelihood estimates.

I used model-based estimates of the effective area occupied and centre of gravity to identify changes in the range and location of flatfish distributions (Thorson et al. 2016). Centre of gravity (longitude and latitude) was estimated by

$$\bar{x}(c, t) = \frac{\sum_{s=1}^{n_s} d(s, c, t) \times x(s)}{\sum_{i=1}^{n_s} d(s, c, t)} \quad (2.6)$$

where $x(s)$ is a latitudinal or longitudinal description of location for knot s and $d(s, c, t)$ is the predicted density across knots, categories, and time.

Effective area occupied (h_t) was estimated by

$$h_t = \frac{b_t}{m_t} = \frac{(\int D_t(s) ds)^2}{\int D_t^2(s) ds} \quad (2.7)$$

where b_t is total biomass, m_t is average population density (kg km^{-2}), and $D_t(s)$ is the density function for that year. The estimation of this metric is done within VAST and Eqn. 2.7 is a simplification used for brevity (for a full derivation, description, and validation see Thorson et al. 2016). This formulation of effective area occupied measures the area required to contain a population given its average population density. As a result, this metric can identify changes in area occupied regardless of changes in total biomass. To identify potential density-dependent changes in distribution, I used Pearson correlation to relate the estimated total biomass index with the effective area occupied for both species. Although correlation between total biomass and effective area occupied can provide evidence of density-dependent changes in distribution, this correlation may also be indicative of other mechanisms driving shifts in distribution (Borregaard and Rahbek 2010).

2.2.3 Testing for density-dependent habitat selection

I wanted to account for the effects of density-dependent habitat selection to ensure that distribution shifts were not the result of changes in biomass. I tested for the existence of density-dependent habitat selection by examining the relationship between local and

global biomass (Myers and Stokes 1989; Shackell et al. 2005). This relationship serves as a proxy for habitat suitability because theory predicts that when density-dependent habitat selection exists, increased abundance will decrease population growth rates in optimal habitats and increase growth rates in marginal habitats (MacCall 1990). I considered the null hypothesis to be that variation in local density responses is independent of habitat suitability (i.e., a single positive linear or exponential relationship between local and total population biomass). This relationship would indicate that as global biomass increases, so does density at all locations. Using the output of the VAST model, I used a simple linear regression to model the relationship between annual global biomass estimates and annual local density estimates (at all 50 knots). If there was a positive relationship and no evidence of model misfit (e.g., non-normal residuals would indicate locally varying relationships) this would serve as evidence for the null hypothesis (density-dependent habitat selection does not play a large role in local population growth rates). If there was no relationship and/or evidence of model misfit, this would serve as evidence for the alternative hypothesis and I would test whether there are location specific relationships between local density and global biomass.

If there was evidence against the null hypothesis, I wanted to account for the effects of density-dependent habitat selection. To accomplish this, I developed a non-linear random effects model using,

$$\widehat{y}_{k,t} = a_k x_t^{b_k} \quad (2.8)$$

to examine local variability in the density-dependent habitat selection relationship (Myers and Stokes 1989; Swain and Morin 1996; Shackell et al. 2005). Where \widehat{y}_k is the log of local density +10, with the +10 ensuring that all y_k 's are positive (the log of local

density was <1 for some knots in some years), and x_t representing the log of total biomass +10 in a given year. Both a_k and b_k are random effects to provide unique estimates for all knots. I would expect that the estimate of b_k for locations would be least/concave in prime/core habitats and highest/convex in marginal habitats. Weaker responses (i.e., $b_k \leq 1$) would specifically indicate that a location is not sensitive to regional biomass changes. Since the residuals should represent deviations from the density-dependent relationship (i.e., the density-independent influence on distribution) I used them in the remaining analyses to ensure that my results would not be affected by density-dependent habitat selection. The model was fit in Template Model Builder (TMB; Kristensen et al. 2016) in R (R Core Team 2018), where convergence was assessed using the same criteria that I used for the VAST model.

2.2.4 Correlation analysis for recovery response

Knot specific density estimates (or residuals) were correlated with knot specific bottom-water temperature estimates across all years using rank-based Spearman correlation,

$$d_{s,t_i} = \frac{\text{cov}(\text{rnk}(d_{s,t_i}), \text{rnk}(\text{temp}_{s,t_j}))}{\sigma_{\text{rnk}(d_{s,t_i})} \sigma_{\text{rnk}(\text{temp}_{s,t_j})}} \quad (2.9)$$

Rank correlation allowed a comparison of the relative densities and temperatures, such that total population size and warmer or colder years would not affect correlations. Since both species modified their distributions in unique ways and magnitudes, I opted to use relative correlation between years rather than identifying a threshold of correlation as a cut-off to decide which years were correlated. In addition, I correlated the spatial

distribution of temperature and fish with themselves across time (Appendix A Figs. A6, A18, & A19) to identify their relative change in regards to their historical distributions.

2.3 Results

2.3.1 Bottom water temperature interpolation

Bottom water temperature was spatially heterogeneous on the Grand Banks. The spatial distribution of bottom water temperatures was relatively consistent throughout the study period with the southern and northeastern sections of the bank being the warmest (see Fig. 2.2 for geographical reference) and the interior, northern half of the bank and Avalon channel being the coldest (Fig. 2.4a; Appendix A Figs. A1-A5). From 1977-1990, temperature throughout the bank declined and eventually reached a minimum in 1990. During 1989-1991, the Grand Banks had large areas, specifically in the interior, northern half of the bank, where water temperature was lower than any other location on the bank during any of the years examined here ($< -1^{\circ}\text{C}$; Fig. 2.4). Following this cold period, water temperature increased throughout the bank and returned to and even exceeded the levels observed in the late-1970's and early-1980's. I examined the spatiotemporal correlation of temperature across space through time (Appendix A Fig. A6), which provided further evidence that the spatial pattern of water temperature was similar through time. Therefore, this relatively constant spatial distribution of bottom water temperature is used as a spatial reference for changes in fish distributions in later analyses.

2.3.2 VAST Estimates

Both yellowtail flounder and American plaice on the Grand Banks underwent distributional changes between 1985 and 2018 (Appendix A Figs. A7 & A8). Yellowtail

flounder were initially distributed throughout the interior of the Grand Banks. Their spatial distribution contracted and moved ~80 km south and ~20 km west (Appendix A Figs. A7 & A9d) during the cold period between 1985 and 1995, and re-expanded northeastwards across the interior of the bank afterwards (Appendix A Fig. A9d). The contraction and re-expansion of yellowtail flounder, as measured by the effective area occupied, was positively correlated with changes in the population's biomass which declined and then recovered ($\rho = 0.73$, $p\text{-value} < 0.01$; Appendix A Fig. A9c). American plaice were distributed throughout the entire Grand Banks in the mid-1980's. Their distribution contracted and shifted ~200 km southwards during the cold period (Appendix A Figs. A8 & A9b). Since contracting southwards, American plaice have not re-distributed to their previous location 200 km north, instead they have moved 50 km northeast (Appendix A Fig. A9b). Further, the contraction of the American plaice distribution, as measured by the effective area occupied, was correlated with changes in the population's biomass which declined and has yet to recover ($\rho = 0.73$, $p\text{-value} < 0.01$; Appendix A Fig. A9a).

2.3.3 Density-dependent habitat selection

A linear relationship without evidence of model misfit between total population biomass and local population density (the population density at each of the fifty locations estimated in the VAST) was detected for American plaice (Appendix A Fig. A10 & A12) but not for yellowtail flounder (Appendix A Fig. A11 & A13). After fitting a linear model to the total and local population size, the model had a relatively high R^2 (0.38) and the residuals showed a normal distribution for American plaice (Appendix A Fig. A12).

Whereas, for yellowtail flounder, the model had a low R^2 (0.07) and the residuals had a bimodal distribution (Appendix A Fig. A13). Density-dependent habitat selection is expected to yield differential growth rates in optimal and marginal habitats as population size increases (MacCall 1990). The relationship observed for American plaice was indicative of a proportional response in density to increasing population size, while yellowtail flounder's bimodal residuals and low R^2 indicated locally varying relationships between local and global biomass. Therefore, these analyses indicated that density-dependent habitat selection was strong for yellowtail flounder yet not detectable in American plaice. As a result, I was able to test for the response of American plaice's spatial distribution to changing water temperature using the local density estimates from VAST directly.

Using an exponential mixed-effects model, I identified local variability in the relationship between local density and total population biomass for yellowtail flounder (Appendix A Figs. A14 & A15). The model indicated that the preferred habitat for yellowtail flounder existed throughout the southern Grand Banks with ideal habitat ($b_k < 1$) on the southeast shoal and the most marginal habitat on the northern edge of the Grand Banks ($b_k > 1$; Fig. 2.3). The spatiotemporal residuals from these models were grouped in space and time (Appendix A Fig. A16) indicating that density-dependent habitat selection alone could not fully explain the shifts in spatial distribution for yellowtail flounder. Therefore, I used these residuals to test for the effects of water temperature on yellowtail flounder's spatial distribution.

2.3.4 Distribution – temperature correlation

The relationship between yellowtail flounder's spatial distribution and bottom water temperatures recovered after water temperature returned and exceeded previous levels. The residuals from the density-dependent habitat selection model were positive in the northern Grand Banks prior to the cold period, indicating more fish than expected by density-dependence alone (Appendix A Fig. A16). Following the cold period, the residuals in the north became negative, and these negative values persisted when warm temperatures returned throughout the Grand Banks (Appendix A Fig. A16). The residuals did not become positive again until 2010, the year with the warmest mean temperature on record for the Grand Banks ($\sim 2.5^{\circ}\text{C}$). Using the correlation between these residuals and the spatial distribution of temperature, I observed an abrupt shift from negative to positive correlation in the coldest year (1992; Fig. 2.4c). The positive correlation between temperature and yellowtail flounder distribution persisted until the warmest year (2010) which marked a second abrupt shift to negative correlation, which has mostly persisted since (Fig. 2.4c). Therefore, there was evidence of multiple distribution states for the same environmental conditions (temperature), where the switch between states corresponded with particularly cold and particularly warm temperatures.

Non-recovery in the relationship between spatial distribution and bottom water temperatures was observed for American plaice. American plaice distribution was negatively correlated with spatial temperatures prior to 1991 but became positively correlated in the years after 1991 (Fig. 2.4d). Unlike yellowtail flounder, the distribution of American plaice has yet to be negatively correlated with temperature since 1991 (Fig.

2.4d). Therefore, the American plaice population has evidence of two distinct spatial states: an early state with a wide distribution throughout the bank that was negatively correlated with temperature, and a recent state with a more contracted and southerly distribution that is positively correlated with temperature. Similar to yellowtail flounder, both states have existed during years with similar temperatures and the shift from the early state to the recent state corresponded with the timing of the coldest years. However, unlike yellowtail flounder, American plaice have yet to return to their previous distribution even when temperature became warmer than the levels before the cold period.

2.4 Discussion

I identified evidence that yellowtail flounder and American plaice have undergone shifts in their distribution over the past 35 years. These shifts differed in scale, where American plaice contracted and shifted their distribution hundreds of km's, while yellowtail flounder contracted and had relatively small changes in their central location. Furthermore, both species experienced a population collapse in the early 1990's but only yellowtail flounder has recovered since. To account for the potential effects of changing population size on distribution, I examined the role of density-dependent habitat selection which appeared to influence the distributional shift for yellowtail flounder but not American plaice. Past studies have reached the same conclusions for both populations (Myers and Stokes 1989; Simpson and Walsh 2004). However, density-dependent habitat selection did not fully describe the distributional changes for yellowtail flounder.

Furthermore, American plaice have yet to return to the northern Grand Banks where their distribution was initially centered, despite the Grand Banks warming in recent years.

By testing for changes in the correlation between spatial temperature and the spatial distribution of populations, I detected periods of change and non-recovery in the distribution of yellowtail flounder and American plaice. The cold-period that I observed from 1990 – 1992 matched previous observations of below average water temperatures on the Grand Banks that were accompanied by record high ice extent and record low salinity (Colbourne et al. 1994; Dempsey et al. 2017). My results suggest that anomalous temperatures can elicit long-term changes, which may represent alternative distributional states that can be difficult to reverse (Scheffer and Carpenter 2003). In both species, local fish density in the northern Grand Banks has shown the smallest amount of recovery. In addition, yellowtail flounder returned to their initial distributional state following a recent period of warm temperatures in 2011, while American plaice did not. This indicates that although both species exhibited a lack of recovery following the same cold period (i.e., a temperature threshold) they appear to have unique temperature thresholds that must be reached to return to their initial states. In the following paragraphs, I will discuss the possible ecological mechanisms, management implications, and future research directions of non-recovery of spatial distributions following an anomalous climate event.

Non-recovery of spatial distributions may be caused by spatially varying environmental effects acting on local populations (i.e., lower-level effects). The initial effects of a disturbance on local populations will depend on the level of exposure to the disturbance (Pascual and Guichard 2005). For example, American plaice have historically

preferred colder temperatures than yellowtail flounder (Appendix A Fig. A26- A28) and as a result were exposed to colder temperatures. The locations with the coldest temperatures in the northern half of the Grand Banks were also the locations with the largest reductions in local density. Furthermore, exposure to the coldest temperatures may have played a role in the trajectory of shifting thermal habitats for both species where American plaice's median occupied temperature increased by approximately 2°C following the cold period, while yellowtail flounder's increase was relatively small (approximately 0.5°C) in comparison (Appendix A Fig. A28). The change in occupied temperature for American plaice coupled with their relatively sedentary nature (Pitt 1969; Morgan 1996) and reductions in local density may indicate that rather than migrating to maintain a preferred temperature, changes in their distribution may represent a mass mortality event in locations with the coldest temperatures. The combined effects of this increased level of exposure may affect population recovery, since the northern component of the American plaice population was historically a major source of recruitment success (Walsh et al. 2004). The dramatic reductions and lack of recovery in local densities in the northern component of the American plaice population may be indicative of the existence of depensatory dynamics (i.e., Hutchings 2014). In addition, the magnitude of the effect of disturbance on local density is dependent on the resilience of local populations (Allen et al. 2016). Resilience to major disturbances may be decreased in populations that have previously been affected by persistent minor disturbances and, as such, populations that have been exposed to anthropogenic pressures (e.g., prolonged fishing pressure; Hsieh et al., 2010) may experience greater risk of prolonged change. Furthermore, reduced population density and productivity in certain locations can affect metapopulation

dynamics (Hastings and Botsford 2006; Revilla and Wiegand 2008). Connectivity and productivity of sub-populations within a metapopulation are necessary for the persistence of sub-populations through time, and spatially heterogeneous disturbances have the ability to fragment habitat and reduce connectivity and productivity (Kallimanis et al. 2005; Vuilleumier et al. 2007). Finally, spatial differences in individual physiology (Eliason et al. 2011; Sorte et al. 2011) and/or demographic traits (Davis and Shaw 2001; Valladares et al. 2014) could impact the recovery of a population. If the organisms that survived the disturbance lack the physiological or demographic traits that permitted survival or reproductive success in the disturbed areas, then re-colonization of those areas would be reliant on demographic or physiological changes.

Non-recovery of spatial distributions could also be caused by spatially reorganized community structure (i.e., higher-level effects; Scheffer & Carpenter, 2003). Biotic interactions (e.g., competition, predation) define community structure and these interactions are dependent on the abundance and presence (i.e., spatial overlap) of interacting species (Morin 2011a). Therefore, spatially heterogeneous disturbances can initiate unique successional pathways (i.e., changes in an ecological community following a disturbance) that reorganize local community structure (Connell and Slatyer 1977; Noble and Slatyer 1980). For example, the cold period on the Grand Banks may have promoted population growth of previously non-dominant species (e.g., snow crab; Mullaney et al., 2014) while also reducing the abundance of dominant species (e.g., Atlantic cod) in specific locations. This shift in dominance can modify biotic interactions in those locations and force long-term community reorganization (Morin 2011b). These

local reorganizations would create a spatially heterogeneous interaction network that may impede recovery by modifying the spatial availability of suitable habitat for a particular species (Rietkerk et al. 2004). Such changes have been previously observed in plant communities and were proposed as a potential leading indicator for regime shifts (Rietkerk et al. 2004). Additionally, I observed distributional shifts of both species (more dramatically for American plaice) towards warmer waters during a warming period, rather than moving to maintain prior thermal conditions as would generally be expected (Dulvy et al. 2008; Lenoir and Svenning 2015). Regardless of the direction, distributional shifts can modify ecological communities by forcing the development of novel interactions between species that did not previously overlap (Alexander et al. 2016). Although I did not examine the effects of species interactions on species distributions and productivity here, hypotheses about modified interactions on the Grand Banks could be examined in the future with VAST by allowing for species densities to impact one another across space and time (Thorson et al. 2019). Overall, non-recovering distributions may be indicative of drastic changes in local community ecology, despite only being an observable pattern for a few species.

It is important to note that the non-recovery of distributions discussed here may be only partially related to changes in temperature. For example, changes in the ecological community on the Grand Banks are hypothesized to be the result of both fishing and environmental drivers (Dempsey et al. 2017). Furthermore, although there was not an increase in reported American plaice landings in the 1980's, fishing in NAFO Division 3L is reported to have accounted for >50% of American plaice landings in most years

during the pre-collapse period. These landings may have affected local densities and increased the susceptibility of fish in the northern Grand Banks to collapse when exposed to particularly low temperatures. However, due to a lack of fine-scale spatiotemporal time-series of fishing pressure (see Appendix A Fig. A17 for spatially aggregated time-series), I was unable to directly examine the influence of fishing on population distributions. Despite not being able to account for fishing pressure directly, I was able to assess the relationship between changes in population size (one effect of fishing pressure) and spatial distribution. However, it is also worth noting that given the observational nature of the data used, I was only able to test for the effects of population size through the mechanism of density-dependent habitat selection. It is possible that population size could interact with changing temperatures or affect distribution through other mechanisms. Developing VAST or other spatiotemporal models to allow for estimates of density-dependent habitat selection and non-stationary covariate effects would allow for a more integrated propagation of uncertainty than was possible with the multi-model approach used here. Furthermore, being unable to observe all potential drivers is an inevitable challenge of empirical study in natural systems, since it is impossible to collect data on all aspects of an ecosystem. Therefore, future research on long-term changes in spatial distributions would benefit from theoretical examinations capable of controlling for additional drivers. Finally, the observed pattern is dependent on the scale of observation. For example, if this study had examined the northern and southern Grand Banks separately, I may conclude that American plaice in the northern section of the bank had not recovered while the southern section of the bank had. Although I cannot yet identify the mechanisms responsible for the distribution shift, an ability to identify the

pattern of change is a necessary first step towards producing plausible, testable hypotheses that will inform conservation and resource management.

Modified spatial distributions of species can affect conservation and resource harvesting strategies. Distributional shifts have been observed as a response to changing climate (Dulvy et al. 2008; Lenoir and Svenning 2015) and the identification of these shifts has led to the development of protected areas and management plans that estimate future distributions using species distribution models (Guisan et al. 2013). Although I observed that species on the Grand Banks initially tracked local climate (cooler temperatures) by shifting their distributions southwards, the lack of recovery has maintained the southerly distributions despite the return of warm temperatures. This potentially irreversible shift is problematic because distributional shifts in unexpected directions (e.g., towards warm waters during a warming period) and non-recovery of distributions following environmental recovery may not be predicted with species distribution models (Wheeland and Morgan 2020). These unexpected changes will affect the efficacy of protected areas developed for areas with presumed stationary landscape structure or protected areas that shift with climate (Runge et al. 2016). Therefore, the development of connected, protected area networks throughout a heterogeneous environment may be the best strategy for buffering the effects of disturbance and minimizing the risk of non-recovery (Van Teeffelen et al. 2012). Additionally, the non-linear response of spatial distributions provides evidence for the necessity of using various ecological indicators (including spatial distributions) when assessing the status of an ecosystem or a population (Shepard et al. 2015). Population status is often assessed

based on population change within specific management boundaries, and unacknowledged distributional shifts across a management boundary may impact the perceived population size and/or vital rates (growth, reproduction, mortality) that are used for the development of management strategies (Link et al. 2011b; Kerr et al. 2017). I have only examined species within their management boundaries here and therefore cannot assess whether this problem may exist for populations in the Northwest Atlantic. Successful management of species affected by non-recovering spatial distributions will require a recognition of the change, as well as a determination of the effects of the spatial change on estimates of population status and recovery potential.

I have used the concept of non-recovery (i.e., non-linear response) to describe the observed patterns of spatial change, and have provided various lines of evidence for what may be causing this pattern and why it merits further investigation. Future studies should continue to examine spatial distribution shifts following anomalous events to identify if non-recovery is a widespread phenomenon. Additionally, further study on the role of biotic interactions in shaping the distribution of species will improve our understanding of how modified feedbacks may promote persistent changes in spatial distributions (Araújo and Luoto 2007; Ockendon et al. 2014). Finally, continued exploration of the mechanisms that erode spatial population structure are necessary to develop conservation and management strategies that will minimize the possibility of degrading spatial distributions (Hsieh et al. 2010). In conclusion, by analyzing the non-recovery of species distributions following anomalous climate events, we will gain a better understanding of the causes and consequences of prolonged distributional changes, the diversity of responses to

climate change, and be able to better identify ways to mitigate their negative socio-ecological effects.

2.5 List of Figures

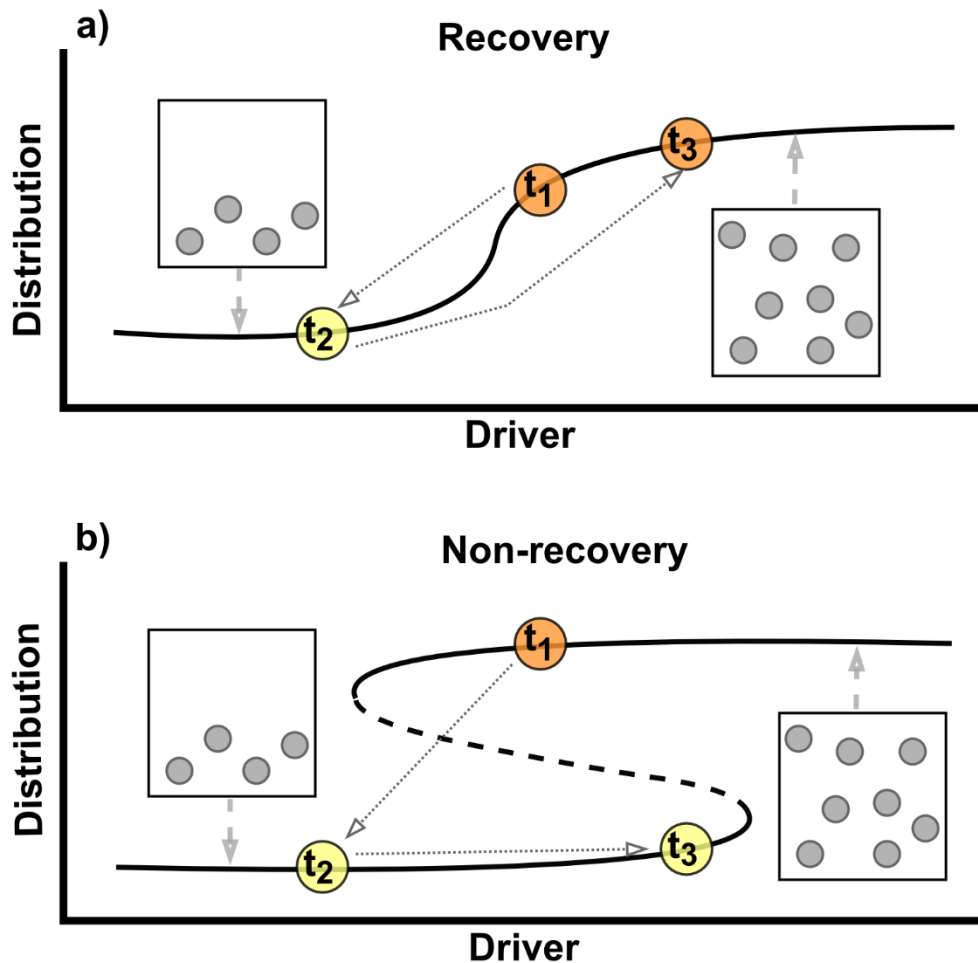


Figure 2.1 Conceptual diagram of spatial distribution recovery and non-recovery. The curved lines represent how an organism's spatial distribution will change with an environmental driver where, a) is a distribution that recovers when the environmental driver returns to previous conditions and b) is a distribution that does not recover when the environmental driver returns to previous conditions. The S-shape in b) represents an unstable equilibrium between distributional states, where a distribution above the dashed line will be driven to the upper asymptote and distributions below the dashed line will be driven to the lower asymptote (similar to the concept of hysteresis in ecosystem states; Scheffer et al. 2001). The colored circles on the lines represent three snapshots in time (t_1 – t_3) that are meant to represent the same environmental driver conditions between panels a) and b), and the dotted grey arrows represent the transition between each snapshot. The circles within boxes represent the snapshots of the spatial states for the organism's distribution.

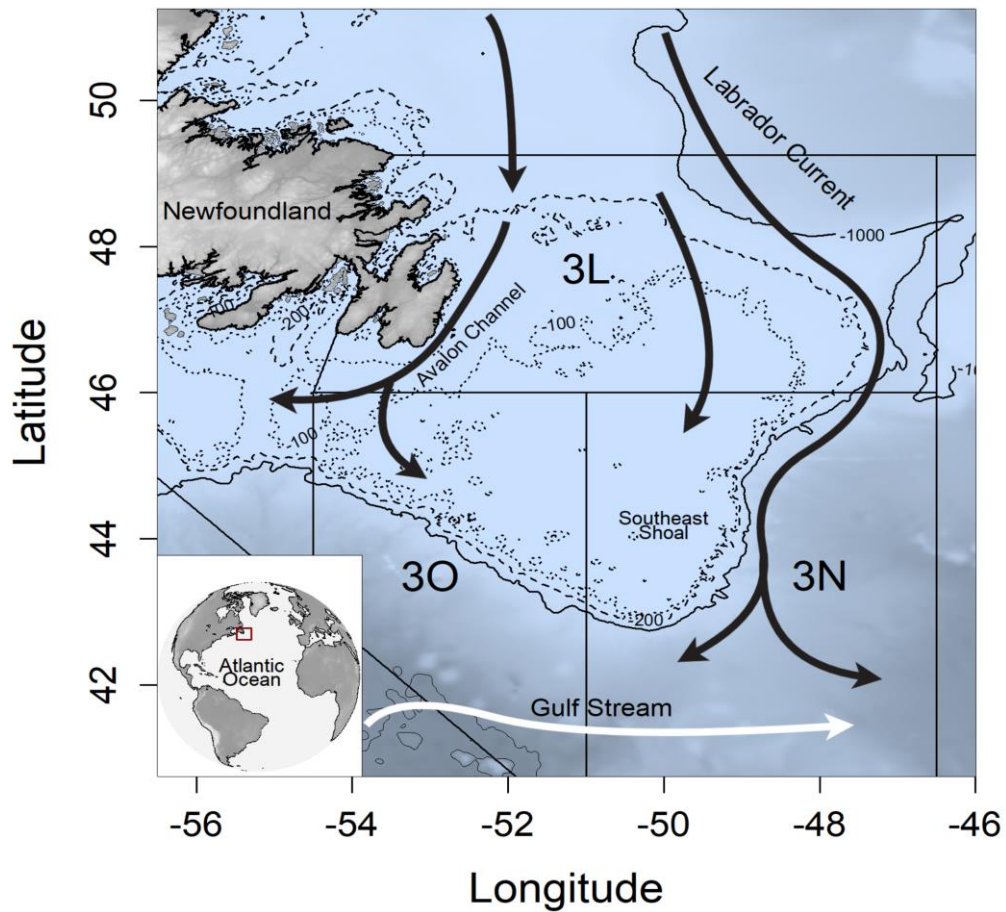


Figure 2.2 Bathymetry and dominant currents of the Grand Banks region/North Atlantic Fisheries Organization (NAFO) divisions 3LNO. Bathymetric contours shown for 100 (dotted lines), 200 (dashed lines), and 1000 m (solid lines). Approximate pathways for the Labrador Current represented by black arrows and the Gulf Stream represented by white arrows. Inset in the bottom left shows the position of the study area (red rectangle) in reference to the rest of the Atlantic Ocean.

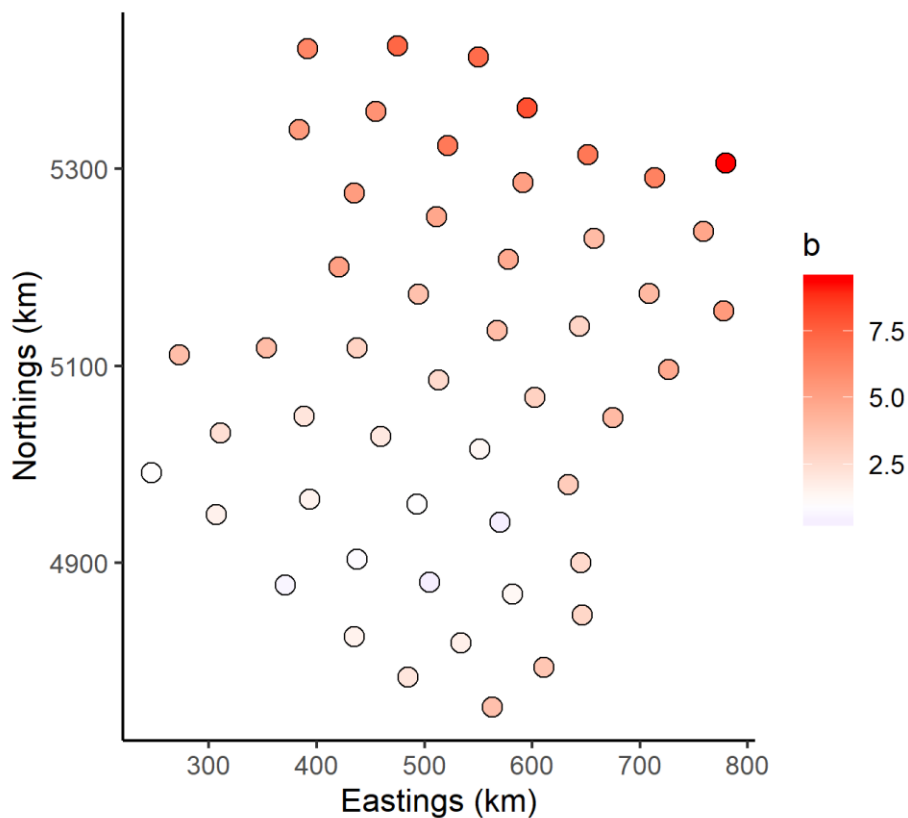


Figure 2.3 The estimate of the slope (exponent) between local and total biomass (b_k) from the knot specific exponential models comparing yellowtail flounder local density based on total biomass across the fifty knots in the VAST. Red circles represent a $b_k > 1$ which indicate large local biomass changes with total biomass changes (i.e., marginal habitat), white circles represent a $b_k = 1$, and blue circles represent a $b_k < 1$ which indicate that local biomass is stable with changes in total biomass (i.e., ideal habitat).

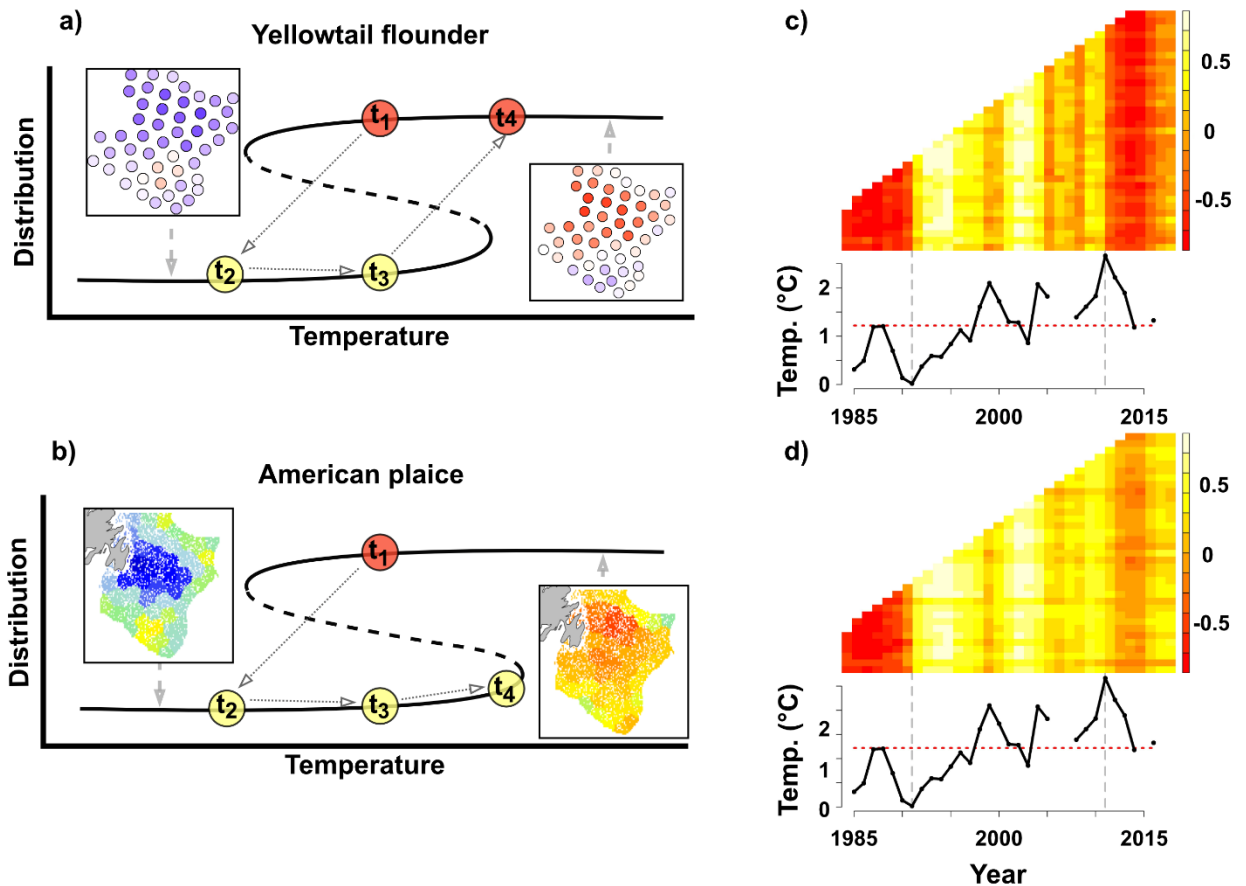


Figure 2.4 Diagram of spatial distribution recovery results, format based on Figure 2.2. Line drawings for a-b) represent the theoretical pattern that matches the observations for each species. t_1 and t_3 represent snapshots in time with equal temperature, while t_2 and t_4 represent a snapshot with a higher temperature. Maps for a-b) represent snapshots that define each spatial state, where the maps for a) represent the residuals (blue = negative, red = positive) of the density-dependent model for yellowtail flounder (see Appendix A Fig. A16) and maps for b) represent the spatial distribution (blue = low density, red = high density) of American plaice from the Vector Autoregressive Spatiotemporal model [VAST] (see Appendix A Fig. A8). Finally, c-d) is the correlation analysis of spatial distributions (y-axis) and bottom water temperature distributions (x-axis) over time (yellow = high correlation, red = negative correlation) along with the mean annual temperature trend on the Grand Banks shown beneath the correlation plots (dashed grey lines represent the minimum [1991] and maximum [2011] mean temperatures; dotted red line represents the mean temperature over the entire time-series). Positive correlation in panels c-d) indicates that areas with high density occur in areas with warmer temperatures and negative correlation indicates that areas with high density occur in areas with cold temperatures.

3 Accounting for a non-linear functional response when estimating prey dynamics using predator diet data

Authors: Robertson, M.D.^{1*}, Koen-Alonso, M.², Regular, P.M.², Cadigan, N.¹, & Zhang, F.^{1,3}

Author Affiliations

1. Centre for Fisheries Ecosystems Research, Fisheries and Marine Institute of Memorial University of Newfoundland, P.O. Box 4920, St. John's, NL, A1C 5R3, Canada.
2. Fisheries and Oceans Canada, Northwest Atlantic Fisheries Centre, P.O. Box 5667, 80 East White Hills Rd., St. John's, NL, A1C 5X1, Canada.
3. College of Marine Science, Shanghai Ocean University, 999 Huchenghuan Road, Shanghai, 201306, China.

A version of this chapter was published in *Methods in Ecology and Evolution*:

Robertson, M.D., Koen-Alonso, M., Regular, P.M., Cadigan, N., & Zhang, F. (2022). Accounting for a non-linear functional response when estimating prey dynamics using predator diet data. Methods in Ecology and Evolution, 13(4), 880-893
<https://doi.org/10.1111/2041-210X.13795>

Abstract

Forage fish species are key in the transfer of energy from lower to upper trophic levels in marine ecosystems. Therefore, understanding their population dynamics, including population levels, is crucial for understanding productivity and the regulation of marine food webs. However, many forage fishes are poorly sampled by bottom trawl surveys, leading to poor estimates of their abundance. These estimates can be improved by using predator stomach contents as an additional sampling strategy; however, non-linear relationships between prey abundance and predator consumption (i.e., the functional response) may bias stomach data as well. Using predator stomach contents and bottom trawl survey data, this study aimed to minimize this bias by developing a model to estimate prey dynamics and account for the predator functional response. This model was tested using a series of simulations and applied to a case-study of northern sand lance (*Ammodytes dubius*) on the Newfoundland Grand Banks, Canada. The simulations revealed that when predators consumed prey following a non-linear functional response, the model outperformed a classical model (the model adopted by most studies) that assumed a linear functional response. In the case study, I estimated the relative abundance of sand lance from 1995 – 2018, which exhibited oscillatory dynamics with a period of approximately seven years. These results demonstrate that this model is capable of more accurately estimating the abundance of data-limited prey populations, which contributes to a better understanding of food web dynamics.

3.1 Introduction

In marine ecosystems, intermediate trophic level species (i.e., forage fishes) play a key role in regulating the energy flow from primary and secondary producers to top predators (Pikitch et al. 2014), and understanding their population dynamics is crucial for food web studies and ecosystem-based fisheries management (Tam et al. 2017; Link et al. 2020). However, reliably estimating the abundance of forage fishes is challenging; these species are often data-limited because they are not directly targeted and/or poorly sampled by fisheries, and while they often spend time in pelagic habitats, regular research surveys typically focus on demersal species and use bottom trawls as the sampling gear (O'Driscoll et al. 2002; Stockwell et al. 2006).

Estimation of forage fish abundance can be improved by employing multiple sampling strategies that provide alternative perspectives (Yule et al. 2007; Jech and McQuinn 2016). For example, predator stomach contents are increasingly used as an additional data source to estimate prey abundance (Mills et al. 2007; Deroba 2018), especially for species that lack targeted and effective surveys (e.g., Staudinger et al. 2020). Since predators are often the main targets of research surveys and commercial harvests, they tend to be better sampled and their stomach contents can be indicative of prey abundance/biomass (Link 2004; Dwyer et al. 2010; Ng et al. 2021). For instance, trends in the frequency of occurrence of capelin and sand lance in fish predator stomach contents in the Gulf of Alaska matched abundance estimates from research surveys and seabird diet data (Piatt et al. 2018). Similar analyses have been conducted using a variety of methods (e.g., generalized linear models, generalized additive models) that have

tended to assume that the frequency and/or amount (e.g., number, weight) of prey in stomachs is linearly correlated to the abundance of that prey (Roseneau and Byrd 1997; Buchheister and Latour 2015; but see Mills et al. 2007).

Non-linear relationships between consumption and prey abundance can affect estimates of abundance based on stomach contents data. The relationship between prey abundance and consumption rate is known as the functional response (Koen-Alonso 2007). Single species functional responses are often described following Holling (1959): linear with an asymptote (type I), decelerating (type II), or sigmoidal (type III), but evidence from studies of marine fishes indicates that type II and III functional responses are the most common forms (Moustahfid et al. 2010; Uiterwaal et al. 2018). Given these observations, and considering that many estimates of abundance from stomach contents still rely on linear assumptions, a research gap exists for methods that account for more realistic functional response forms when using stomach contents to estimate trends in prey abundance.

To address this gap, I developed the Non-Linear Functional response Prey dynamics Model (NLFPM). This model estimates prey dynamics by combining survey and predator stomachs contents data, and accounting for the predator functional response. The functional response is modeled by treating average survey catch as a relative index of prey population abundance to compare to the probability of consumption of prey from stomach contents data. These two sources of data are combined to provide an improved index of prey abundance. This method was tested using simulations and was then applied to a case study for northern sand lance (*Ammodytes dubius*) on the Grand Banks,

Newfoundland, Canada. The case study used bottom trawl survey data and stomach contents data from two groundfish predator species (Atlantic cod [*Gadus morhua*] and American plaice [*Hippoglossoides platessoides*]). These two predator species were specifically chosen because they are commonly caught and sampled by the trawl survey and stomach contents sampling programs on the Grand Banks, and because both species have been observed to regularly consume northern sand lance on the Grand Banks (e.g., Gonzalez et al. 2006; Koen-Alonso 2018).

Northern sand lance is a forage fish that substantially contributes to the diet of several commercially important species on the Newfoundland Grand Banks in Northwest Atlantic Fisheries Organization (NAFO) divisions 3LNO (Koen-Alonso 2018). Despite their importance in this ecosystem, sand lance has received little research attention. For example, our understanding of their population dynamics and ecology on the Grand Banks has been limited to potentially inaccurate abundance and biomass estimates from bottom trawl surveys (Winters 1983; Lilly and Simpson 2000; Nogueira et al. 2015). The inaccuracy of the survey estimates is driven by sand lance's limited catchability in bottom trawl surveys due to their narrow, anguilliform morphology, and alternating pelagic and burrowing behaviors (Staudinger et al. 2020). Therefore, alternative methods are required to more accurately estimate sand lance abundance and population dynamics.

3.2 Materials and Methods

3.2.1 Non-Linear Functional response Prey dynamics Model (NLFPM)

I developed a model to estimate a relative index of abundance for a prey species and account for a type II/III functional response. The model uses comparable trawl and

stomach content data, where data are reduced to presence/absence of prey (i.e., their most basic form of information). Although categorizing data as presence/absence removes information on abundance/biomass per tow for trawl surveys and gravimetric (i.e., weight) estimates for stomach contents, doing so removes the need to determine how comparable individual stomach content weights are to abundance/biomass of fish in a tow. The model has process and observation components, where process components specify the underlying dynamics of the unobserved response variable (i.e., prey population abundance) while the observation components link the observed data (i.e., survey catch and predator stomach contents) to the unobserved response (Aeberhard et al. 2018).

The latent variable of interest is the total abundance of a prey population (N_y) over time (y). Whole populations are, however, rarely available to a survey, especially for forage species. Therefore, a relative index of average population abundance (n_y) is used as the response variable. The process component of the model estimates n_y as a random effect that follows a Gaussian random walk likelihood function,

$$n_y \sim N(n_{y-1}, \sigma^2). \quad (3.1)$$

There are two observation components to the model: 1) fitting the trawl data and 2) fitting the stomach contents data. The first component involves modeling the probability of encountering at least one prey in a random trawl tow (pt) in a given year (y),

$$pt_y = 1 - \exp(-n_y), \quad (3.2)$$

such that $pt_y \rightarrow 1$ as $n_y \rightarrow \infty$ (Thorson 2017). Although the spatial distribution of prey is likely not homogenous (e.g., prey distribution may depend on habitat availability), I assumed that prey are distributed homogeneously throughout the sampling area here as a first step. Since trawl data are reduced to binomial (presence/absence) data, pt_y is then directly estimated using a Bernoulli distribution,

$$trawl_i \sim \text{Bernoulli}(pt_y), \quad (3.3)$$

where $trawl_i$ is a single presence/absence observation of prey in the i 'th trawl tow. This transformation and estimation process matches the first step in delta/hurdle models (specifically a Poisson-link delta model; Thorson 2017) that are commonly used to standardize catch-per-unit-effort fisheries data (Maunder and Punt 2004; Zuur et al. 2009). If the prey is homogeneously distributed and trawl catches are Poisson distributed then the probability of catching at least one of the prey is given by Eqn. (3.2), which is the motivation for this equation. Assuming an exponential relationship between relative abundance and encounter probability is reasonable because encounter probability has been found to scale with abundance for many taxa (e.g., Gaston et al., 2000; McCarthy et al., 2013). Furthermore, non-linear relationships between encounter probability and abundance can occur as a result of species biology/ecology and data collection methodology (Walsh 1996; Harley et al. 2001; Maunder et al. 2006).

The second observation component of the model involves fitting the stomach contents data. These data are indirect samples of presence/absence that are dependent on direct sampling by predators via consumption. Being indirect, the probability of encountering prey in stomach contents data may be dependent on the functional response

of the predator. One flexible parameterization that can account for type II and III functional response shapes is the general form described by Real (1979),

$$r = \frac{k(d^\beta)}{\chi^\beta + d^\beta}, \quad (3.4)$$

where r represents the rate of consumption of prey, d is the density of prey, k represents the upper asymptote of the curve, χ is a shape parameter, and β describes the form of the curve ($\beta=1$: type II, $\beta>1$: type III). This representation assumes a single species functional response, where the consumption rate only depends on prey density and it is not affected by other changes in the prey field. Furthermore, if both sides of Eqn. (3.4) are divided by k , the consumption rate can be expressed as a fraction of its maximum, and the probability of encountering a prey in a random stomach could be used as a proxy for the r/k fraction. I use this approximation to represent the connection between stomach and trawl information,

$$ps_y = \frac{(pt_y)^\beta}{\chi^\beta + (pt_y)^\beta}, \quad (3.5)$$

where the probability of encountering a prey in a random predator's stomach in a given year (ps_y) is a proxy for the (r/k) ratio, and the probability of encountering a prey in a random trawl tow in a given year (pt_y ; Eqn. 3.2) represents a proxy for the local prey density (d). This proxy is more valid at lower prey densities (e.g., when the relationship between pt_y and n_y is more linear; see Section 3.2.2.2 and Appendix B1). This approach effectively bounds the functional response between (0,1), but preserves the ability of producing a wide variety of shapes consistent with type II and III formulations. Finally, ps_y is estimated using a Bernoulli distribution function,

$$stomach_i \sim Bernoulli(ps_y), \quad (3.6)$$

where $stomach_i$ is a single presence/absence observation of prey in a predator stomach.

I used the Template Model Builder (TMB, Kristensen et al. 2016) package in R (R Core Team 2018) to evaluate the negative logarithms of the marginal likelihoods (nll) of these models and the data, and to evaluate the nll gradients. Further, I used the R function `nllminb()` to find the maximum likelihood estimates. Model convergence was evaluated by ensuring that the nll gradient for all parameters was $<10^{-4}$ and that the Hessian matrix was positive definite at the maximum-likelihood estimates.

3.2.2 Simulation

3.2.2.1 Overview of simulation structure

To identify whether this model could reliably account for non-linear functional responses and estimate prey abundance, I implemented simulations that involved four types of models: operating, observation, estimation, and evaluation (Fig. 3.1). The operating models simulated random time-series for both predator and prey species and simulated the consumption of prey by predator following a functional response. The observation models simulated bottom trawl sampling of prey and stomach content sampling of predators. The estimation models included the NLFPM model, a model that uses the trawl data and assumes a linear functional response (Linear Functional response Prey dynamics Model [LFPM]), and a model that only used trawl data. Finally, the evaluation models compared the mean squared error (MSE) and bias between the estimated and true prey population dynamics as well as the precision of estimates

between the NLFPM and the trawl data only model. Each aspect of the simulation is described in detail in the subsequent sub-sections.

3.2.2.2 Operating models

Simulations were run with time-series of 25 years, where both the size of predator and prey populations varied following a Gaussian random walk with an initial mean of 10,000 and variability of 200,

$$N_1 \sim N(10,000, 200), \quad (3.7)$$

$$N_t = N_{t-1} + \sim N(0,200). \quad (3.8)$$

For simplicity I allowed the size of the populations to vary independently. All uses of prey abundance in the simulations relied on inputting abundance into Eqn. 3.2. However, since the prey abundance specified in Eqns. 3.7-3.8 is large, estimated pt_y from Eqn. 3.2. would always be equal to 1 if abundance was not scaled. To account for this, I scaled prey abundance by normalization using the standard score equation,

$$N_{t,normalized} = \frac{N_t - \bar{N}_t}{\sigma_{N_t}}, \quad (3.9)$$

and then logit transformed the normalized abundance to bound the values between (0,1) before using them in Eqn. 3.2. In addition to requiring scaled abundance, I bounded abundance between (0,1) to maintain abundances that would not approach the asymptote of the exponential relationship (values >1) where large changes in abundance may only yield small changes in probability of encounter. Abundance values are still estimable but become less accurate as they approach the asymptote (see Appendix B1).

This simulation allowed predation to follow a specified type II or III functional response (Eqn. 3.4). Prey density in the functional response equation was based on inputting scaled prey abundance into Eqn. 3.2. Every predator in the population sampled the prey field using a random draw from a binomial distribution where p in that distribution represented the probability of consumption that was calculated using the functional response (Eqn. 3.5).

3.2.2.3 Observation models

Both prey and predator populations were sampled using simulated trawl surveys. I used 200 random trawl samples per year. The trawl samples of the prey population were taken using a binomial distribution, where the probability of encountering prey increased with average population abundance and was based on inputting scaled prey abundance into Eqn. 3.2. The trawl survey for the predator population represented the stomach sampling configuration used on the Grand Banks, where <20 fish per species have their stomachs sampled per trawl sample, and less than half of the trawl samples (75) examine predator stomachs (Koen-Alonso 2018). This process involved samples being derived from a Poisson distribution with mean λ that was proportional to predator population size following,

$$\lambda = \alpha + \frac{N - \min(N)}{(\max(N) - \min(N))} (\omega - \alpha), \quad (3.10)$$

where α describes the minimum scaled value (here 10), ω describes the maximum scaled value (here 20), and N is the number of predators in the population. By representing the process in this way, the number of predators sampled varies randomly based on the size of the predator population and a minimum of 10 and maximum of 20 predators are

sampled on each tow (see Appendix B4 for analyses on the effects of stomach sample size). Every predator captured had its stomach sampled and stomach samples always correctly identified whether the predator had consumed prey or not.

3.2.2.4 Estimation

For each simulation, I compared estimates from the NLFPM to the LFPM and a model with only trawl data. The LFPM was identical to the NLFPM except for how stomach contents data were treated in the process model. Rather than assuming that these data followed a general functional response (Eqn. 3.5) they were assumed to be relative indices of abundance like the trawl data in the NLFPM (Eqn. 3.2). The trawl data model was formulated in the same way as the LFPM and NLFPM for the trawl data component (i.e., Eqn. 3.1-3.3) and had all stomach content components (i.e., Eqn. 3.5-3.6) removed. By comparing these estimation models I was able to determine whether the NLFPM would provide improved estimates of prey abundance.

3.2.2.5 Evaluation

I ran 1,000 simulations for operating models with predators using type II and type III functional response forms, where the shape parameters for the type II form were $\chi = 0.3$, $\beta = 1$ and $\chi = 0.3$, $\beta = 3$ for the type III form (Fig. 3.2). These forms were chosen to represent distinct functional response forms to evaluate how model performance varied with the shape of the functional response. The ability of the models to recover true estimates of changes in the prey population size were evaluated by comparing the MSE and mean difference (i.e., bias) between model estimates of n_y and the true values for relative (normalized and logit transformed) population size that were used in the

simulation (Section 3.2.2.2). To determine whether adding predation data would improve model precision, I also compared model estimates of standard deviation in each year for n_y between the NLFPM and the model with only trawl data. I then tested whether the model representing the true dynamics (i.e., the NLFPM) would be identified using Akaike's Information Criterion (AIC) when compared to the LFPM. I could not compare the NLFPM or LFPM to the trawl data model due to differing amounts of input data (i.e., no stomach contents data in the model with only trawl data). Finally, I compared NLFPM estimates of the functional response shape parameters and the median shape of the estimated functional response to the true values.

3.2.3 Case Study

3.2.3.1 Data

I used catch per unit effort data from annual stratified-random bottom-trawl surveys, conducted in the spring (April – June) by the Canadian Department of Fisheries and Oceans (DFO), on the Newfoundland Grand Banks, Canada in NAFO divisions 3LNO from 1995 – 2018. Due to the model assumption that prey are distributed homogeneously, I removed samples from locations where sand lance were never caught since adding samples from locations that don't match the distribution of prey could bias estimates of abundance (see Appendix B2).

I used two types of stomach contents data, 'called' and full, collected during the bottom trawl surveys for two predators, Atlantic cod (*Gadus morhua*) and American plaice (*Hippoglossoides platessoides*). Called stomach data records the presence/absence of prey species, where the top two prey species that are present in a stomach are recorded

to estimate the frequency of consumption of dominant prey. Atlantic cod called stomach data were collected every year from 1995 – 2018, while American plaice called stomachs were not collected in 2006 or 2016 – 2018. Full stomach contents data (gravimetric stomach analyses) recorded the mass of each prey item in a predator’s stomach. However, these data generally had smaller sample sizes and were only available for a limited number of years (Atlantic cod: 1995 – 1997 & 2013 – 2018, American plaice: 2013 – 2018). I only examined stomach contents data for Atlantic cod and American plaice >25 cm in length (see Appendix B3 for rationale) because both predators undergo ontogenetic diet shifts.

To allow comparability between data types, all data were converted to presence/absence. This reduced some of the information that was available from trawls (numbers and weight) and full stomach content data (weight). However, it has been acknowledged that the Campelen surveys were not designed to capture forage species, and while they can provide useful presence/absence information, their ability to provide reliable quantitative estimates is more limited (O’Driscoll et al. 2002; DFO 2012).

I ran separate models for each predator species. These models used both called and full stomach contents data to estimate a shared functional response. However, the models estimated separate probabilities of encounter for the different types of stomach content data since the data represented different observation processes and therefore may have unique temporal trends. In addition to running models for each predator species separately, I ran one model that included both types of stomach contents data from both predator species. This model estimated separate encounter probabilities for each type of

stomach contents and for each predator species (six total encounter probabilities, one pt_y for each species, and one ps_y for each stomach contents data source for each species), but all data contributed to a single, fully integrated relative index of abundance.

3.3 Results

3.3.1 Simulation

The simulation indicated that the NLFPM estimated relative prey abundance trends that were close to the true relative prey abundance trends (i.e., MSE close to zero) regardless of the true form of the functional response (Fig. 3.3). The NLFPM had a median MSE that was approximately 39 and 499 times lower than the LFPM and 2.1 and 4.9 times lower than the model with only trawl data when the true dynamics were type II and III respectively. Estimates from the NLFPM were less biased than estimates from the LFPM but slightly more biased than the trawl data only model (Fig. 3.4). The NLFPM median bias was 2.1 and 3.2 times higher than the model with only trawl data but was 44 and 62 times lower than the LFPM when the true dynamics were type II and III respectively. These results indicate that the NLFPM is capable of accounting for type II and III functional responses to provide more precise estimates of the actual changes in prey abundance, although using prey data can slightly bias abundance estimates when compared to a model with only trawl data. Furthermore, these improved estimates from the LFPM are observable in model AIC score, where the median decreases in AIC for the NLFPM in comparison to the LFPM were 536 and 1337 for operating models with type II and III functional responses respectively (Fig. 3.5).

The NLFPM estimated functional response shape parameter values that were close to, but sometimes less than, the true shape parameter values (Fig. 3.6). When type II dynamics were the true form of the functional response, the median estimate of χ was approximately equal to the true value and β was underestimated by 0.05. When type III dynamics were the true form of the functional response, the median estimate of χ was approximately equal to the true value and β was underestimated by 0.150. Despite the underestimates of β , the median functional response shapes were not much different from the true shapes, indicating that these small deviations from the truth will not have a large effect on prey abundance estimates (Appendix B Fig. B4.4).

When compared to a model with only trawl data, the NLFPM always had smaller annual standard deviation estimates for the prey abundance index for both operating models (Fig. 3.7). These results indicate that adding diet information can improve the precision of abundance index estimates.

3.3.2 Case Study

Estimated relative prey density (Eqn. 3.2) and probability of consumption (Eqn. 3.5) indicated that both American plaice and Atlantic cod have exhibited type III functional responses (i.e., $\beta > 1$; Fig. 3.8, Table 3.1) and the NLFPM had smaller AIC scores compared to the LFPM (Table 3.2). American plaice were estimated to have a relatively shallow type III functional response curve compared to Atlantic cod, and American plaice had a lower probability of consuming sand lance (maximum probability 0.27) compared to 0.36 for Atlantic cod. Furthermore, the range of estimated prey density was small ($\sim 0.3 - 0.55$) indicating that any changes in sand lance abundance were relatively small (see

Appendix B4 for analyses on the effects of a narrow range of prey density). All data were below the midpoint of the estimated functional responses indicating that any increases in prey abundance should yield relatively large increases in the probability of consumption. Finally, when American plaice and Atlantic cod were used in the same model, their functional response shape parameters differed slightly from when they were modeled separately. Both curves became flatter, with larger values for χ and smaller values for β (Fig. 3.8).

All three models estimated trends indicating that sand lance abundance has fluctuated since 1995, with approximately three peaks and four valleys estimated at a period of around seven years (Fig. 3.9). Each of these time-series varied slightly, with Atlantic cod having a less pronounced peak in the middle of the time-series (2005 – 2010), and the American plaice and both species models having a lower initial peak (1997 – 1998). Finally, when American plaice and Atlantic cod data were combined, the trend was similar to what had been observed when those species were modeled separately.

3.4 Discussion

This study aimed to develop a model that can estimate prey dynamics by integrating survey and stomach content data, while accounting for predator functional responses. The efficacy of the NLFPM was justified by simulations and I then applied the NLFPM to a case study for northern sand lance on the Grand Banks. When predators exhibited non-linear functional responses in the simulations, the NLFPM outperformed the LFPM in all assessed metrics. The NLFPM also outperformed a model with only trawl data in mean-squared error and standard deviation but produced estimates that were

slightly biased in comparison. Furthermore, the NLFPM was capable of estimating functional response shape parameter values that closely corresponded with the true values. In the case study, the model estimated sand lance dynamics using bottom trawl survey and two types of predator stomach contents data from two predators. Results indicated that both predators consume sand lance following a type III functional response. Furthermore, I identified coherent patterns between all data sources, indicating that sand lance abundance followed an oscillating pattern over time from 1995 – 2018. Here, I discuss the advantages of my model, its assumptions, future directions, and the implications of estimated dynamics of sand lance in the case study.

3.4.1 Model Advantages

I developed a model that estimates and accounts for non-linear predator functional responses when combining predator diet data with survey trawl data to estimate prey dynamics. Estimating and accounting for the predator functional response improves the biological realism of the processes that influence predator consumption since predators are unlikely to consume prey at rates that are linearly proportional to prey population size (Holling 1959; Koen-Alonso 2007). Furthermore, as shown in simulations, if predator diet data are assumed to be linearly proportional to prey population size, when predators consume prey following a non-linear functional response, estimates of prey dynamics can be biased. Aside from minor increases in bias, simulation results also indicate that precision is improved when predator diet data are used in concert with trawl data to inform changes in prey dynamics. The NLFPM was capable of substantially reducing this

bias and improving the precision, thus providing an improved index for the modeled prey species when including stomach contents data.

Another advantage of the NLFPM is that it can integrate multiple data sources to estimate prey dynamics. Integrating data sources into a combined index using a joint likelihood is preferred over comparing separate indices because it reduces the loss of information and better accounts for uncertainty than non-integrated analyses (Link 1999; Maunder and Punt 2013). To my knowledge, the model developed here is the first to integrate fisheries survey data with predator stomach contents data to estimate prey dynamics, therefore avoiding two-step procedures that have been used previously (e.g., Mills et al. 2007; Richardson et al. 2014). Additionally, by combining multiple sources of data with different sampling approaches, the NLFPM increases the sampling resolution in time and space. By increasing sample sizes with stomach contents data, my prey abundance index had improved mean-squared error and precision when compared to a model with only trawl data. However, including stomach contents data led to slightly more biased estimates when compared to a trawl data only model, likely in response to slight misspecifications in shape parameter estimates. Integrated models occasionally weight the influence of data on the joint likelihood to account for conflicting signals (Maunder and Piner 2017). I did not observe conflicting data signals in my case-study, but data-weighting may be a future research direction for improving the NLFPM, where data from individual stomachs could be weighted less than data from a trawl tow. Overall, combining data sources can result in estimates that are more representative of the true

dynamics than any index would have been on their own (Yule et al. 2007; Gibson-Reinemer et al. 2017).

The final major advantage of the NLFPM is that it is flexible enough to account for a variety of saturating and sigmoidal functional response shapes. Oftentimes, permitting shape flexibility requires models to estimate numerous shape parameters which can be challenging and uncertainty around those parameter estimates can result in cumulative errors that reduce model accuracy (Ludwig and Walters 1981, 1985; Fulton et al. 2003). Here, I reduced the number of estimated shape parameters in the functional response by modifying the general form (Eqn. 3.4), to express the consumption rate as a fraction of its maximum (Eqn. 3.5). By expressing the consumption rate in this way, my formulation consistently achieved convergence and yielded more accurate, less biased shape parameter estimates and functional response curves that were close to the simulated truth. As a result, my formulation should provide a relatively robust platform for estimating functional responses that will minimize problems with convergence and error aggregation. However, it is worth noting that model convergence and estimate accuracy will depend on the quality and quantity of data used when fitting the model (see Appendix B4). Furthermore, future simulation tests could explore how NLFPM abundance estimate bias varies with a wider variety of functional response curves than were explored here.

3.4.2 Model Assumptions and Future Directions

The NLFPM relies on several assumptions that may need to be addressed by future studies to permit more general applications. One of the main assumptions is that

presence/absence in trawl surveys can act as an unbiased indicator of prey abundance. Presence/absence of pelagic fishes in bottom trawl surveys can be a more appropriate measure of abundance than the number or weight of fish caught in that survey due to their behavior and size/body form (O'Driscoll et al. 2002). Furthermore, indices of abundance based on presence/absence from survey trawls have been used previously for several species (Overholtz and Friedland 2002) including northern sand lance (Frank et al. 2013). However, by assuming that there is a direct relationship between the probability of encountering prey in trawl and diet samples, I also assumed that prey distribution and predation are equal through space and time which may not be correct. Variability in prey distribution across space and time may be accounted for by using habitat covariates (e.g., bottom type, temperature) in a similar way to how covariates are added to delta models (Zuur et al. 2009) or by adding spatiotemporal error structures (Ng et al. 2021). Further, I assumed perfect detection of prey in predator stomachs which is likely incorrect and may have yielded underestimates of prey consumption by predators, however, further simulation testing would be required to identify the magnitude of these underestimates (Hyslop 1980). Incorporating covariates to account for variability in gut evacuation rates (e.g., predator body size) may also improve estimates of prey detection in stomach contents. As such, I advocate future research to examine the validity of extending the NLFPM to include covariates and spatiotemporal error.

The NLFPM is based on a prey-dependent, single prey species functional response formulation. The number of predators in a population can affect consumption rates (i.e., predator-dependent functional response) through interference or facilitation behaviors

(Yodzis 1994; Skalski and Gilliam 2001). These formulations tend to be acknowledged as more biologically realistic than the prey-dependent functional response formulation that I have used (DeLong and Vasseur 2011; Arditi and Ginzburg 2012). Additionally, I used a single species functional response formulation. Most marine predators are generalists that consume a variety of prey species and their consumption rates may be more realistically modeled using multi-species formulations that account for the behaviors associated with this type of predation (Yodzis 1994; Koen-Alonso 2007). One important consideration for generalist predators is that changes in their diet composition will match relative changes in the availability among prey rather than absolute changes, which may lead to observations of increases in a diet despite the abundance of that prey declining. However, estimating predator-dependent and multi-species functional responses requires additional data sources and the estimation of more parameters. The increased complexity of predator-dependent and multi-species formulations may be valuable, and even necessary in some systems, and are important future research directions for extending the NLFPM. Despite the advantages of more complex models, the current formulation of the NLFPM is an important step to account for a basic predation process that has yet to be accounted for, and the low data demand enables the NLFPM to be potentially widely applicable to data-limited situations.

3.4.3 Case-Study

The two predators examined in my case study were estimated to consume northern sand lance following a type III functional response. Type III functional responses are sigmoidal and have a variety of proposed mechanisms including predator learning to

capture prey as density increases and predators switching prey types in the presence of alternative prey species (Koen-Alonso 2007). However, the functional responses estimated here may not reflect the true functional responses of the predators at the behavioral scale due to this approach representing a population-level functional response. As a result, using these estimates to examine behavioral scale mechanisms should be approached with caution. Nonetheless, these estimates may provide information on the aggregate behaviors of predator fish populations. I estimated that Atlantic cod consumed more sand lance than American plaice and were more sensitive to changes in sand lance population size. It is possible that the importance of sand lance in these predator's diets may have implications for their population productivity as has been observed for Atlantic cod productivity on the Newfoundland shelf (NAFO div. 2J3KL) and its link with capelin (*Mallotus villosus*) availability (Buren et al. 2014).

The oscillatory pattern in sand lance abundance could be driven by both abiotic and biotic factors. For example, environmental indicators (e.g., sea surface temperature), chlorophyll, and zooplankton biomass have all had oscillatory dynamics in the last twenty years (Colbourne et al. 2018; NAFO 2019) which may have driven some of the variability in sand lance population dynamics. In fact, the oscillatory pattern observed here for sand lance loosely matches the patterns that have been estimated for 2J3KL capelin (Lewis et al. 2019), indicating that capelin and sand lance may be affected by similar environmental drivers. Additionally, dynamics of sand lance may further affect or be affected by species at upper trophic levels. For example, juvenile Atlantic cod natural mortality among several Newfoundland stocks (NAFO Divs. 2J3KL, 3NO, and 3Ps) have been estimated

to fluctuate over a similar period to what was observed for sand lance here (Zhang et al. 2020), suggesting that sand lance may affect predator population dynamics. Although examining the drivers and effects of variability in sand lance abundance is beyond the scope of this study, given their role as an intermediate trophic level species on the Grand Banks, such examinations are an important future research direction. Overall, our understanding of sand lance species throughout the Northwest Atlantic is limited despite their important functional role in food webs (Staudinger et al. 2020). My analysis of sand lance here may allow their inclusion in food web, ecosystem, or stock assessment models to better understand their population dynamics and role in the Grand Banks ecosystem.

Ecosystem based management requires understanding interactions among species in an ecosystem. To model species interactions, we need information on species dynamics which may not be available for all species in a community from abundance/biomass samples in bottom trawl surveys (Link 2004; Sydeman et al. 2017). Therefore, the index from the NLFPM may bolster our understanding of poorly sampled species dynamics and thus serve as a stepping stone towards including those species in ecosystem models. This approach may be particularly useful because predator diets are relatively easily measured, are responsive to changes in the environment, and can enhance the information that is collected during research surveys (Mills et al. 2007; Dwyer et al. 2010). Furthermore, past research has identified that directly including diet data in multispecies population dynamics models yields more accurate estimates of multispecies interactions (Trijoulet et al. 2019). Therefore, directly including the NLFPM in multispecies population dynamics models may present a promising approach for informing interactions while allowing the

propagation of uncertainty about these effects. Additionally, multi-species and ecosystem models rely on information about interactions between species, including the functional response, yet the parameterization of these models is often uninformed due to a lack of empirical research (Hunsicker et al. 2011). The NLFPM may be able to help inform the parameterization of the functional response in such models and potentially improve the accuracy of model estimates.

3.5 List of Tables

Table 3.1 Functional response shape parameter estimates and associated 95% confidence intervals.

Species	Parameter	Estimate	95% C.I.
American plaice	χ	0.78	[0.66, 0.90]
	β	2.98	[2.17, 3.79]
Atlantic cod	χ	0.62	[0.57, 0.68]
	β	5.50	[4.06, 6.94]
American plaice & Atlantic cod	χ_{plaice}	0.97	[0.77, 1.16]
	β_{plaice}	2.20	[1.61, 2.79]
	χ_{cod}	0.67	[0.60, 0.73]
	β_{cod}	4.62	[3.44, 5.80]

Table 3.2 Model outputs for all three models run. Δ represents difference and NLL represents the negative log-likelihood (NLL) from the NLFPM.

Species	LFPM AIC	NLFPM AIC	Δ AIC	NLL
American plaice	30507	28440	2068	14217
Atlantic cod	20289	18339	1950	9166
American plaice & Atlantic cod	40853	38374	2479	19183

3.6 List of Figures

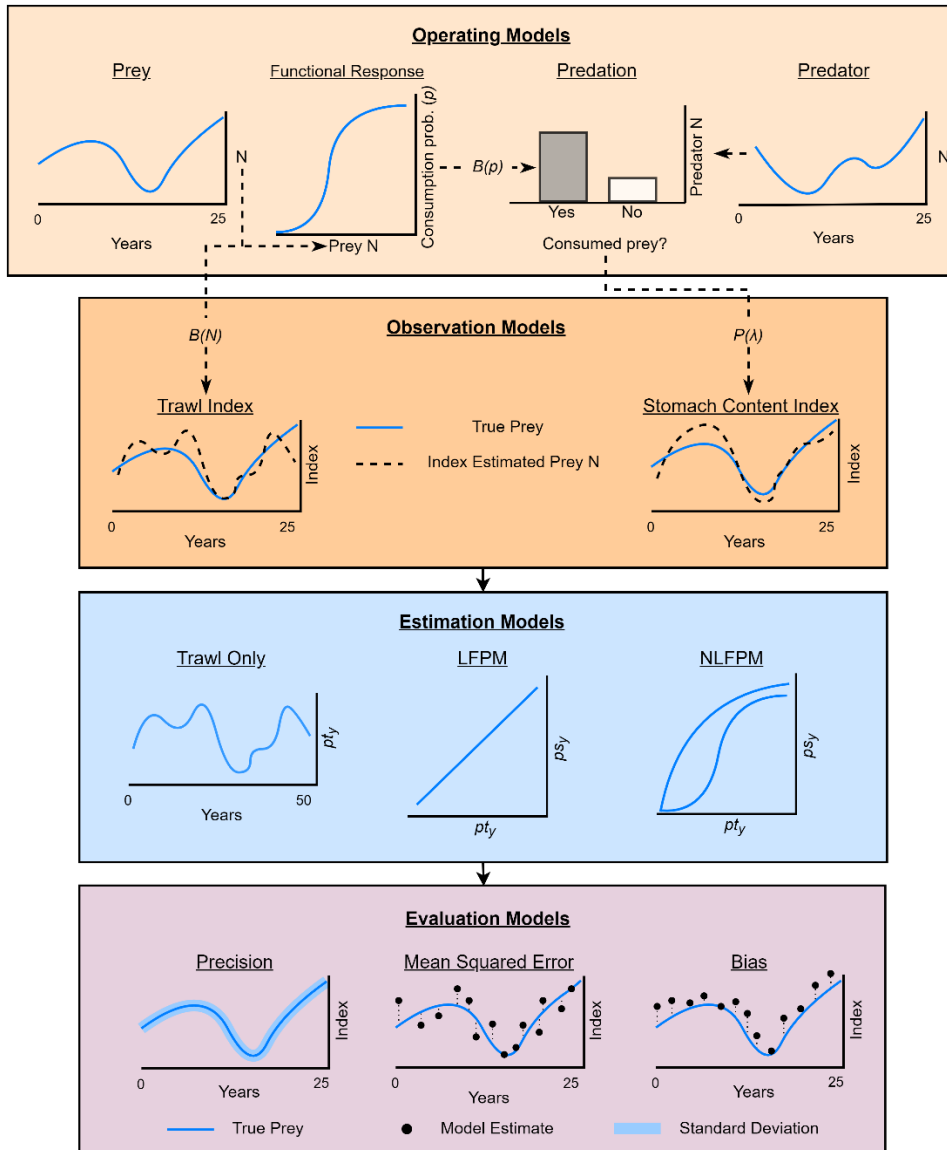


Figure 3.1 Overview diagram for the simulation. The Operating Models panel portrays prey and predator abundance over time (Eqn. 3.7-3.8), the functional response (Eqn. 3.4), and the number of predators that have consumed prey (Eqn. 3.10). The Observation Models panel portrays comparisons between the true dynamics and a trawl index estimated based on the random draws from a binomial distribution and a stomach contents index estimated from a Poisson distribution. The Estimation Models panel portrays functional response curves from the LFPM and NLFPM as well as an estimate of prey dynamics from a model with only trawl data. The Evaluation Models panel portrays the calculations of precision, mean squared error, and bias between the Estimation Models and the true prey dynamics.

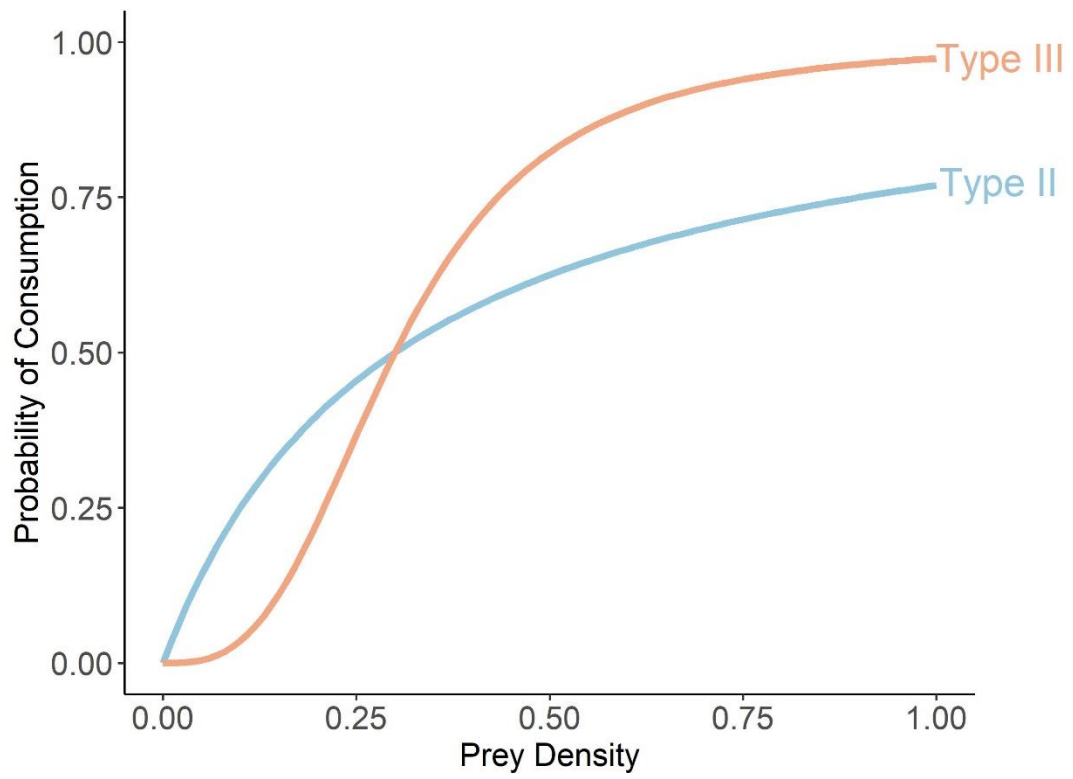


Figure 3.2 The different functional response shapes used in the simulation.

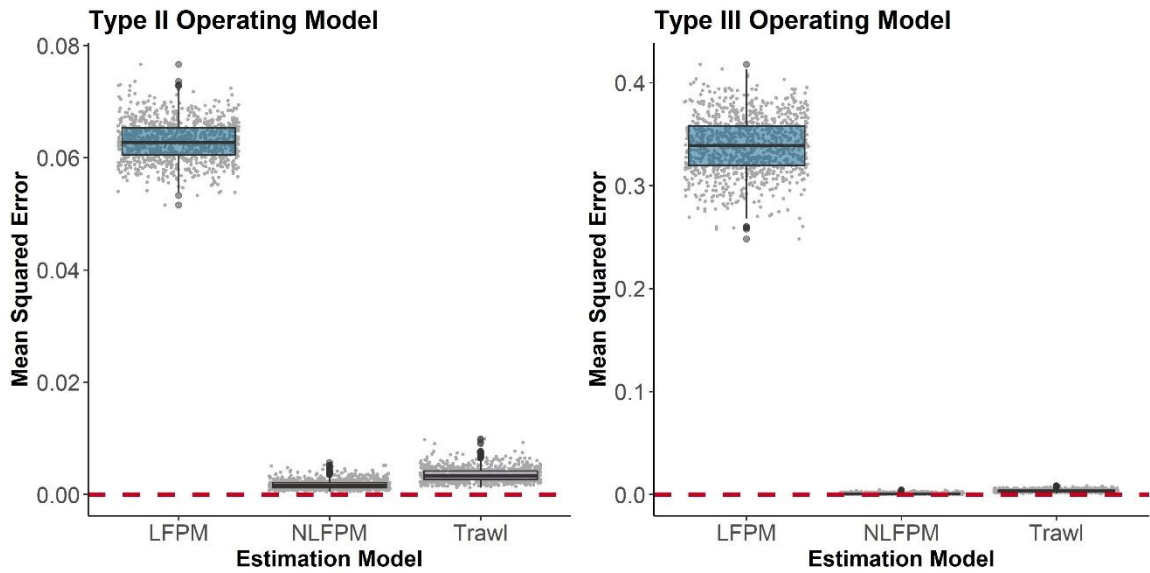


Figure 3.3 MSE between estimated relative index of prey abundance and the scaled true prey abundance from all simulations. Grey points represent the MSE from each simulation and the dashed red line represents zero. The grey points were jittered on the x-axis to improve visualization. The boxplots were created using the default settings in the ggplot2 package in R (Wickham 2009), where the boxes represent the 25th – 75th percentiles, the horizontal line represents the median, the vertical lines represent 1.5 * the interquartile range, and black points represent any data outside 1.5 * the interquartile range.

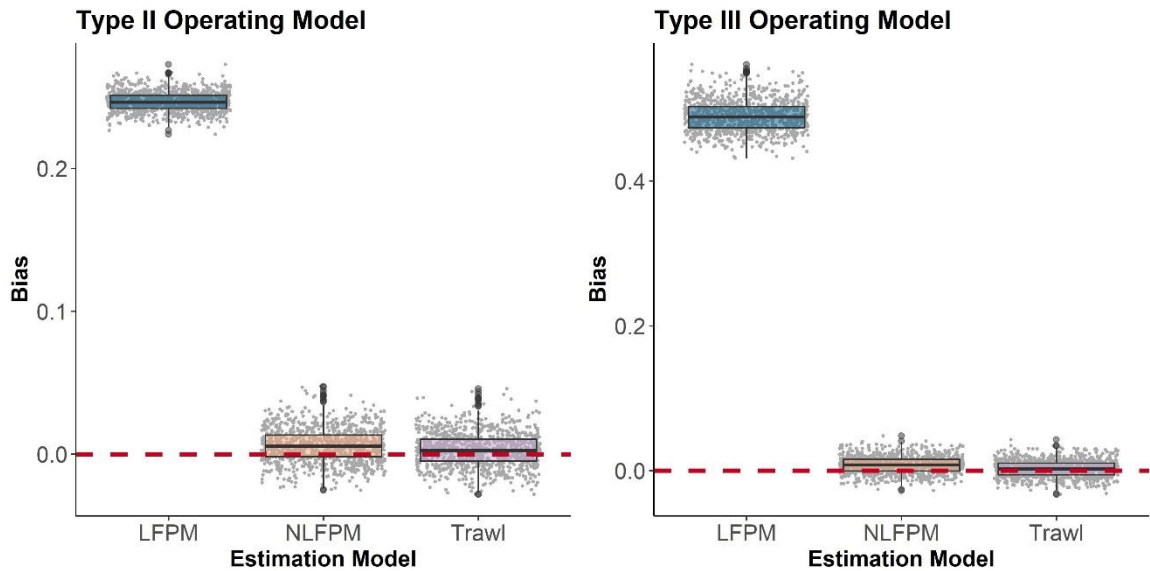


Figure 3.4 Bias between estimated relative index of prey abundance and the scaled true prey abundance from all simulations.

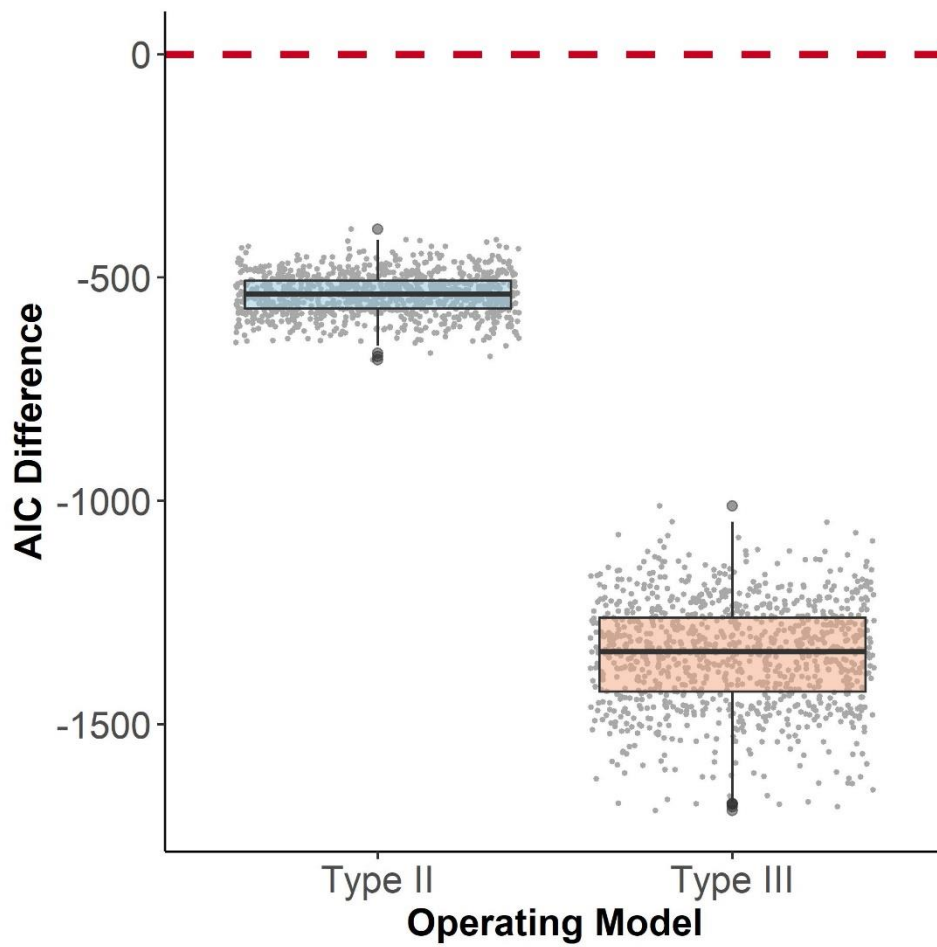


Figure 3.5 Difference in AIC between the NLFPM and LFPM for both operating models. Negative values indicate that the LFPM had a larger AIC than the NLFPM.

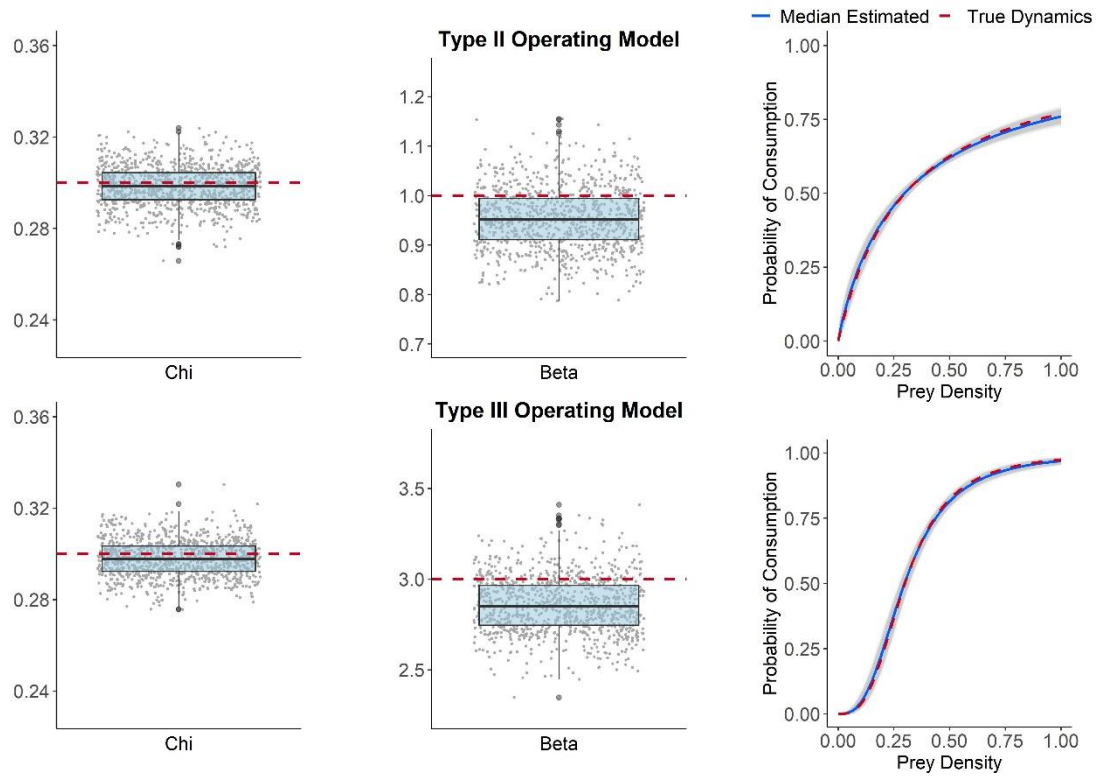


Figure 3.6 Estimates for the shape parameter values in the functional response from the simulation. The dashed red line indicates the true parameter value for each shape. The panels on the far right represent the true shape of the functional response (red lines), the shapes given by all estimated shape parameter values (grey lines), and the median shape parameter values (dark blue lines).

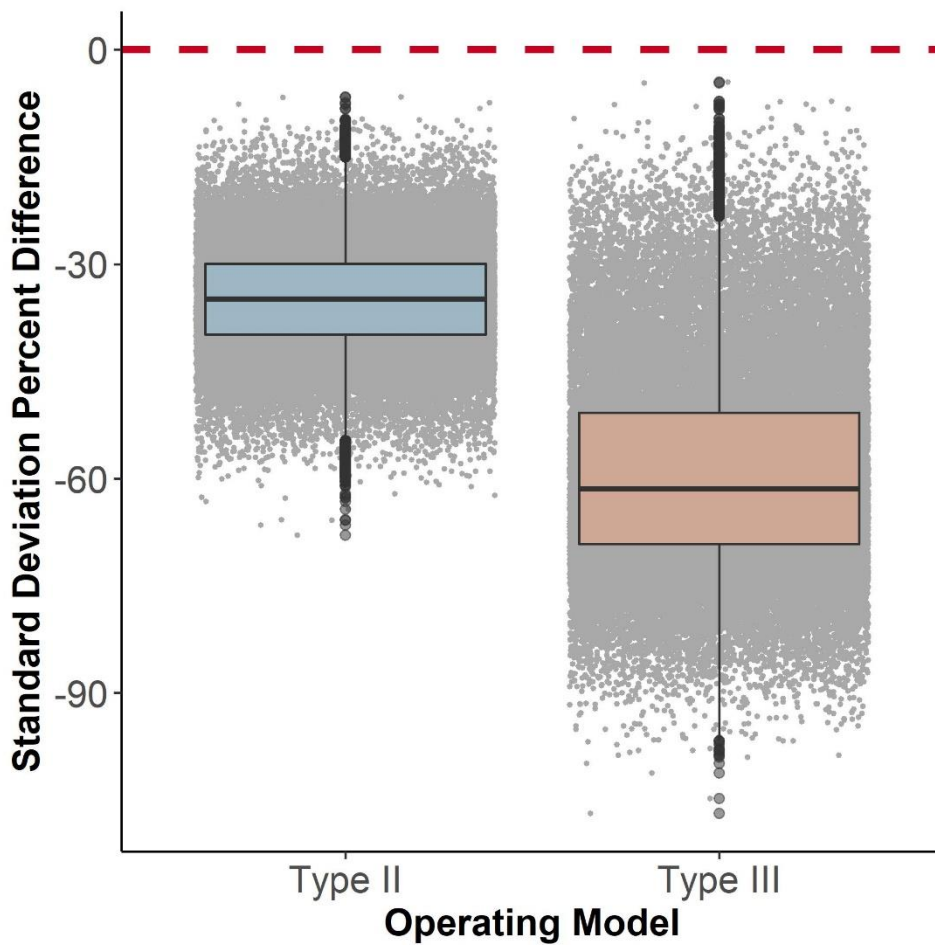


Figure 3.7 Percent difference in annual standard deviation estimates for the prey abundance index between the NLFPM and a model with no stomach contents data for both operating models. Percent difference was based on the mean of the standard deviation estimates from the model with no stomach contents data. Negative values indicate a smaller standard deviation for a particular year in the NLFPM.

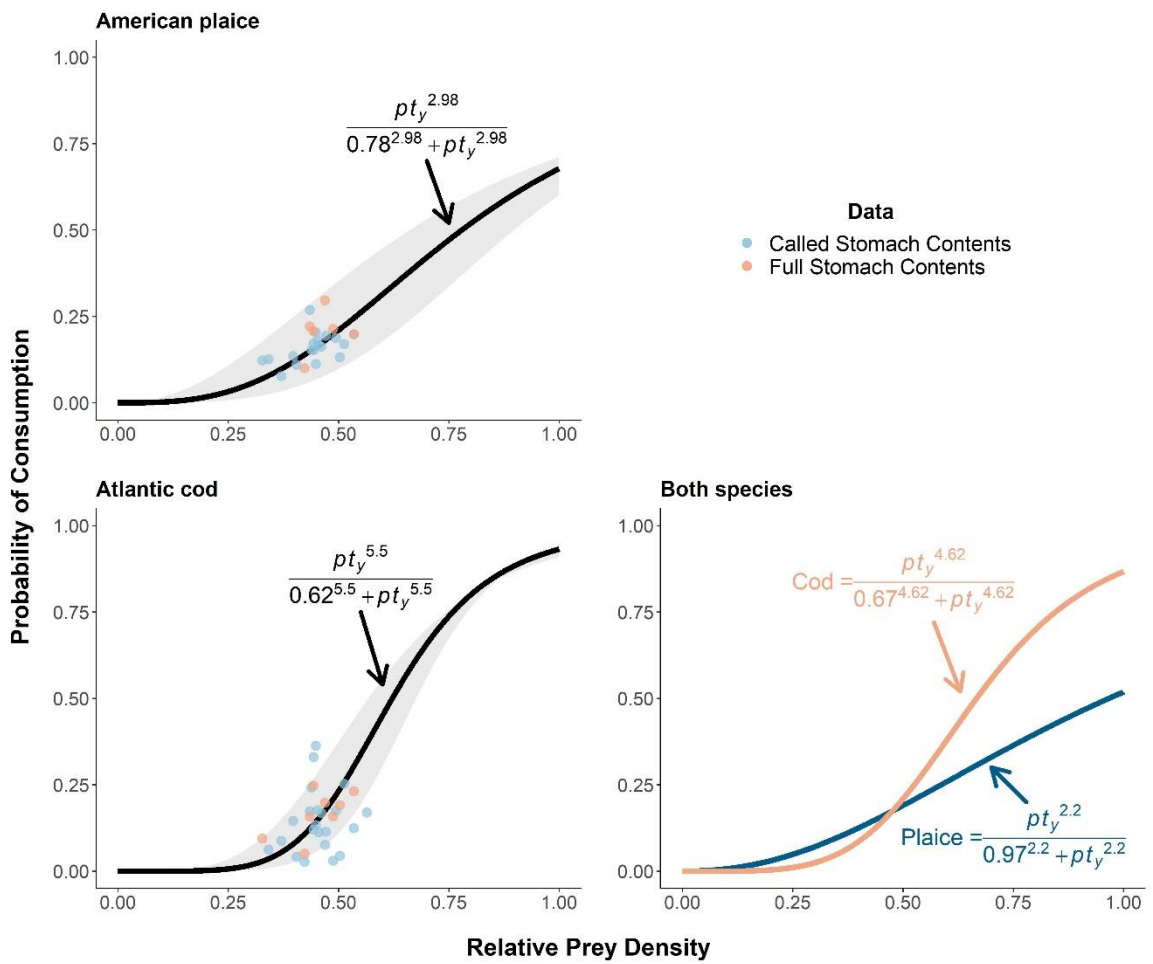


Figure 3.8 Estimated functional responses (lines) and 95% confidence interval (shaded grey polygon) for both predator species when modeled separately and together.

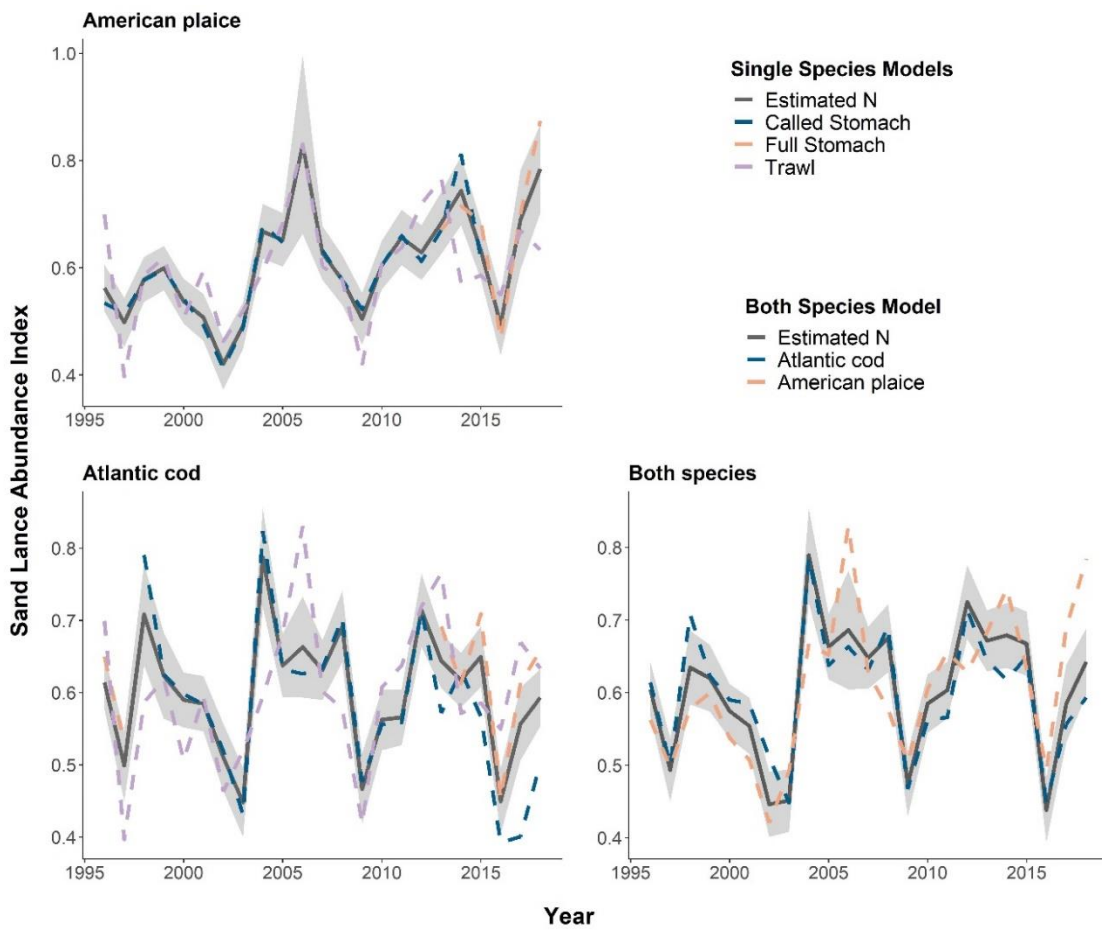


Figure 3.9 Estimated sand lance relative abundance index and 95% confidence interval (shaded grey polygon) from models that used each predator's data separately and one that modeled American plaice and Atlantic cod data together.

4 Limited temporal variability in natural mortality for juvenile American plaice on the Newfoundland Grand Banks

Authors: Robertson, M.D.^{1*}, Regular, P.M.², & Cadigan, N.¹

Author Affiliations

1. Centre for Fisheries Ecosystems Research, Fisheries and Marine Institute of Memorial University of Newfoundland, P.O. Box 4920, St. John's, NL, A1C 5R3, Canada.
2. Fisheries and Oceans Canada, Northwest Atlantic Fisheries Centre, P.O. Box 5667, 80 East White Hills Rd., St. John's, NL, A1C 5X1, Canada.

A version of this chapter was published in the Journal of Northwest Atlantic Fishery Science:

Robertson, M.D., Regular, P.M., & Cadigan, N. (2022). Limited temporal variability in natural mortality for juvenile American plaice on the Grand Bank of Newfoundland, 53, 47-56 <https://doi.org/10.2960/J.v53.m738>

Abstract

Increases in natural mortality have been suggested as a potential driver for both the collapse and lack of recovery for the American plaice (*Hippoglossoides platessoides*) population on the Newfoundland Grand Banks in NAFO Divisions 3LNO. However, natural mortality is among the most difficult parameters to estimate since it can be confounded with other parameters and model misspecifications. One method used to avoid this confounding involves modeling unfished components of a population where total mortality and natural mortality are equal. Here, I used a state-space metapopulation dynamics model to investigate whether there is evidence that natural mortality rates for unfished juvenile American plaice have varied since the population collapse. In addition, this model examined the degree of synchrony in age-1 recruitment signals between each management Division. The best fitting model included temporal variability in natural mortality rates, but estimates did not frequently differ from zero. This indicates that change in natural mortality rates is not an important driver of current juvenile 3LNO American plaice stock dynamics. Instead, this model identified that juvenile stock dynamics were mainly affected by variations in age-1 recruitment. Furthermore, a correlation analysis of the temporal variations in recruitment showed that trends were somewhat dissimilar between NAFO Divisions 3L and 3NO. Overall, although increases in M have been suggested by recent studies, I did not find strong evidence for this in juvenile American plaice.

4.1 Introduction

Increases in natural mortality rates (M 's) have been suggested as a potential driver for both the collapse and lack of recovery for the American plaice (*Hippoglossoides platessoides*) population on the Newfoundland Grand Banks in NAFO Divisions 3LNO (Morgan and Brodie 2001; COSEWIC 2009; Morgan et al. 2011; Perreault et al. 2020). In fact, in the most recent run of the ADAPT model for this stock (Wheeland et al. 2021) and in previously accepted models (e.g., Wheeland et al. 2018), the assumed M was increased from 0.2 to 0.53 for all ages from 1989 to 1996. In the late 1980s – early 1990s 3LNO American plaice collapsed, and despite a moratorium on directed commercial fishing since 1994, the population has yet to recover (Figure 4.1; Wheeland et al. 2021). Despite an expectation that the collapse and lack of recovery were mainly driven by overfishing (directed fishing for the collapse, and bycatch for the lack of recovery), population dynamics models have indicated that known catches are unlikely to account for observed increases in total mortality rates (Z) both during and after the collapse (Morgan and Brodie 2001; Perreault et al. 2020). Such increases in Z have consequently been, at least partially, attributed to shifts in M . These shifts are hypothesized to be linked to particularly low bottom-water temperatures that covered the Grand Banks during this time-period (Morgan 1992; Walsh et al. 2004; Robertson et al. 2021); however, direct estimation of the temporal variability in M and its drivers has yet to occur.

Although M is often considered to be one of the most important parameters in a fish stock assessment model, it is also among the most difficult parameters to estimate using commonly available data (Punt et al. 2021). It can be confounded with survey gear

selectivity and fishing mortality rates (Pope et al. 2021). Even when M can be estimated numerically, it may be confounded or aliased with other model misspecifications and M estimates may then be unreliable. There are two main methods capable of avoiding the confounding issue. The first is integration of additional data that can inform M estimates. This usually involves tagging data (e.g., Pine, Pollock, Hightower, Kwak, & Rice 2003; Cadigan, 2015), but there are recent examples that used fish condition indices (e.g., Regular et al. 2022). Another approach involves examinations of unfished components of a population (Myers and Cadigan 1993a, 1993b; Gudmundsson 2004; Zhang et al. 2020). Although 3LNO American plaice lack a time-series of mark-recapture data (but see Morgan (1996) for a tagging experiment), this stock benefits from having research surveys that catch a wide range of ages, including juvenile age-classes (ages 1-5) that are too small to be captured by the fishery. Survey indices of these age-classes provide a means to examine trends in M for the juvenile component of this population since their Z and M should be equal.

Here I used a state-space metapopulation dynamics model to investigate whether there is evidence that American plaice juvenile M has varied since the population collapse. This model is applied to juvenile (ages 1-5) abundance indices on the Newfoundland Grand Banks since 1995. American plaice have spatiotemporally varying, sexually dimorphic growth with juveniles growing from approximately 5 to 20 cm, female maturation occurring around age eight, and male maturation occurring around age four in recent years in NAFO divisions 3LNO (Zheng et al. 2020a, 2020b). A previous use of this model assessed juvenile cod M around Newfoundland and Labrador, where

both cohort strength and M were found to vary across space and time (Zhang et al. 2020). Here, I limited my analysis to one stock on the Grand Banks, but allowed for separate estimates in each management division due to previous findings of divisional-level recruitment asynchrony (Kumar et al. 2019).

4.2 Materials and Methods

4.2.1 Metapopulation dynamics process model

The model used here was developed by Zhang et al. (2020) and a more detailed description can be found there. Briefly, this model framework uses age-based survey indices of unfished juvenile fish abundance to estimate changes in juvenile M and cohort strength within metapopulation units. The model is based on the common cohort population model, $N_{a,y} = N_{a-1,y-1} \exp(-M_{a-1,y-1})$, where $N_{a,y}$ represents stock abundance at age a in year y and $M_{a,y}$ is the natural mortality rate. I assume that $M_{a,y}$ can be modelled in terms of age- and year-effects, $M_{a,y} = M_a + \delta_y$, where M_a ($a = 0, \dots, A$) is the overall level of juvenile mortality at age a and δ_y ($y = 0, \dots, Y$) is the annual deviation $M_{a,y} - M_a$ that I assume is common for all juvenile ages. If $c = y - a$ indicates the cohort and $n_{a,y} = \log(N_{a,y})$, then I can show through recursive applications of the basic cohort model that

$$n_{a,c} = n_{0,c} - \sum_{i=0}^{a-1} (M_i + \delta_{c+i}), \quad a > 0. \quad (4.1)$$

Where δ_y for $y = 1, \dots, Y$ is modeled using a stationary Gaussian autoregressive process with a correlation parameter φ_δ and stationary variance $\sigma_\delta^2 / (1 - \varphi_\delta^2)$:

$$\delta_0 \sim N\left(0, \frac{\sigma_\delta^2}{1 - \varphi_\delta^2}\right), \quad \delta_y | \delta_{y-1} \sim N(\varphi_\delta \delta_{y-1}, \sigma_\delta^2), \quad y = 1, \dots, Y. \quad (4.2)$$

Note that $\delta_y|\delta_{y-1}$ denotes the distribution of δ_y conditional on the value δ_{y-1} , and $\sigma_\delta^2 = \text{Var}(\delta_y|\delta_{y-1}) \leq \text{Var}(\delta_y)$.

In addition, I model the time-series of the initial cohort abundance ($n_{0,c}$; i.e., recruits) using an intercept plus a Gaussian autoregressive cohort effect (γ_c),

$$n_{0,c} = n_0 + \gamma_c, \quad (4.3)$$

where

$$\gamma_0 \sim N\left(0, \frac{\sigma_\gamma^2}{1-\phi_\gamma^2}\right), \quad \gamma_c|\gamma_{c-1} \sim N(\phi_\gamma\gamma_{c-1}, \sigma_\gamma^2), \quad c = 1, \dots, C \quad (4.4)$$

4.2.2 Observation model

My model is based on bottom trawl research survey indices ($I_{s,a,y}$), where s denotes the survey, a denotes the age, and y denotes the year. Each age-class in the surveys is expected to have unique catchability ($Q_{s,a}$) which is based on gear selectivity and availability of fish at different ages (and sizes) to the survey. My basic observation model is

$$I_{s,a,y} \approx Q_{s,a} N_{s,a,y} \exp\{-f_s(M_{s,a} + \delta_{s,y})\}, \quad (4.5)$$

where f_s is the fraction of the year that survey s occurs and the $\exp\{-f_s(M_{s,a} + \delta_{s,y})\}$ term simply projects beginning of year abundance ($N_{s,a,y}$) to the survivors at the time of the survey. I collect all of the M deviations and cohort abundance random effects into the set $\Psi = \{\delta_y, \gamma_c; y = 1, \dots, Y, c = 1, \dots, C\}$. Let $q_{s,a} = \log(Q_{s,a})$ and define $\mu_{s,a,y} =$

$E\{\log(I_{s,a,y})|\Psi\}$ to be the statistical expected value of $\log(I_{s,a,y})$ given all the random effects. The expectations are

$$\mu_{s,a=0,y=c} = q_{s,0}^* + n_{s,0,c} - f_s \delta_{s,c}, \quad (4.6)$$

and

$$\mu_{s,a,y=c+a} = q_{s,a}^* + n_{s,0,c} - \sum_{i=0}^{a-1} (\delta_{s,c+i} - f_s \delta_{s,c+a}), \quad a > 0, \quad (4.7)$$

where $q_{s,0}^* = q_{s,0} - f_s M_{s,0}$ and $q_{s,a}^* = q_{s,a} - \sum_{i=0}^{a-1} M_{s,i} - f_s M_{s,a}$. As described in Zhang et al. (2020), the $q_{s,a}$ and $M_{s,a}$ values are completely confounded, therefore I cannot directly estimate $M_{s,a}$ without additional information on $q_{s,a}$. As a result, I estimate their combined effect, $q_{s,a}^*$.

The survey index observation equation is

$$\log(I_{s,a,y}) = \mu_{s,a,y} + \tau_{s,y} + \varepsilon_{s,a,y}, \quad (4.8)$$

where $\tau_{s,y}$ and $\varepsilon_{s,a,c}$ are normally distributed [i.e., $\tau_{s,y} \stackrel{iid}{\sim} N(0, \sigma_{s,\tau}^2)$] survey measurement errors. The random year-effects ($\tau_{s,y}$) allow for measurement errors to be correlated across ages within surveys and years, which is common for survey indices of juvenile ages. However, these errors are independent for different years and surveys. Due to this structure, these year-effects will only affect estimates in a particular year, rather than having a cumulative effect on cohort dynamics like the temporal deviations in M.

Furthermore, $q_{s,a=5}^*$ is constrained to be zero for each survey to eliminate the confounding between the values of $q_{s,a}^*$ and $n_{s,0,c}$ in Equation (4.7). Finally, I estimate between-survey

and unstructured correlations in both $M_{s,a,y}$ and $n_{s,0,c}$, which is described in Zhang et al. (2020). These correlations represent the metapopulation aspect of the model, where population processes may be similar among NAFO divisions. These correlations were examined with a hierarchical cluster analysis using the `hclust` function in R on the Pearson dissimilarity between surveys.

4.2.3 Data

I used six relative abundance indices of juvenile (ages 1 – 5; aged from otoliths) American plaice from stratified random research bottom-trawl surveys in NAFO Divisions 3LNO. These surveys were conducted in the spring (~April – June) and fall (~October – November) and were separated based on NAFO Divisions (i.e. spring 3L, spring 3N, spring, 3O, fall 3L, fall 3N, and fall 3O). I limited the time-series for my analysis to spring surveys conducted after 1996 and fall surveys after 1995 due to low catchability of age 1 American plaice with the bottom trawl gear used in prior years (Morgan et al. 1998). Surveys were not completed in some years and any indices with zero or very small values (i.e., $<e^{-5}$) were not used (see Appendix C Figure C1).

4.2.4 Model fitting

I examined thirteen parameterizations of the model, with varying numbers of random effects ($\gamma_c, \tau_{s,y}, \delta_c$) to determine which components were necessary to account for the variability in the sampled survey indices (Table 4.1). In addition to sequentially adding components, I tested various correlation structures to identify if cohort effects or M deviations varied across space and season. Model selection was completed using a combination of Akaike's information criterion (AIC), Bayesian information criterion

(BIC), and examinations of residuals. BIC measures goodness-of-fit, while AIC is a measure of prediction accuracy (Sober 2002). I used the Template Model Builder (TMB, Kristensen et al. 2016) package in R (R Core Team 2018) to evaluate the negative logarithms of the marginal likelihoods (nll) of these models and the data, and to evaluate the nll gradients to improve estimation. Further, I used the R function nlminb() to find the maximum likelihood estimates. Model convergence was evaluated by ensuring that the nll gradient for all parameters was $<10^{-4}$ and that the Hessian matrix was positive definite at the maximum-likelihood estimates.

4.3 Results

My model comparisons indicated that the model with the best fit was model M5 which had cohort and year-effects, as well as M deviations that were shared across Divisions (Table 4.1). Model M5 fit the data well, with no observable trends in residual plots (see Appendix C Figures C6-C16). This model was an improvement over the simpler model M4, and had no survey year-effects in standardized residuals (Appendix C Figures C2 & C3). M4 had clear residual year-effects (Appendix C Figure C2) that were substantially reduced in M5, although a similar trend of small magnitude remained (Appendix C Figure C3). M5 included spatial and temporal variability in cohort effects (Figure 4.2). Despite 3LNO being managed as a single stock, the model selection process showed substantial improvements in estimates when cohort effects were allowed to vary by Division and season (Table 4.1). The temporal trends indicated that in NAFO Division 3L, cohort effects decreased until 1996, increased after this until 2012, and have since declined somewhat steadily. Meanwhile, there was much less of a trend in NAFO

Divisions 3NO, where cohort effects generally oscillated around a mean with a period of around 5-6 years. The similarity in cohort effect trends between 3N and 3O was identified in the spatial cohort effect correlation matrix (Figure 4.3) where 3N and 3O surveys always had a high correlation with each other (>0.9). Meanwhile, the correlations between cohort strength derived from 3L surveys and those in 3N and 3O were often lower (≤ 0.5). This was further illustrated using a cluster analysis that identified that the cohort effects for 3NO were dissimilar from the cohort effects for 3L (Figure 4.4).

Model M5 indicated that accounting for M deviations was necessary to produce the best fits to the survey indices. M5 had the simplest formulation of M deviations, where they were assumed to be equal across NAFO Divisions 3LNO (Table 4.1). Therefore, unlike cohort effects, my results indicate that M deviations may not vary by Division or season and may be driven by a larger scale process. Finally, despite improving model fit, the estimates of M deviations only differed significantly from zero in four years: 1999, 2005, 2015, and 2016 (Figure 4.5). At the extreme, the estimates suggest M's in 2015-16 were slightly more than double those in 1999-2000. Estimated changes in M were much smaller in other years.

4.4 Discussion

I applied a state-space metapopulation dynamics model to identify whether American plaice juvenile natural mortality rates (M's) have affected stock dynamics since the population collapse. Model comparison identified that estimating temporal variability in M improved the model fit to juvenile 3LNO American plaice survey indices which indicates that temporal variability in M may influence the dynamics of the unfished

portion of the stock. The best fitting model included spatial cohort and survey year-effects, along with non-spatial M deviations. Although this best fitting model included temporal M deviations, estimates were rarely significantly different from zero. The limited variation in these M deviations in comparison to the larger magnitude variations in age-1 recruitment indicated that juvenile stock dynamics were mainly affected by recruitment. Furthermore, temporal variations in cohort effects were more dissimilar between NAFO Divisions 3L and 3NO, implying that drivers of age-1 recruitment may differ between these regions.

Recent analyses have indicated that current assumptions about M in 3LNO American plaice stock assessments underestimate its impact on the slow recovery for this stock (Perreault et al. 2020; Wheeland 2021). Here, I observed that estimating temporal variability in juvenile M improved estimates of juvenile stock dynamics. However, annual M deviations were rarely significantly different from zero, indicating that the variation is less important compared to spatial and temporal variations in cohort strength. This finding matches results from a previous cohort model used for this stock that assessed the potential for changes in M graphically rather than modelling it as I have done here (Kumar et al. 2019). Furthermore, this finding matches broader findings that demersal fish juvenile natural mortality tends to show limited temporal variability (Myers and Cadigan 1993a; Gudmundsson 2004). The limited variability in juvenile M may affect our ability to understand the drivers of current stock assessment problems for this stock. For example, my findings differ from a recent exploration of M deviations where there was an indication that accounting for temporal change in M at young ages would

help reduce retrospective patterns (Perreault et al. 2020). This difference in magnitude of influence of natural mortality may have been generated by M deviations at young ages producing better fits by reducing recruitment variance since the Perreault et al. (2020) model formulation did not include an M deviation variance penalty like the model employed here. Therefore, future examinations of state-space catch-at-age models for this stock may seek to estimate M deviations for young ages using the approach demonstrated here to identify if the limited variability in M is still capable of reducing retrospective patterns. Overall, although increases in M have been suggested by recent studies, I did not find strong evidence for this in juvenile fish.

I did not find evidence of large changes in juvenile M since the fishing moratorium in 1995 but this does not mean that high juvenile M is not a factor in the delayed recovery of the stock. It is possible that recent M's are much higher than those prior to 1995. However, my model and the available survey data only allow the estimation of M deviations which cannot inform the magnitude of M to provide any direct indication of whether current M is high relative to expected levels of juvenile M. As a result, investigating how juvenile M has varied pre- and post-collapse would require a longer historical time series. Since Fall survey indices are only available since 1990, they cannot provide much information about pre-collapse M. Spring survey indices go back to 1985, but the survey trawl used in the Spring during 1985-1995 had a larger mesh size than the current trawl and indices for age 1-2 seem less reliable. They include many zeroes that I cannot use in the current model formulation. Although Spring indices at ages 3-5 are more reliable, it would be difficult to differentiate between a change in M and

year-effects with survey indices for only three ages. Hence, extending my model back to the mid-1980's does not seem useful. This juvenile metapopulation dynamics model is only practically useful with indices produced by surveys that are effective at monitoring juveniles, such as the current DFO bottom trawl surveys that use the Campelen trawl.

Unlike the cohort effect, there was little evidence of differences in juvenile M across NAFO Divisions, indicating that the main driver(s) of mortality is likely a large scale process. Large-scale processes affecting juvenile M could include bottom-up processes like bottom-water temperature or prey availability, or top-down processes like predation. Regardless of the particular driver, it is interesting that the spatiotemporal structure of M and age-1 recruitment (e.g., cohort effects) differed. Although differences in the spatial scales affecting different aspects of population dynamics are likely inherent in many populations (i.e., Levin 1992) recognizing these differences can produce an improved mechanistic understanding of the observed patterns.

The cohort strength effects for juvenile 3LNO American plaice are much larger than the effects of time-varying M . This finding is not particularly novel since understanding recruitment dynamics has been at the core of fisheries science for over a century due to its large influence on population dynamics (e.g., Houde 2008). However, in a recent analysis of juvenile Atlantic cod dynamics around Newfoundland and Labrador, oscillations with a similar period to those estimated here were identified in both M deviations and cohort effects (Zhang et al. 2020). Furthermore, these oscillations are similar to estimates of weight-at-length (an indicator of condition and potentially starvation induced mortality) for 3Ps Atlantic cod (Cadigan et al. 2022). The 3Ps Atlantic

cod model estimates were compared to regional drivers and significant correlations were identified for oceanographic (e.g., bottom water temperature), basal food web (e.g., zooplankton), and direct prey abundance (3LNO northern sand lance (*Ammodytes dubius*)). Therefore, it is possible that Atlantic cod and American plaice recruitment and/or M are affected by similar environmental and/or trophic mechanisms.

In addition to the influence of age-1 recruitment, I also observed a substantial influence of survey year-effects on model estimates. Survey year-effects are used to account for correlated observation error among ages in a particular survey that can occur for a variety of unknown reasons (Myers and Cadigan 1995). For example, catchability may vary annually depending on environmental conditions, there may be anomalous sets accounting for a majority of catch, or there could be differences in how survey crew handles the fishing gear. Additionally, the survey year-effects may be necessary to account for stock distributional shifts (Swain and Sinclair 1994; Swain and Benoit 2003). Accounting for these year-effects is important when modelling juvenile dynamics based on survey indices; however, their source(s) remains speculative.

There is substantial evidence that M varies with body size and age, often by orders of magnitude over the life cycle (Lorenzen et al. 2022). Although the metapopulation dynamics model was based on separate age-dependent M 's for each metapopulation, I assumed that annual deviations in M were the same for all ages even though the absolute value of M could differ substantially among ages. Yet, this simplifying assumption may be unrealistic. For example, if M at age 1 is 2.0 and M at age 5 is 0.3 then it is possible that annual M deviations at age 2 are larger than at age 5. However, additive M deviations

have a multiplicative effect on cohort survival; that is, if $M_{a,y} = M_a + \delta_y$ then $N_{a+1,y+1} = N_{a-1,y-1} \exp(-M_a) \exp(-\delta_{y-1})$. If annual M deviations are multiplicative in nature then a more realistic M model would be $M_{a,y} = M_a \exp(\delta_y)$ or $\log(M_{a,y}) = \log(M_a) + \delta_y$ (Cadigan 2015; Stock and Miller 2021). Using the approximation $\exp(\delta_y) \approx 1 + \delta_y$, then $M_{a,y} = M_a \exp(\delta_y) \approx M_a + M_a \delta_y$. Note that if δ_y is normally distributed with mean zero and stationary variance $\sigma_\delta^2 / (1 - \varphi_\delta^2)$ then $M_a \delta_y$ is also normally distributed with mean zero but with stationary variance $M_a^2 \sigma_\delta^2 / (1 - \varphi_\delta^2)$. As a result, the necessity for using multiplicative rather than additive M deviations for a population where M_a decreases with age could be explored by examining whether there is higher residual variation at younger ages in an additive M deviation model. This is exactly the pattern I found (see Appendix C Figure C4). However, it is also possible that the $\varepsilon_{s,a,c}$ survey measurement error variances (see Equation 4.8) are higher at younger ages, which is another possible model misspecification. The within-survey variance of the indices may indicate if the patterns in Appendix C Figure C4 are consistent with sampling variability or not, but these sampling variances were not available to us. Therefore, given the current data, these effects are confounded and I cannot identify whether the observed residual variance pattern is the result of process or observation error. Finally, implementing a model with multiplicative M deviations would also require that I specify the age pattern in M's. However, I am unsure why the residual variation in Appendix C Figure C4 usually increases at age 5 but sometimes at age 4. These are areas that require further research.

I identified that the recruitment trends appear to differ between NAFO Divisions 3L and 3NO despite these management Divisions comprising the same stock. Similar results were found in a different cohort model used for American plaice stocks throughout all of Newfoundland and Labrador (NAFO Divisions 2J3KLNOPs; Kumar et al. 2019). The spatial extent of management on the Grand Banks varies by species. Yellowtail flounder and American plaice are the only two species whose management occurs across NAFO Divisions 3LNO, whereas other species are managed separately between 3L and 3NO (e.g., 2J3KL vs. 3NO Atlantic cod). Previous studies have argued that American plaice in NAFO Division 3L differ from those in 3NO (see review by Brodie 2002). These arguments have stemmed from various lines of evidence including differences in growth and maturity (Zheng et al. 2020b), in divisional research surveys indicating different trends in abundance, and as a result of the general sedentary nature of American plaice in this region (Pitt 1969; Morgan 1996). Since incorrect delineation of stock spatial structure can affect estimates of productivity and in turn affect management decision-making (e.g., Kerr et al. 2017), further work on addressing this question for 3LNO American plaice is warranted.

4.5 List of Tables

Table 4.1 Model names, descriptions and comparisons using AIC and BIC. + represents effects that were included, while a blank space indicates that the effect was not included. n_0 represents cohort effects, τ represents survey year effects, and δ_c represents M deviations. The subscript d indicates that the effect was only allowed to vary by Division rather than by survey (i.e., season and Division), the subscript s represents when an effect varied by survey, and the subscript c represented when an effect varied by cohort. k is the number of parameters, nll is the negative log-likelihood and the Δ columns represent the difference in the number of criterion points from the model with the lowest respective criterion points. The bolded row (M5) indicates the model that I determined to have the best fit.

Model	$n_{0,c}$	$n_{s,0,c}$	$\tau_{s,y}$	δ_c	$\delta_{d,c}$	$\delta_{d,c}$ Corr.	$\delta_{s,c}$	$\delta_{s,c}$ Corr.	k	nll	AIC	Δ AIC	BIC	Δ BIC
M1	+								53	834	1773	272	2011	232
M2		+							58	763	1642	141	1902	123
M3		+	+						60	706	1532	31	1801	22
M4		+		+					60	709	1538	37	1807	28
M5		+	+	+					62	689	1501	0	1779	0
M6		+			+				62	714	1551	50	1829	50
M7		+	+		+				64	696	1520	19	1807	28
M8		+			+	+			65	702	1533	32	1825	46
M9		+	+		+	+			67	687	1508	7	1809	30
M10		+					+		65	737	1604	103	1895	116
M11		+	+				+		67	702	1537	36	1838	59
M12		+					+	+	80	692	1544	43	1902	123
M13		+	+				+	+	82	683	1529	28	1897	118

4.6 List of Figures

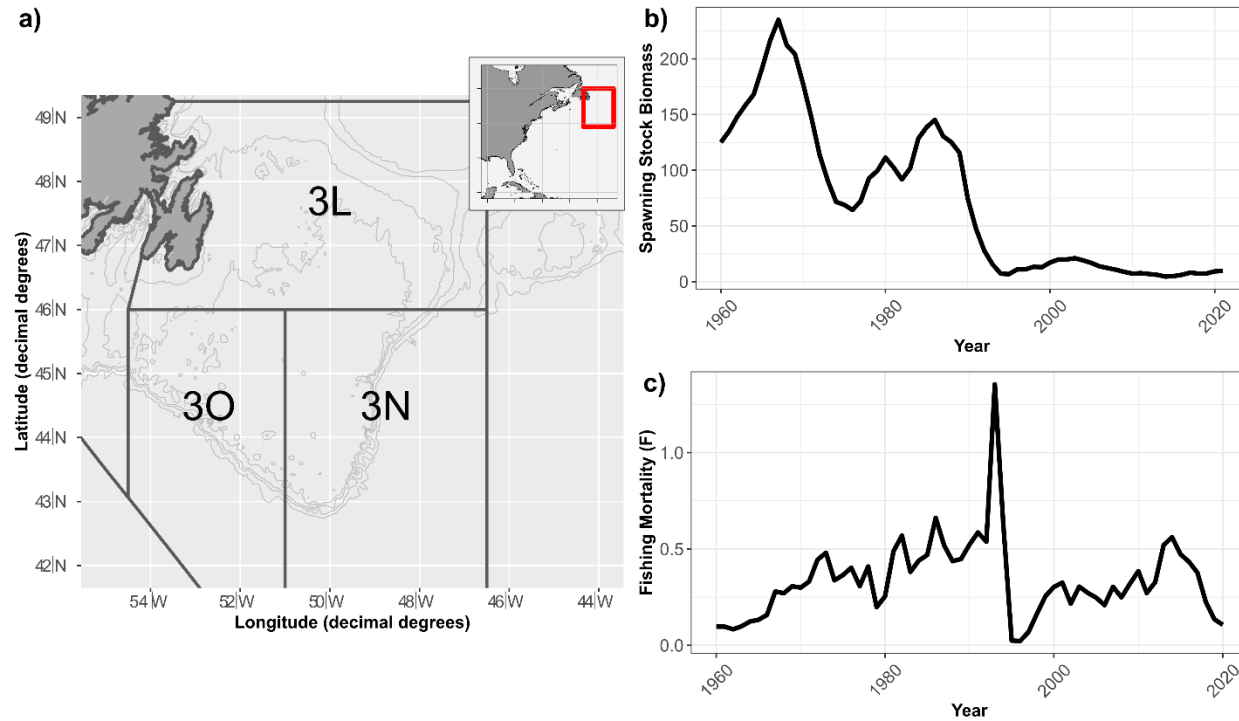


Figure 4.1 Map of NAFO Divisions 3LNO (a) and estimates of recent spawning stock biomass (b) and fishing mortality (c) from the most recent run of the stock assessment model (Wheeland et al. 2021). Light grey lines in panel a represent bathymetric contours at 100, 200, 400, and 1000 m depth. Spawning stock biomass estimates are in the 1,000's of tons and estimates of fishing mortality are the average estimates for ages 9-14.

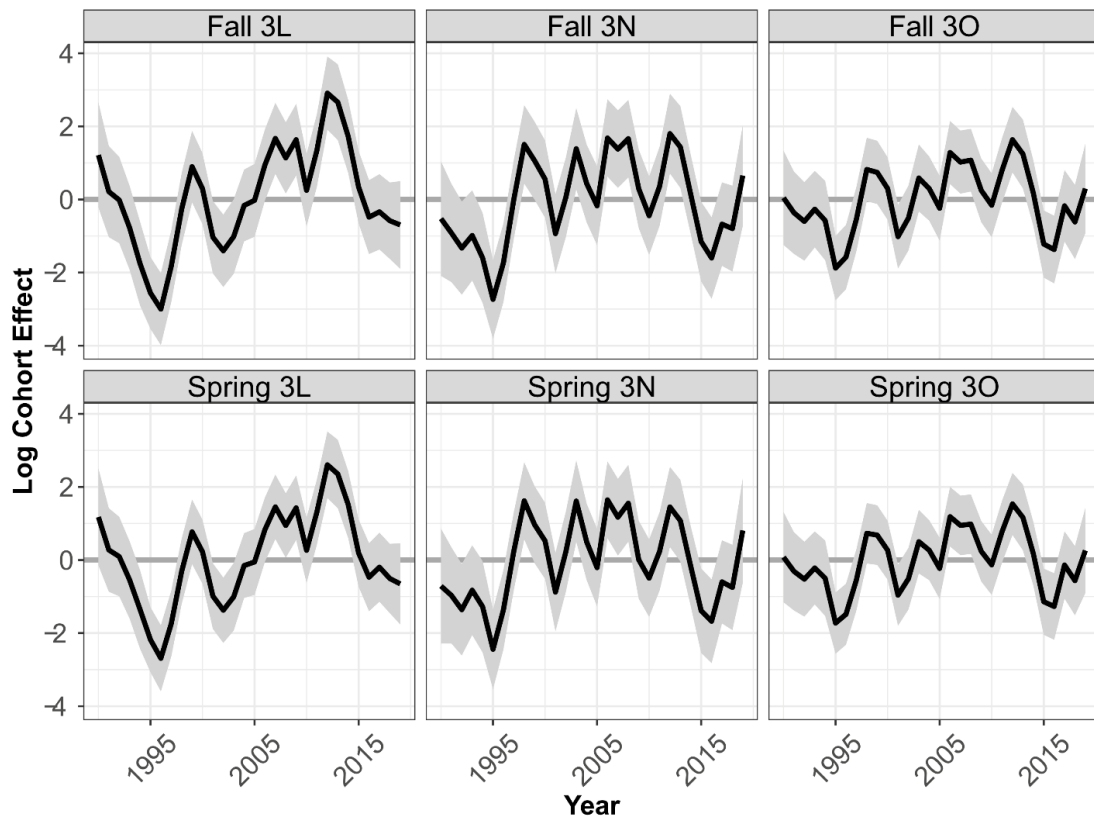


Figure 4.2 Time-series of cohort effect deviations estimated for each survey index using model M5. The black lines represent the point-estimates while the shaded grey area represents the 95% confidence intervals.

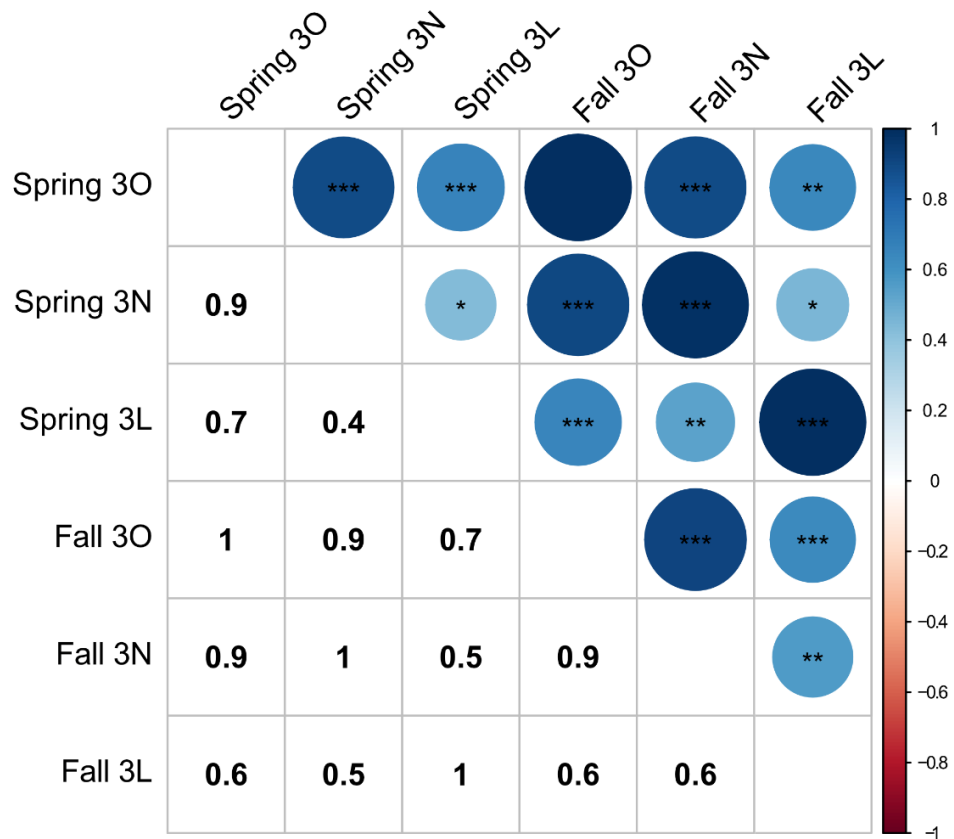


Figure 4.3 Spatial correlations of the cohort effects between the six survey indices from model M5. The size and darkness of the circles indicate the magnitude of the correlations. The stars indicate significance, where more stars represent lower p -values (1 star = $P < 0.05$, 3 stars = $P < 0.01$).

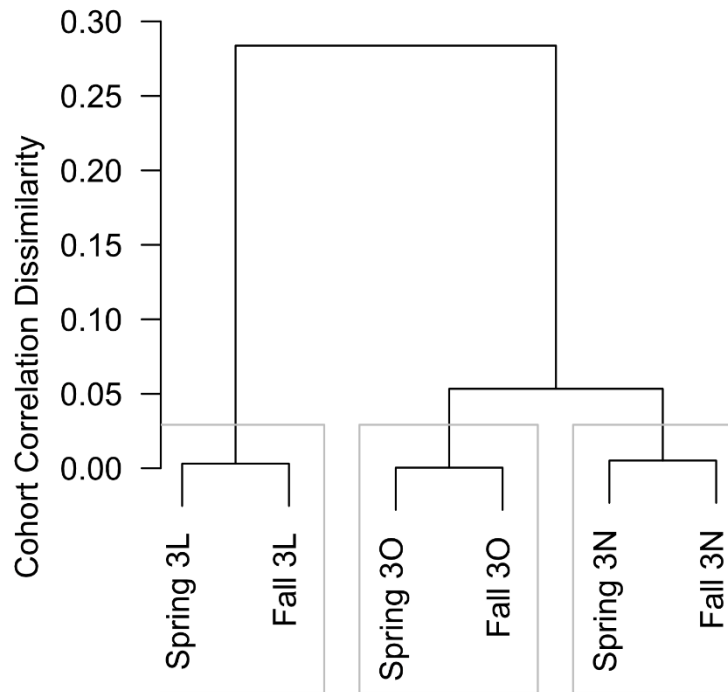


Figure 4.4 Dendrogram of a dissimilarity matrix of the spatial correlations of cohort effects in model M5.

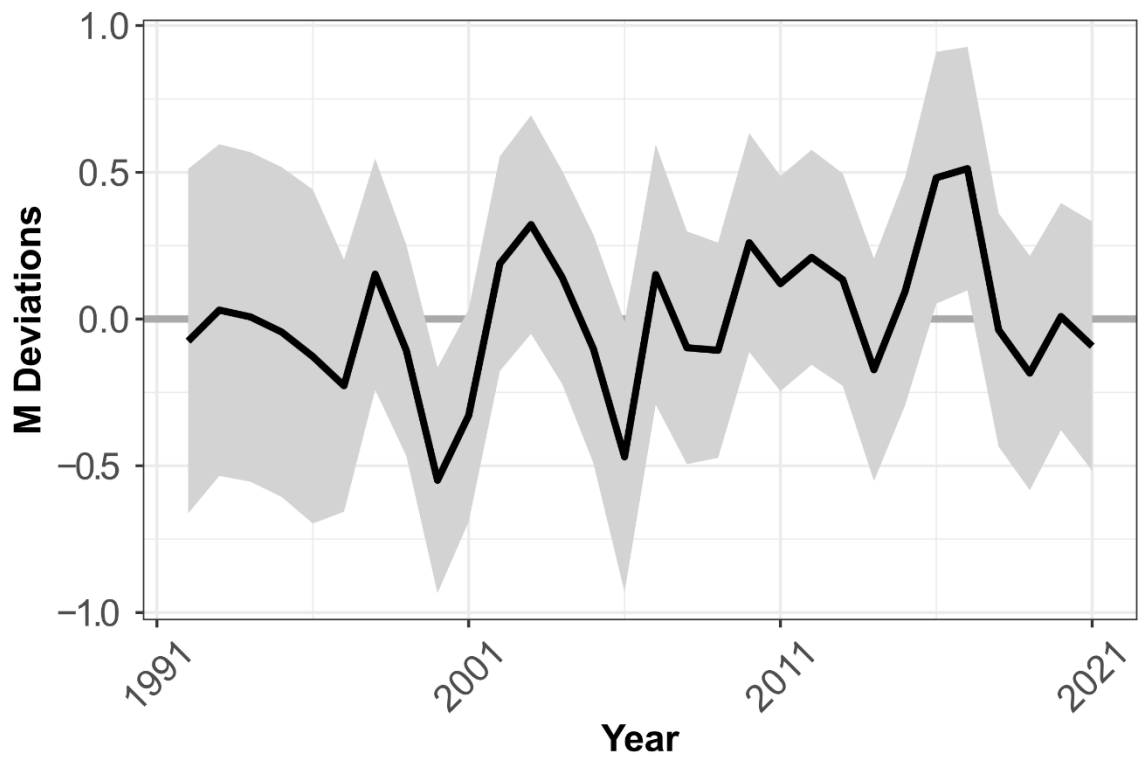


Figure 4.5 Time-series of annual natural mortality rate deviations from model M5. The black line represents the point-estimates and the shaded grey area represents 95% confidence intervals.

5 Testing models of increasing complexity to develop ecosystem-informed fisheries advice

Authors: Robertson, M.D.^{1*}, Cadigan, N.¹, Regular, P.M.², Koen-Alonso, M.², Bélanger, D.², Cyr, F.², Zhang, F.^{1,3}, & Eddy, T.¹

Author Affiliations

1. Centre for Fisheries Ecosystems Research, Fisheries and Marine Institute of Memorial University of Newfoundland, P.O. Box 4920, St. John's, NL, A1C 5R3, Canada.
2. Fisheries and Oceans Canada, Northwest Atlantic Fisheries Centre, P.O. Box 5667, 80 East White Hills Rd., St. John's, NL, A1C 5X1, Canada.
3. College of Marine Science, Shanghai Ocean University, 999 Huchenghuan Road, Shanghai, 201306, China.

A version of this chapter is being prepared for submission in *Fish and Fisheries*:

Robertson, M.D., Cadigan, N., Regular, P.M., Koen-Alonso, M., Bélanger, F., Cyr, F., Zhang, F., & Eddy, T. Sequentially testing models of increasing complexity to develop ecosystem-informed fisheries advice. In Prep. Fish and Fisheries.

Abstract

Despite continued calls for the application of ecosystem-based fisheries management, tactical fisheries management continues to be heavily based on single-species stock assessments that rarely quantitatively assess the effects of ecosystem processes on fish stock productivity. Examining models with varying assumptions can help identify sources of uncertainty and their relative importance. Testing and comparing models of increasing complexity may present a transparent hypothesis testing method that underscores the importance of incorporating various population and ecosystem processes. Here, I compare population dynamics models of increasing complexity to assess the population and ecosystem processes that most likely affected the differential recovery of two flatfish populations (American plaice and yellowtail flounder) on the Newfoundland Grand Banks over the past three decades. I observed that yellowtail flounder population dynamics were primarily driven by recruitment variability, which was negatively affected by warmer climatological conditions, as indicated by an integrated regional climate index. Meanwhile, American plaice population dynamics were affected by a combination of temporal variability in recruitment and natural mortality, where natural mortality increased during colder than average conditions. Furthermore, despite both species sharing similar life-history traits, habitat, and prey, I did not observe any indication that direct competition between yellowtail flounder and American plaice is influencing either of their population dynamics. Overall, the framework explored here may provide a transparent hypothesis testing method for exploring plausible population and ecosystem processes that have influenced stock productivity over time.

5.1 Introduction

Despite continued calls for the application of ecosystem-based fisheries management (EBFM: DFO, 2007; Denit, 2017; Koen-Alonso et al., 2019), tactical fisheries management continues to be primarily based on single-species stock assessments that rarely quantitatively assess the effects of ecosystem drivers on fish stock productivity (Skern-Mauritzen et al., 2016 but see Marshall et al., 2019; Pepin et al., 2022). Contrary to the historical population dynamic assumption of stationary productivity (i.e., lack of temporal variability), fish stock productivity varies over time in response to bottom-up processes (Smith et al. 2011; Regular et al. 2022), top-down processes (Baum and Worm 2009; Walters et al. 2018), and climate impacts on recruitment (Szuwalski et al. 2015). Given the increasing ability of state-space stock assessment models to estimate time-varying parameters (e.g., growth, maturity; Cadrin et al., 2020; Lorenzen, 2016; Punt et al., 2020), further exploration of the population and ecosystem processes driving variability in stock productivity over time may yield improved management outcomes.

The assumption of stationarity in natural mortality rates (M) in single-species stock assessments limits our ability to assess the effects of ecosystem processes on this aspect of population dynamics (Plagányi et al. 2022). Estimating M is difficult (Pope et al. 2021) and therefore, many stock assessments assume a stationary value rather than estimating it. When the assumption of stationary M is violated, any variability in M will be misattributed to another population process that is estimated to vary over time (e.g., recruitment, fishing mortality) or to survey catchability. Such misattributions of process variability will not only affect management advice (Hordyk et al. 2019; Stawitz et al.

2019; Punt et al. 2021), but will also affect our ability to identify relationships between population processes and ecosystem drivers. Therefore, misattribution of process variability may be partially responsible for the well-known inability of estimated recruitment-environment correlations to persist over time (i.e., Myers, 1998; Haltuch et al., 2019). However, recent model advances have improved our ability to estimate M and evidence indicates that the benefits of estimating time-varying M now outweigh the costs (Punt et al. 2021).

Examining models with different assumptions can help identify sources of uncertainty and their relative importance (Gårdmark et al. 2013; Heneghan et al. 2021; Reum et al. 2021; IPCC 2022). Model comparison is one way to examine models with different assumptions and occurs during the development of most ecosystem models. For instance, models of intermediate complexity (MICE) attempt to focus only on key species and processes to explain unaccounted variability in population dynamics (Plagányi et al. 2014; Collie et al. 2016), and thus serve as an intermediary between single-species population dynamics models and larger ecosystem models. During MICE development, population and ecosystem processes are included in a stepwise manner to identify their consistency with observed data and their impact on model fit (Plagányi et al. 2022). However, the inherent complexity in the development of MICE and other ecosystem models (see Geary et al., 2020) often results in a disconnect in understanding how model formulations and hypotheses were tested to yield the final model. This issue could be resolved by comparing models of increasing complexity. For example, to include ecosystem considerations in single-species stock assessments, extended models with

additional time-varying parameters (e.g., M), environmental integration, and/or multispecies extensions could be compared. In doing so, modellers may present a transparent hypothesis testing methodology that underscores the importance of incorporating different population and ecosystem processes to explain non-stationary stock productivity.

Here, I extend and compare population dynamics models of increasing complexity to assess the population and ecosystem processes that most likely affected the differential recovery of two flatfish populations on the Newfoundland Grand Banks (Northwest Atlantic Fisheries Organization [NAFO] Divisions 3LNO) over the past three decades. NAFO Divisions 3LNO yellowtail flounder (*Limanda ferruginea*) and American plaice (*Hippoglossoides plattesoides*) collapsed in the early 1990s following decades of over-exploitation (Parsons et al. 2021; Wheeland et al. 2021). Since this collapse, yellowtail flounder has recovered while American plaice has remained at a low population level, despite both species having relatively similar life-history characteristics (e.g., slow growth, late maturation, long lifespan), having been under the same fishing moratorium until 2000, and American plaice still maintaining no directed fishing pressure. The magnitude of collapse for American plaice was larger than yellowtail flounder, however, it remains unknown whether this difference in magnitude is the sole reason why yellowtail flounder recovered so rapidly from their lowest ever recorded biomass in the mid-1990s (Brodie et al. 2010) while American plaice continue to exhibit limited recovery despite low fishing pressure and several relatively strong recruitment events (Morgan and Brodie 2001; Walsh et al. 2004; Perreault et al. 2020). This difference in

recovery has specifically been hypothesized to be related to environmental drivers that may have differentially affected these populations because yellowtail flounder has historically been distributed in shallow, warmer water in NAFO divisions 3NO, while American plaice has historically been distributed in deeper, colder water in NAFO division 3L (Figure 5.1; Robertson et al., 2021). By extending and comparing models that include hypotheses regarding time-varying M , environmental and bottom-up effects on recruitment and M , and competitive interactions between these flatfishes, I attempt to gain insight into the most likely population and ecosystem processes that have affected recovery.

5.2 Materials and Methods

5.2.1 Modeling Approach

I extended single-species population dynamics models for yellowtail flounder and American plaice in NAFO Divisions 3LNO on the Newfoundland Grand Banks to include population and ecosystem processes that may have affected population recovery (Figure 5.2). The population dynamics model for yellowtail flounder was a newly developed delay-difference model (Section 5.2.2.1), while the American plaice model was a simplified formulation of a previously developed age-based model (Section 5.2.2.2; Perreault et al. 2020). I checked that the most basic parameterizations of these models estimated similar biomass trends to the current stock assessment models to ensure that models driven by similar assumptions produced similar results.

I added complexity to the basic population dynamic models to explore hypotheses explaining differences in recovery trajectories between yellowtail flounder and American plaice, namely, variability in M (Morgan et al. 2011; Wheeland 2021; Robertson et al.

2022b), variable responses to environmental drivers (Larraneta 1986; Brodie et al. 2010; Robertson et al. 2021), and competitive interactions between the two species (Figure 5.2; Walsh et al., 2004). First, I incorporated estimation of time and/or age-varying M (Section 5.2.3.1) to the single-species parameterizations. If model selection criteria (Section 5.2.5) indicated that estimating M improved model performance, then those models were used in subsequent analyses because M may have been influenced by environmental drivers or competition. Subsequent analyses included environmental drivers that modified recruitment and M (Section 5.2.3.2) and multispecies competitive interactions between American plaice and yellowtail flounder (Section 5.2.4). I then examined model selection criteria for the environmental and multispecies extended models to determine if including any of these processes improved model performance (Section 5.2.5). Once a best performing model was identified, I simulated how recovery trajectories would have differed for both stocks if their most informative environmental or multispecies driver had varied at low, average, or high values since collapse (Section 5.2.6). In doing so, I present an example of the framework for testing and comparing models of increasing complexity.

5.2.2 Single-Species Dynamics

5.2.2.1 Yellowtail flounder delay-difference model

The current 3LNO yellowtail flounder stock assessment model is a Bayesian stock production model (Parsons et al. 2021). Stock production models have been used for this stock due to a lack of age-structured time-series. However, stock production models are notoriously challenging to create extensions for, or to include in multispecies models, due to the correlation between the carrying capacity and intrinsic rate of growth parameters (pers. comm. É. Plagányi). The parameters are also not directly informative about

structured population processes (e.g., recruitment, growth, mortality) and therefore understanding the mechanisms driving population change is not possible. As a result, I opted to model yellowtail flounder population dynamics using a state-space parameterization of a Deriso-Schnute delay-difference model (Deriso 1980; Schnute 1987). This model still estimates unstructured population dynamics on an annual timeframe but explicitly estimates recruitment and survival parameters, and has previously been used in single-species extensions and multispecies approaches (Walters and Bonfil 1999; Plagányi and Butterworth 2012; Tulloch et al. 2017). My model estimated population dynamics for yellowtail flounder from 1965 – 2017 and included annual catch data from 1965 – 2017 and biomass estimates from five bottom-trawl research surveys (Parsons et al. 2021): Yankee (1971 – 1982), Russian (1984 – 1991), Campelen Spring (1984 – 2017), Campelen Fall (1990 – 2017), and Spanish (1995 – 2017). A full model description can be found in Appendix D1.

5.2.2.2 American plaice age-based model

The current American plaice stock assessment model is conducted using an adaptive framework-virtual population analysis (ADAPT-VPA; Wheeland et al., 2021). However, this type of assessment cannot include uncertainty in the landings data, a key concern for this stock where there is evidence of substantial underreporting in historical landings (Dwyer et al. 2016). As a result, a state-space age-based model was recently developed for this stock (Perreault et al. 2020). I used a modified version of this model to estimate American plaice dynamics here (see Appendix D2 for description and rationale for modifications). This model estimates population dynamics from 1960 – 2017 and

includes survey catch-at-age data from two research bottom trawl surveys: spring (1985 – 2017; 2006 & 2015 omitted due to poor survey coverage) and fall (1990 – 2017; 2004 & 2014 omitted due to poor survey coverage). These bottom trawl surveys changed gears from the Engel to Campelen in 1995, where the Campelen had improved catchability for juvenile fish (ages 1 – 4; Morgan et al., 1998). To account for the gear change, the model estimates separate survey catchabilities for the Engel and Campelen surveys for juvenile fish. Proportion of mature fish at age and stock weight at age estimates were taken from the most recent stock assessment (Wheeland et al. 2021). In addition, this model includes landings from 1960 – 2017, commercial average weights-at-age, as well as commercial catch proportions at age (all commercial data is for ages 5+). A full model description can be found in Appendix D2.

5.2.3 Environmental Drivers

5.2.3.1 Recruitment and M deviations

To identify whether recruitment and M varied over time (and/or age) I compared two major model parameterizations for yellowtail flounder and three for American plaice. The single-species parameterizations for yellowtail flounder had 1) only time-varying recruitment deviations or 2) time-varying recruitment deviations and natural mortality deviations. Meanwhile, the American plaice parameterizations included 1) only time-varying recruitment deviations, 2) time-varying recruitment deviations and natural mortality deviations or 3) time-varying recruitment deviations and time- and age-varying natural mortality deviations. I modeled recruitment and M deviations following a common approach (Maunder and Watters 2003; Schirripa et al. 2009; O’Leary et al.

2019) and in a way that would permit covariate inclusion (Section 5.2.3.2). I modeled these time (or time- and age-) varying processes (X_y) as,

$$X_y = f(x) \exp(\varepsilon_y), \quad (5.1)$$

$$\log(\varepsilon_y) \sim RW(\sigma), \quad (5.2)$$

where $f(x)$ is the mean function of the individual process, ε_y are temporal deviations of that process, RW refers to a zero-mean Gaussian random walk, and σ is the standard deviation of the time-varying deviations. The mean function for M deviations was input as the traditional assumption of 0.2. For American plaice parameterizations, I only considered models where M deviations varied for ages 5+ since a recent study identified that the influence of M deviations on juvenile American plaice dynamics (ages 1-5) has been relatively small since the early 1990s (Robertson et al. 2022b). Additionally, to penalize M deviations (Punt et al. 2021), I included a zero-mean Gaussian prior with a standard deviation of 0.05. This prior ensures that the likelihood function will increase when M deviations are estimated, ensuring that the model will only maintain those estimates if there is sufficient evidence that the added explanatory power of estimating M deviations (i.e., as indicated by the likelihood function) is greater than the imposed penalty. Meanwhile, the mean recruitment function for yellowtail flounder was based on the number of mature fish in the population and a maximum juvenile survival rate, where the deviations essentially modified survival downwards (see Appendix D1 for full description and equations). Finally, American plaice mean recruitment was based on a Beverton-Holt recruitment function (see Appendix D2 for full description and equations).

5.2.3.2 Environmental extensions

Many of the explanations for the difference in recovery trajectories between species involves different environmental drivers. As a result, I examined parameterizations where environmental time-series were input to explain recruitment or M deviations. To allow this, I used the general formulation for integrating environmental time-series into population dynamics models that was developed by Maunder & Watters (2002),

$$X_y = f(x) \exp(\varphi_0 + \varphi_1 I_y + \varepsilon_y), \quad (5.3)$$

$$\log(\varepsilon_y) \sim RW(\sigma), \quad (5.4)$$

where φ_0 is a scaling parameter, I_y is the environmental time-series, and φ_1 relates the environmental time-series to the process of interest. Although non-linear (e.g., quadratic) relationships between environmental time-series and process deviations are plausible, data exploration indicated that relationships with my data were linear (see Appendix D3). By modeling the environmental drivers in this way, I was able to determine whether the population dynamics of a species are better described when environmental drivers are explicitly used to reduce the process deviations (ε_y). Furthermore, by estimating autocorrelated ε_y , even with the inclusion of environmental drivers (Eqn. 5.2), this modeling approach does not rely on the relationship between population processes and environmental drivers to fully describe non-stationary processes, but instead allows these drivers to act as a component of the non-stationarity.

I considered including the role of 1) climatic variability using the Newfoundland and Labrador (NL) climate index, mean spring bottom-water temperature from the bottom

trawl research surveys, and the area of the cold-intermediate layer (CIL; Cyr & Galbraith, 2021), 2) bottom-up drivers using a time-series of two key forage fishes: capelin (*Mallotus villosus*) biomass (Koen-Alonso et al. 2021), northern sand lance (*Ammodytes dubius*) abundance (Robertson et al. 2022a) and 3) a potential competitor for food and habitat, thorny skate (*Amblyraja radiata*) using a time-series of estimated biomass (Simpson et al. 2018).

To account for longer term climatological effects and the period of influence on processes, climate time-series were included differently for recruitment and natural mortality for both species. Yellowtail flounder recruitment was tested with one-sided five-year moving averages (i.e., averaging the five years prior to a given year) because recruitment was estimated to occur over a five-year period (see Appendix D1). American plaice recruitment was tested against one-sided three-year moving averages to account for limited catchability of age 1-2 American plaice by the surveys (Morgan et al. 1998). Meanwhile, M for both species was tested against climate time-series without a moving average, because M was most likely affected by the direct impacts of climate within a given year. The northern sand lance index was extended back to 1984 by combining estimates from separate non-linear functional response models (Robertson et al. 2022a) for Engels and Campelen data. Every covariate was standardized using the standard score equation ($X_{standard} = \frac{X - \bar{X}}{\sigma_X}$) prior to inclusion to improve model convergence and to determine whether longer time-series could serve as proxies for correlated shorter time-series (see Appendix D3). As a result, my environmental covariate hypotheses were reduced from six to five. The capelin time-series were relatively short in comparison to

other covariates and were highly negatively correlated with the NL climate index, CIL area, and bottom-water temperature so they were not directly tested. Each of the five directly tested covariates had specific hypotheses regarding their influence on flatfish population dynamics. The NL climate index informed whether the flatfish populations responded to macro-scale climatic variability, while bottom-water temperature informed benthic habitat availability, and area of the CIL indicated habitat and prey availability (e.g., by modifying the distribution of prey; Davoren et al., 2006; Harvey et al., 2009). The northern sand lance time-series provided one indication of whether direct prey availability had negatively affected either species. Finally, the thorny skate biomass time-series indicated whether it has competed with the American plaice and yellowtail flounder populations.

5.2.4 Competition

To determine whether any of the observed recruitment or M deviations were driven by competitive interactions with the other flatfish population, I compared several parameterizations of a basic multispecies model. This multispecies model included both population dynamics models in a joint likelihood where stock size and vital rates were linked using Eqn. 5.3. Specifically, the spawning stock biomass of each population was linked to either the recruitment or M deviations of the other stock to test for the possibility of competition and predation of juveniles by mature fish or direct competition for habitat or food between mature fish. Recruitment was also linked to the recruitment deviations of the other stock to test whether there may be juvenile habitat competition. Because yellowtail flounder recruitment deviations modelled births that occurred five years prior

(see Appendix D1), the spawning stock biomass and recruitment of American plaice were lagged five years.

5.2.5 Estimation

Model selection was completed using a combination of Akaike's information criterion (AIC), Bayesian information criterion (BIC), and examination of residuals. BIC measures goodness-of-fit, while AIC is a measure of prediction accuracy (Sober 2002). I first compared single-species models to determine which formulation had the best performance; the best performing model was then used in all single-species extensions and multispecies formulations. All covariates except the NL climate index and CIL area did not exist for the entirety of the time-period examined with the population dynamics models. To account for this, I conducted model selection with covariates only affecting process deviations from 1984 – 2017, when data existed for every covariate, to ensure that differing data lengths did not influence model selection results. Although necessary for model selection, it is worth noting that this may affect my ability to identify environmental drivers of population dynamics prior to 1984 and limits the number of samples used to identify relationships with the environment. I used the Template Model Builder (TMB, Kristensen et al. 2016) package in R (R Core Team 2018) to evaluate the negative logarithms of the marginal likelihoods (nll) of these models and the data, and to evaluate the nll gradients to improve estimation. Further, I used the R function `nlminb()` to find the maximum likelihood estimates.

5.2.6 Recovery simulations

If any models that included environmental covariates or multispecies competitive interactions outperformed the single-species formulations, I ran simulations to determine how recovery trajectories would have varied under alternative histories of the most important (i.e., best performing) ecosystem process. These simulations gave an indication of the magnitude difference in population dynamics under different environmental and ecosystem considerations. Simulations began two years prior (1992) to when the fishing moratoria were announced (1994) to account for the delay between the collapse occurring and when it had been officially recognized. All model parameters (including fishing mortality) were fixed at values from prior model runs so that variability in population dynamics was only driven by differences in environmental trajectories. Simulated environmental time-series followed a Gaussian random walk with mean zero and standard deviation of 0.2. This standard deviation value was chosen to allow variability over time while minimizing overlap between alternative histories. Since all covariates and multispecies interactions were standardized prior to inclusion in models, the alternative histories involved starting the random walk at initial values of -1, 0, and 1 to represent low, average, and high values for each covariate. Population dynamics at each of the initial values were then simulated 1000 times and the 20:80% and 10:90% quantiles of the simulations were visualized to identify the most common range of dynamics under each alternative history. Although it is likely that variability in recruitment and/or natural mortality would yield additional consequences for the population dynamics (e.g., modifying fishing history), the main goal of this simulation exercise was to determine the

magnitude of the effect that ecosystem processes may have had on the recovery of these stocks.

5.3 Results

5.3.1 Single-species models

The best performing single-species models for both yellowtail flounder and American plaice included time-varying M deviations (YTFL2; AMPL2; Table 5.1). However, the improvements to model criterion score and residuals for the yellowtail flounder model were minor (e.g., mean reduction of survey index standard deviation estimates <0.01) and the estimates of time-varying M deviations were negatively correlated with the recruitment deviations. As a result, further analyses for yellowtail flounder were conducted with the model that did not estimate M deviations (YTFL1). Including time-varying M deviations improved the fit to the survey indices, catch proportions-at-age, and landings data for the American plaice model (see Appendix D2 for residual plots). Specifically, including M deviations reduced all standard deviation estimates for catch proportions-at-age (reduction mean = 0.38) and reduced standard deviation estimates for survey indices for all (mean reduction = 0.07) but the oldest ages (age 14 – 15) which were approximately equal to estimates from the model without time-varying M (difference <0.01). However, extending this further to include time- and age-varying M deviations had worse model performance than the model with only time-variations in M . This would indicate that although the data were informative about time-variations in M , there was not enough information to parse both time and age variation.

The best performing models followed similar trends in spawning stock biomass (SSB) and biomass to the current stock assessments (Figure 5.3). The yellowtail flounder models estimated a very similar trend to the current stock assessment until the mid-1990s. After this point, both models estimated rapid increases followed by a plateau and a decline, however, both models estimated the magnitude of the increase to be smaller than the current stock assessment (peak of 124 kt rather than a peak of 176 kt). This difference in estimated biomass appears to be driven by differing survey catchability estimates. The null American plaice model (AMPL1) did not estimate as large of a peak in SSB in the late-1960s or in the mid-1980s as the current stock assessment. Meanwhile, the model with time-varying M deviations (AMPL2) estimated a slightly larger peak in SSB in the late-1960s and a much larger peak in SSB in the mid-1980s. These differences in SSB are most likely driven by the increasing estimates of M in the 1980s – 1990s. AMPL1 assumes that M is stationary at 0.2, the current stock assessment inputs M as 0.53 from 1989 – 1996 for all ages (Wheeland et al. 2021), and AMPL2 estimates that M for fish ages 5+ is higher (mean = 0.84) during that time period. The models account for this increase in M by modifying SSB to maintain landings estimates. Finally, AMPL2 estimated a higher, fluctuating SSB that declined rather than increased in the terminal years of the model (2016 – 2017).

5.3.2 Environmental Drivers

Both yellowtail flounder and American plaice models were improved by using environmental covariates to account for either recruitment or M deviations (Table 5.2; Appendices D1 & D2). The best performing yellowtail flounder model included the five-

year moving average NL climate index to account for recruitment deviations (YTFLE1). Including the five-year moving average NL climate index completely accounted for recruitment deviations (recruitment deviation standard deviation in YTFLE1 = 0.35, YTFLE1 < 0.001; Figure 5.4) but also reduced model fit to survey indices (mean standard deviation estimate increase = 0.02; Appendix D1 Figs. D1.2, D1.3, D1.6, & D1.7). Furthermore, the landings residuals developed a slight pattern from the 1970s – early 1990s when the NL climate index was used to modify recruitment deviations (Appendix D1 Figs D1.5 & D1.9), although the magnitude of these trends are small (see Appendix D1 Figs D1.4 & D1.8). Even though the NL climate index only modified the deviations from 1984 onwards, the time-series accounted for enough variability that recruitment deviations did not need to be estimated to yield similar population dynamics estimates to YTFLE1.

The best performing model for American plaice included the NL climate index to account for *M* deviations (AMPLE6; Table 5.2). Including the NL climate index reduced the standard deviation estimate for the *M* deviations by 0.05 and did not substantially affect recruitment deviations (Figure 5.4) or model fit to catch proportions-at-age or survey indices (standard deviation estimate differences <0.01; Appendix D2 Figs. D2.11 – D2.15, D2.18 – D2.20, D2.21 – D2.25, D2.28 – D2.30, & D2.31 – D2.35). *M* deviations in AMPLE6 were modified throughout the time-series. The biggest change from the non-extended model (AMPL2) occurred from 1989 onwards, where the deviations were reduced in the late 1980s – early 1990s as was the oscillating trend during the late 1990s – 2017. However, all changes remained within the 95% confidence intervals of both

models. These estimated changes may indicate that the NL climate index was not related to M prior to collapse and that it does not explain all of the variability during or after the collapse. Finally, although none of the models that used covariates to account for recruitment deviations produced a better performance than AMPLE6, the model with three-year moving average bottom-water temperatures (AMPLE3) produced the best performance of the recruitment deviation models.

5.3.3 Competition

Multispecies formulations with competitive interactions did not produce an improved model performance over the null multispecies model that did not include competitive interactions (Table 5.3). This lack of improvement indicates no evidence that the dynamics of these two stocks are primarily driven by direct competitive interactions with one another.

5.3.4 Best-performing models

Since there was no improvement in model performance with multispecies model formulations, the best performing models for both species were the models that included environmental covariates (YTFLE1 and AMPLE6). The NL climate index was estimated to have a negative effect on M and recruitment deviations for American plaice and yellowtail flounder, respectively (Figure 5.5). The estimated effect of the NL climate index on yellowtail flounder indicated that a negative climate index (i.e., colder conditions) promoted strong recruitment while a positive climate index (i.e., warmer conditions) substantially reduced recruitment success. Meanwhile, American plaice M

increased when there were colder conditions and decreased in warm conditions, although the 95% confidence interval for this effect only differed from 1 at the coldest conditions.

The best performing models did not substantially modify population dynamics estimates from the single-species formulations (Figure 5.6). SSB, fishing mortality (F), and recruitment estimates were only slightly modified for American plaice between the non-extended model (AMPL2) and the best performing model (AMPLE6), with the only observable differences occurring prior to 1990 and no estimates falling outside of the 95% confidence interval of the extended model. Meanwhile, yellowtail flounder biomass, F , and recruitment estimates were modified throughout the time-series between the non-extended model (YTFL1) and the best performing model (YTFLE1). In general, the differences in estimates between models fell within the 95% confidence intervals of YTFLE1 in recent years. These changes were likely driven by the lack of estimated recruitment deviations.

5.3.5 Recovery simulations

Simulations for AMPL6 and YTFLE1 indicated that recovery trajectories for these stocks would have differed substantially with alternative histories for their most important environmental drivers (Figure 5.7). If environmental conditions had followed a warmer than average trajectory, yellowtail flounder would have continued to decline after collapse, with most simulations indicating lower than current biomass. Average conditions could have yielded a wide range of population trajectories, with population levels below, equal to, or higher than currently observed. Finally, the simulations for cold conditions indicate that yellowtail flounder biomass would most likely have been higher

than current levels. It is worth noting that the magnitude of this increase is likely an artefact of the lack of carrying capacity term in the delay-difference formulation. Meanwhile, the American plaice simulation indicates that given warmer than average conditions, the American plaice stock would not have collapsed and would have experienced an uncertain population trajectory from the early 2000s onwards, with most simulations yielding larger SSB than is currently estimated. However, with both average and cold conditions, American plaice SSB would have declined and frequently remained below 100,000 tonnes.

5.4 Discussion

I sought to determine whether using a framework of testing models of increasing complexity could identify the population and ecosystem processes that affected the population dynamics for two flatfish populations on the Newfoundland Grand Banks. I observed that NAFO Divisions 3LNO yellowtail flounder population dynamics were primarily driven by recruitment variability, which was negatively affected by warmer climatological conditions, as indicated by the NL climate index. Meanwhile, American plaice population dynamics were affected by a combination of temporal variability in recruitment and M , where M increased during colder than average conditions. Simulations based on these best performing models indicated that if there had been a different trajectory for the environmental drivers that affected these stocks, they may have exhibited drastically different pathways to recovery following their collapses in the early 1990s.

5.4.1 Yellowtail flounder

The observations that yellowtail flounder population dynamics were affected by recruitment and the NL climate index lend support to hypotheses that have been put forward for this stock in the past. For example, Robertson et al. (2021) observed a shift in stock distribution in response to the cold period in the early-1990s, and hypothesized that this may have affected population productivity. Additionally, Walsh & Colbourne, (2007) observed that 3LNO yellowtail flounder biomass was positively correlated with bottom water temperatures and hypothesized that temperature affected recruitment and growth. Despite these findings supporting hypotheses that productivity is affected by climatological conditions, I estimated a negative relationship between recruitment and the NL climate index rather than a positive relationship as found by Walsh & Colbourne, (2007). This difference in sign is likely driven by differences in estimation method (e.g., population dynamics model) and the estimated value that was used to represent productivity (i.e., biomass compared to recruitment deviations). The negative relationship identified here may indicate that temperature ultimately represents an indirect effect. The northernmost extent of the range for yellowtail flounder in the Northwest Atlantic is the Grand Banks, where their distribution is centered around the Southeast Shoal, representing some of the shallowest and warmest habitats on the Grand Banks (Figure 5.1; Pitt, 1970). Therefore, cold temperatures in this region would most likely induce a negative physiological effect rather than a positive effect as I observed here. As a result, the negative correlation between recruitment and the NL climate index may indicate that cold conditions are an ecological indicator of beneficial recruitment habitat or reduced juvenile predation or competition. For example, a study on yellowtail flounder in the

Middle Atlantic Bight (Sullivan et al. 2005) identified a strong negative correlation between recruitment and temperature and discussed that this relationship may be related to the match/mismatch hypothesis (Cushing 1975). In this case, colder temperatures delay phytoplankton and zooplankton blooms, which may then better align zooplankton availability with the timing of initial feeding for yellowtail flounder larvae. Overlapping timing of peaks in yellowtail flounder larvae and zooplankton abundance were linked to the production of strong year classes on George's Bank, although this relationship was not statistically significant (Johnson 2000). Phytoplankton bloom timing on the Grand Banks is negatively correlated with the NL climate index (Belanger et al., 2021), where colder temperatures are specifically related to delays in the peak and end of the spring bloom (Appendix D3 Figs. D3.8 & D3.9). This relationship indicates that yellowtail flounder recruitment on the Grand Banks may also be affected by match/mismatch of larvae and their prey.

5.4.2 American plaice

The collapse and lack of population recovery for American plaice was affected by recruitment success and variability in adult M , where M increased under cold conditions as indicated by the NL climate index. I observed substantial temporal variability in American plaice adult M which is not accounted for in the current stock assessment model (Wheeland et al. 2021). My model estimated that M increased dramatically just prior to and during the population collapse and has shown increasing fluctuations since. Estimated increases in M corroborate research on this stock that has indicated that assuming that $M=0.2$ is an underestimate in recent years (Perreault et al. 2020; Wheeland

2021). This assumption may be responsible for inducing retrospective patterns in the stock assessment model and may be affecting fisheries management advice. Although separating relative changes in M , fishing mortality (F), and catchability is notoriously difficult, I followed recent advice and estimated M with a prior (Punt et al. 2021). It seems increasingly likely that changes in American plaice adult M have affected stock collapse and recovery, however, specifying different model configurations may influence the trend and magnitude of M estimates.

The NL climate index accounted for variability in M during and after the population collapse. American plaice were historically spatially distributed throughout the Grand Banks with the largest centers of biomass and productivity in the coldest region of the Grand Banks in 3L (Figure 5.1; Robertson et al., 2021; Walsh et al., 2004). This distribution shifted dramatically following the period of cold conditions that occurred in the late 1980s – early 1990s. Additionally, American plaice in this region are generally sedentary, indicating that a large migration in response to cold temperatures was unlikely (Pitt 1969; Morgan 1996). By coupling the evidence that the timing of a distributional shift away from the coldest areas on the Grand Banks matches the timing of estimated increases in M that are explained by the NL climate index, it is possible that the observed distributional shift represents a mass mortality event for the stock. However, the exact mechanisms regarding past and continued high levels of natural mortality remain uncertain. Because the NL climate index integrates indices of environmental conditions, it provided a better fit than CIL area or bottom water temperature alone, even if those variables may have played a role in the observed effect. For example, in cold years the

CIL can reach the seafloor in 3L (e.g., Colbourne et al., 2018) which may directly induce mortality or restrict habitat and feeding opportunities for American plaice. The CIL is a layer of relatively fresh, sub-zero °C water located between warmer surface and shelf waters on the Newfoundland shelf in the summer (Colbourne 2000). Temperatures below physiological thresholds can induce lethal effects (Donaldson et al. 2008), however, previous research has indicated that this may be unlikely for American plaice given their tolerance of low temperatures (Morgan 1992). Instead, larger CIL areas in 3L could impact mortality by either limiting foraging directly due to its physiological impacts (e.g., feeding cessation; Morgan, 1992) or indirectly by producing thermal refuges from predation by prey (e.g., northern sand lance and capelin; Davoren et al., 2006; Lilly, 1982; Rose & Leggett, 1989). These types of effects would fall in line with hypotheses regarding starvation-induced mortality as has been observed for northern cod (Regular et al. 2022) and hypothesized for other local stocks (Cadigan et al. 2022). As a result, further research on changes in American plaice growth and body condition are warranted. Finally, unlike the effects of the NL climate index on yellowtail flounder recruitment, the NL climate index did not account for all variability in M , indicating that there may have been multiple drivers that affected M over time. It is possible that the NL climate index impacted M prior to the collapse of American plaice but this effect was not identified here because it was either obscured by the large magnitude effect of F or because the survey catch-at-age data capable of parsing F and M effects was only available from 1984 onwards.

The population processes and environmental drivers that affected American plaice population collapse (early 1990s) may not be the same as those that limited its recovery (late 1990s – present). My models indicate that population collapse occurred in response to a dramatic decline in recruitment and increase in M and F in the late 1980s – early 1990s. However, these models indicated that recruitment deviations have been at or above-average since the late 1990s. Large pulses of pre-recruits (aged 0-5) have been identified in the recent stock assessment models as well (Wheeland et al. 2018, 2021). This indicates that population dynamics since the collapse have been primarily affected by the increasing fluctuations in M (and to some extent F in the early 2000s) rather than poor recruitment. Although the particularly cold temperatures ($<0^{\circ}$ C) that covered the Grand Banks in the early 1990s may have crossed a threshold that impacted both recruitment and M , the comparatively warm temperatures since may not have had such a large effect. The NL climate index was capable of accounting for some of the fluctuations in M since the collapse but did not explain the continued increase in M deviations since the late 1990s which represents a concerning pattern for a collapsed stock.

5.4.3 Competition

I did not observe any indication that direct competition between yellowtail flounder and American plaice is influencing either of their population dynamics. Although both populations have relatively similar life history traits, they are not expected to predate one another (Tam and Bundy 2019) and the Grand Banks has sustained larger populations of both species, indicating that habitat should not necessarily be limiting. The main mechanism which may have driven competition would have been dietary overlap, where

small American plaice and yellowtail flounder both rely on echinoderms and crustaceans (Pitt 1976; Pérez-Rodríguez et al. 2011). This dietary overlap is reduced for larger fishes since American plaice preferentially consume substantially more sand lance and capelin than yellowtail flounder. However, if capelin and sand lance were not available in large enough quantities, competition between larger American plaice and yellowtail flounder for food is possible. Despite the low population size of capelin in recent years, my model did not identify competition as an important driver of dynamics for either species. This does not mean that competition can be completely disregarded. The American plaice population has shifted its spatial distribution in recent years and is much more overlapped with the distribution of yellowtail flounder than previously (Robertson et al. 2021). As a result, methods with higher spatial resolution may be more likely to identify signals of competition if present.

5.4.4 Management implications

Comparing alternative representations of population dynamics can highlight potential sources of uncertainty for fisheries management advice. Here, the biomass estimates from my models differed from the most recent stock assessment model estimates for both species. My delay-difference formulation of yellowtail flounder population dynamics estimated that the magnitude of biomass recovery was lower than was estimated using the surplus production stock assessment model (Parsons et al. 2021). This difference appears to be derived from differences in catchability estimates. The current stock assessment estimates that biomass is near B_{MSY} , and therefore, any decreases in magnitude of recent biomass may affect current stock status and harvest advice. Meanwhile, estimating time-

varying M in the American plaice stock assessment model yielded different estimates of SSB and F from the current stock assessment model (Wheeland et al. 2021). Although the differences in SSB are unlikely to affect stock status, the high levels of M for adults may change the context for allowable levels of bycatch (Shelton and Morgan 2006).

Identifying differences in model estimates is not uncommon when exploring alternative representations of population dynamics (e.g., Brodziak & Legault, 2005; Brodziak & Piner, 2010). Although my approach of testing models of increasing complexity focused on identifying a best performing model, another benefit from this approach is the examination of different formulations and how they affect model estimates. It is often beneficial to combine estimates from multiple plausible models as advice from ensembles may better represent the sources of uncertainty for the stock(s) of interest (Jardim et al. 2021).

Testing models of increasing complexity can help identify the most important processes influencing population dynamics. Traditional single-species population dynamics models are generally limited to attributing changes in populations to shifts in recruitment or fishing mortality, however, there are other processes that may be more important for describing fish population dynamics (*sensu* Rice, 2011). This framework allows modellers to explore hypotheses related to shifts in other population vital rates and interactions with the environment or other species. Similar to other related frameworks that focus on developing multispecies and ecosystem models (Collie et al. 2016; Plagányi et al. 2022), model structural uncertainty may limit the application of these models to directly inform tactical fisheries management. Despite this potential limitation, this

modeling framework may indicate future research directions to facilitate the development of ecosystem-informed management advice. For example, providing evidence that natural mortality has varied through time and impacted population dynamics may elucidate a need to further explore the drivers of these shifts, to include additional data in a stock assessment (e.g., body condition; Cadigan, 2015; Regular et al., 2022), or to use ecosystem models to rescale target F (i.e., F_{eco} ; Howell et al., 2021). Additionally, this framework may assist in the determination of reference points that guide fishery management decisions. For example, when stocks exhibit non-stationary productivity, reference points may need to be modified to ensure a match between their productivity state and the allowable levels of harvest (Berger 2019; Zhang et al. 2021a). However, a major barrier to implementation of so-called “dynamic reference points” has been uncertainty about whether a change has occurred and is lasting (Eddy et al. In Press). By estimating non-stationary patterns in productivity that are linked to environmental drivers, this framework could be used to identify when implementing dynamic reference points may be appropriate. Finally, by exploring models with alternative hypotheses about the drivers that have influenced population dynamics, this framework would provide a natural starting point for identifying potential operating models for management strategy evaluations (MSE). MSE are being increasingly advocated to provide ecosystem-informed management advice (Smith et al. 2007; Goethel et al. 2022). However, MSE currently lack standardized methods and can struggle to provide an open, transparent process to the managers, scientists, and stakeholders that are involved (Miller et al. 2019; Townsend et al. 2019). Using a framework like the one described here to identify operating models and describe why some hypotheses were prioritized over others may

create a straightforward process where results could be more easily communicated to stakeholders.

5.5 List of Tables

Table 5.1 Model comparisons for different formulations of both single-species models. *nll* represents the negative log-likelihood, *k* represents the number of parameters, Δ represents the difference in model criterion score from the model with the lowest model criterion score. The bolded row indicates the model with the lowest AIC and BIC.

Name	<i>M dev.</i>	<i>nll</i>	<i>k</i>	AIC	BIC	Δ AIC	Δ BIC
Yellowtail flounder							
YTFL1	Input	96	14	221	258	6	3
YTFL2	Estimated	93	15	215	255	0	0
American plaice							
AMPL1	Input	1126	55	2362	2622	335	331
AMPL2	Time-Varying	958	56	2027	2291	0	0
AMPL3	Time & Age-Varying	978	66	2087	2399	60	108

Table 5.2 Model comparisons for different formulations of the two best null models. *nll* represents the negative log-likelihood, *k* represents the number of parameters, Δ represents the difference in model criterion score from the model with the lowest model criterion score. The bolded row indicates the model with the lowest AIC and BIC.

Name	Process	Covariate	<i>nll</i>	<i>k</i>	AIC	BIC	Δ AIC	Δ BIC
Yellowtail flounder								
YTFL1			96	14	221	258	21	16
YTFLE1	Rec.	Climate index	84	16	200	242	0	0
YTFLE2	Rec.	CIL	94	16	220	262	20	20
YTFLE3	Rec.	Bot. temp	96	16	225	267	25	25
YTFLE4	Rec.	Sand lance	96	16	224	266	24	24
YTFLE5	Rec.	Thorny Skate	95	16	222	264	22	22
American plaice								
AMPLE2			958	56	2027	2291	20	11
AMPLE1	Rec.	Climate index	957	58	2029	2303	22	23
AMPLE2	Rec.	CIL	957	58	2031	2304	24	24
AMPLE3	Rec.	Bot. temp.	950	58	2016	2289	9	9
AMPLE4	Rec.	Sand lance	957	58	2031	2304	24	24
AMPLE5	Rec.	Thorny Skate	957	58	2031	2304	24	24
AMPLE6	<i>M</i>	Climate index	945	58	2007	2280	0	0
AMPLE7	<i>M</i>	CIL	953	58	2021	2295	14	15
AMPLE6	<i>M</i>	Bot. temp	954	58	2025	2298	18	18
AMPLE9	<i>M</i>	Sand lance	957	58	2031	2304	24	24
AMPLE10	<i>M</i>	Thorny skate	957	58	2030	2304	23	24

Table 5.3 Model comparisons for the multispecies formulations. Ampl is an abbreviation for American plaice and Ytfl is an abbreviation of yellowtail flounder. The column headers represent the process (Rec. or M) for a given species that was estimated to have a relationship with a covariate. Text within the Ampl. Rec, Ampl M , and Ytfl Rec. columns indicates the covariate modeled to explain a particular process, where SSB refers to the other species spawning stock biomass while Rec. refers to the other species recruitment. nll represents the negative log-likelihood, k represents the number of parameters, Δ represents the difference in model criterion score from the model with the lowest model criterion score. The bolded row indicates the model with the lowest AIC and BIC.

Name	Ampl Rec.	Ampl M	Ytfl Rec.	nll	k	AIC	BIC	Δ AIC	Δ BIC
MS1				1035	70	2211	2549	0	0
MS2	SSB			1035	72	2214	2562	3	13
MS3	Rec.			1035	72	2213	2561	2	12
MS4			SSB	1034	72	2213	2560	2	11
MS5			Rec.	1039	72	2223	2570	12	21
MS6		SSB		1227	72	2598	2946	387	397
MS7	SSB		SSB	1034	74	2216	2574	5	25
MS8	Rec.		Rec.	1033	74	2215	2572	4	23
MS9		SSB	SSB	1226	74	2600	2957	389	408
MS10		SSB	Rec.	1228	74	2605	2962	394	413

5.6 List of Figures

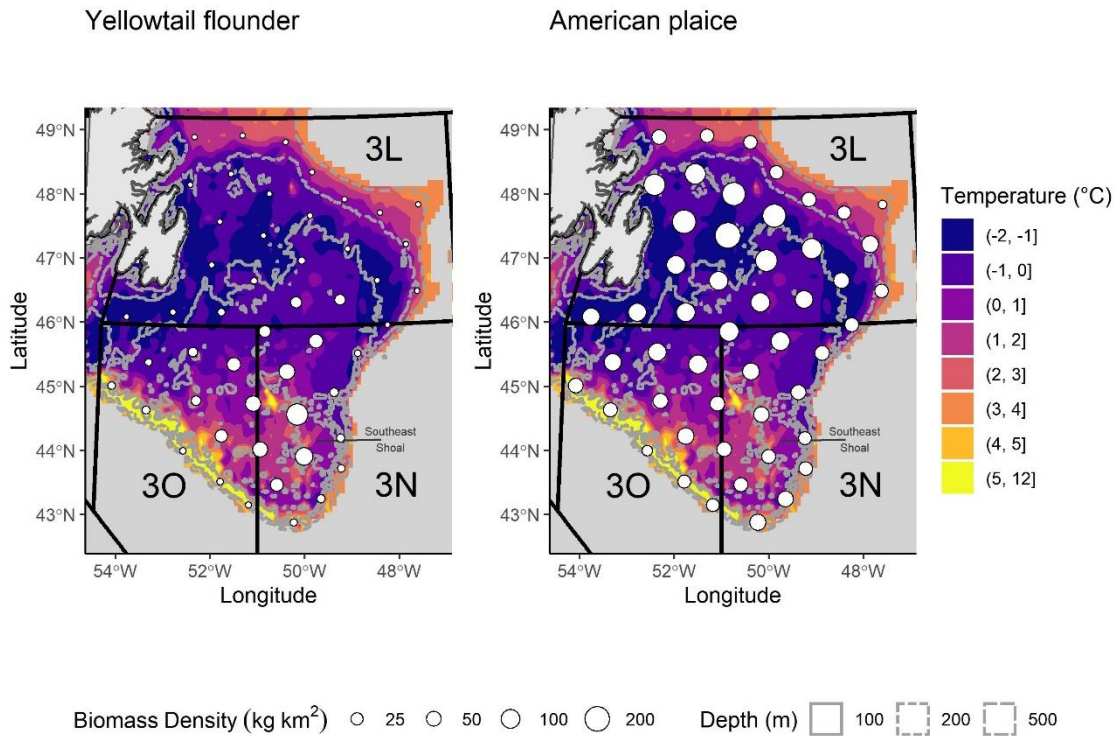


Figure 5.1 Mean historical distribution (1985-1989) of NAFO Divisions 3LNO yellowtail flounder and American plaice overlaid on spring bottom water temperatures from the same time-period. Circle size represents biomass density (kg km⁻²) estimates for each stock estimated using VAST models in Robertson et al., (2021). Spring bottom temperatures were derived from all available temperature profiles collected annually (e.g., DFO monitoring programs, international oceanographic campaigns, Argo program) between April and June on a regular 0.1° x 0.1° (latitudinal x longitudinal) grid using a linear interpolation method introduced in Cyr et al. (2019).

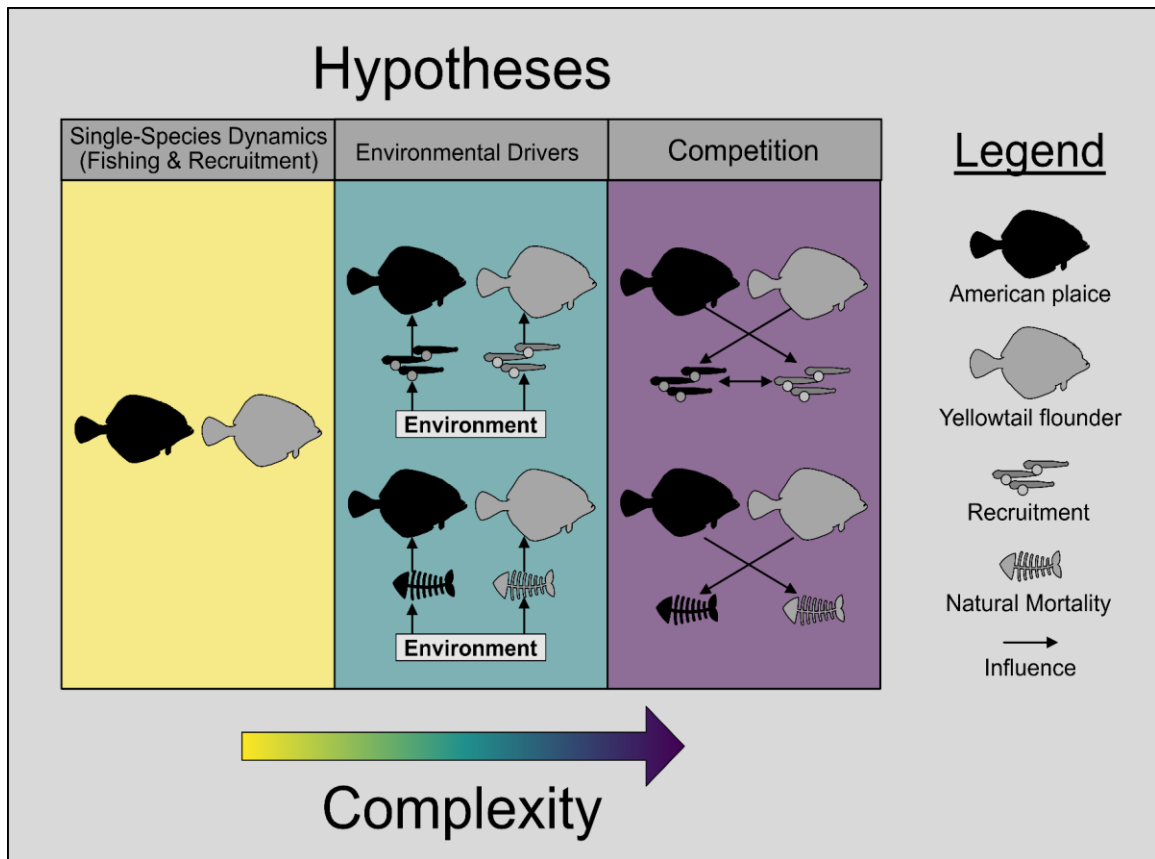


Figure 5.2 Conceptual diagram of the process of extending and comparing population dynamics models of increasing complexity.

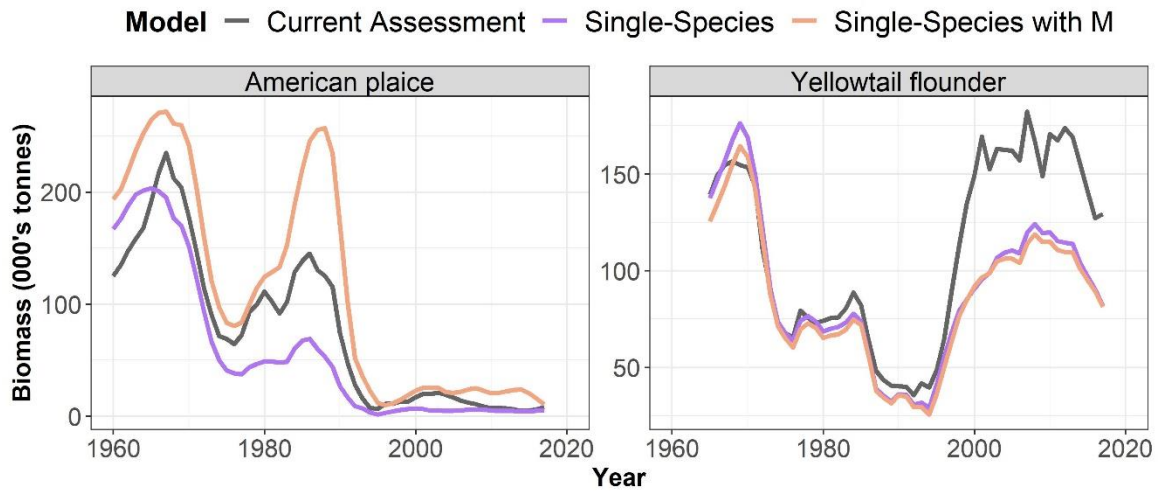


Figure 5.3 Model comparisons between spawning stock biomass (American plaice) or biomass (yellowtail flounder) from the current stock assessment (grey lines) to the single-species model (purple lines; YTFL1 & AMPL1 from Table 5.1), and the single-species model with M deviations (orange lines; AMPL2 & YTFL2 from Table 5.1).

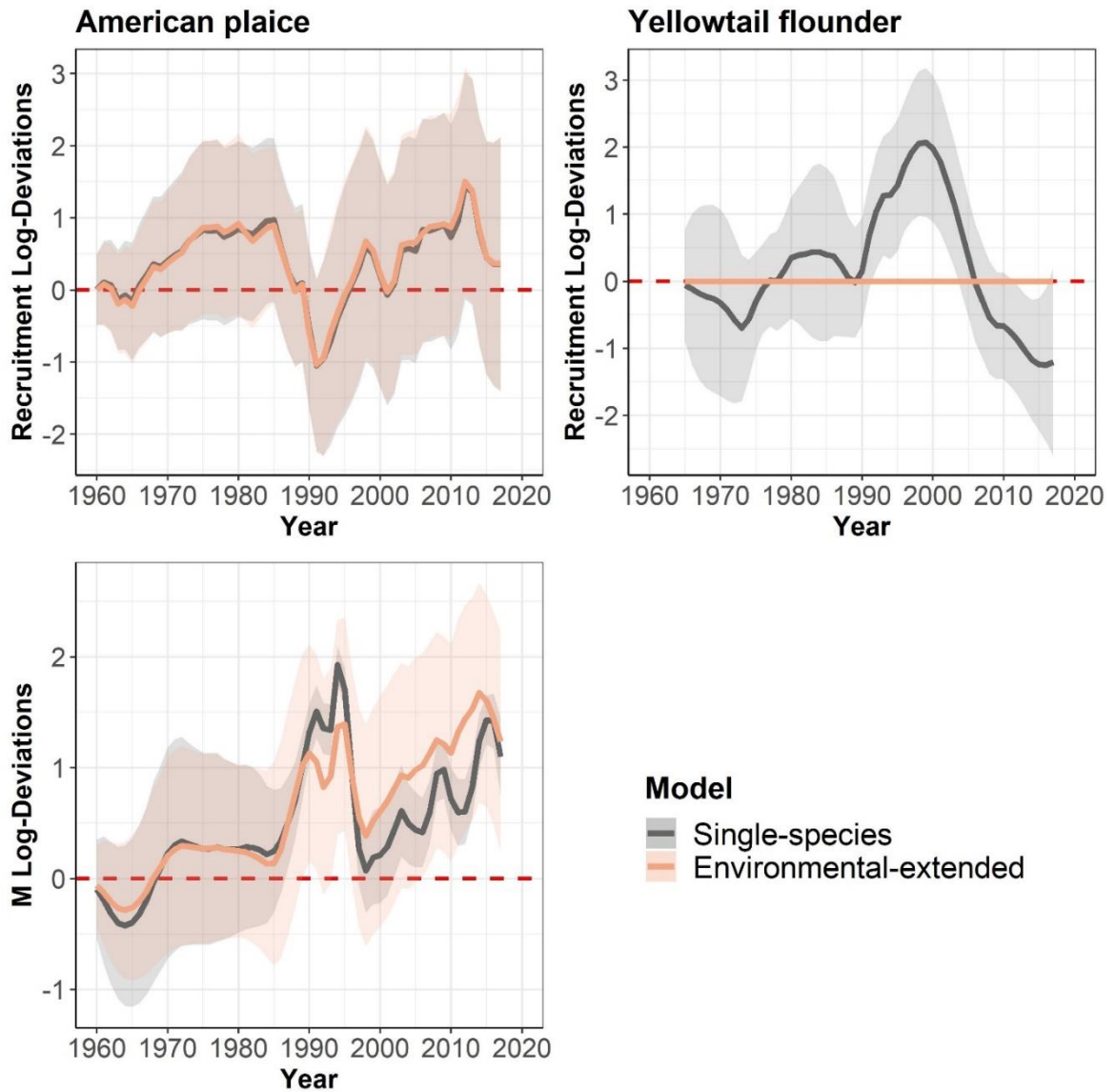


Figure 5.4 Comparison of deviation parameters (recruitment and M) between the best performing non-extended models (orange lines; AMPL2, YTF1) and the best performing extended models (grey lines; AMPLE6, YTFLE1). 95% confidence interval for estimates from best performing extended models are shown as grey polygons.

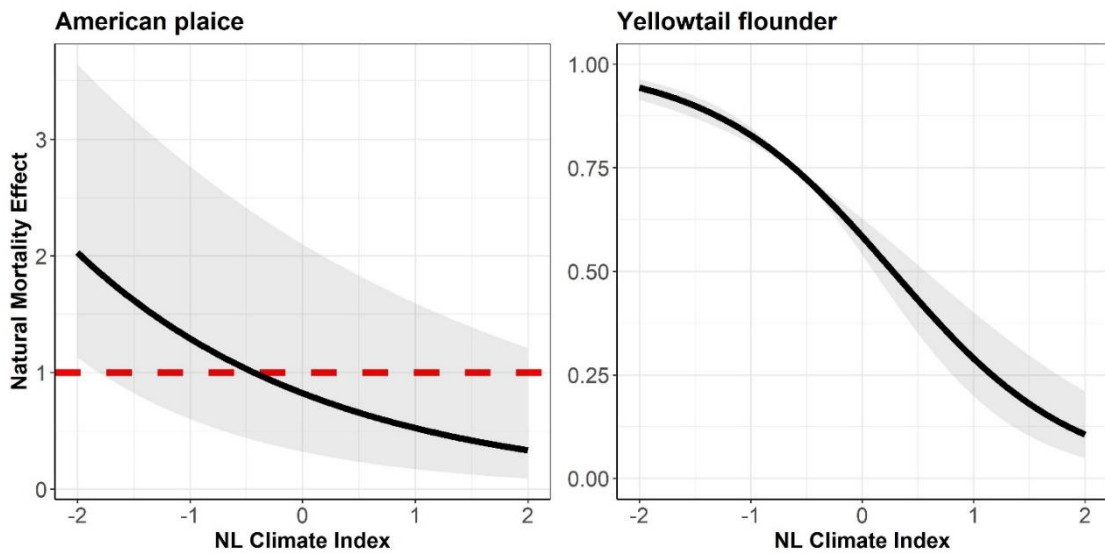


Figure 5.5 Estimates of the effects (black lines) and 95% confidence intervals (grey polygons) of environmental covariates for AMPLE6 and YTFLE1. The red dashed line in the American plaice panel represents 1, which would indicate no effect on M since the effect is multiplicative.

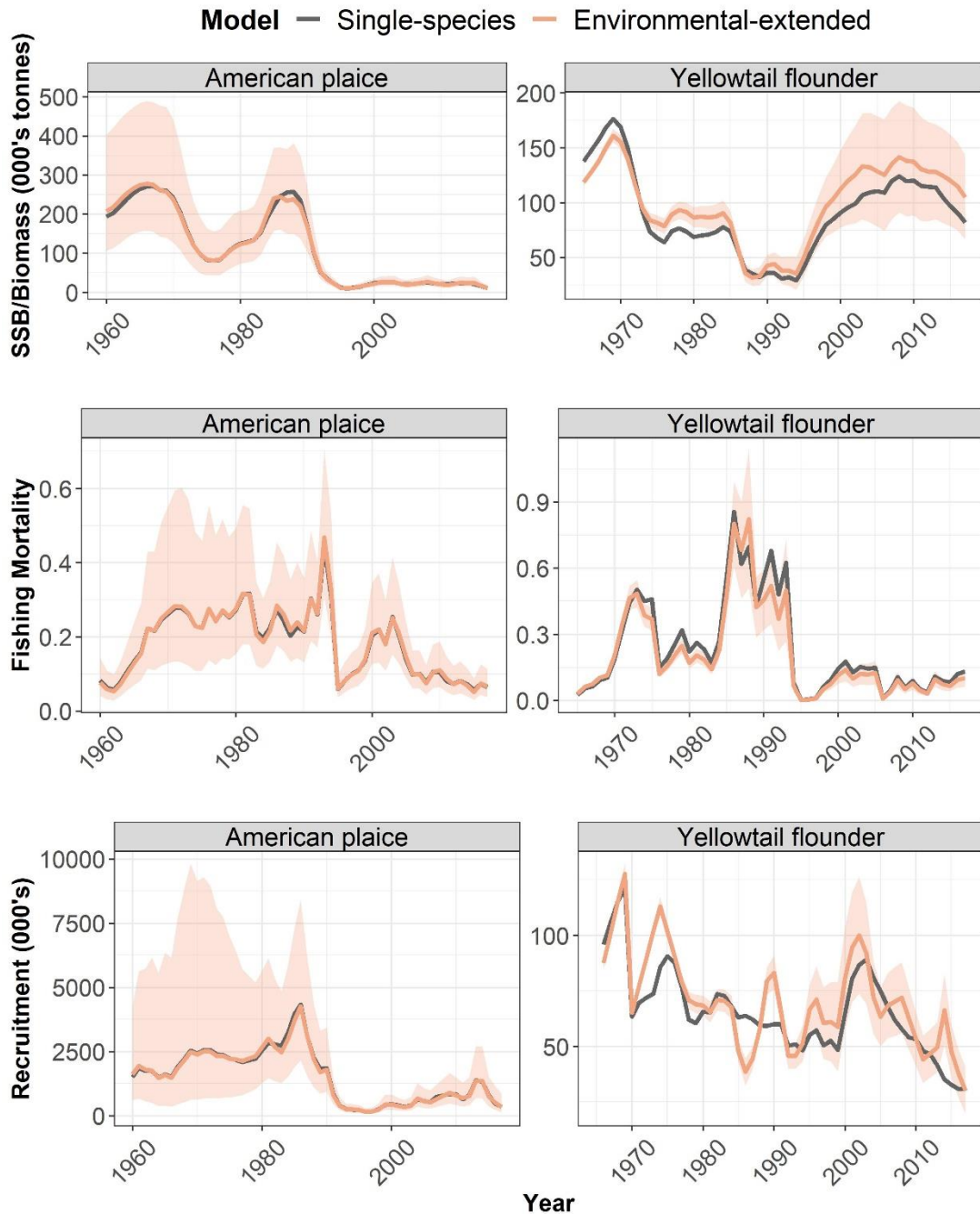


Figure 5.6 Comparison of SSB/biomass estimates and fishing mortality between the best performing non-extended models (grey lines; AMPL2, YTFL1) and the best performing extended models (orange lines; AMPLE6, YTFLE1). 95% confidence interval for estimates from best performing extended models are shown as orange polygons. Estimates of SSB are shown for American plaice while yellowtail flounder estimates are for biomass. Fishing mortality estimates for American plaice are averaged from ages 9-14 years.

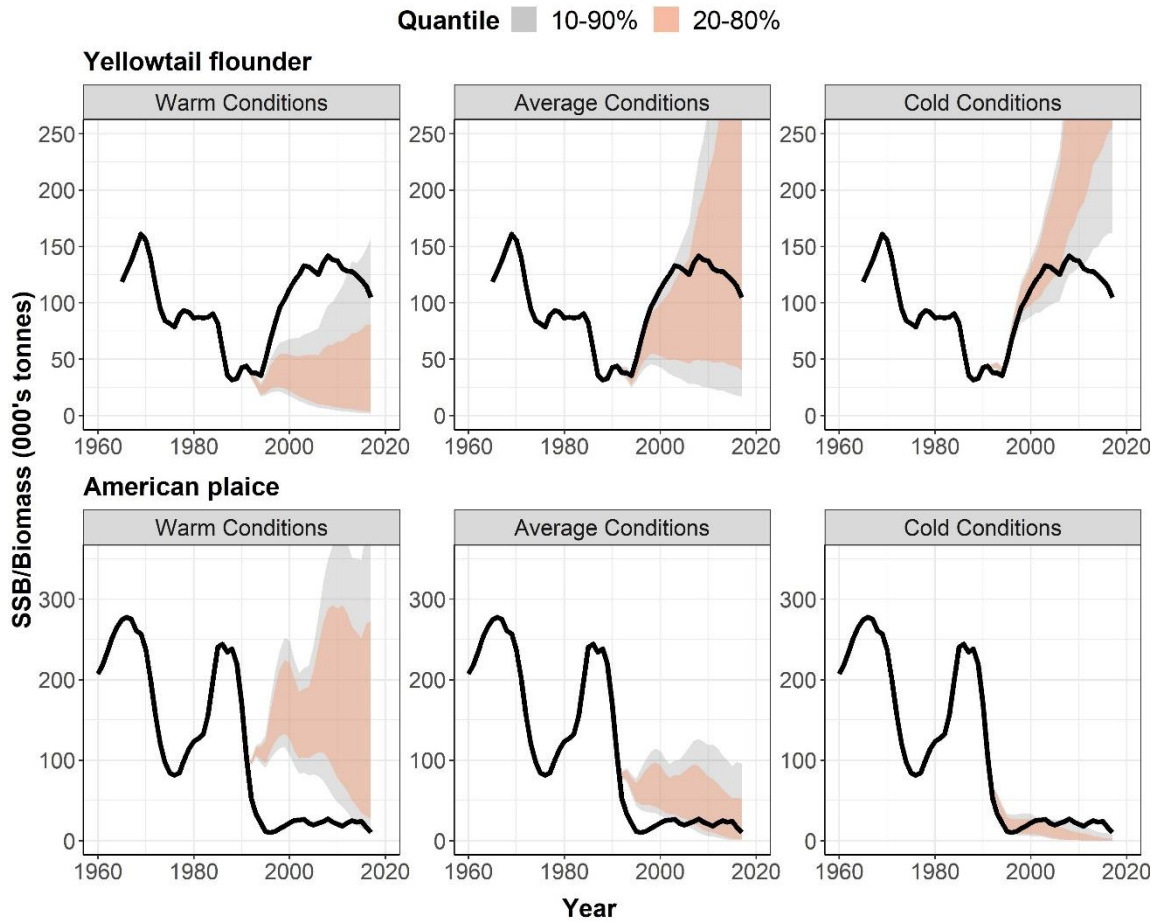


Figure 5.7 Simulations of how population dynamics would have differed if their environmental drivers followed different trajectories from 1992 onwards. The polygons represent the 20-80% (orange) and 10-90% quantiles (grey) of dynamics from 1,000 simulations. The different trajectories are based on the starting value of the random walk for the environmental covariates in each simulation. Since environmental covariates were scaled, -1 was used for lower values (left panels), 0 was used for average values (middle panels), and 1 was used higher values (right panels).

6 General Conclusions

6.1 Thesis Overview

The central objective of this thesis was to investigate the interactive effects of overfishing and environmental variability on fish population recovery. This objective was addressed by exploring the differential recovery trajectories of yellowtail flounder (*Limanda ferruginea*) and American plaice (*Hippoglossoides platessoides*) populations on the Newfoundland Grand Banks (Northwest Atlantic Fisheries Organization [NAFO] Divisions 3LNO). In Chapter Two, I modeled the spatial distribution of bottom water temperatures, yellowtail flounder, and American plaice populations over a 30-year period. The results showed that anomalous cold water across the Grand Banks in the early 1990s shifted the distributions of both species southwards and that neither species responded to the subsequent increasing temperatures linearly. Chapter Three focused on the development of a model to estimate prey dynamics while accounting for the predator functional response, which was tested on a case study of northern sand lance on the Grand Banks. The model outperformed prior models that had been used and estimated that sand lance, an important forage fish prey species for American plaice, has exhibited oscillatory dynamics over time. In Chapter Four, I explored whether there is evidence that natural mortality has been a primary driver of juvenile American plaice population dynamics since the 1990s. Model selection using various parameterizations of a juvenile metapopulation dynamics model indicated that although estimating natural mortality improved model fit, it was not a primary driver of juvenile dynamics. Instead, juvenile American plaice population dynamics were primarily influenced by recruitment. Finally, Chapter Five focused on developing a modeling framework to use models of increasingly

complexity to underscore the importance of incorporating various population and ecosystem processes in population dynamics models. Using the case study of differential recovery of American plaice and yellowtail flounder populations on the Grand Banks, the results indicated that yellowtail flounder population dynamics were primarily driven by recruitment variability, which was negatively affected by the Newfoundland and Labrador (NL) Climate Index. Meanwhile, American plaice population dynamics were affected by a combination of temporal variability in recruitment and natural mortality, where natural mortality was negatively affected by the NL Climate Index. Throughout this discussion, I will focus on the overall themes of this thesis to describe how the findings will impact regional fisheries management and future research on the interactive effects of fishing pressure and environmental variability for rebuilding fisheries.

6.2 Implications for Regional Fisheries Management

This thesis focused on analyzing the collapse and recovery of two flatfish populations that had been overfished for decades. Although I primarily focused on identifying the role of environmental variability in population collapse and recovery, or lack thereof, the population trajectories of yellowtail flounder and American plaice would have been substantially different had the populations been harvested at a more sustainable rate in the years prior to their collapse. For example, yellowtail flounder stock recovery occurred shortly after the implementation of a directed fishing moratorium and when the moratorium was lifted, several new fisheries management measures were implemented (e.g., mandatory observer coverage, gear modifications, seasonal and spatial closures; Brodie et al., 2010). The improvements in stock health following the implementation of

these fisheries management measures is indicative that prior management measures were not adequate, even if some of the recovery can be explained by the presence of beneficial environmental conditions. Additionally, there is evidence that growth and maturity of these stocks were modified during a period of overfishing (Morgan and Colbourne 1999; Walsh and Morgan 1999; Barot et al. 2005; Zheng et al. 2020b). These types of fisheries induced reductions in population size and modifications to stock vital rates likely made these stocks more susceptible to environmental variability.

Incorporating the effects of environmental variability into stock assessment advice requires a combination of ecological and population dynamics research. I attempted to accomplish this by focusing Chapters Two and Three on ecological questions regarding the influence of temperature on spatial distributions and the influence of prey availability on the rate of consumption, while Chapters Four and Five assessed variability in population dynamics processes and how they may have been influenced by the environment. This combination of approaches is necessary because identifying causal relationships between environmental drivers and population dynamics is desired if those environmental drivers are to affect fisheries management decision making (Sugihara et al. 2012; Link et al. 2020). Given that the most important environmental influence on the population dynamics of both stocks examined in Chapter Five was determined to be an integrated index of the regional climate, further research regarding the causal relationships between components of the environment and hypothesized population dynamics processes is necessary. For example, a greater understanding of the relationship between the timing of phytoplankton and zooplankton blooms and recruitment success

would generate an improved causal link between the NL Climate Index and 3LNO yellowtail flounder recruitment. However, despite lacking a complete causal understanding of the effects of climate on population dynamics, there is strong evidence that the environment has influenced these stocks and therefore, including environmental considerations in their management is warranted.

Canadian stock assessments are increasingly considering environmental conditions, however, the quantitative and qualitative inclusion of environmental conditions still occurs in <40% of assessments and often follow ad-hoc approaches (Kulka et al. 2022; Pepin et al. 2022). There are many reasons for this lack of inclusion, including a lack of mechanistic understanding regarding the impact of the environment on short term management advice (Kulka et al. 2022). However, the fisheries management process in Canada also lacks a clear framework for systematically considering ecosystem and climate-induced effects on fisheries (Boyce et al. 2021). Since these ecosystem factors can substantially affect stock productivity and represent a large source of uncertainty, foregoing their inclusion will minimize the efficacy of the precautionary approach decision-making framework (DFO 2021). Therefore, developing a framework for incorporating ecosystem considerations at different points in the fisheries management process should improve management outcomes (Boyce et al. 2020; Duplisea et al. 2021; Link et al. 2021).

A framework was recently developed to incorporate ecosystem advice in NAFO, the Regional Fisheries Management Organization (RFMO) for the northwest Atlantic (Koen-Alonso et al. 2019). This framework is separated into three primary tiers: 1)

ecosystem-state assessments, 2) multispecies assessments, and 3) single-species assessments. NAFO Division 3LNO yellowtail flounder and American plaice populations occur within and outside of the Canadian Exclusive Economic Zone (EEZ) and are therefore managed by NAFO, and the work conducted within this thesis will primarily contribute to the scientific understanding of the second and third tiers described in the NAFO framework. Much of this thesis focused on furthering the single-species assessment tier by examining environmental sources of mortality, recruitment, and shifts in spatial distribution. However, Chapter Three contributed to the multispecies tier by examining the predation process of Atlantic cod and American plaice on northern sand lance, while Chapter Five examined the possibility of competitive multispecies interactions between American plaice and yellowtail flounder. In addition to providing further scientific exploration of ecosystem-based questions relevant for NAFO management, the results from Chapter Two indicated rapidly shifting spatial distributions for both stocks which may affect ecological community structure and catch shares for components of these stocks that persist outside of the Canadian EEZ. For example, the shifts in distribution that were observed for American plaice have likely resulted in a larger relative proportion of the stock being available for harvest outside of the EEZ, which is represented by the larger proportion of bycatch by non-Canadian fisheries in recent years (COSEWIC 2009; Wheeland et al. 2021). These types of changes are likely to become more prevalent among managed stocks in the future as more stocks modify their spatial distributions to keep pace with climate change (Pinsky et al. 2020). Therefore, continuing to develop and implement ecosystem-based fisheries management approaches in RFMOs will likely be necessary to recognize changes and ensure that

management advice is capable of being modified accordingly (Pentz et al. 2018; Pinsky et al. 2018).

6.3 Implications for Rebuilding Fisheries

This thesis reveals further evidence that fishing pressure and environmental variability interactively affect fish stock collapse and recovery. Despite indications that reducing fishing pressure can promote population rebuilding following overfishing and collapse (Hilborn et al. 2020), the population and ecosystem level change induced by fishing can yield substantial variability in population responses to rebuilding strategies (Frank et al. 2022). Unfortunately, accounting for this variability is complicated by selective harvesting and environmental variability inducing similar changes to fish populations (e.g., modifications to growth, maturity, spatial distributions) and communities (Planque et al. 2010; Bell et al. 2015). As a result, applications of ecosystem-based fisheries management often require methods capable of disentangling of the relative effects of top-down (including fishing mortality) and bottom-up processes on population dynamics (Link et al. 2021). For example, in Chapter Two, I examined how bottom water temperatures may have influenced the spatial distributions of the flatfish populations on the Grand Banks. Because changes in distribution can be non-additive and non-stationary (Ciannelli et al. 2012), accounting for the variability induced by fishing and the environment required a combination of density-dependent and density-independent analytical approaches. Although I identified that bottom water temperatures have modified the distribution of American plaice and yellowtail flounder, this relationship was influenced by degradation to the spatial structure of the stocks through

decades of overharvesting. The presence of such non-additive and non-stationary effects of fishing and environmental change indicate that disentangling the relative effects of top-down and bottom-up processes will always be complex.

The effects of interactions between fishing and environmental variability on population recovery depend on population and ecosystem context (e.g., life history strategies, habitat use, and food web interactions; Stier et al. 2016). For example, fisheries-induced selection and warming temperatures can induce faster growth (Neuheimer and Taggart 2007; Heino et al. 2015; Pauly 2021). However, many overfished species, including American plaice and yellowtail flounder, have slow life history strategies (e.g., slow growth rates, larger size at maturity) which inherently tend to recover at slower rates than species with fast life history strategies (Denney et al. 2002; Neubauer et al. 2013). Additionally, population growth and recovery can be constrained by habitat availability (Fahrig 2001). This is particularly of interest with ongoing global climate change, where warming waters are reducing available habitat for marine species (Deutsch et al. 2015; Boyce et al. 2022). The impacts of reductions in habitat availability may be strongest for species with limited mobility or dispersal (Angert et al. 2011; Sunday et al. 2015). For instance, the cold temperatures that covered the Grand Banks in the 1990s may have had a large effect on American plaice not only due to how temperatures modified total habitat availability, but also because American plaice are relatively sedentary (Morgan 1996) and may not have been able to easily migrate to warmer waters. Furthermore, following shifts to the southern Grand Banks, American plaice have yet to substantially recolonize the northern Grand Banks, which was a

historical center of productivity. Although yellowtail flounder are also relatively sedentary (Morgan and Walsh 1996; Walsh et al. 2001), Chapter Two showed that cold water induced modifications to their habitat were not as dramatic and generally resulted in contraction towards their preferred habitat, potentially improving their likelihood of recovery in comparison to American plaice. When communities undergo shifts in the relative abundance and spatial distributions of their component species, as occurred on the Grand Banks in the 1990s (Dawe et al. 2012; Dempsey et al. 2018), the number and strength of species interactions (e.g., predation, competition) will be modified (Bartley et al. 2019; D’Alelio et al. 2019). These shifts in interactions may further affect population recovery (Gilman et al. 2010). For example, the southward shift of American plaice may have modified interactions with prey and competitor species based on changes to spatial overlap. Our understanding of marine food webs are often limited due to difficulties associated with collecting empirical data on interactions (Libralato et al. 2014). Therefore, as novel methods of data collection continue to emerge (Nielsen et al. 2018; Pethybridge et al. 2018; McCormack et al. 2019), continued research on the impact of species interaction shifts in marine food webs may promote a better understanding about discrepancies between population recovery for similar species. Overall, research on population and ecosystem context can be used to inform which ecosystem components may be most influential on population dynamics.

State-space population dynamics models (i.e., models that separate measurement and process error) allow estimation of time-varying processes (Cadigan 2015; Pedersen and Berg 2017). Although estimating time-varying processes can increase model

complexity, they can also improve estimates by incorporating mechanistic drivers of changes in productivity (Collie et al. 2016; Holt and Michielsens 2020; Zhang et al. 2021b). Extensions of single-species stock assessments to include these mechanistic drivers have often focused on estimating time-varying predation mortality (Lewy and Vinther 2004; Howell et al. 2021), while the inclusion of bottom-up effects has generally been limited to relationships with recruitment or catchability (Haltuch et al. 2019; Marshall et al. 2019). However, bottom-up processes can have a larger influence on population dynamics processes other than recruitment (e.g., growth, natural mortality, maturity; Lorenzen, 2016; Rice, 2011). With the increasing capacity of integrated stock assessment models to estimate time-varying processes (Cadrin et al., 2020; Lorenzen, 2016; Punt et al., 2020), the inclusion of relationships between the environment and population dynamics are becoming possible (Lee et al. 2018; Plagányi et al. 2022). For example, by estimating natural mortality over time, Chapter Five identified that American plaice population dynamics had been affected by a relationship between climatological conditions and natural mortality. This conclusion could not have been reached by using a population dynamics model with assumed stationary natural mortality or by only examining the relationship between environmental variability and recruitment. Therefore, continued progress on estimating time-varying population dynamics processes within stock assessments may increase the possibility of identifying more robust relationships with the environment.

The inclusion of environmental drivers in fisheries management advice often requires determining whether evidence of a relationship between an environmental

variable and population productivity crosses a sufficient threshold (Klaer et al. 2015; Link et al. 2021). Requiring some threshold level of evidence may ensure that fisheries management does not continually shift baselines of productivity and thereby produce inappropriate reference points (Pauly 1995; Schijns and Pauly 2021; Leadbitter et al. 2022). However, determining the required threshold of evidence and how it may be represented to inform fisheries management decisions likely cannot be generalized across systems (Fu et al. 2020; Hillebrand et al. 2020). As a result, there have been increasing calls for incorporating environmental considerations as a potential source of uncertainty that may affect the risks associated with management decisions. These approaches include ensemble models, climate change conditioned advice, and using environmentally-driven operating models in management strategy evaluation (Brodziak and Piner 2010; Punt et al. 2016; Duplisea et al. 2021; Jacobsen et al. 2021; Jardim et al. 2021). The modeling framework that I developed in Chapter Five adds a potential method for directly comparing a range of hypothesised sources of uncertainty on current population status. Although my framework contains unique components to address population and ecosystem processes, each approach recognizes that population dynamics modeling choices can be used to represent varying sources of uncertainty (including environmental uncertainty) regarding how or why a population changes over time. These sources of uncertainty can then be used to evaluate their potential effects on management outcomes. In general, although these approaches require some degree of process-based understanding of the relationship between an environmental variable and population productivity, they can be used to broadly consider the implications of management

decisions in the context of environmental variability without requiring the definition of a threshold of evidence for the environmental drivers.

In conclusion, this thesis analysed differential population recovery for two collapsed stocks on the Newfoundland Grand Banks to describe the interactive effects of overfishing and environmental variability on fish population recovery. By applying various ecological and population dynamics based approaches, I disentangled the effects of fishing and environmental variability on collapse and recovery. Results indicated that although overfishing was important in the collapse of these stocks, environmental variability also contributed to their collapse and differential recovery trajectories. Specifically, my thesis provided evidence that the cold temperatures that covered the Grand Banks in the late 1980s – early 1990s influenced the spatial distributions, recruitment, and natural mortality of these stocks. These analyses contribute to the ongoing development of ecosystem-based fisheries management in Canadian and regional (i.e., NAFO) fisheries management organizations and indicate that including climate considerations for these stocks may yield more precautionary management advice. Furthermore, this thesis fits within the growing body of research that the interactive, non-stationary effects of fishing and environmental variability on population dynamics are necessary to account for in fisheries management more broadly. Fisheries science that couples ecological and population dynamics research provides a more holistic understanding of fishing and environmental interactions, enriching ecosystem-informed management advice to identify appropriate rebuilding strategies for collapsed populations.

Bibliography

- Aeberhard, W.H., Flemming, J.M., and Nielsen, A. 2018. Review of State-Space Models for Fisheries Science. *Annu. Rev. Stat. Its Appl.* **5**: 215–235. doi:10.1146/annurev-statistics-031017-100427.
- Alexander, J.M., Diez, J.M., Hart, S.P., and Levine, J.M. 2016. When climate reshuffles competitors: a call for experimental macroecology. *Trends Ecol. Evol.* **31**(11): 831–841. doi:10.1016/j.tree.2016.08.003.
- Allen, C.R., Angeler, D.G., Cumming, G.S., Folke, C., Twidwell, D., and Uden, D.R. 2016. Quantifying spatial resilience. *J. Appl. Ecol.* **53**: 625–635. doi:10.1111/1365-2664.12634.
- Angert, A.L., Crozier, L.G., Rissler, L.J., Gilman, S.E., Tewksbury, J.J., and Chunco, A.J. 2011. Do species' traits predict recent shifts at expanding range edges? *Ecol. Lett.* **14**(7): 677–689. doi:10.1111/j.1461-0248.2011.01620.x.
- Araújo, M.B., and Luoto, M. 2007. The importance of biotic interactions for modelling species distributions under climate change. *Glob. Ecol. Biogeogr.* **16**(6): 743–753. doi:10.1111/j.1466-8238.2007.00359.x.
- Arditi, R., and Ginzburg, L.R. 2012. How species interact: altering the standard view on trophic ecology. Oxford University Press.
- Barot, S., Heino, M., Morgan, M.J., and Dieckmann, U. 2005. Maturation of Newfoundland American plaice (*Hippoglossoides platessoides*): Long-term trends in maturation reaction norms despite low fishing mortality? *ICES J. Mar. Sci.* **62**(1): 56–64. doi:10.1016/j.icesjms.2004.10.004.
- Bartley, T.J., McCann, K.S., Bieg, C., Cazelles, K., Granados, M., Guzzo, M.M., MacDougall, A.S., Tunney, T.D., and McMeans, B.C. 2019. Food web rewiring in a changing world. *Nat. Ecol. Evol.* **3**(3): 345–354. doi:10.1038/s41559-018-0772-3.
- Baum, J.K., and Worm, B. 2009. Cascading top-down effects of changing oceanic predator abundances. *J. Anim. Ecol.* **78**(4): 699–714. doi:10.1111/j.1365-2656.2009.01531.x.
- Bélangier, D., Pepin, P., and Maillet, G. 2021. Biogeochemical oceanographic conditions in the Northwest Atlantic (NAFO subareas 2-3-4) during 2020. *NAFO Sci. Council. Res. Doc.* **21/010**(N7177): 1–24.
- Bell, R.J., Richardson, D.E., Hare, J.A., Lynch, P.D., and Fratantoni, P.S. 2015. Disentangling the effects of climate, abundance, and size on the distribution of marine fish: an example based on four stocks from the Northeast US shelf. *ICES J. Mar. Sci.* **72**(5): 1311–1322.
- Berger, A.M. 2019. Character of temporal variability in stock productivity influences the utility of dynamic reference points. *Fish. Res.* **217**(July 2018): 185–197. Elsevier.

doi:10.1016/j.fishres.2018.11.028.

- Berkeley, S., Hixon, M., Larson, R., and Love, M. 2004. Fisheries sustainability via protection of age structure and spatial distribution of fish populations. *Fisheries* **29**: 23–32.
- Blanchard, J.L., Dulvy, N.K., Jennings, S., Ellis, J.R., Pinnegar, J.K., Tidd, A., and Kell, L.T. 2005. Do climate and fishing influence size-based indicators of Celtic Sea fish community structure? *ICES J. Mar. Sci.* **62**(3): 405–411. doi:10.1016/j.icesjms.2005.01.006.
- Borregaard, M., and Rahbek, C. 2010. Causality of the relationship between geographic distribution and species abundance. *Q. Rev. Biol.* **85**(1): 3–25.
- Boyce, D.G., Fuller, S., Karbowski, C., Schleit, K., and Worm, B. 2021. Leading or lagging: How well are climate change considerations being incorporated into canadian fisheries management? *Can. J. Fish. Aquat. Sci.* **78**(8): 1120–1129. doi:10.1139/cjfas-2020-0394.
- Boyce, D.G., Schleit, K., and Fuller, S. 2020. Incorporating climate change into fisheries management in Atlantic Canada and the Eastern Arctic. Halifax, Nova Scotia, Canada.
- Boyce, D.G., Tittensor, D.P., Garilao, C., Henson, S., Kaschner, K., Kesner-Reyes, K., Pigot, A., Reyes, R.B., Reygondeau, G., Schleit, K.E., Shackell, N., Sorongon-Yap, P., and Worm, B. 2022. A climate risk index for marine life. *Nat. Clim. Chang.* **12**(9): 854–862. Springer US. doi:10.1038/s41558-022-01437-y.
- Brodie, W., Walsh, S.J., and Parsons, D.M. 2010. An evaluation of the collapse and recovery of the yellowtail flounder (*Limanda ferruginea*) fishery on the Grand Bank. *ICES J. Mar. Sci.* **67**(9): 1887–1895. doi:10.1016/j.seares.2003.08.004.
- Brodie, W.B. 2002. American Plaice *Hippoglossoides platessoides* on the Grand Bank (NAFO Divisions 3LNO) – a Review of Stock Structure in Relation to Assessment of the Stock.
- Brodziak, J., and Legault, C.M. 2005. Model averaging to estimate rebuilding targets for overfished stocks. *Can. J. Fish. Aquat. Sci.* **62**(3): 544–562. doi:10.1139/f04-199.
- Brodziak, J., and Piner, K. 2010. Model averaging and probable status of north pacific striped marlin, *Tetrapturus audax*. *Can. J. Fish. Aquat. Sci.* **67**(5): 793–805. doi:10.1139/F10-029.
- Buchheister, A., and Latour, R.J. 2015. Dynamic trophic linkages in a large estuarine system – support for supply-driven dietary changes using delta generalized additive mixed models. *Can. J. Fish. Aquat. Sci.* **73**(1): 5–17.
- Buren, A.D., Koen-Alonso, M., and Stenson, G.B. 2014. The role of harp seals, fisheries and food availability in driving the dynamics of northern cod. *Mar. Ecol. Prog. Ser.* **511**: 265–284. doi:10.3354/meps10897.

- Burrows, M.T., Schoeman, D.S., Buckley, L.B., Moore, P., Poloczanska, E.S., Brander, K.M., Brown, C., Bruno, J.F., Duarte, C.M., Halpern, B.S., Holding, J., and Kappel, C. V. 2011. The pace of shifting climate in marine and terrestrial ecosystems. *Science*. **334**(6056): 652–656. doi:10.1126/science.1210288.
- Caddy, J.F., and Agnew, D.J. 2005. An overview of recent global experience with recovery plans for depleted marine resources and suggested guidelines for recovery planning. *Rev. Fish Biol. Fish.* **15**(1–2): 165. doi:10.1007/s11160-005-4305-1.
- Cadigan, N.G. 2015. A state-space stock assessment model for northern cod, including under-reported catches and variable natural mortality rates. *Can. J. Fish. Aquat. Sci.* **73**(2): 296–308.
- Cadigan, N.G., Robertson, M.D., Nirmalkanna, K., and Zheng, N. 2022. The complex relationship between weight and length of Atlantic cod off the south coast of Newfoundland. *Can. J. Fish. Aquat. Sci.*: 1–33. doi:10.1139/cjfas-2021-0325.
- Cadrin, S.X., Maunder, M.N., and Punt, A.E. 2020. Spatial Structure: Theory, estimation and application in stock assessment models. *Fish. Res.* **229**. doi:10.1016/j.fishres.2020.105608.
- Charbonneau, J.A., Keith, D.M., MacNeil, M.A., and Hutchings, J.A. 2022. Effects of fishing mortality on the age structure of marine fishes. *Can. J. Fish. Aquat. Sci.* **2236**: 2225–2236. doi:10.1139/cjfas-2021-0338.
- Chen, I.C., Hill, J.K., Ohlemüller, R., Roy, D.B., and Thomas, C.D. 2011. Rapid range shifts of species associated with high levels of climate warming. *Science*. **333**(6045): 1024–1026. doi:10.1126/science.1206432.
- Cheung, W.W.L., Lam, V.W.Y., Sarmiento, J.L., Kearney, K., Watson, R., and Pauly, D. 2009. Projecting global marine biodiversity impacts under climate change scenarios. *Fish Fish.* **10**(3): 235–251. doi:10.1111/j.1467-2979.2008.00315.x.
- Chaine, I. 2010. Why does phenology drive species distribution? *Philos. Trans. R. Soc. B Biol. Sci.* **365**(1555): 3149–3160. doi:10.1098/rstb.2010.0142.
- Ciannelli, L., Bartolino, V., and Chan, K.S. 2012. Non-additive and non-stationary properties in the spatial distribution of a large marine fish population. *Proc. R. Soc. B Biol. Sci.* **279**(1743): 3635–3642. doi:10.1098/rspb.2012.0849.
- Ciannelli, L., Fisher, J.A.D., Skern-Mauritzen, M., Hunsicker, M.E., Hidalgo, M., Frank, K.T., and Bailey, K.M. 2013. Theory, consequences and evidence of eroding population spatial structure in harvested marine fishes: A review. *Mar. Ecol. Prog. Ser.* **480**: 227–243. doi:10.3354/meps10067.
- Colbourne, E. 2000. Interannual variations in the stratification and transport of the Labrador Current on the Newfoundland Shelf. *ICES Counc. Meet.* **2000**(2): 1–20.
- Colbourne, E., Holden, J., Snook, S., Lewis, S., Cyr, F., Senciall, D., Bailey, W., and Higdon, J. 2018. Physical oceanographic environment on the Newfoundland and

- Labrador Shelf in NAFO subareas 2 and 3 during 2017. NAFO SCR Doc **18**(009): 40.
- Colbourne, E., Narayanan, S., and Prinsenberg, S. 1994. Climatic changes and environmental conditions in the Northwest Atlantic, 1970-1993. *ICES J. Mar. Sci. Symp.* **198**: 311–322.
- Collie, J., Bell, R.J., Collie, S.B., Minto, C., Conservancy, T.N., and Road, S.F. 2021. Harvest strategies for climate-resilient fisheries. *ICES J. Mar. Sci.* **78**(8): 2774–2783. Oxford University Press.
- Collie, J., Rochet, M., and Bell, R.J. 2013. Rebuilding fish communities : the ghost of fisheries past and the virtue of patience. *Ecol. Appl.* **23**(2): 374–391. doi:10.1890/12-0877.1.
- Collie, J.S., Botsford, L.W., Hastings, A., Kaplan, I.C., Largier, J.L., Livingston, P.A., Plagányi, É., Rose, K.A., Wells, B.K., and Werner, F.E. 2016. Ecosystem models for fisheries management: Finding the sweet spot. *Fish Fish.* **17**(1): 101–125. doi:10.1111/faf.12093.
- Connell, J.H., and Slatyer, R.O. 1977. Mechanisms of succession in natural communities and their role in community stability and organization. *Am. Nat.* **111**(982): 1119–1144. doi:10.1086/283241.
- COSEWIC. 2009. COSEWIC assessment and status report on the American Plaice *Hippoglossoides platessoides*, Maritime population, Newfoundland and Labrador population and Arctic population, in Canada. Ottawa.
- Cushing, D. 1975. *Marine ecology and fisheries*. Cambridge University Press.
- Cyr, F., and Galbraith, P.S. 2021. A climate index for the Newfoundland and Labrador shelf. *Earth Syst. Sci. Data* **13**: 1807–1828. doi:https://doi.org/10.5194/essd-13-1807-2021.
- D’Alelio, D., Hay Mele, B., Libralato, S., Ribera d’Alcalà, M., and Jordán, F. 2019. Rewiring and indirect effects underpin modularity reshuffling in a marine food web under environmental shifts. *Ecol. Evol.* **9**(20): 11631–11646. doi:10.1002/ece3.5641.
- Davies, R.W.D., and Rangeley, R. 2010. Banking on cod: Exploring economic incentives for recovering Grand Banks and North Sea cod fisheries. *Mar. Policy* **34**(1): 92–98. Elsevier. doi:10.1016/j.marpol.2009.04.019.
- Davis, M.B., and Shaw, R.G. 2001. Range shifts and adaptive responses to quaternary climate change. *Science*. **292**(5517): 673–679. doi:10.1126/science.292.5517.673.
- Davoren, G.K., Anderson, J.T., and Montevecchi, W.A. 2006. Shoal behaviour and maturity relations of spawning capelin (*Mallotus villosus*) off Newfoundland: Demersal spawning and diel vertical movement patterns. *Can. J. Fish. Aquat. Sci.* **63**(2): 268–284. doi:10.1139/f05-204.

- Dawe, E.G., Koen-Alonso, M., Chabot, D., Stansbury, D., and Mullooney, D. 2012. Trophic interactions between key predatory fishes and crustaceans: Comparison of two Northwest Atlantic systems during a period of ecosystem change. *Mar. Ecol. Prog. Ser.* **469**: 233–248. doi:10.3354/meps10136.
- Delong, J.P., and Vasseur, D.A. 2011. Mutual interference is common and mostly intermediate in magnitude. *BMC Ecol.* **11**(1): 1–8.
- Dempsey, D.P., Gentleman, W.C., Pepin, P., and Koen-Alonso, M. 2018. Explanatory power of human and environmental pressures on the fish community of the Grand Bank before and after the biomass collapse. *Front. Mar. Sci.* **5**(37): 1–16. doi:10.3389/fmars.2018.00037.
- Dempsey, D.P., Koen-Alonso, M., Gentleman, W.C., and Pepin, P. 2017. Compilation and discussion of driver, pressure, and state indicators for the Grand Bank ecosystem, Northwest Atlantic. *Ecol. Indic.* **75**: 331–339. Elsevier Ltd. doi:10.1016/j.ecolind.2016.12.011.
- Denit, K. 2017. Ecosystem-based fisheries management road map. *In* National marine fisheries service procedure.
- Denney, N.H., Jennings, S., and Reynolds, J.D. 2002. Life-history correlates of maximum population growth rates in marine fishes. *Proc. R. Soc. B Biol. Sci.* **269**(1506): 2229–2237. doi:10.1098/rspb.2002.2138.
- Deriso, R. 1980. Harvesting strategies and parameter estimation for an age-structured model. *Can. J. Fish. Aquat. Sci.* **37**: 268–282.
- Deroba, J.J. 2018. Sources of variation in stomach contents of predators of Atlantic herring in the Northwest Atlantic during 1973-2014. *ICES J. Mar. Sci.* **75**(4): 1439–1450. doi:10.1093/icesjms/fsy013.
- Deutsch, C., Ferrel, A., Seibel, B., Pörtner, H.O., and Huey, R. 2015. Climate change tightens a metabolic constraint on marine habitats. *Science.* **348**(6239): 1132–1136.
- DFO. 2007. A new ecosystem science framework in support of integrated management.
- DFO. 2012. Results and recommendations from the Ecosystem Research Initiative - Newfoundland and Labrador's Expanded Research on Ecosystem Relevant but Under-Surveyed Splicers. *CSAS* **058**: 15.
- DFO. 2020. Integrated fisheries management plans: Groundfish Newfoundland and Labrador Region NAFO Subarea 2 + Divisions 3KLMNO. Available from https://www.dfo-mpo.gc.ca/fisheries-peches/ifmp-gmp/groundfish-poisson-fond/2020/groundfish-poisson-fond-2_3klmno-eng.htm.
- DFO. 2021. A fishery decision-making framework incorporating then precautionary approach. Available from <https://www.dfo-mpo.gc.ca/reports-rapports/regs/sff-cpd/precaution-back-fiche-eng.htm>.

- Donaldson, M.R., Cooke, S.J., Patterson, D.A., and Macdonald, J.S. 2008. Cold shock and fish. *J. Fish Biol.* **73**: 1491–1530. doi:10.1111/j.1095-8649.2008.02061.x.
- Doubleday, W. 1981. Manual on groundfish surveys in the Northwest Atlantic. NAFO Sci. Coun. Stud. **2**: 7–55.
- Dulvy, N.K., Rogers, S.I., Jennings, S., Stelzenmüller, V., Dye, S.R., and Skjoldal, H.R. 2008. Climate change and deepening of the North Sea fish assemblage: A biotic indicator of warming seas. *J. Appl. Ecol.* **45**(4): 1029–1039. doi:10.1111/j.1365-2664.2008.01488.x.
- Duplisea, D.E., Roux, M., Hunter, K.L., and Rice, J. 2021. Fish harvesting advice under climate change : A risk-equivalent empirical approach. *PLoS One* **16**(2): e0239503. doi:10.1371/journal.pone.0239503.
- Dwyer, K.S., Buren, A., and Koen-Alonso, M. 2010. Greenland halibut diet in the Northwest Atlantic from 1978 to 2003 as an indicator of ecosystem change. *J. Sea Res.* **64**(4): 436–445. doi:10.1016/j.seares.2010.04.006.
- Dwyer, K.S., Rideout, R., Ings, D., Power, D., Morgan, J., Brodie, B., and Healey, B.P. 2016. Assessment of American plaice in Div. 3LNO. NAFO SCS **16/30**(N6573): 1–19.
- Dwyer, K.S., Walsh, S.J., and Campana, S. 2003. Age determination, validation and growth of Grand Bank yellowtail flounder (*Limanda ferruginea*). *ICES J. Mar. Sci. J. du ...* **60**: 1123–1138. doi:10.1016/S1054.
- Eddy, T.D., Duplisea, D.E., Robertson, M.D., Ruiz-Díaz, R., Solberg, C.A., and Zhang, F. (In Press). Barriers to implementation of dynamic reference points in fisheries management. FACETS.
- Eliason, E.J., Clark, T.D., Hague, M.J., Hanson, L.M., Gallagher, Z.S., Jeffries, K.M., Gale, M.K., Patterson, D.A., Hinch, S.G., and Farrell, A.P. 2011. Differences in thermal tolerance among sockeye salmon populations. *Science*. **332**(6025): 109–112.
- Fahrig, L. 2001. How much habitat is enough? *Biol. Conserv.* **100**: 65–74.
- Fahrig, L., Lilly, G.R., and Miller, D.S. 1993. Predator stomachs as sampling tools for prey distribution: Atlantic cod (*Gadus morhua*) and capelin (*Mallotus villosus*). *Can. J. Fish. Aquat. Sci.* **50**(7): 1541–1547. doi:10.1139/f93-175.
- FAO. 2003. Fisheries management. 2. The ecosystem approach to fisheries. *In* FAO Technical Guidelines for Responsible Fisheries. Rome, Italy.
- Fey, S.B., Vasseur, D.A., Alujević, K., Kroeker, K.J., Logan, M.L., O’Connor, M.I., Rudolf, V.H.W., DeLong, J.P., Peacor, S., Selden, R.L., Sih, A., and Clusella-Trullas, S. 2019. Opportunities for behavioral rescue under rapid environmental change. *Glob. Chang. Biol.* **25**(9): 3110–3120. doi:10.1111/gcb.14712.
- Frank, K.T., Fisher, J.A.D., and Leggett, W.C. 2022. The dynamics of exploited marine

- fish populations and Humpty Dumpty : similarities and differences. *Restor. Ecol.* **e13680**. doi:10.1111/rec.13680.
- Frank, K.T., Leggett, W.C., Petrie, B.D., Fisher, J.A.D., Shackell, N.L., and Taggart, C.T. 2013. Irruptive prey dynamics following the groundfish collapse in the Northwest Atlantic: an illusion? *ICES J. Mar. Sci.* **70**(7): 1299–1307.
- Fu, C., Xu, Y., Grüss, A., Bundy, A., Shannon, L., Heymans, J.J., Halouani, G., Akoglu, E., Lynam, C.P., Coll, M., Fulton, E.A., Velez, L., and Shin, Y.J. 2020. Responses of ecological indicators to fishing pressure under environmental change: Exploring non-linearity and thresholds. *ICES J. Mar. Sci.* **77**(4): 1516–1531. doi:10.1093/icesjms/fsz182.
- Fulton, E.A., Smith, A.D.M., and Johnson, C.R. 2003. Effect of complexity on marine ecosystem models. *Mar. Ecol. Prog. Ser.* **253**: 1–16.
- Garcia, S.M., Ye, Y., Rice, J., and Charles, A. 2018. Rebuilding of marine fisheries Part 1 : Global review. *In* *FAO Fisheries and Aquaculture Technical Paper*. Rome, Italy.
- Gårdmark, A., Lindegren, M., Neuenfeldt, S., Blenckner, T., Heikinheimo, O., Müller-Karulis, B., Niiranen, S., Tomczak, M.T., Aro, E., Wikström, A., and Möllmann, C. 2013. Biological ensemble modeling to evaluate potential futures of living marine resources. *Ecol. Appl.* **23**(4): 742–754. doi:10.1890/12-0267.1.
- Garrison, L., and Link, J. 2002. Fishing effects on spatial distribution and trophic guild structure of the fish community in the Georges Bank region. *ICES J. Mar. Sci.* **57**(3): 723–730. doi:10.1006/jmsc.2000.0713.
- Gaston, K.J., Blackburn, T.I.M.M., Greenwood, J.D., Gregory, R.D., Quinn, M., and Lawton, J.H. 2000. Abundance - occupancy relationships. *J. Appl. Ecol.* **37**: 39–59.
- Geary, W.L., Bode, M., Doherty, T.S., Fulton, E.A., Nimmo, D.G., Tulloch, A.I.T., Tulloch, V.J.D., and Ritchie, E.G. 2020. A guide to ecosystem models and their environmental applications. *Nat. Ecol. Evol.* **4**: 1459–1471. Springer US. doi:10.1038/s41559-020-01298-8.
- Gibson-Reinemer, D.K., Ickes, B.S., and Chick, J.H. 2017. Development and assessment of a new method for combining catch per unit effort data from different fish sampling gears : multigear mean standardization (MGMS). *Can. J. Fish. Aquat. Sci.* **74**: 8–14.
- Gilman, S.E., Urban, M.C., Tewksbury, J., Gilchrist, G.W., and Holt, R.D. 2010. A framework for community interactions under climate change. *Trends Ecol. Evol.* **25**(6): 325–331. Elsevier Ltd. doi:10.1016/j.tree.2010.03.002.
- Goethel, D.R., Omori, K.L., Punt, A.E., Lynch, P.D., Berger, A.M., Moor, C.L. De, Plagányi, É.E., Cope, J.M., Dowling, N.A., MCGarvey, R., Preece, A.L., Thorson, J.T., Chaloupka, M., Gaichas, S., Gilman, E., Hesp, S.A., Longo, C., Yao, N., and Methot, R.D. 2022. Oceans of plenty? Challenges, advancements, and future

- directions for the provision of evidence - based fisheries management advice. *Rev. Fish Biol. Fish.* Springer International Publishing. doi:10.1007/s11160-022-09726-7.
- Gonzalez, C., Paz, X., Roman, E., and Hermida, M. 2006. Feeding habits of fish species distributed on the Grand Bank (NAFO Divisions 3NO, 2002-2005). *NAFO SCR* **06**(31): 22.
- Gudmundsson, G. 2004. Time-series analysis of abundance indices of young fish. *ICES J. Mar. Sci.* **61**: 176–183. doi:10.1016/j.icesjms.2003.12.001.
- Guisan, A., Tingley, R., Baumgartner, J.B., Naujokaitis-Lewis, I., Sutcliffe, P.R., Tulloch, A.I.T., Regan, T.J., Brotons, L., McDonald-Madden, E., Mantyka-Pringle, C., Martin, T.G., Rhodes, J.R., Maggini, R., Setterfield, S.A., Elith, J., Schwartz, M.W., Wintle, B.A., Broennimann, O., Austin, M., Ferrier, S., Kearney, M.R., Possingham, H.P., and Buckley, Y.M. 2013. Predicting species distributions for conservation decisions. *Ecol. Lett.* **16**(12): 1424–1435. doi:10.1111/ele.12189.
- Haddon, M. 2001. Fisheries, population dynamics, and modelling. *In* *Modeling and Quantitative Methods in Fisheries*. Chapman & Hall/CRC. pp. 1–16.
- Haltuch, M.A., Brooks, E.N., Brodziak, J., Devine, J.A., Johnson, K.F., Klibansky, N., Nash, R.D.M., Payne, M.R., Shertzer, K.W., Subbey, S., and Wells, B.K. 2019. Unraveling the recruitment problem : A review of environmentally-informed forecasting and management strategy evaluation. *Fish. Res.* **217**: 198–216. Elsevier. doi:10.1016/j.fishres.2018.12.016.
- Harley, C.D.G., and Paine, R.T. 2009. Contingencies and compounded rare perturbations dictate sudden distributional shifts during periods of gradual climate change. *PNAS* **106**(27): 11172–11176. doi:10.1073/pnas.0904946106.
- Harley, S.J., Myers, R.A., and Dunn, A. 2001. Is catch-per-unit-effort proportional to abundance ? *Can. J. Fish. Aquat. Sci.* **58**(9): 1760–1772.
- Harvey, M., Galbraith, P.S., and Descroix, A. 2009. Vertical distribution and diel migration of macrozooplankton in the St. Lawrence marine system (Canada) in relation with the cold intermediate layer thermal properties. *Prog. Oceanogr.* **80**(1–2): 1–21. Elsevier Ltd. doi:10.1016/j.pocean.2008.09.001.
- Hastings, A., and Botsford, L.W. 2006. Persistence of spatial populations depends on returning home. *Proc. Natl. Acad. Sci.* **103**(15): 6067–6072.
- Healey, B., Brodie, W., Ings, D., and Power, D. 2012. Performance and description of Canadian multi-species surveys in NAFO subarea 2+ Divisions 3KLMNO, with emphasis on 2009-2011. *In* *Scientific Council Reports*. St. John's Newfoundland.
- Heino, M., Díaz Pauli, B., and Dieckmann, U. 2015. Fisheries-Induced Evolution. *Annu. Rev. Ecol. Evol. Syst.* **46**: 461–480. doi:10.1146/annurev-ecolsys-112414-054339.
- Heneghan, R.F., Galbraith, E., Blanchard, J.L., Harrison, C., Barrier, N., Bulman, C., Cheung, W., Coll, M., Eddy, T.D., Erauskin-Extramiana, M., Everett, J.D.,

- Fernandes-Salvador, J.A., Gascuel, D., Guiet, J., Maury, O., Palacios-Abrantes, J., Petrik, C.M., du Pontavice, H., Richardson, A.J., Steenbeek, J., Tai, T.C., Volkholz, J., Woodworth-Jefcoats, P.A., and Tittensor, D.P. 2021. Disentangling diverse responses to climate change among global marine ecosystem models. *Prog. Oceanogr.* **198**(102659). Elsevier Ltd. doi:10.1016/j.pocean.2021.102659.
- Hiemstra, P. 2015. Automatic interpolation package. CRAN. Available from <http://cran.r-project.org/web/packages/automap/automap.pdf>.
- Hilborn, R., Amoroso, R.O., Anderson, C.M., Baum, J.K., Branch, T.A., Costello, C., De Moor, C.L., Faraj, A., Hively, D., Jensen, O.P., Kurota, H., Little, L.R., Mace, P., McClanahan, T., Melnychuk, M.C., Minto, C., Osio, G.C., Parma, A.M., Pons, M., Segurado, S., Szuwalski, C.S., Wilson, J.R., and Ye, Y. 2020. Effective fisheries management instrumental in improving fish stock status. *Proc. Natl. Acad. Sci.* **117**(4): 2218–2224. doi:10.1073/pnas.1909726116.
- Hilborn, R., and Walters, C. 1992a. *Quantitative Fisheries Stock Assessment*. Chapman & Hall, London.
- Hilborn, R., and Walters, C.J. 1992b. Biomass dynamic models. *In* *Quantitative Fisheries Stock Assessment*. Chapman & Hall, London. pp. 297–329.
- Hillebrand, H., Donohue, I., Harpole, W.S., Hodapp, D., Kucera, M., Lewandowska, A.M., Merder, J., Montoya, J.M., and Freund, J.A. 2020. Thresholds for ecological responses to global change do not emerge from empirical data. *Nat. Ecol. Evol.* **4**(11): 1502–1509. Springer US. doi:10.1038/s41559-020-1256-9.
- Holling, C.S. 1959. Some characteristics of simple types of predation and parasitism. *Can. Entomol.* **91**(7): 385–398.
- Holt, C.A., and Michielsens, C.G.J. 2020. Impact of time-varying productivity on estimated stock – recruitment parameters and biological reference points. *Can. J. Fish. Aquat. Sci.* **847**: 836–847.
- Hordyk, A.R., Huynh, Q.C., and Carruthers, T.R. 2019. Misspecification in stock assessments: Common uncertainties and asymmetric risks. *Fish Fish.* **20**(5): 888–902. doi:10.1111/faf.12382.
- Houde, E.D. 2008. Emerging from Hjort’s shadow. *J. Northwest Atl. Fish. Sci.* **41**: 53–70. doi:10.2960/J.v41.m634.
- Howell, D., Schueller, A., Bentley, J., Buchheister, A., Chagaris, D., Cieri, M., Drew, K., Lundy, M., Pedreschi, D., Reid, D., and Townsend, H. 2021. Combining Ecosystem and Single-Species Modeling to Provide Ecosystem-Based Fisheries Management Advice Within Current Management Systems. *Front. Mar. Sci.* **7**. doi:10.3389/fmars.2020.607831.
- Hsieh, C., Yamauchi, A., Nakazawa, T., and Wang, W.F. 2010. Fishing effects on age and spatial structures undermine population stability of fishes. *Aquat. Sci.* **72**(2):

165–178. doi:10.1007/s00027-009-0122-2.

- Hunsicker, M.E., Ciannelli, L., Bailey, K.M., Buckel, J.A., Wilson White, J., Link, J.S., Essington, T.E., Gaichas, S., Anderson, T.W., Brodeur, R.D., Chan, K.S., Chen, K., Englund, G., Frank, K.T., Freitas, V., Hixon, M.A., Hurst, T., Johnson, D.W., Kitchell, J.F., Reese, D., Rose, G.A., Sjodin, H., Sydeman, W.J., Van der Veer, H.W., Vollset, K., and Zador, S. 2011. Functional responses and scaling in predator-prey interactions of marine fishes: Contemporary issues and emerging concepts. *Ecol. Lett.* **14**(12): 1288–1299. doi:10.1111/j.1461-0248.2011.01696.x.
- Hutchings, J.A. 2000. Collapse and recovery of marine fishes. *Nature* **406**: 882–885.
- Hutchings, J.A. 2014. Renaissance of a caveat : Allee effects in marine fish. *ICES J. Mar. Sci.* **71**(8): 2152–2157.
- Hutchings, J.A., and Reynolds, J.D. 2004. Marine fish population collapses: Consequences for recovery and extinction risk. *Bioscience* **54**(4): 297–309. doi:10.1641/0006-3568(2004)054[0297:MFPCCF]2.0.CO;2.
- Hyslop, E.J. 1980. Stomach contents analysis—a review of methods and their application. *J. Fish Biol.* **17**(4): 411–429. doi:10.1111/j.1095-8649.1980.tb02775.x.
- IPCC. 2022. Contribution of Working Group II to the Sixth Assessment Report of the Intergovernmental Panel on Climate Change. *In Climate Change 2022: Impacts, Adaptation, and Vulnerability. Edited by H. Portner, D. Roberts, M. Tignor, E. Poloczanska, K. Mintenback, A. Algeria, M. Craig, S. Langsdorf, S. Loschke, V. Moller, A. Okem, and B. Rama.* Cambridge University Press, Cambridge (UK).
- Jacobsen, N., Marshall, K., Berger, A., Grandin, C., and Taylor, I. 2021. Management Strategy Evaluation of Pacific Hake: Exploring the Robustness of the Current Harvest Policy to Spatial Stock Structure, Shifts in Fishery Selectivity, and Climate-Driven Distribution Shifts. *In U.S. Department of Commerce, NOAA Technical Memorandum.*
- Jardim, E., Azevedo, M., Brodziak, J., Brooks, E.N., Johnson, K.F., Klibansky, N., Millar, C.P., Minto, C., Mosqueira, I., Nash, R.D.M., Vasilakopoulos, P., and Wells, B.K. 2021. Operationalizing ensemble models for scientific advice to fisheries management. *ICES J. Mar. Sci.* **78**(4): 1209–1216. doi:10.1093/icesjms/fsab010.
- Jech, J.M., and McQuinn, I.H. 2016. Towards a balanced presentation and objective interpretation of acoustic and trawl survey data, with specific reference to the eastern Scotian Shelf. *Can. J. Fish. Aquat. Sci.* **73**(12): 1914–1921. doi:10.1139/cjfas-2016-0113.
- Johnson, D.L. 2000. Preliminary examination of the match-mismatch hypothesis and recruitment variability of yellowtail flounder, *Limanda ferruginea*. *Fish. Bull.* **98**(4): 854–863.
- Kallimanis, A.S., Kunin, W.E., Halley, J.M., and Sgardelis, S.P. 2005. Metapopulation

- extinction risk under spatially autocorrelated disturbance. *Conserv. Biol.* **19**(2): 534–546. doi:10.1111/j.1523-1739.2005.00418.x.
- Kerr, L.A., Hintzen, N.T., Cadrin, S.X., Clausen, L.W., Dickey-Collas, M., Goethel, D.R., Hatfield, E.M.C., Kritzer, J.P., and Nash, R.D.M. 2017. Lessons learned from practical approaches to reconcile mismatches between biological population structure and stock units of marine fish. *ICES J. Mar. Sci.* **74**(6): 1708–1722. doi:10.1093/icesjms/fsw188.
- Khan, A.S., and Neis, B. 2010. The rebuilding imperative in fisheries: Clumsy solutions for a wicked problem? *Prog. Oceanogr.* **87**(1–4): 347–356. Elsevier Ltd. doi:10.1016/j.pocean.2010.09.012.
- Klaer, N.L., O’Boyle, R.N., Deroba, J.J., Wayte, S.E., Little, L.R., Alade, L.A., and Rago, P.J. 2015. How much evidence is required for acceptance of productivity regime shifts in fish stock assessments: Are we letting managers off the hook? *Fish. Res.* **168**: 49–55. Elsevier B.V. doi:10.1016/j.fishres.2015.03.021.
- Koen-Alonso, M. 2007. A process-oriented approach to the multispecies functional response. *In* *From Energetics to Ecosystems: The Dynamics and Structure of Ecological Systems*, 1st edition. *Edited by* N. Rooney, K. McCann, and D. Noakes. Springer Science & Business Media. pp. 1–36. doi:10.1007/978-1-4020-5337-5.
- Koen-Alonso, M. 2018. Newfoundland and Labrador Region Stomach Content Collection and Processing. *In* *Pacific Region Science Workshop on Stomach Contents Analyses*. Nanaimo, BC.
- Koen-Alonso, M., Lindstrøm, U., Cuff, A., and Pennino, M.G. 2021. Comparative Modeling of Cod-Capelin Dynamics in the Newfoundland-Labrador Shelves and Barents Sea Ecosystems. *Front. Mar. Sci.* **8**(579946): 1–15. doi:10.3389/fmars.2021.579946.
- Koen-Alonso, M., Pepin, P., Fogarty, M.J., Kenny, A., and Kenchington, E. 2019. The Northwest Atlantic Fisheries Organization Roadmap for the development and implementation of an Ecosystem Approach to Fisheries: structure, state of development, and challenges. *Mar. Policy* **100**: 342–352. doi:10.1016/j.marpol.2018.11.025.
- Kristensen, K., Nielsen, A., Berg, C.W., Skaug, H., and Bell, B. 2016. TMB: Automatic Differentiation and Laplace Approximation. *J. Stat. Softw.* **70**(5): 21. doi:10.18637/jss.v070.i05.
- Krkošek, M., and Drake, J.M. 2014. On signals of phase transitions in salmon population dynamics. *Proc. R. Soc. B Biol. Sci.* **281**(1784). doi:10.1098/rspb.2013.3221.
- Kulka, D.W., Thompson, S., Cogliati, K., Olmstead, M., Austin, D., and Pepin, P. 2022. An Accounting of Integration of Environmental Variables in Fishery Stock Assessments in Canada. *Can. Tech. Rep. Fish. Aquat. Sci.* **3473**: viii + 79 p.

- Kumar, R., Cadigan, N.G., and Morgan, M.J. 2019. Recruitment synchrony in spatially structured Newfoundland and Labrador populations of American plaice (*Hippoglossoides platessoides*). *Fish. Res.* **211**: 91–99. Elsevier. doi:10.1016/j.fishres.2018.10.027.
- Larraneta, M.G. 1986. Dynamics of yellowtail flounder and american plaice populations on the Grand Bank. *NAFO Sci. Council. Stud.* **10**: 35.
- Leadbitter, D., Staples, D.J., Porobic, J., Ye, Y., Phoonsawat, R., and Kulanujaree, N. 2022. Shifting baselines and deciding on the desirable form of multispecies maximum sustainable yield. *ICES J. Mar. Sci.* **0**: 1–17. doi:10.1093/icesjms/fsac150.
- Lee, Q., Thorson, J.T., Gertseva, V. V., and Punt, A.E. 2018. The benefits and risks of incorporating climate-driven growth variation into stock assessment models, with application to Splitnose Rockfish (*Sebastes diploproa*). *ICES J. Mar. Sci.* **75**(1): 245–256. doi:10.1093/icesjms/fsx147.
- Lenoir, J., and Svenning, J.C. 2015. Climate-related range shifts - a global multidimensional synthesis and new research directions. *Ecography (Cop.)*. **38**(1): 15–28. doi:10.1111/ecog.00967.
- Levin, S. 1992. The problem of pattern and scale in ecology. *Ecology* **73**(6): 1943–1967. doi:10.2307/1941447.
- Lewis, K.P., Buren, A.D., Regular, P.M., Mowbray, F.K., and Murphy, H.M. 2019. Forecasting capelin *Mallotus villosus* biomass on the Newfoundland shelf. *Mar. Ecol. Prog. Ser.* **616**: 171–183. doi:10.3354/meps12930.
- Lewy, P., and Vinther, M. 2004. A stochastic age-length-structured multispecies model applied to North Sea stocks. *ICES C.M.* **33**: 1–33.
- Libralato, S., Pranovi, F., Stergiou, K.I., and Link, J.S. 2014. Trophodynamics in marine ecology : 70 years after Lindeman. *Mar. Ecol. Prog. Ser.* **512**: 1–7. doi:10.3354/meps11033.
- Lilly, G.R. 1982. Influence of the Labrador Current on predation by cod on capelin and sand lance off eastern Newfoundland. *NAFO Sci. Council. Stud.* **3**: 77–82.
- Lilly, G.R., and Simpson, M. 2000. Distribution and biomass of capelin, Arctic cod and sand lance on the Northeast Newfoundland Shelf and Grand Bank as deduced from bottom-trawl surveys. *DFO Can. Sci. Advis. Sec. Res. Doc.* **091**: 40.
- Link, J.S. 2004. Using fish stomachs as samplers of the benthos: Integrating long-term and broad scales. *Mar. Ecol. Prog. Ser.* **269**: 265–275. doi:10.3354/meps269265.
- Link, J.S., and Browman, H.I. 2014. Integrating what? Levels of marine ecosystem-based assessment and management. *ICES J. Mar. Sci.* **71**(5): 1170–1173.
- Link, J.S., Bundy, A., Shackell, N., Overholtz, W.J., Manderson, J., Duplisea, D., Hare, J., Friedland, K., and Koen-Alonso, M. 2011a. Ecosystem-based fisheries

- management in the Northwest Atlantic. *Fish Fish.* (12): 152–170.
doi:10.1017/CBO9780511973956.005.
- Link, J.S., Huse, G., Gaichas, S., and Marshak, A.R. 2020. Changing how we approach fisheries: A first attempt at an operational framework for ecosystem approaches to fisheries management. *Fish Fish.* **21**(2): 393–434. doi:10.1111/faf.12438.
- Link, J.S., Karp, M., Lynch, P., Morrison, W., and Peterson, J. 2021. Proposed business rules to incorporate climate-induced changes in fisheries management. *ICES J. Mar. Sci.* **78**(10): 3562–3580. Oxford University Press.
- Link, J.S., Nye, J.A., and Hare, J.A. 2011b. Guidelines for incorporating fish distribution shifts into a fisheries management context. *Fish Fish.* **12**(4): 461–469.
doi:10.1111/j.1467-2979.2010.00398.x.
- Link, W. 1999. Modeling pattern in collections of parameters. *J. Wildl. Manage.* **63**(3): 1017–1027.
- Lorenzen, K. 2016. Toward a new paradigm for growth modeling in fisheries stock assessments: Embracing plasticity and its consequences. *Fish. Res.* **180**: 4–22. Elsevier B.V. doi:10.1016/j.fishres.2016.01.006.
- Lorenzen, K., Camp, E. V, and Garlock, T.M. 2022. Natural mortality and body size in fish populations. *Fish. Res.* **252**(106327). Elsevier B.V. doi:10.1016/j.fishres.2022.106327.
- Lotze, H.K., Coll, M., Magera, A.M., Ward-Paige, C., and Airoidi, L. 2011. Recovery of marine animal populations and ecosystems. *Trends Ecol. Evol.* **26**(11): 595–605. Elsevier Ltd. doi:10.1016/j.tree.2011.07.008.
- Lozier, M.S., Owens, W.B., and Curry, R.G. 1995. The climatology of the North Atlantic. *Prog. Oceanogr.* **36**(1): 1–44. doi:10.1016/0079-6611(95)00013-5.
- Ludwig, D., and Walters, C.J. 1981. Measurement Errors and Uncertainty in Parameter Estimates for Stock and Recruitment. *Can. J. Fish. Aquat. Sci.* **38**: 711–720.
- Ludwig, D., and Walters, C.J. 1985. Are age-structured models appropriate for catch-effort data? *Can. J. Fish. Aquat. Sci.* **42**: 1066–1072.
- MacCall, A. 1990. Dynamic geography of marine fish populations. Washington Sea Grant Program, Seattle, WA.
- Marshall, K.N., Jensen, O.P., Koehn, L.E., Levin, P.S., and Essington, T.E. 2019. Inclusion of ecosystem information in US fish stock assessments suggests progress toward ecosystem-based fisheries management. *ICES J. Mar. Sci.* **76**(1): 1–9. doi:10.1093/icesjms/fsy152.
- Matthysen, E. 2005. Density-dependent dispersal in birds and mammals. *Ecography (Cop.)*. **28**(3): 403–416. doi:10.1111/j.0906-7590.2005.04073.x.

- Maunder, M.N., and Piner, K.R. 2017. Dealing with data conflicts in statistical inference of population assessment models that integrate information from multiple diverse data sets. *Fish. Res.* **192**: 16–27. Elsevier B.V. doi:10.1016/j.fishres.2016.04.022.
- Maunder, M.N., and Punt, A. 2004. Standardizing catch and effort data : a review of recent approaches. *Fish. Res.* **70**: 141–159. doi:10.1016/j.fishres.2004.08.002.
- Maunder, M.N., and Punt, A.E. 2013. A review of integrated analysis in fisheries stock assessment. *Fish. Res.* **142**: 61–74. doi:10.1016/j.fishres.2012.07.025.
- Maunder, M.N., Sibert, J.R., Fonteneau, A., Hampton, J., Kleiber, P., and Harley, S.J. 2006. Interpreting catch per unit effort data to assess the status of individual stocks and communities. *ICES J. Mar. Sci.* **63**: 1373–1385. doi:10.1016/j.icesjms.2006.05.008.
- Maunder, M.N., and Watters, G.M. 2003. A general framework for integrating environmental time series into stock assessment models: model description, simulation testing, and example article. *Fish. Bull.* **101**: 89–99.
- McCarthy, M.A., Moore, J.L., Morris, W.K., Parris, K.M., Garrard, G.E., Vesk, P.A., Rumpff, L., Giljohann, K.M., Camac, J.S., Bau, S.S., Friend, T., Harrison, B., and Yue, B. 2013. The influence of abundance on detectability. *Oikos* **122**: 717–726. doi:10.1111/j.1600-0706.2012.20781.x.
- McCormack, S.A., Trebilco, R., Melbourne-Thomas, J., Blanchard, J.L., Fulton, E.A., and Constable, A. 2019. Using stable isotope data to advance marine food web modelling. *Rev. Fish Biol. Fish.* **29**(2): 277–296. Springer International Publishing. doi:10.1007/s11160-019-09552-4.
- Miller, S.K., Anganuzzi, A., Butterworth, D.S., Davies, C.R., Donovan, G.P., Nickson, A., Rademeyer, R.A., and Restrepo, V. 2019. Improving communication: The key to more effective MSE processes. *Can. J. Fish. Aquat. Sci.* **76**(4): 643–656. doi:10.1139/cjfas-2018-0134.
- Mills, K., Laidig, T., Ralston, S., and Sydeman, W. 2007. Diets of top predators indicate pelagic juvenile rockfish (*Sebastes* spp.) abundance in the California Current System. *Fish. Oceanogr.* **16**(3): 273–283. doi:10.1111/j.1365-2419.2006.00429.x.
- Morgan, M.J. 1992. Low-Temperature Tolerance of American Plaice in Relation to Declines in Abundance. *Trans. Am. Fish. Soc.* **121**: 399–402. doi:10.1577/1548-8659(1992)121<0399:ltoapi>2.3.co;2.
- Morgan, M.J. 1996. Preliminary results of tagging experiments on American plaice in NAFO Divs. 3LNO. NAFO SCR Doc **96/61**(N2737): 13.
- Morgan, M.J., Bailey, J., Healey, B.P., Maddock Parsons, D., and Rideout, R. 2011. Recovery potential assessment of American Plaice (*Hippoglossoides platessoides*) in Newfoundland and Labrador. *In* DFO Can. Sci. Advis. Sec. Res. Doc.
- Morgan, M.J., and Brodie, W. 2001. An Exploration of Virtual Population Analyses for

- Divisions 3LNO American Plaice. NAFO SCR Doc **01/4**(N4638): 1–20.
- Morgan, M.J., Brodie, W., Bowering, W., Maddock Parsons, D., and Orr, D. 1998. Results of Data Conversions for American Plaice in Div. 3LNO from Comparative Fishing Trials Between the Engel Otter Trawl and the Campelen 1800 Shrimp Trawl. NAFO SCR Doc **98/70**(N3062): 10.
- Morgan, M.J., and Colbourne, E.B. 1999. Variation in maturity-at-age and size in three populations of American plaice. *ICES J. Mar. Sci.* **56**(5): 673–688. doi:10.1006/jmsc.1999.0487.
- Morgan, M.J., and Walsh, S. 1996. Tracking movements of juvenile yellowtail flounder in the nursery area on the southern Grand Bank, NAFO Divisions 3LNO. NAFO SCR Doc **96/66**(N2742): 10.
- Morin, P. 2011a. Communities: basic patterns and elementary processes. *In Community Ecology*, Second. Blackwell Science. pp. 1–23.
- Morin, P. 2011b. Causes and consequences of diversity. *In Community Ecology*, Second. Blackwell Science. pp. 283–318.
- Moustahfid, H., Tyrrell, M.C., Link, J.S., Nye, J.A., Smith, B.E., and Gamble, R.J. 2010. Functional feeding responses of piscivorous fishes from the northeast US continental shelf. *Oecologia* **163**(4): 1059–1067. doi:10.1007/s00442-010-1596-2.
- Mullowney, D.R.J., Dawe, E.G., Colbourne, E.B., and Rose, G.A. 2014. A review of factors contributing to the decline of Newfoundland and Labrador snow crab (*Chionoecetes opilio*). *Rev. Fish Biol. Fish.* **24**(2): 639–657. doi:10.1007/s11160-014-9349-7.
- Myers, R.A. 1998. When do environment - recruitment correlations work? *Rev. Fish Biol. Fish.* **8**: 285–305.
- Myers, R.A., and Cadigan, N.C. 1993a. Is juvenile natural mortality in marine demersal fish variable? *Can. J. Fish. Aquat. Sci.* **50**: 1591–1598.
- Myers, R.A., and Cadigan, N.G. 1993b. Density-dependent juvenile mortality in marine demersal fish. *Can. J. Fish. Aquat. Sci.* **50**: 1576–1590.
- Myers, R.A., and Cadigan, N.G. 1995. Statistical-Analysis of Catch-at-Age Data with Correlated Errors. *Can. J. Fish. Aquat. Sci.* **52**(6): 1265–1273. doi:10.1139/f95-123.
- Myers, R.A., Hutchings, J.A., and Barrowman, N.J. 1997. Why do fish stocks collapse? The example of cod in Atlantic Canada. *Ecol. Appl.* **7**(1): 91–106. doi:10.1890/1051-0761(1997)007[0091:WDFSCCT]2.0.CO;2.
- Myers, R.A., and Stokes, K. 1989. Density-dependent habitat utilization of groundfish and the improvement of research survey. *In ICES Committee Meeting D15*.
- NAFO. 2019. Report of the Scientific Council Meeting. NAFO SCS Doc **19/20**(N6966):

245. doi:10.1017/CBO9781107415324.004.
- Neubauer, P., Jensen, O.P., Hutchings, J.A., and Baum, J.K. 2013. Resilience and recovery of overexploited marine populations. *Science*. **340**(6130): 347–349. doi:10.1126/science.1230441.
- Neuheimer, A.B., and Taggart, C.T. 2007. The growing degree-day and fish size-at-age: the overlooked metric. *Can. J. Fish. Aquat. Sci.* **64**(2): 375–385. doi:10.1139/f07-003.
- Ng, E.L., Deroba, J.J., Essington, T.E., Smith, B.E., and Thorson, J.T. 2021. Predator stomach contents can provide accurate indices of prey biomass. *ICES J. Mar. Sci.* **78**(3): 1146–1159. doi:10.1093/icesjms/fsab026.
- Nielsen, J.M., Clare, E.L., Hayden, B., Brett, M.T., and Kratina, P. 2018. Diet tracing in ecology: Method comparison and selection. *Methods Ecol. Evol.* **9**(2): 278–291. doi:10.1111/2041-210X.12869.
- Noble, I., and Slatyer, R. 1980. The use of vital attributes to predict successional changes in plant communities subject to recurrent disturbances. *Vegetatio* **43**: 5–21.
- Nogueira, A., Paz, X., and Gonzalez-Troncoso, D. 2015. Changes in the exploited demersal fish assemblages in the Southern Grand Banks (NAFO Divisions 3NO): 2002-2013. *ICES J. Mar. Sci.* **72**(3): 753–770. doi:10.1093/icesjms/fst153.
- O’Driscoll, R.L., Rose, G.A., and Anderson, J.T. 2002. Estimating abundance and management: Counting capelin: A comparison of acoustic density and trawl catchability. *ICES J. Mar. Sci.* **59**(5): 1062–1071. doi:10.1006/jmsc.2002.1262.
- O’Leary, C.A., Miller, T.J., Thorson, J.T., and Nye, J.A. 2019. Understanding historical summer flounder (*Paralichthys dentatus*) abundance patterns through the incorporation of oceanography-dependent vital rates in Bayesian hierarchical models. *Can. J. Fish. Aquat. Sci.* **76**: 1275–1294.
- Ockendon, N., Baker, D.J., Carr, J.A., White, E.C., Almond, R.E.A., Amano, T., Bertram, E., Bradbury, R.B., Bradley, C., Butchart, S.H.M., Doswald, N., Foden, W., Gill, D.J.C., Green, R.E., Sutherland, W.J., Tanner, E.V.J., and Pearce-Higgins, J.W. 2014. Mechanisms underpinning climatic impacts on natural populations: Altered species interactions are more important than direct effects. *Glob. Chang. Biol.* **20**(7): 2221–2229. doi:10.1111/gcb.12559.
- Oliver, M.A., and Webster, R. 2015. *Basic Steps in Geostatistics: The Variogram and Kriging*. Springer.
- Overholtz, W.J., and Friedland, K.D. 2002. Recovery of the Gulf of Maine – Georges Bank Atlantic herring (*Clupea harengus*) complex : perspectives based on bottom trawl survey data. *Fish. Bull.* **100**(3): 593–608.
- Parsons, D., Rideout, R., and Rogers, R. 2021. 2021 Assessment of Yellowtail Flounder in NAFO Divisions 3LNO using a Stock Production Model in a Bayesian

- Framework. NAFO SCR Doc **21/018**(7186): 48.
- Parsons, D.M., Morgan, M., and Rogers, R. 2018. Assessment of yellowtail flounder in NAFO divisions 3LNO using a new stock production model in a Bayesian framework. NAFO SCR Doc **18/038**(N6828): 1–14.
- Pascual, M., and Guichard, F. 2005. Criticality and disturbance in spatial ecological systems. *Trends Ecol. Evol.* **20**(2): 88–95. doi:10.1016/j.tree.2004.11.012.
- Pauly, D. 1995. Anecdotes and the shifting baseline syndrome of fisheries. *Trends Ecol. Evol.* **10**(10): 1995.
- Pauly, D. 2021. The gill-oxygen limitation theory (GOLT) and its critics. *Sci. Adv.* **7**(eabc6050): 18.
- Pedersen, M.W., and Berg, C.W. 2017. A stochastic surplus production model in continuous time. *Fish Fish.* **18**(2): 226–243. doi:10.1111/faf.12174.
- Pentz, B., Klenk, N., Ogle, S., and Fisher, J.A.D. 2018. Can regional fisheries management organizations (RFMOs) manage resources effectively during climate change? *Mar. Policy* **92**: 13–20. Elsevier Ltd. doi:10.1016/j.marpol.2018.01.011.
- Pepin, P., King, J., Holt, C., Smith, H.G., Shackell, N., Hedges, K., and Bundy, A. 2022. Incorporating knowledge of changes in climatic, oceanographic and ecological conditions in Canadian stock assessments. *Fish Fish.* **23**: 1332–1346. doi:10.1111/faf.12692.
- Pérez-Rodríguez, A., Koen-Alonso, M., González-Iglesias, C., and Saborido-Rey, F. 2011. Analysis of common trends in the feeding habits of main demersal fish species on the Flemish Cap. NAFO SCR Doc **11/77**(N6009): 31.
- Perreault, A.M.J., Wheeland, L.J., and Morgan, M.J. 2020. A state-space stock assessment model for American plaice on the Grand Bank of Newfoundland. *J. Northwest Atl. Fish. Sci.* **51**: 45–104.
- Perry, R.I., and Smith, S.J. 1994. Identifying Habitat Associations of Marine Fishes Using Survey Data: An Application to the Northwest Atlantic. *Can. J. Fish. Aquat. Sci.* **51**(3): 589–602. doi:10.1139/f94-061.
- Pethybridge, H.R., Choy, C.A., Polovina, J.J., and Fulton, E.A. 2018. Improving marine ecosystem models with biogeochemical tracers. *Ann. Rev. Mar. Sci.* **10**(1): 199–228. doi:10.1146/annurev-marine-121916-063256.
- Petrik, C.M., Stock, C.A., Andersen, K.H., van Denderen, P.D., and Watson, J.R. 2019. Bottom-up drivers of global patterns of demersal, forage, and pelagic fishes. *Prog. Oceanogr.* **176**(June): 102124. Elsevier. doi:10.1016/j.pocean.2019.102124.
- Piatt, J.F., Arimitsu, M.L., Sydeman, W.J., Thompson, S.A., Renner, H., Zador, S., Douglas, D., Hatch, S., Kettle, A., and Williams, J. 2018. Biogeography of pelagic food webs in the North Pacific. *Fish. Oceanogr.* **27**(4): 366–380.

doi:10.1111/fog.12258.

- Pikitch, E.K., Rountos, K.J., Essington, T.E., Santora, C., Pauly, D., Watson, R., Sumaila, U.R., Boersma, P.D., Boyd, I.L., Conover, D.O., Cury, P., Heppell, S.S., Houde, E.D., Mangel, M., Plagányi, É., Sainsbury, K., Steneck, R.S., Geers, T.M., Gownaris, N., and Munch, S.B. 2014. The global contribution of forage fish to marine fisheries and ecosystems. *Fish Fish.* **15**(1): 43–64. doi:10.1111/faf.12004.
- Pikitch, E.K., Santora, C., Babcock, E.A., Bakun, A., Bonfil, R., Conover, D.O., Dayton, P., Doukakis, P., Fluharty, D., Heneman, B., Houde, E.D., and Link, J. 2004. Ecosystem-Based Fishery Management. *Science.* **305**: 346–348.
- Pine, W.E., Pollock, K.H., Hightower, J.E., Kwak, T.J., & Rice, J.A. 2003. A review of tagging methods for estimating fish population size and components of mortality. *Fisheries* **28**(10): 10–23. doi:10.1577/1548-8446(2003)28.
- Pinsky, M., Worm, B., Fogarty, M., Sarmiento, J., and Levin, S. 2013. Marine taxa track local climate velocities. *Science.* **341**: 1239–1242.
- Pinsky, M.L., Reygondeau, G., Caddell, R., Palacios-Abrantes, J., Spijkers, J., and Cheung, W.W.L. 2018. Preparing ocean governance for species on the move. *Science.* **360**(6394): 1189–1191. doi:10.1126/science.aat2360.
- Pinsky, M.L., Selden, R.L., and Kitchel, Z.J. 2020. Climate-Driven Shifts in Marine Species Ranges: Scaling from Organisms to Communities. *Ann. Rev. Mar. Sci.* **12**(1): 153–179. doi:10.1146/annurev-marine-010419-010916.
- Pitt, T.K. 1969. Migrations of American Plaice on the Grand Bank and in St. Mary's Bay, 1954, 1959, and 1961. *J. Fish. Res. Board Canada* **26**: 1301–1319. doi:10.1139/f69-115.
- Pitt, T.K. 1970. Distribution, Abundance, and Spawning of Yellowtail Flounder, *Limanda ferruginea*, in the Newfoundland Area of the Northwest Atlantic. *J. Fish. Res. Board Canada* **27**(12). doi:10.1139/f70-254.
- Pitt, T.K. 1976. Food of Yellowtail Flounder on the Grand Bank and a comparison with American Plaice. *ICNAF Res. Bull.* **12**: 23–27.
- Plagányi, É.E., Blamey, L.K., Rogers, J.G.D., and Tulloch, V.J.D. 2022. Playing the detective : Using multispecies approaches to estimate natural mortality rates. *Fish. Res.* **249**(106229). doi:10.1016/j.fishres.2022.106229.
- Plagányi, É.E., and Butterworth, D. 2012. The Scotia Sea krill fishery and its possible impacts on dependent predators : modeling localized depletion of prey. *Ecol. Appl.* **22**(3): 748–761.
- Plagányi, É.E., Punt, A.E., Hillary, R., Morello, E.B., Thébaud, O., Hutton, T., Pillans, R.D., Thorson, J.T., Fulton, E.A., Smith, A.D.M., Smith, F., Bayliss, P., Haywood, M., Lyne, V., and Rothlisberg, P.C. 2014. Multispecies fisheries management and conservation: Tactical applications using models of intermediate complexity. *Fish*

- Fish. **15**(1): 1–22. doi:10.1111/j.1467-2979.2012.00488.x.
- Planque, B., Fromentin, J., Cury, P., Drinkwater, K.F., Jennings, S., Perry, R.I., and Kifani, S. 2010. How does fishing alter marine populations and ecosystems sensitivity to climate? *J. Mar. Syst.* **79**(3–4): 403–417. Elsevier B.V. doi:10.1016/j.jmarsys.2008.12.018.
- Poloczanska, E.S., Brown, C.J., Sydeman, W.J., Kiessling, W., Schoeman, D.S., Moore, P.J., Brander, K., Bruno, J.F., Buckley, L.B., Burrows, M.T., Duarte, C.M., Halpern, B.S., Holding, J., Kappel, C. V., O'Connor, M.I., Pandolfi, J.M., Parmesan, C., Schwing, F., Thompson, S.A., and Richardson, A.J. 2013. Global imprint of climate change on marine life. *Nat. Clim. Chang.* **3**(10): 919–925. doi:10.1038/nclimate1958.
- Pope, J.G., Gislason, H., Rice, J.C., and Daan, N. 2021. Scrabbling around for understanding of natural mortality. *Fish. Res.* **240**: 105952. Elsevier B.V. doi:10.1016/j.fishres.2021.105952.
- Pörtner, H.O. 2001. Climate change and temperature-dependent biogeography: Oxygen limitation of thermal tolerance in animals. *Naturwissenschaften* **88**(4): 137–146. doi:10.1007/s001140100216.
- Punt, A.E., Butterworth, D.S., de Moor, C.L., De Oliveira, J.A.A., and Haddon, M. 2016. Management strategy evaluation: best practices. *Fish Fish.* **17**(2): 303–334. doi:10.1111/faf.12104.
- Punt, A.E., Castillo-Jordan, C., Hamel, O.S., Cope, J.M., Maunder, M.N., and Ianelli, J.N. 2021. Consequences of error in natural mortality and its estimation in stock assessment models. *Fish. Res.* **233**: 105759.
- Punt, A.E., Dunn, A., Þór Elvarsson, B., Hampton, J., Hoyle, S.D., Maunder, M.N., Methot, R.D., and Nielsen, A. 2020. Essential features of the next-generation integrated fisheries stock assessment package: A perspective. *Fish. Res.* **229**(105617). Elsevier. doi:10.1016/j.fishres.2020.105617.
- Punt, A.E., Teresa, A., Bond, N.A., Butterworth, D.S., Moor, C.L. De, Oliveira, A.A. De, Haltuch, M.A., Hollowed, A.B., and Szuwalski, C. 2014. Fisheries management under climate and environmental uncertainty: control rules and performance simulation. *ICES J. Mar. Sci.* **71**(8): 2208–2220.
- R Core Team. 2018. R: A language and environment for statistical computing. R Foundation for Statistical Computing, Vienna, Austria.
- Real, L. 1979. Ecological determinants of a functional response. *Ecology* **60**(3): 481–485.
- Regular, P.M., Buren, A.D., Dwyer, K.S., Cadigan, N.G., Gregory, R.S., Koen-alonso, M., Rideout, R.M., Robertson, G.J., Robertson, M.D., Stenson, G.B., Wheeland, L.J., and Zhang, F. 2022. Indexing starvation mortality to assess its role in the population regulation of Northern cod. *Fish. Res.* **247**: 106180. Elsevier B.V.

doi:10.1016/j.fishres.2021.106180.

- Reum, J.C.P., Townsend, H., Gaichas, S., Sagarese, S., Kaplan, I.C., and Grüss, A. 2021. It's Not the Destination, It's the Journey: Multispecies Model Ensembles for Ecosystem Approaches to Fisheries Management. *Front. Mar. Sci.* **8**(631839): 1–14. doi:10.3389/fmars.2021.631839.
- Revilla, E., and Wiegand, T. 2008. Individual movement behavior, matrix heterogeneity, and the dynamics of spatially structured populations. *Proc. Natl. Acad. Sci.* **105**(49): 19120–19125. doi:10.1073/pnas.0801725105.
- Rice, J. 2011. Managing fisheries well: Delivering the promises of an ecosystem approach. *Fish Fish.* **12**(2): 209–231. doi:10.1111/j.1467-2979.2011.00416.x.
- Richardson, D.E., Palmer, M.C., and Smith, B.E. 2014. The influence of forage fish abundance on the aggregation of Gulf of Maine Atlantic cod (*Gadus morhua*) and their catchability in the fishery. *Can. J. Fish. Aquat. Sci.* **71**(9): 1349–1362. doi:10.1139/cjfas-2013-0489.
- Rietkerk, B.M., Dekker, S.C., Ruiter, P.C. De, and Koppel, J. Van De. 2004. Self-organized patchiness and catastrophic shifts in ecosystems. *Science.* **305**(5692): 1926–1929.
- Robertson, M.D., Gao, J., Regular, P.M., Morgan, M.J., and Zhang, F. 2021. Lagged recovery of fish spatial distributions following a cold - water perturbation. *Sci. Rep.* **11**(9513): 1–11. Nature Publishing Group UK. doi:10.1038/s41598-021-89066-x.
- Robertson, M.D., Koen-Alonso, M., Regular, P., Cadigan, N., and Zhang, F. 2022a. Accounting for a nonlinear functional response when estimating prey dynamics using predator diet data. *Methods Ecol. Evol.* **13**(4): 880–893. doi:10.1111/2041-210X.13795.
- Robertson, M.D., Regular, P.M., and Cadigan, N.G. 2022b. Limited temporal variability in natural mortality for juvenile American plaice on the Grand Bank of Newfoundland. *J. Northwest Atl. Fish. Sci.* **53**: 47–56.
- Rose, G., and Leggett, W. 1989. Interactive effects of geophysically-forced sea temperatures and prey abundance on mesoscale coastal distributions of a marine predator, Atlantic cod (*Gadus morhua*). *Can. J. Fish. Aquat. Sci.* **46**: 1904–1913.
- Rose, G.A., deYoung, B., Kulka, D.W., Goddard, S.V., and Fletcher, G.L. 2000. Distribution shifts and overfishing the northern cod (*Gadus morhua*): a view from the ocean. *Can. J. Fish. Aquat. Sci.* **57**(3): 644–663. doi:10.1139/cjfas-57-3-644.
- Roseneau, D.G., and Byrd, G.V. 1997. Using Pacific Halibut to Sample the Availability of Forage Fishes to Seabirds. *In* Forage fishes in marine ecosystems. Alaska Sea Grant College Program. pp. 231–241.
- Runge, C.A., Tulloch, A.I.T., Possingham, H.P., Tulloch, V.J.D., and Fuller, R.A. 2016. Incorporating dynamic distributions into spatial prioritization. *Divers. Distrib.* **22**(3):

- 332–343. doi:10.1111/ddi.12395.
- Scheffer, M., Carpenter, S., Foley, J.A., Folke, C., and Walker, B. 2001. Catastrophic shifts in ecosystems. *Nature* **413**: 591–596. doi:10.1038/35098000.
- Scheffer, M., and Carpenter, S.R. 2003. Catastrophic regime shifts in ecosystems: Linking theory to observation. *Trends Ecol. Evol.* **18**(12): 648–656. doi:10.1016/j.tree.2003.09.002.
- Schijns, R., and Pauly, D. 2021. Management implications of shifting baselines in fish stock assessments. *Fish. Manag. Ecol.* **29**(2): 183–195. doi:10.1111/fme.12511.
- Schindler, D.E., Armstrong, J.B., and Reed, T.E. 2015. The portfolio concept in ecology and evolution. *Front. Ecol. Environ.* **13**(5): 257–263. doi:10.1890/140275.
- Schindler, D.E., Hilborn, R., Chasco, B., Boatright, C.P., Quinn, T.P., Rogers, L.A., and Webster, M.S. 2010. Population diversity and the portfolio effect in an exploited species. *Nature* **465**(7298): 609–612. Nature Publishing Group. doi:10.1038/nature09060.
- Schirripa, M.J., Goodyear, C.P., and Methot, R.M. 2009. Testing different methods of incorporating climate data into the assessment of US west Coast sablefish. *ICES J. Mar. Sci.* **66**(7): 1605–1613. doi:10.1093/icesjms/fsp043.
- Schnute, J. 1987. A general fishery model for a size-structured fish population. *Can. J. Fish. Aquat. Sci.* **44**(5): 924–940. doi:10.1139/f87-111.
- Schrank, W.E. 2005. The Newfoundland fishery: Ten years after the moratorium. *Mar. Policy* **29**(5): 407–420. doi:10.1016/j.marpol.2004.06.005.
- Shackell, N.L., Frank, K.T., and Brickman, D.W. 2005. Range contraction may not always predict core areas: an example from marine fish. *Ecol. Appl.* **15**(4): 1440–1449.
- Shelton, A.O., and Mangel, M. 2011. Fluctuations of fish populations and the magnifying effects of fishing. *Proc. Natl. Acad. Sci.* **108**(17): 7075–7080. doi:10.1073/pnas.1100334108.
- Shelton, P.A., and Morgan, M.J. 2006. Is by-catch mortality preventing the rebuilding of cod (*Gadus morhua*) and American plaice (*Hippoglossoides platessoides*) stocks on the Grand Bank? *J. Northwest Atl. Fish. Sci.* **36**: 1–17. doi:10.2960/J.v36.m544.
- Shepard, S., Greenstreet, S., Piet, G., Rindorf, A., and Dickey-Collas, M. 2015. Surveillance indicators and their use in implementation of the Marine Strategy Framework Directive. *ICES J. Mar. Sci.* **72**(8): 2269–2277. doi:doi:10.1093/icesjms/fst123.
- Sherwood, G.D., Rideout, R.M., Fudge, S.B., and Rose, G.A. 2007. Influence of diet on growth, condition and reproductive capacity in Newfoundland and Labrador cod (*Gadus morhua*): Insights from stable carbon isotopes. *Deep Sea Res. II* **54**: 2794–

2809. doi:10.1016/j.dsr2.2007.08.007.
- Simpson, M.R., Miri, C.M., and Collins, R.K. 2018. Assessment of Thorny skate (*Amblyraja radiata* Donovan, 1808) in NAFO Divisions 3LNO and Subdivision 3Ps. NAFO SCR Doc **18/027**(N6811): 1–34.
- Simpson, M.R., and Walsh, S.J. 2004. Changes in the spatial structure of Grand Bank yellowtail flounder: Testing MacCall’s basin hypothesis. *J. Sea Res.* **51**(3–4): 199–210. doi:10.1016/j.seares.2003.08.007.
- Skalski, G.T., and Gilliam, J.F. 2001. Functional responses with predator interference: Viable alternatives to the Holling type II model. *Ecology* **82**(11): 3083–3092. doi:10.1890/0012-9658(2001)082[3083:FRWPIV]2.0.CO;2.
- Skern-Mauritzen, M., Ottersen, G., Handegard, N.O., Huse, G., Dingsør, G.E., Stenseth, N.C., and Kjesbu, O.S. 2016. Ecosystem processes are rarely included in tactical fisheries management. *Fish Fish.* **67**(3): 165–175. doi:10.1111/faf.12111.
- Smith, A.D.M., Brown, C., Bulman, C., Fulton, E., Johnson, P., Kaplan, I., Lozano-Montes, H., Mackinson, S., Marzloff, M., Shannon, L., Shin, Y., and Tam, J. 2011. Impacts of fishing low-trophic level species on marine ecosystems. *Science.* **333**: 1147–1150.
- Smith, A.D.M., Fulton, E.J., Hobday, A.J., Smith, D.C., and Shoulder, P. 2007. Scientific tools to support the practical implementation of ecosystem-based fisheries management. *ICES J. Mar. Sci.* **64**(4): 633–639. doi:10.1093/icesjms/fsm041.
- Smith, K.A., Dowling, C.E., and Brown, J. 2019. Simmered then boiled: Multi-decadal poleward shift in distribution by a temperate fish accelerates during marine heatwave. *Front. Mar. Sci.* **6**(407): 1–16. doi:10.3389/fmars.2019.00407.
- Sober, E. 2002. Instrumentalism, Parsimony, and the Akaike Framework. *Philosophy Sci.* **69**(S3): 112–123.
- Sorte, C.J.B., Jones, S.J., and Miller, L.P. 2011. Geographic variation in temperature tolerance as an indicator of potential population responses to climate change. *J. Exp. Mar. Bio. Ecol.* **400**(1–2): 209–217. Elsevier B.V. doi:10.1016/j.jembe.2011.02.009.
- Staudinger, M.D., Goyert, H., Suca, J.J., Coleman, K., Welch, L., Llopiz, J.K., Wiley, D., Altman, I., Applegate, A., Auster, P., Baumann, H., Beaty, J., Boelke, D., Richardson, D., Robbins, J., Runge, J., Smith, B., Spiegel, C., and Steinmetz, H. 2020. The role of sand lances (*Ammodytes* sp) in the Northwest Atlantic Ecosystem : A synthesis of current knowledge with implications for conservation and management. *Fish Fish.* **21**(3): 522–556. doi:10.1111/faf.12445.
- Stawitz, C.C., Haltuch, M.A., and Johnson, K.F. 2019. How does growth misspecification affect management advice derived from an integrated fisheries stock assessment model? *Fish. Res.* **213**(January): 12–21. Elsevier. doi:10.1016/j.fishres.2019.01.004.
- Stier, A.C., Samhour, J.F., Novak, M., Marshall, K.N., Ward, E.J., Holt, R.D., and Levin,

- P.S. 2016. Ecosystem context and historical contingency in apex predator recoveries. *Sci. Adv.* **2**(5): 1–15. doi:10.1126/sciadv.1501769.
- Stock, B.C., and Miller, T.J. 2021. The Woods Hole Assessment Model (WHAM): A general state-space assessment framework that incorporates time- and age-varying processes via random effects and links to environmental covariates. *Fish. Res.* **240**(105967). Elsevier B.V. doi:10.1016/j.fishres.2021.105967.
- Stockwell, J.D., Yule, D.L., Gorman, O.T., Isaac, E.J., and Moore, S.A. 2006. Evaluation of bottom trawls as compared to acoustics to assess adult Lake Herring (*Coregonus artedii*) abundance in Lake Superior. *J. Great Lakes Res.* **32**(2): 280–292. doi:10.3394/0380-1330(2006)32[280:EOBTAC]2.0.CO;2.
- Sugihara, G., May, R., Ye, H., Hsieh, C.H., Deyle, E., Fogarty, M., and Munch, S. 2012. Detecting causality in complex ecosystems. *Science.* **338**(6106): 496–500. doi:10.1126/science.1227079.
- Sullivan, M.C., Cowen, R.K., and Steves, B.P. 2005. Evidence for atmosphere-ocean forcing of yellowtail flounder (*Limanda ferruginea*) recruitment in the Middle Atlantic Bight. *Fish. Oceanogr.* **14**(5): 386–399. doi:10.1111/j.1365-2419.2005.00343.x.
- Sunday, J.M., Bates, A.E., and Dulvy, N.K. 2012. Thermal tolerance and the global redistribution of animals. *Nat. Clim. Chang.* **2**(9): 686–690. Nature Publishing Group. doi:10.1038/nclimate1539.
- Sunday, J.M., Pecl, G.T., Frusher, S., Hobday, A.J., Hill, N., Holbrook, N.J., Edgar, G.J., Stuart-Smith, R., Barrett, N., Wernberg, T., Watson, R.A., Smale, D.A., Fulton, E.A., Slawinski, D., Feng, M., Radford, B.T., Thompson, P.A., and Bates, A.E. 2015. Species traits and climate velocity explain geographic range shifts in an ocean-warming hotspot. *Ecol. Lett.* **18**(9): 944–953. doi:10.1111/ele.12474.
- Swain, D.P., and Benoit, H.P. 2003. Accounting for length- and depth-dependent diel variation in catchability of fish and invertebrates in an annual bottom-trawl survey. *ICES J. Mar. Sci.* **60**: 1298–1317. doi:10.1016/S1054.
- Swain, D.P., and Morin, R. 1996. Relationships between geographic distribution and abundance of American plaice (*Hippoglossoides platessoides*) in the southern Gulf of St. Lawrence. *Oceanogr. Lit. Rev.* **11**(43): 1155. doi:10.1139/f95-163.
- Swain, D.P., and Sinclair, A.F. 1994. Distribution and Catchability: What is the Appropriate Measure of Distribution? *Can. J. Fish. Aquat. Sci.* **51**: 1046–1054.
- Sydeman, W.J., Piatt, J.F., Thompson, S.A.N.N., Hatch, S.A., Arimitsu, M.L., Slater, L., Williams, J.C., Rojek, N.A., Zador, S.G., and Renner, H.M. 2017. Puffins reveal contrasting relationships between forage fish and ocean climate in the North Pacific. *Fish. Oceanogr.* **26**(4): 379–395. doi:10.1111/fog.12204.
- Szuwalski, C.S., and Hollowed, A.B. 2016. Climate change and non-stationary population

- processes in fisheries management. *ICES J. Mar. Sci.* **73**(5): 1297–1305.
- Szuwalski, C.S., Vert-Pre, K.A., Punt, A.E., Branch, T.A., and Hilborn, R. 2015. Examining common assumptions about recruitment: A meta-analysis of recruitment dynamics for worldwide marine fisheries. *Fish Fish.* **16**(4): 633–648. doi:10.1111/faf.12083.
- Tam, J.C., and Bundy, A. 2019. Mass-balance models of the Newfoundland and Labrador shelf ecosystem for 1985-1987 and 2013-2015. *Can. Tech. Rep. Fish. Aquat. Sci.* **3328**: 88. Dartmouth, NS.
- Tam, J.C., Link, J.S., Rossberg, A.G., Rogers, S.I., Levin, P.S., Rochet, M.J., Bundy, A., Belgrano, A., Libralato, S., Tomczak, M., Van De Wolfshaar, K., Pranovi, F., Gorokhova, E., Large, S.I., Niquil, N., Greenstreet, S.P.R., Druon, J.N., Lesutiene, J., Johansen, M., Preciado, I., Patricio, J., Palialexis, A., Tett, P., Johansen, G.O., Houle, J., and Rindorf, A. 2017. Towards ecosystem-based management: Identifying operational food-web indicators for marine ecosystems. *ICES J. Mar. Sci.* **74**(7): 2040–2052. doi:10.1093/icesjms/fsw230.
- Van Teeffelen, A.J.A., Vos, C.C., and Opdam, P. 2012. Species in a dynamic world: Consequences of habitat network dynamics on conservation planning. *Biol. Conserv.* **153**: 239–253. Elsevier Ltd. doi:10.1016/j.biocon.2012.05.001.
- Thorson, J.T. 2017. Three problems with the conventional delta-model for biomass sampling data, and a computationally efficient alternative. *Can. J. Fish. Aquat. Sci.* **75**(9): 1369–1382.
- Thorson, J.T. 2019a. Guidance for decisions using the Vector Autoregressive Spatio-Temporal (VAST) package in stock, ecosystem, habitat and climate assessments. *Fish. Res.* **210**: 143–161. Elsevier. doi:10.1016/j.fishres.2018.10.013.
- Thorson, J.T. 2019b. VAST model structure and user interface. : 1–19. Available from https://github.com/James-Thorson-NOAA/VAST/blob/master/manual/VAST_model_structure.pdf.
- Thorson, J.T., Adams, G., and Holsman, K. 2019. Spatio-temporal models of intermediate complexity for ecosystem assessments: A new tool for spatial fisheries management. *Fish Fish.* (March): 1083–1099. doi:10.1111/faf.12398.
- Thorson, J.T., Ianelli, J.N., Munch, S.B., Ono, K., Spencer, P.D., and Vinbrooke, R. 2015a. Spatial delay-difference models for estimating spatiotemporal variation in juvenile production and population abundance. *Can. J. Fish. Aquat. Sci.* **72**(12): 1897–1915. doi:10.1139/cjfas-2014-0543.
- Thorson, J.T., Rindorf, A., Gao, J., Hanselman, D., and Winker, H. 2016. Density-dependent changes in effective area occupied for bottom-associated marine fishes. *Philos. Trans. R. Soc. B Biol. Sci.* **283**: 20161853. doi:10.1098/rspb.2016.1853.
- Thorson, J.T., Scheuerell, M.D., Olden, J.D., and Schindler, D.E. 2018. Spatial

- heterogeneity contributes more to portfolio effects than species variability in bottom-associated marine fishes. *Proc. R. Soc. B Biol. Sci.* **285**(20180915). doi:10.1098/rspb.2018.0915.
- Thorson, J.T., Shelton, A.O., Ward, E.J., and Skaug, H.J. 2015b. Geostatistical delta-generalized linear mixed models improve precision for estimated abundance indices for West Coast groundfishes. *ICES J. Mar. Sci.* **72**(5): 1297–1310.
- Townsend, H., Harvey, C.J., Davis, D., Zador, S.G., Gaichas, S., Weijerman, M., Hazen, E.L., and Kaplan, I.C. 2019. Progress on Implementing Ecosystem-Based Fisheries Management in the United States Through the Use of Ecosystem Models and Analysis. *Front. Mar. Sci.* **6**(641): 1–17. doi:10.3389/fmars.2019.00641.
- Trijoulet, V., Fay, G., Curti, K.L., Smith, B., and Miller, T.J. 2019. Performance of multispecies assessment models: insights on the influence of diet data. *ICES J. Mar. Sci.* doi:10.1093/icesjms/fsz112.
- Tulloch, V.J.D., Richardson, A.J., Plagányi, É.E., Matear, R., and Brown, C.J. 2017. Ecosystem modelling to quantify the impact of historical whaling on Southern Hemisphere baleen whales. *Fish Fish.* **19**(1): 117–137. doi:10.1111/faf.12241.
- Tyrrell, M.C., Link, J.S., Moustahfid, H., and Overholtz, W.J. 2008. Evaluating the effect of predation mortality on forage species population dynamics in the Northeast US continental shelf ecosystem using multispecies virtual population analysis. *ICES J. Mar. Sci.* **65**(9): 1689–1700. doi:10.1093/icesjms/fsn185.
- Uiterwaal, S., Lagerstrom, I., Lyon, S., and DeLong, J. 2018. Data paper: FoRAGE (Functional Responses from Around the Globe in all Ecosystems) database: a compilation of functional responses for consumers and parasitoids. bioRxiv: 503334. doi:10.1101/503334.
- Ummenhofer, C.C., and Meehl, G.A. 2017. Extreme weather and climate events with ecological relevance: A review. *Philos. Trans. R. Soc. B Biol. Sci.* **372**(1723). doi:10.1098/rstb.2016.0135.
- Urrego-Blanco, J., and Sheng, J. 2012. Interannual variability of the circulation over the eastern Canadian shelf. *Atmos. - Ocean* **50**(3): 277–300. doi:10.1080/07055900.2012.680430.
- Valladares, F., Matesanz, S., Guilhaumon, F., Araújo, M.B., Balaguer, L., Benito-Garzón, M., Cornwell, W., Gianoli, E., van Kleunen, M., Naya, D.E., Nicotra, A.B., Poorter, H., and Zavala, M.A. 2014. The effects of phenotypic plasticity and local adaptation on forecasts of species range shifts under climate change. *Ecol. Lett.* **17**(11): 1351–1364. doi:10.1111/ele.12348.
- Vuilleumier, S., Wilcox, C., Cairns, B.J., and Possingham, H.P. 2007. How patch configuration affects the impact of disturbances on metapopulation persistence. *Theor. Popul. Biol.* **72**(1): 77–85. doi:10.1016/j.tpb.2006.11.001.

- Walsh, S., Morgan, J., Brodie, W., Dwyer, K., and Mansfield, L. 2001. A New Tagging Program for Yellowtail Flounder on the Grand Bank, NAFO Divisions 3LNO. NAFO SCR Doc **01/53**(N4431): 14.
- Walsh, S.J. 1996. Efficiency of Bottom Sampling Trawls in Deriving Survey Abundance Indices. NAFO SCS **28**: 9–24.
- Walsh, S.J., and Colbourne, E. 2007. Investigating the effects of variation in surplus production, stock biomass, catch and climate on the Grand Bank yellowtail flounder population. NAFO SCR Doc **07/43**(N5395): 21.
- Walsh, S.J., and Morgan, M.J. 1999. Variation in maturation of yellowtail flounder (*Pleuronectes ferruginea*) on the Grand Bank. *J. Northwest Atl. Fish. Sci.* **25**: 47–59. doi:10.2960/J.v25.a5.
- Walsh, S.J., Simpson, M., and Morgan, M.J. 2004. Continental shelf nurseries and recruitment variability in American plaice and yellowtail flounder on the Grand Bank: Insights into stock resiliency. *J. Sea Res.* **51**(3–4): 271–286. doi:10.1016/j.seares.2003.10.003.
- Walters, C.J., and Bonfil, R. 1999. Multispecies spatial assessment models for the British Columbia groundfish trawl fishery. *Can. J. Fish. Aquat. Sci.* **56**(4): 601–628. doi:10.1139/f98-205.
- Walters, C.J., Neuenhoff, R.D., Trites, A.W., Swain, D.P., Cox, S.P., McAllister, M.K., and Hammill, M.O. 2018. Continued decline of a collapsed population of Atlantic cod (*Gadus morhua*) due to predation-driven Allee effects. *Can. J. Fish. Aquat. Sci.* **76**(1): 168–184. doi:10.1139/cjfas-2017-0190.
- Wernberg, T., Bennett, S., Babcock, R.C., Bettignies, T. De, Cure, K., Depczynski, M., Dufois, F., Fromont, J., Fulton, C.J., Hovey, R.K., Harvey, E.S., Holmes, T.H., Kendrick, G. a, Radford, B., Santana-garcon, J., Saunders, B.J., Smale, D. a, Thomsen, M.S., Tuckett, C. a, and Tuya, F. 2015. Climate-driven regime shift of a temperate marine ecosystem. *Science.* **353**(6295): 169–172. doi:10.1126/science.aad8745.
- Wheeland, L. 2021. An exploration of the impact of natural mortality assumptions in a Virtual Population Analysis for Divisions 3LNO American Plaice. NAFO SCR Doc **21/025**(N7193): 16.
- Wheeland, L., Dwyer, K., Kumar, R., Rideout, R., Perreault, A., and Rogers, B. 2021. Assessment of American plaice in Div. 3LNO. NAFO SCR Doc **21**(035).
- Wheeland, L., Dwyer, K., Morgan, J., Rideout, R., and Rogers, R. 2018. Assessment of American Plaice in Div. 3LNO. NAFO SCS Doc **18/039**(N6829): 77.
- Wheeland, L.J., and Morgan, M.J. 2020. Age-specific shifts in Greenland halibut (*Reinhardtius hippoglossoides*) distribution in response to changing ocean climate. *ICES J. Mar. Sci.* **77**(1): 230–240. doi:10.1093/icesjms/fsz152.

- Wickham, H. 2009. *ggplot2: Elegant Graphics for Data Analysis*. Springer-Verlag New York. Available from <http://ggplot2.org>.
- Winters, G.H. 1983. Analysis of the biological and demographic parameters of northern sand lance, *Ammodytes dubius*, from the Newfoundland Grand Bank. *Can. J. Fish. Aquat. Sci.* **40**(4): 409–419. doi:10.1139/f83-059.
- Worm, B., Hilborn, R., Baum, J.K., Branch, T.A., Collie, J.S., Costello, C., Fogarty, M.J., Fulton, E.A., Hutchings, J.A., Jennings, S., Jensen, O.P., Lotze, H.K., Mace, P.M., McClanahan, T.R., Minto, C., Palumbi, S.R., Parma, A.M., Ricard, D., Rosenberg, A.A., Watson, R., and Zeller, D. 2009. Rebuilding Global Fisheries. *Science*. **325**(5940): 578–585. doi:10.1126/science.1173146.
- Yodzis, P. 1994. Predator-Prey Theory and Management of Multispecies Fisheries. *Ecol. Appl.* **4**(1): 51–58.
- Yule, D.L., Adams, J. V., Stockwell, J.D., and Gorman, O.T. 2007. Using Multiple Gears to Assess Acoustic Detectability and Biomass of Fish Species in Lake Superior. *North Am. J. Fish. Manag.* **27**(1): 106–126. doi:10.1577/m06-090.1.
- Zhang, F., Regular, P.M., Wheeland, L., Rideout, R.M., and Morgan, M.J. 2021a. Accounting for non-stationary stock-recruitment relationships in the development of MSY-based reference points. *ICES J. Mar. Sci.* **78**(6): 2233–2243. doi:10.1093/icesjms/fsaa176.
- Zhang, F., Reid, K.B., and Nudds, T.D. 2021b. The longer the better ? Trade-offs in fisheries stock assessment in dynamic ecosystems. *Fish Fish.* **22**: 789–797. doi:10.1111/faf.12550.
- Zhang, F., Rideout, R., and Cadigan, N. 2020. Spatiotemporal variations in juvenile mortality and cohort strength of Atlantic cod (*Gadus morhua*) off Newfoundland and Labrador. *Can. J. Fish. Aquat. Sci.* **77**(3): 625–635.
- Zheng, N., Cadigan, N.G., and Morgan, M. 2020a. A spatiotemporal Richards–Schnute growth model and its estimation when data are collected through length-stratified sampling. *Environ. Ecol. Stat.* **27**(3): 415–446.
- Zheng, N., Robertson, M., Cadigan, N., Zhang, F., Morgan, J., and Wheeland, L. 2020b. Spatiotemporal variation in maturation : A case study with American plaice (*Hippoglossoides platessoides*) on the Grand Bank off Newfoundland. *Can. J. Fish. Aquat. Sci.* **77**(10): 1688–1699. doi:10.1139/cjfas-2020-0017.
- Zuur, A., Ieno, E., Walker, N., Saveliev, A., and Smith, G. 2009. *Mixed Effects Models and Extensions in Ecology with R*. 1st edition. Springer, New York.

Appendices

A. Appendix for Chapter 2

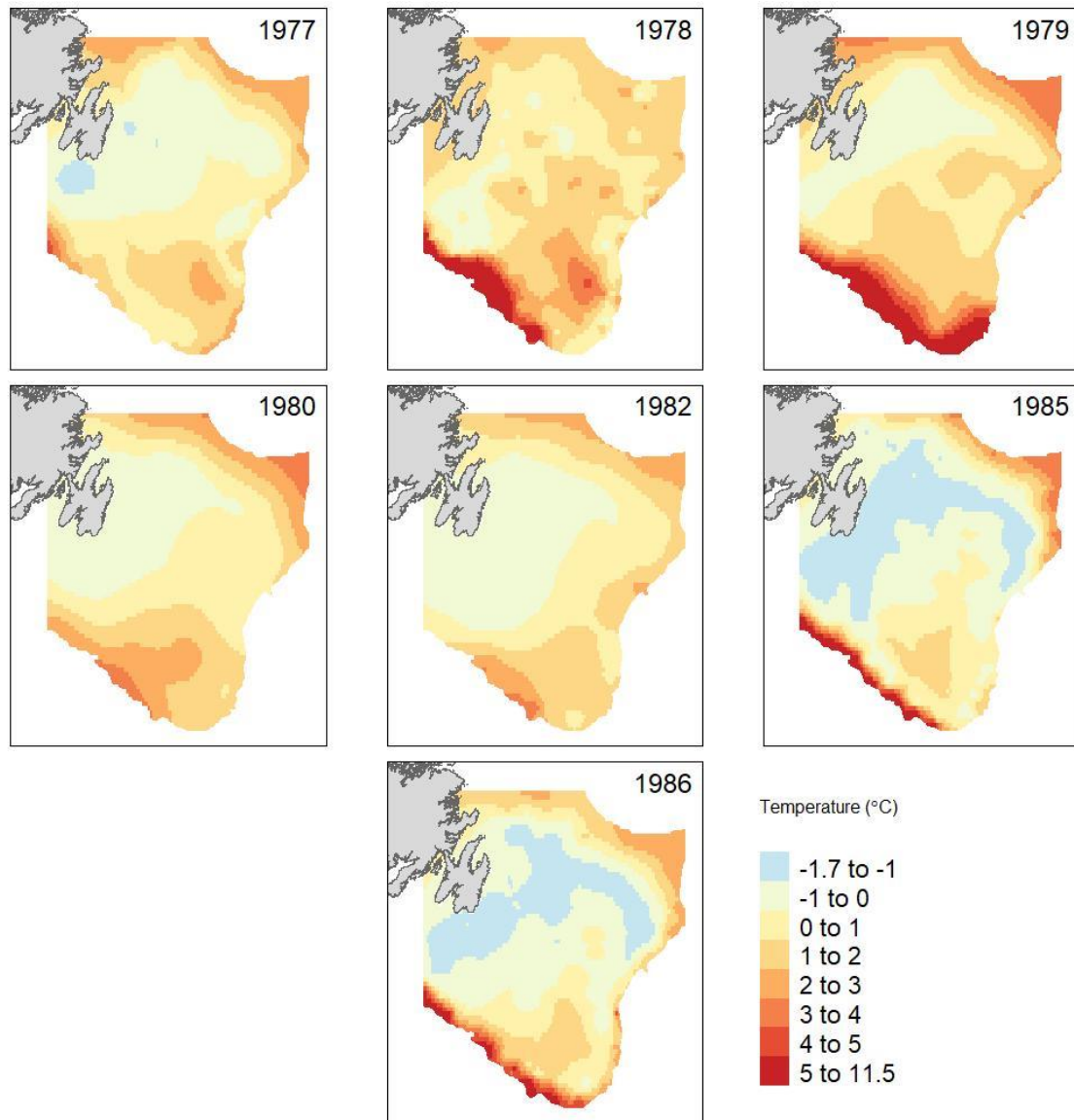


Figure A1. Kriged, non-modified, survey temperatures from 1977-1986, 100x100 raster grid. Darkest red represents all temperatures above 5°C because those temperatures have a very limited spatial coverage.

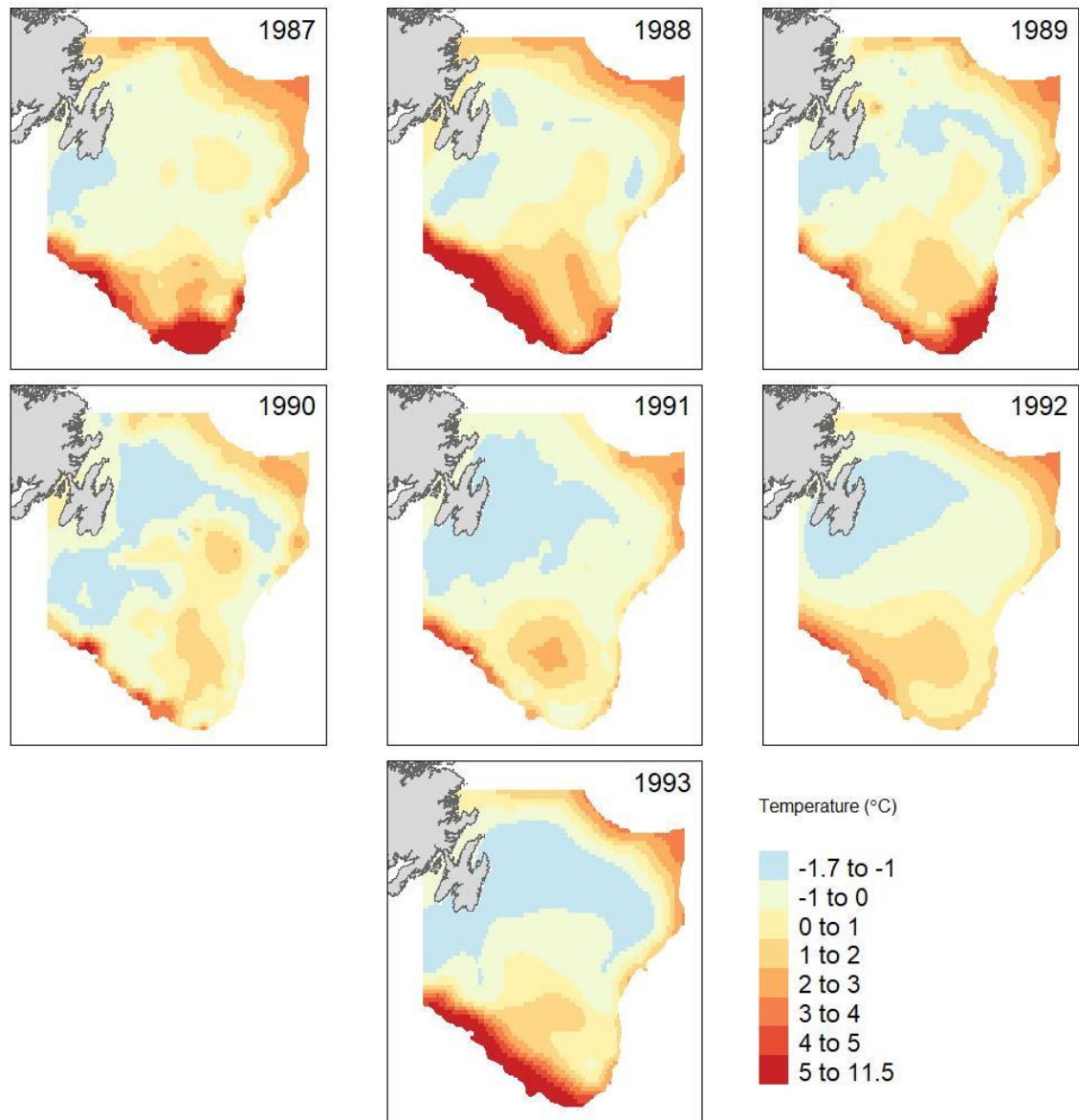


Figure A2. Kriged, non-modified, survey temperatures from 1987-1993, 100x100 raster grid. Darkest red represents all temperatures above 5° C because those temperatures have a very limited spatial coverage.

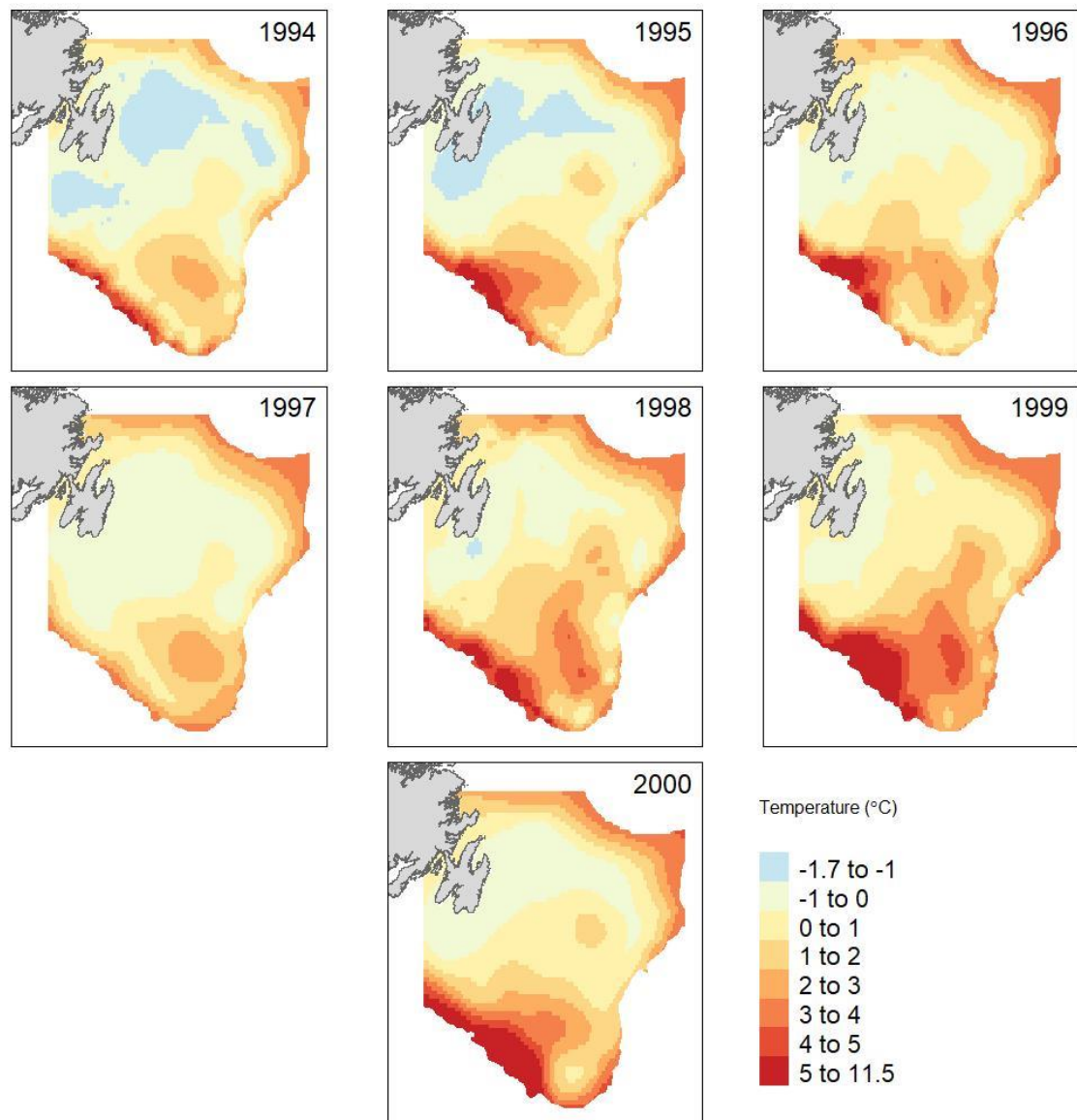


Figure A3. Kriged, non-modified, survey temperatures from 1994-2000, 100x100 raster grid. Darkest red represents all temperatures above 5° C because those temperatures have a very limited spatial coverage.

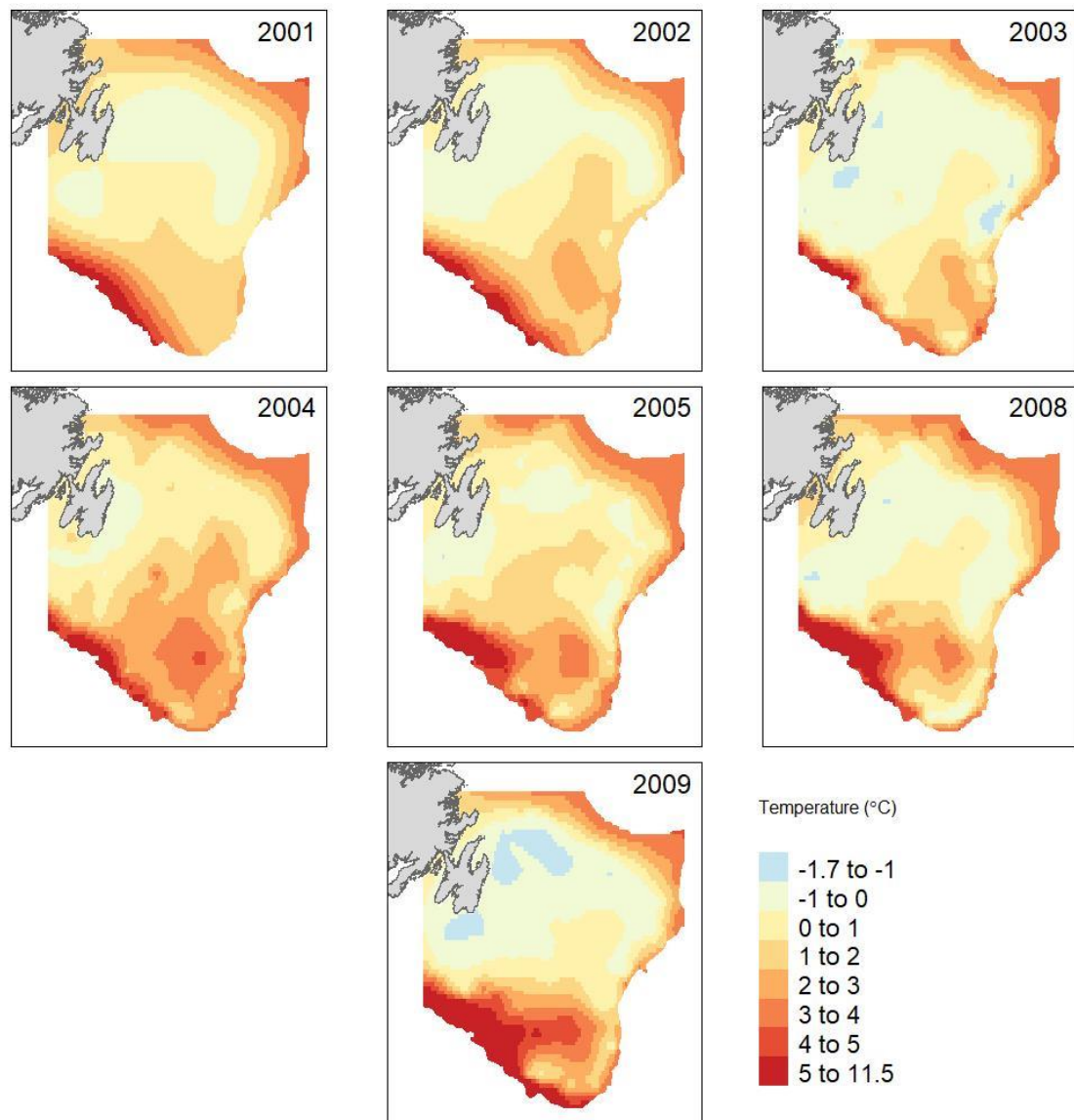


Figure A4. Kriged, non-modified, survey temperatures from 2001-2009, 100x100 raster grid. Darkest red represents all temperatures above 5° C because those temperatures have a very limited spatial coverage.

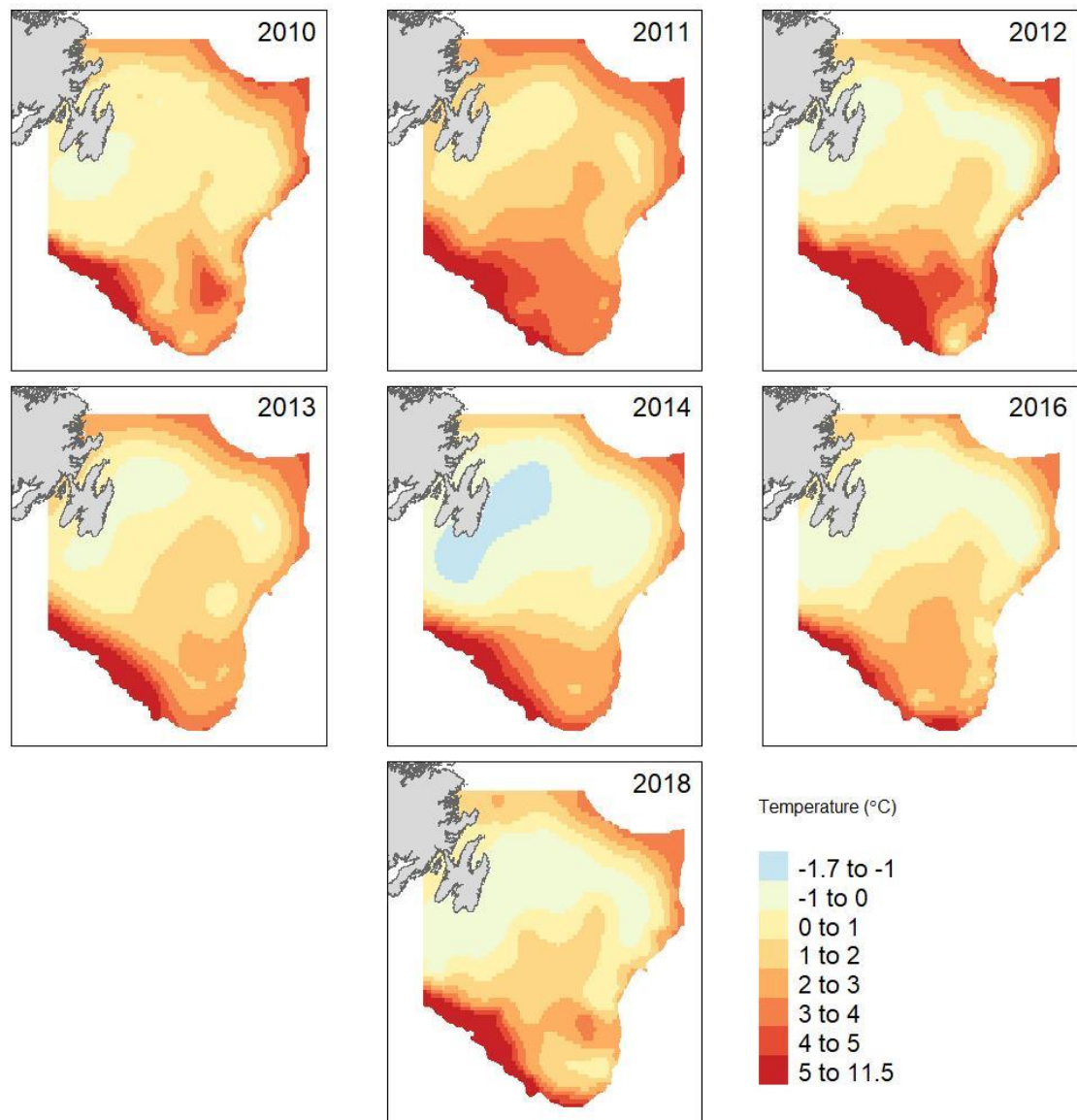


Figure A5. Kriged, non-modified, survey temperatures from 2010-2018, 100x100 raster grid. Darkest red represents all temperatures above 5°C because those temperatures have a very limited spatial coverage.

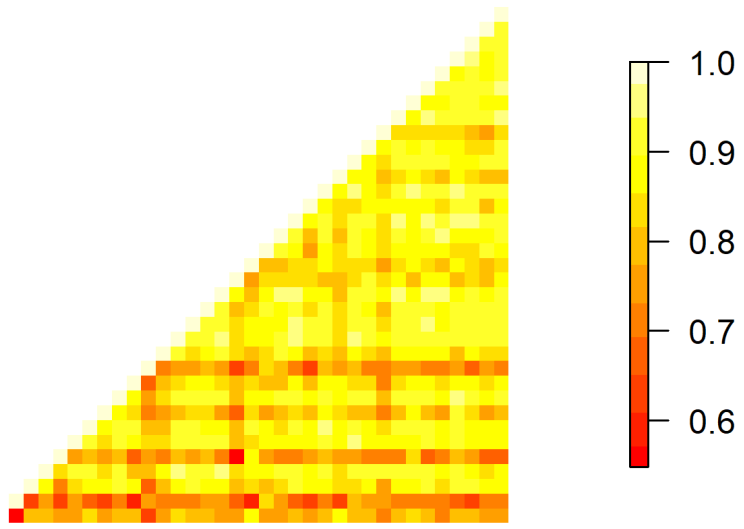


Figure A6. Spearman correlation of spatial temperatures over time (1977 – 2018) with itself. 1977 is on the left of the x-axis and bottom of the y-axis.

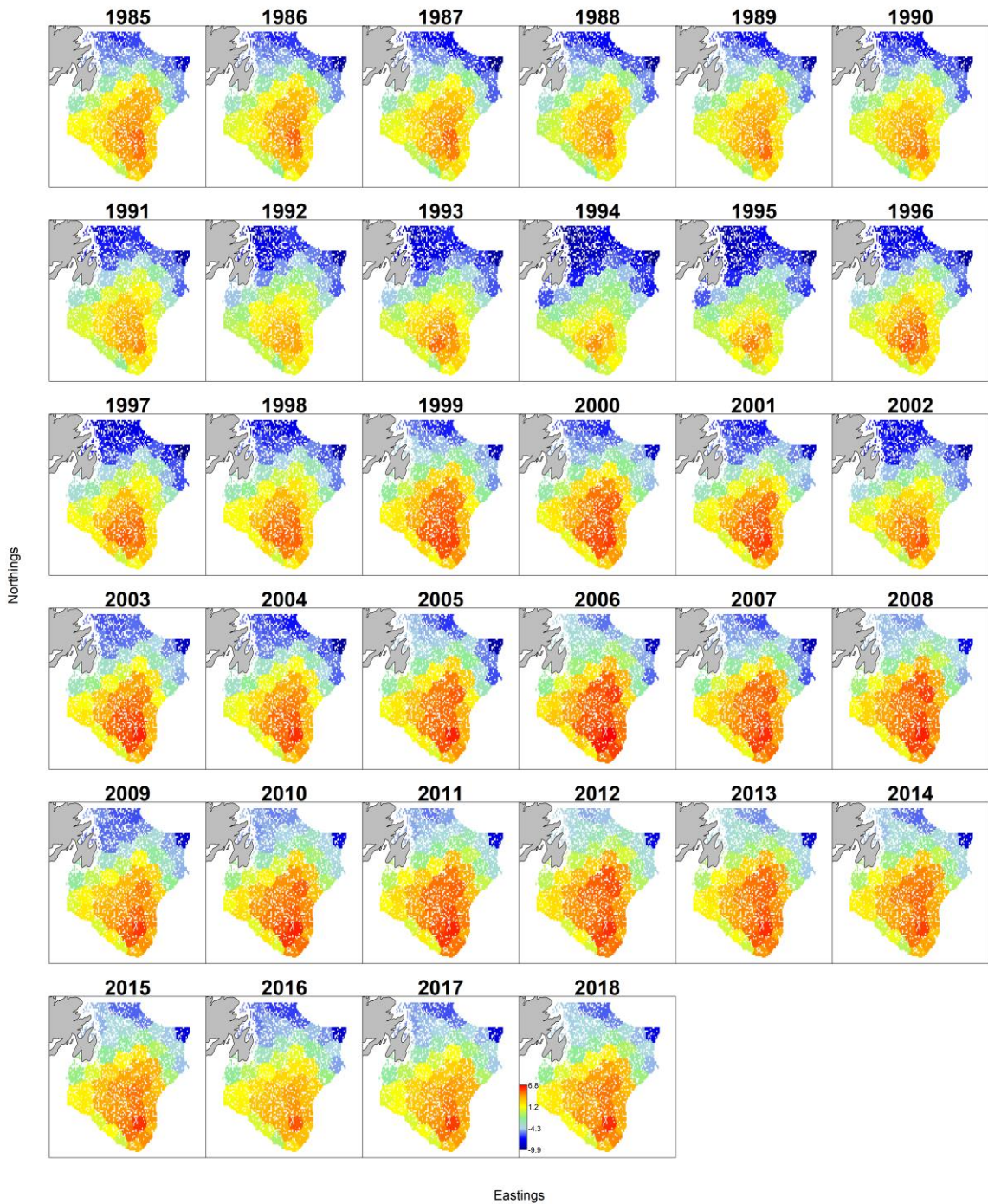


Figure A7. Yellowtail flounder distribution over time using the 50 knot VAST model, red indicates high density and blue indicates low density.

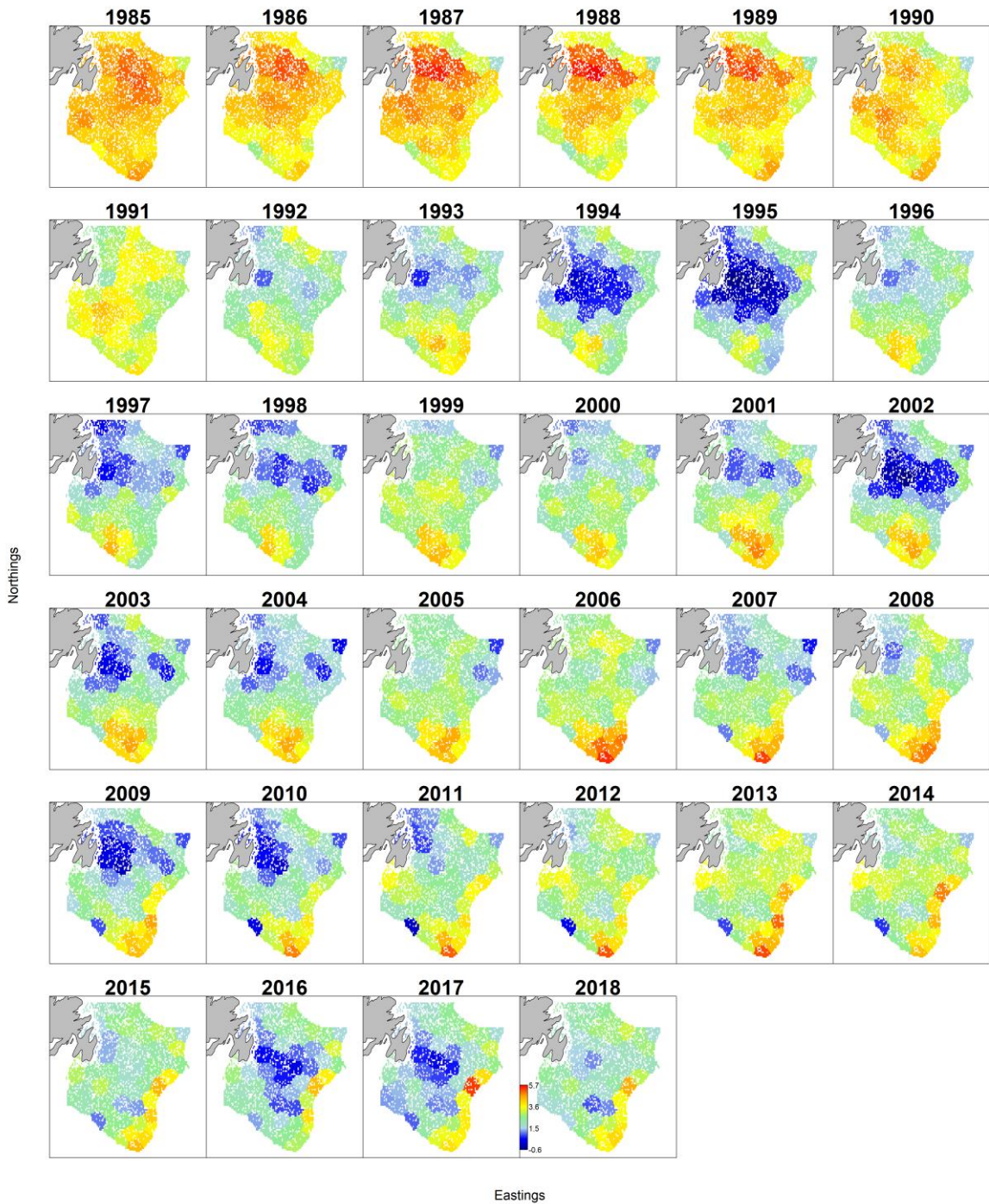


Figure A8. American plaice distribution over time using the 50 knot VAST model, red indicates high density and blue indicates low density.

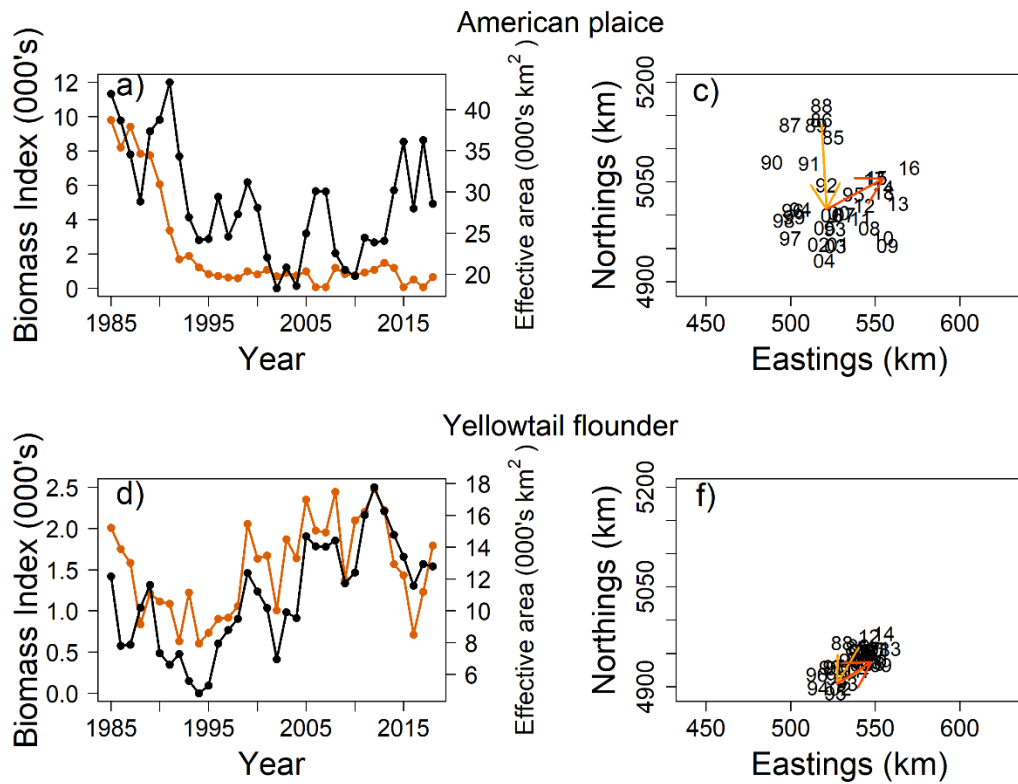


Figure A9. Biomass index (tonnes) and effective area for a) American plaice and c) yellowtail flounder (biomass index = orange lines, effective area = black lines). Center of gravity for b) American plaice (black text) and d) yellowtail flounder (black text). The orange arrows in b & d) represent the median direction of change of fish distributions from 1985 – 1993, and the red arrows represent the median change from 1993 – 2018.

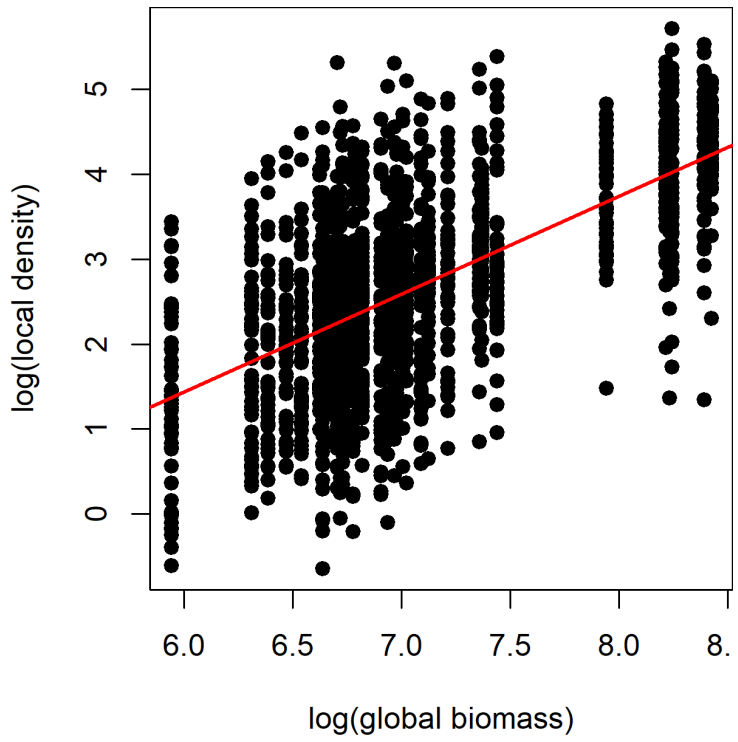


Figure A10. American plaice relationship between global (total) population biomass and local population density. The red line indicates the fit of a linear model.

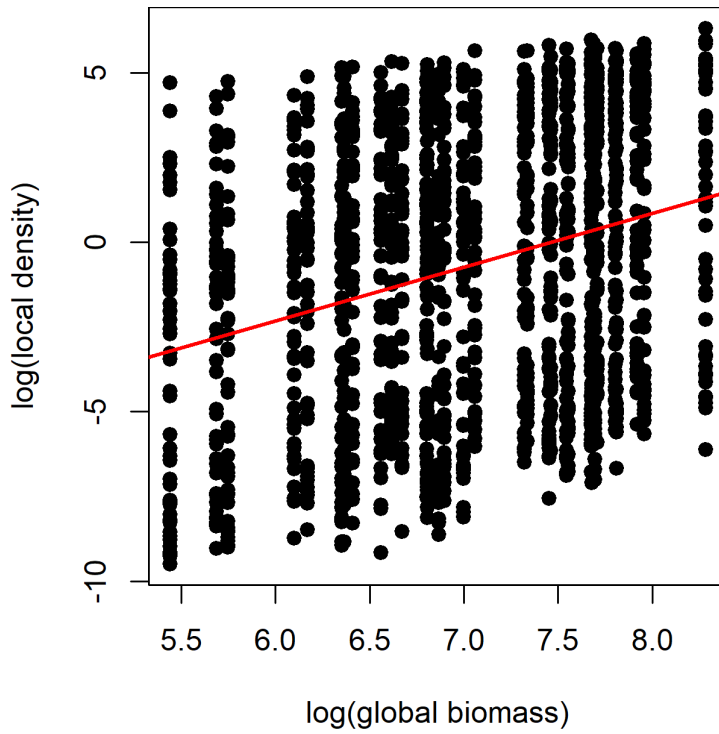


Figure A11. Yellowtail flounder relationship between global (total) population biomass and local population density. The red line indicates the fit of a linear model.

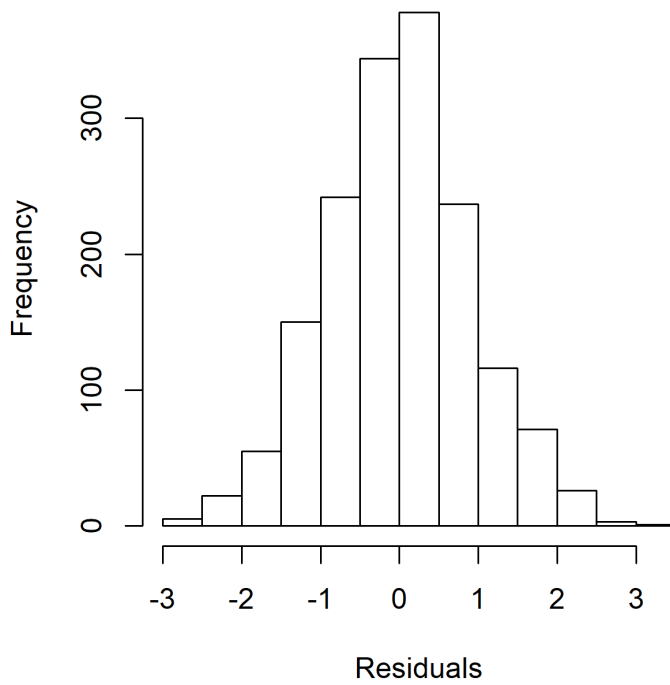


Figure A12. Histogram of residuals from the linear model between American plaice global population biomass and local population density.

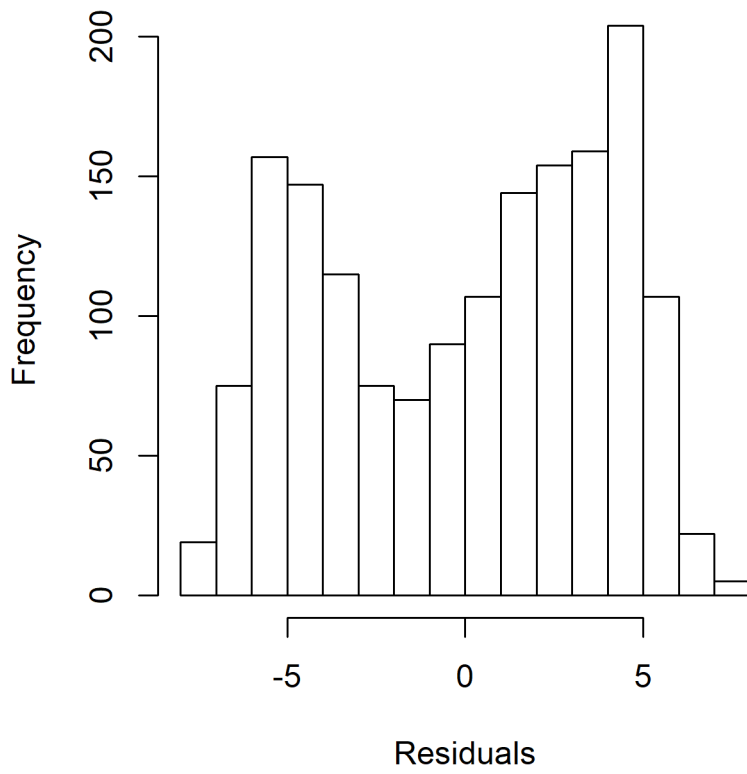


Figure A13. Histogram of residuals from the linear model between yellowtail flounder global population biomass and local population density.

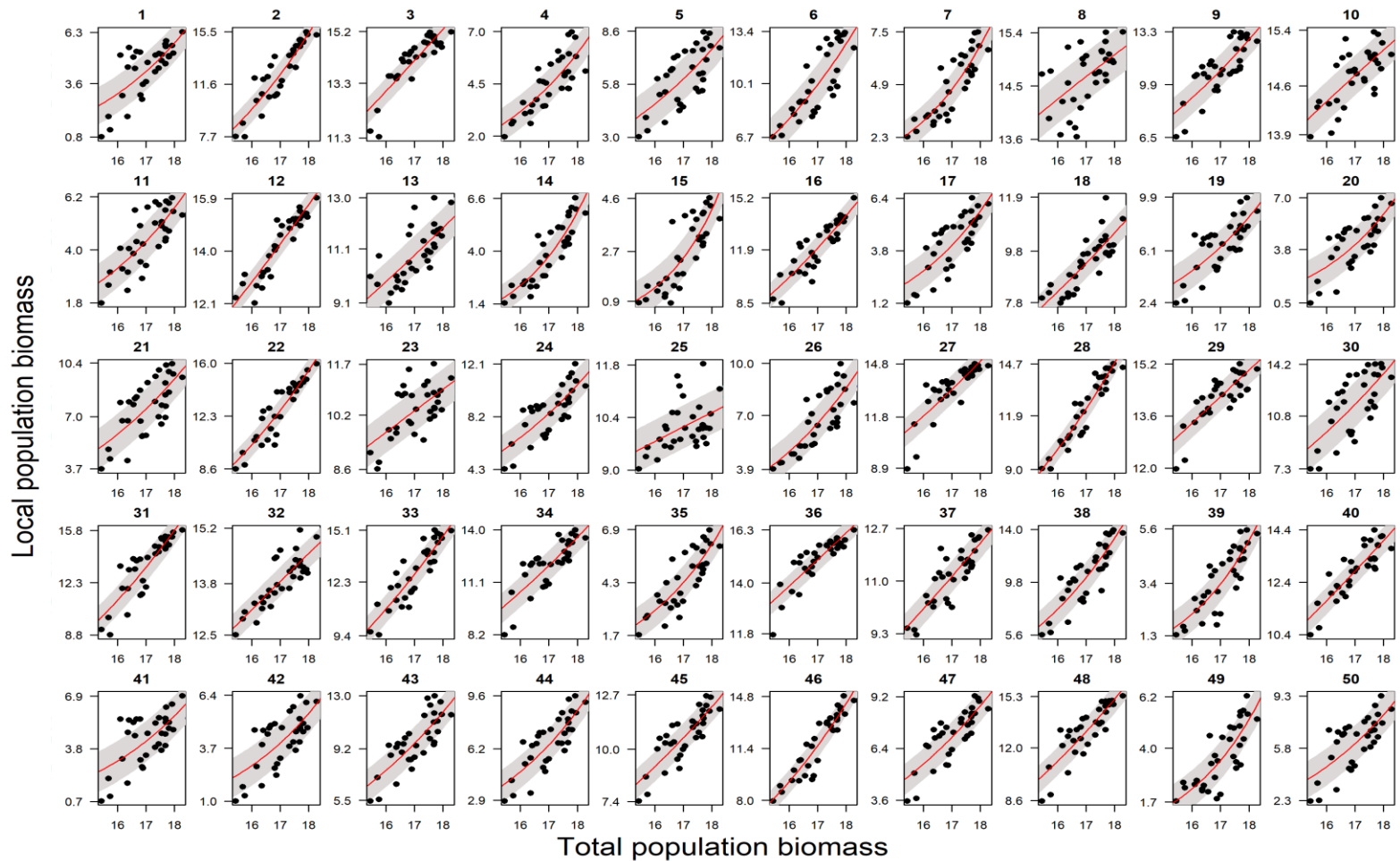


Figure A14. Yellowtail flounder relationships between global (total) population biomass (x-axis) and local population biomass (y-axis) at all 50 knots (panels) from the VAST. The red lines represent the predicted local relationship from the random effects model and grey polygon represents the root mean square error for those relationships.

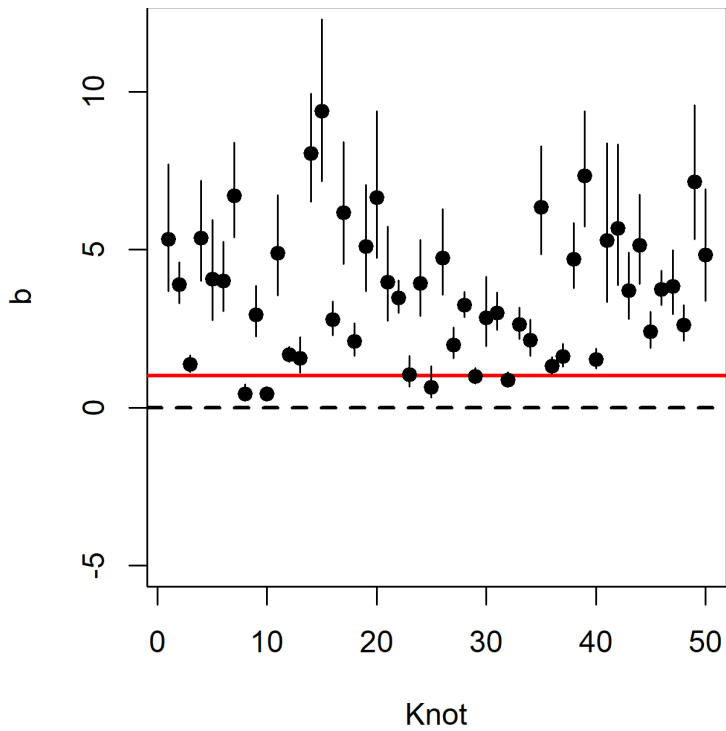


Figure A15. Model estimates of b_k at each knot. The segments represent $\pm 1.96 \cdot \text{SD}$. The solid red line indicates 1, the dashed black line indicates 0.

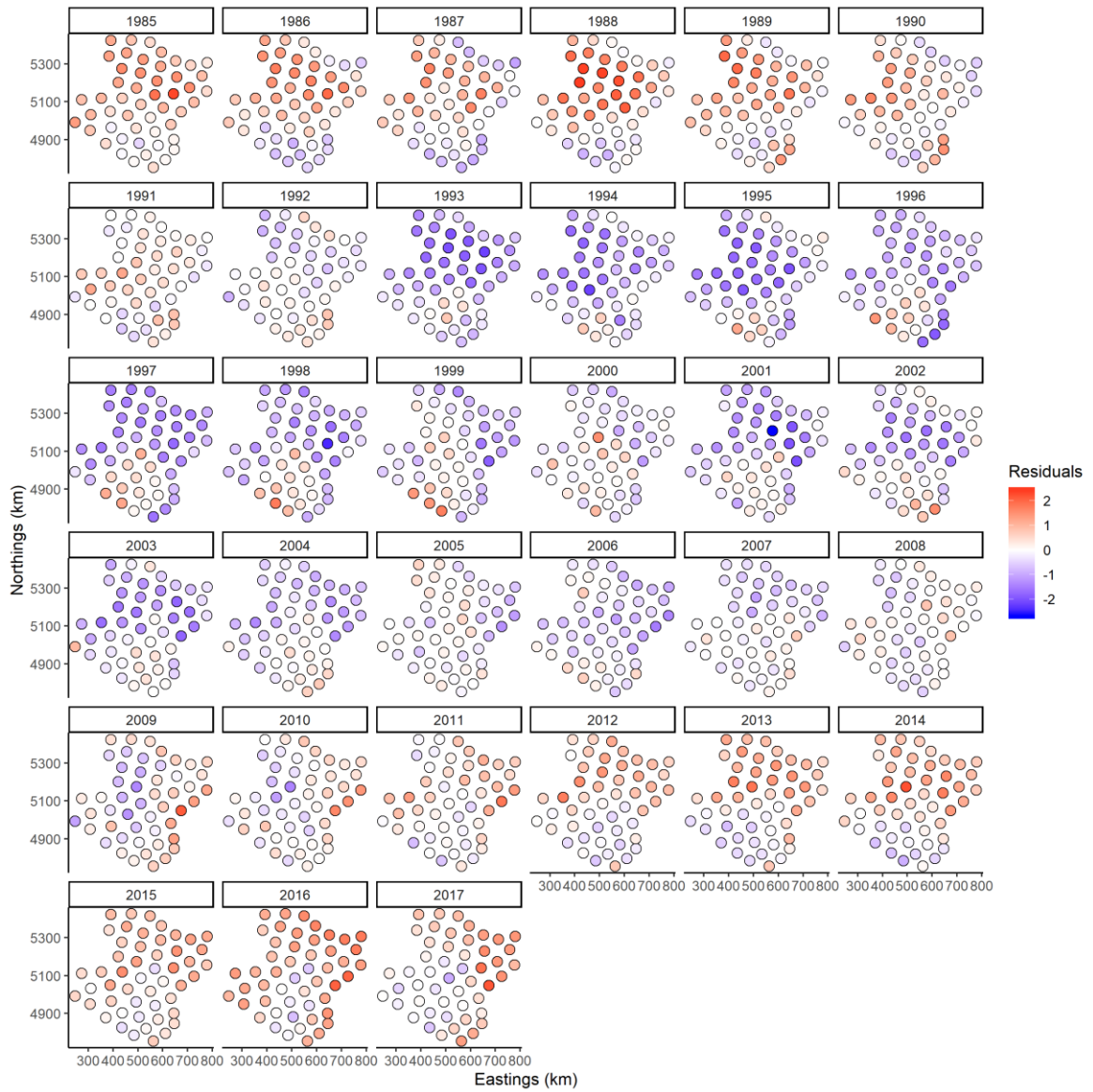


Figure A16. Yellowtail flounder local density residuals from the density dependent habitat selection model.

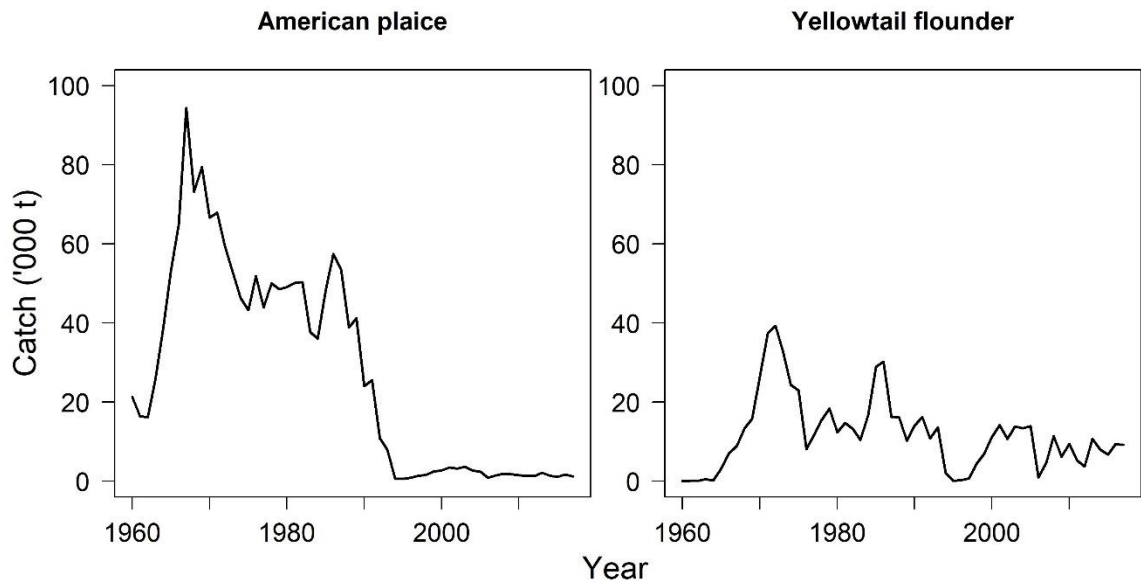


Figure A17. Time-series of catch ('000 t) for American plaice (Wheeland et al. 2018) and yellowtail flounder (Parsons et al. 2018) in NAFO divisions 3LNO.

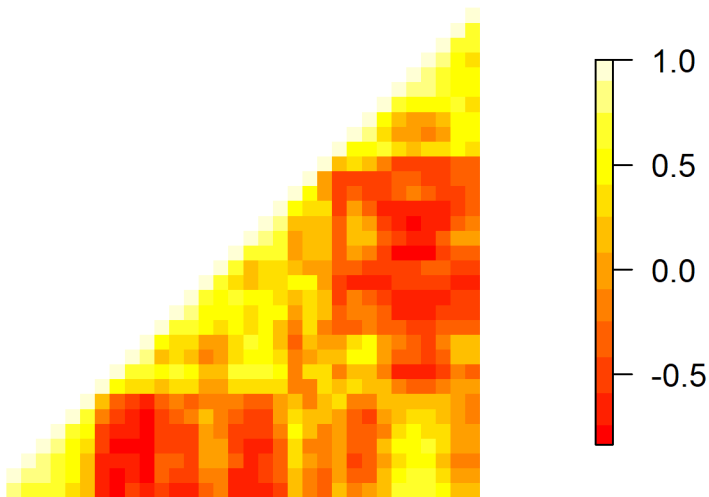


Figure A18. Spearman correlation of the spatial distribution of yellowtail flounder density-dependent residuals over time (1985 – 2018) with itself. 1985 is on the left of the x-axis and bottom of the y-axis.

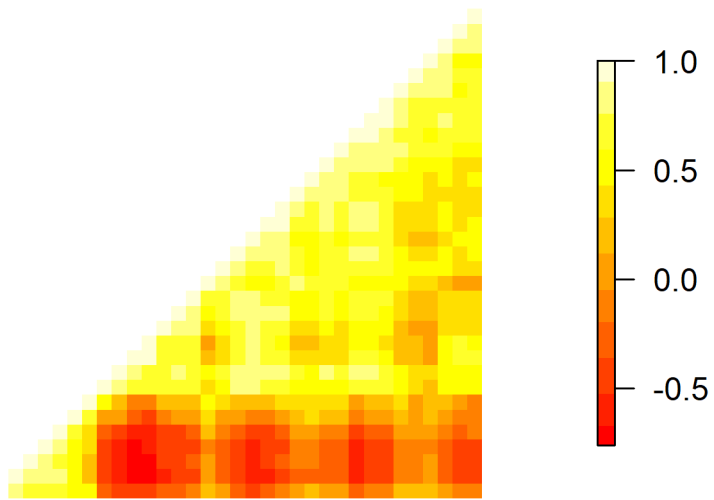


Figure A19. Spearman correlation of the spatial distribution of American plaice over time (1985 – 2018) with itself. 1985 is on the left of the x-axis and bottom of the y-axis.

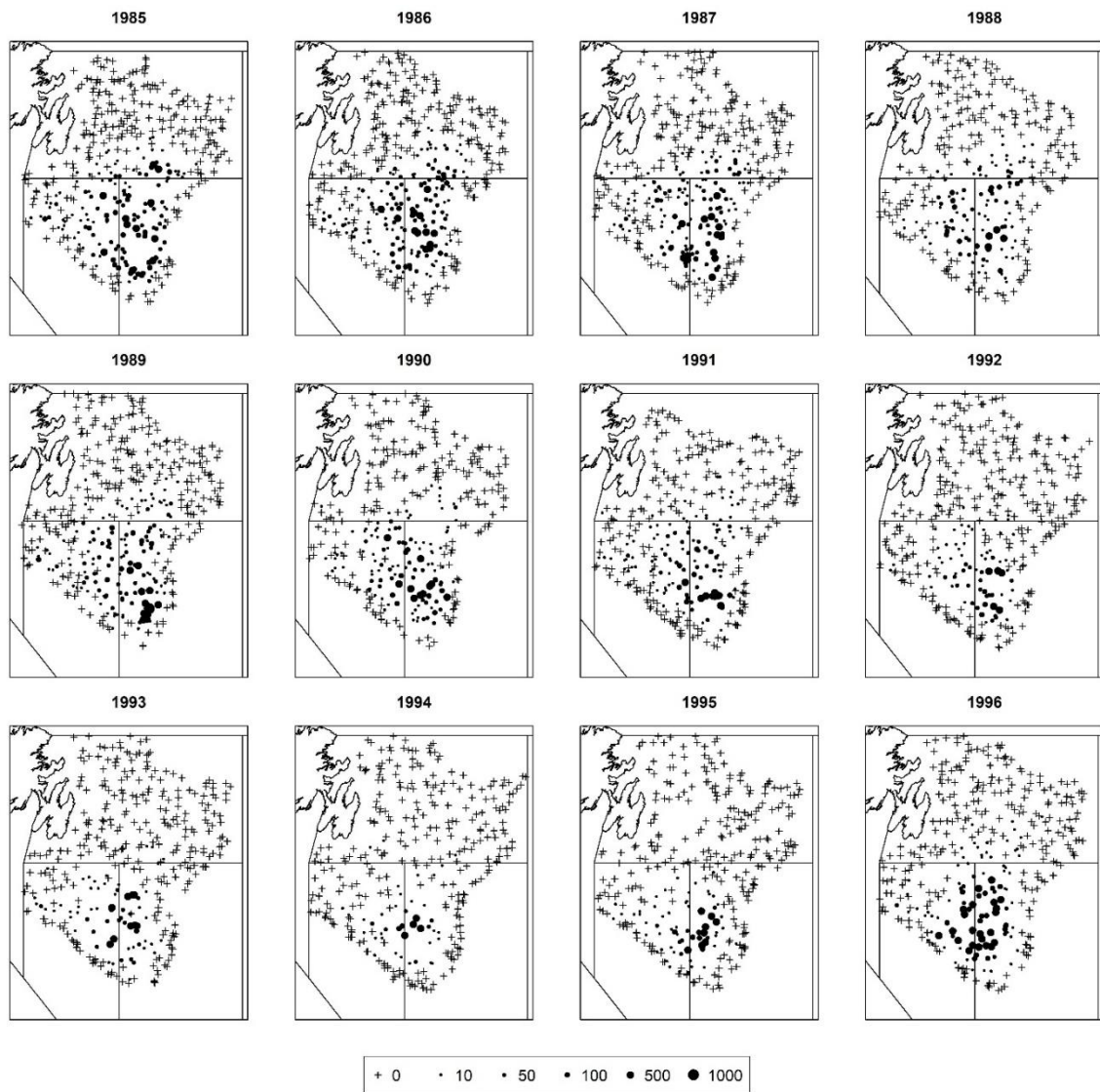


Figure A20. Observed survey catches for yellowtail flounder in NAFO divisions 3LNO from 1985 – 1996. No catch is denoted as a plus symbol and positive catches (biomass [kg]) are shown as points that increase in size with increased biomass caught.

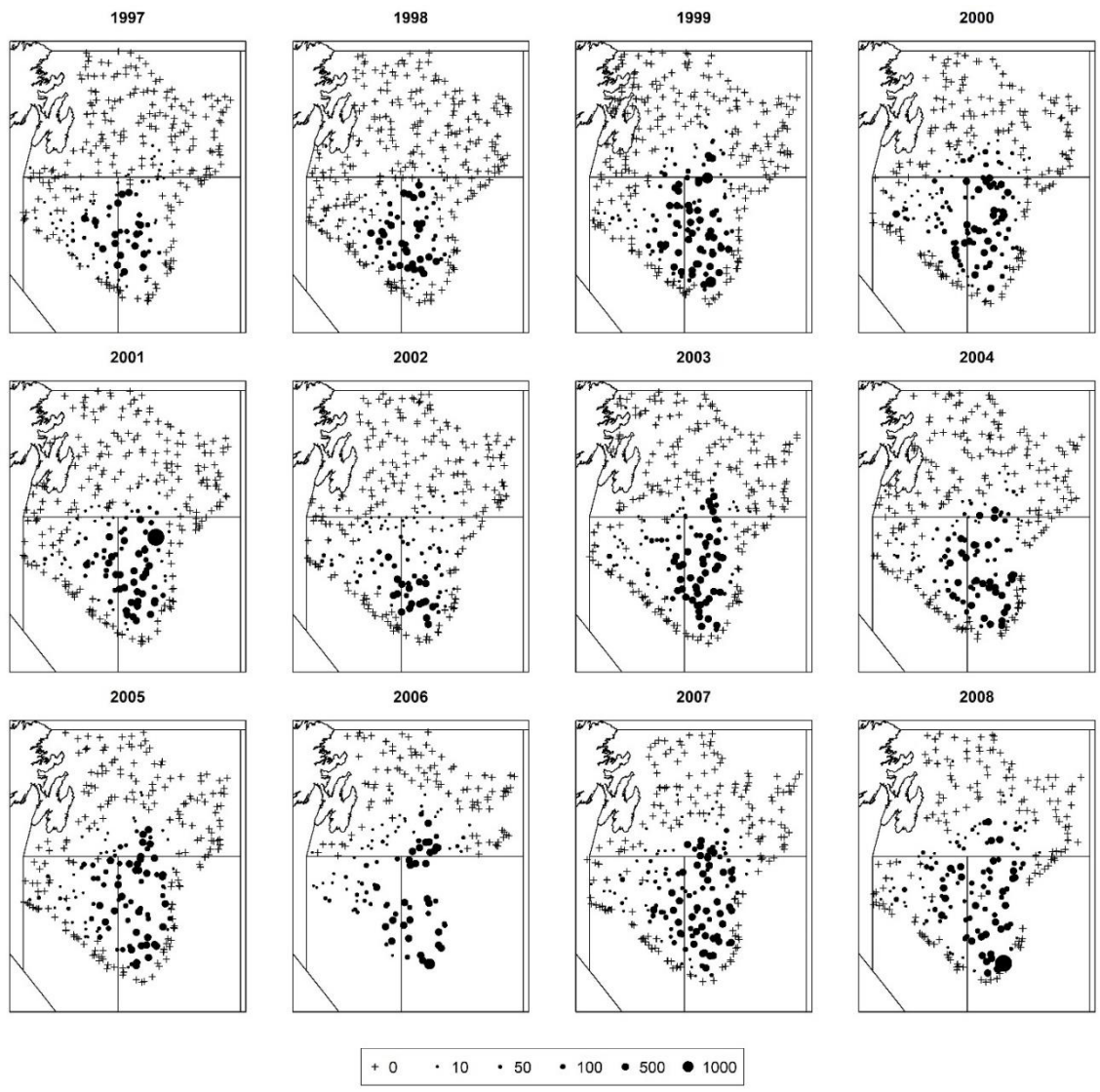


Figure A21. Observed survey catches for yellowtail flounder in NAFO divisions 3LNO from 1997 – 2008. No catch is denoted as a plus symbol and positive catches (biomass [kg]) are shown as points that increase in size with increased biomass caught.

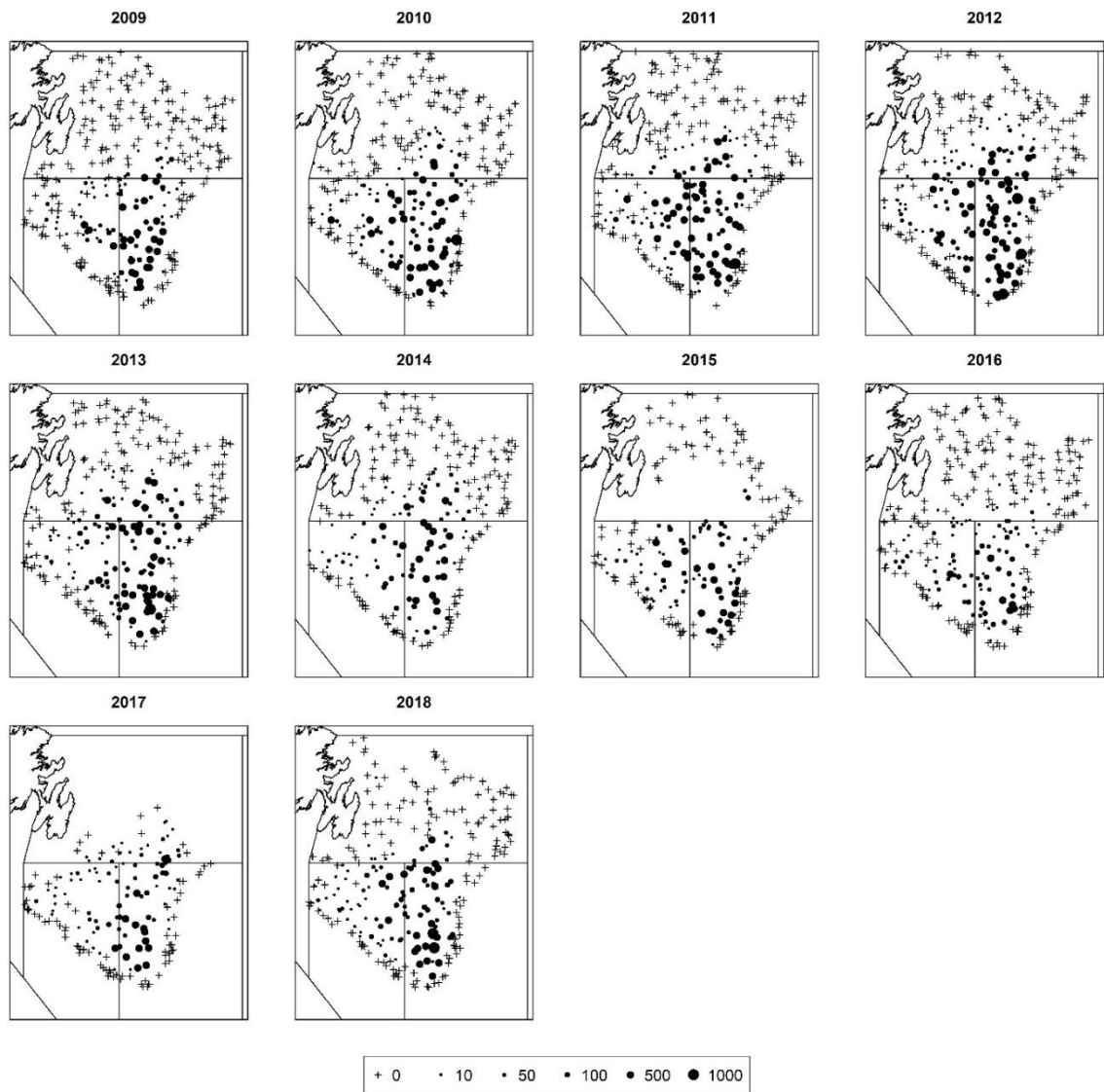


Figure A22. Observed survey catches for yellowtail flounder in NAFO divisions 3LNO from 2009 – 2018. No catch is denoted as a plus symbol and positive catches (biomass [kg]) are shown as points that increase in size with increased biomass caught.

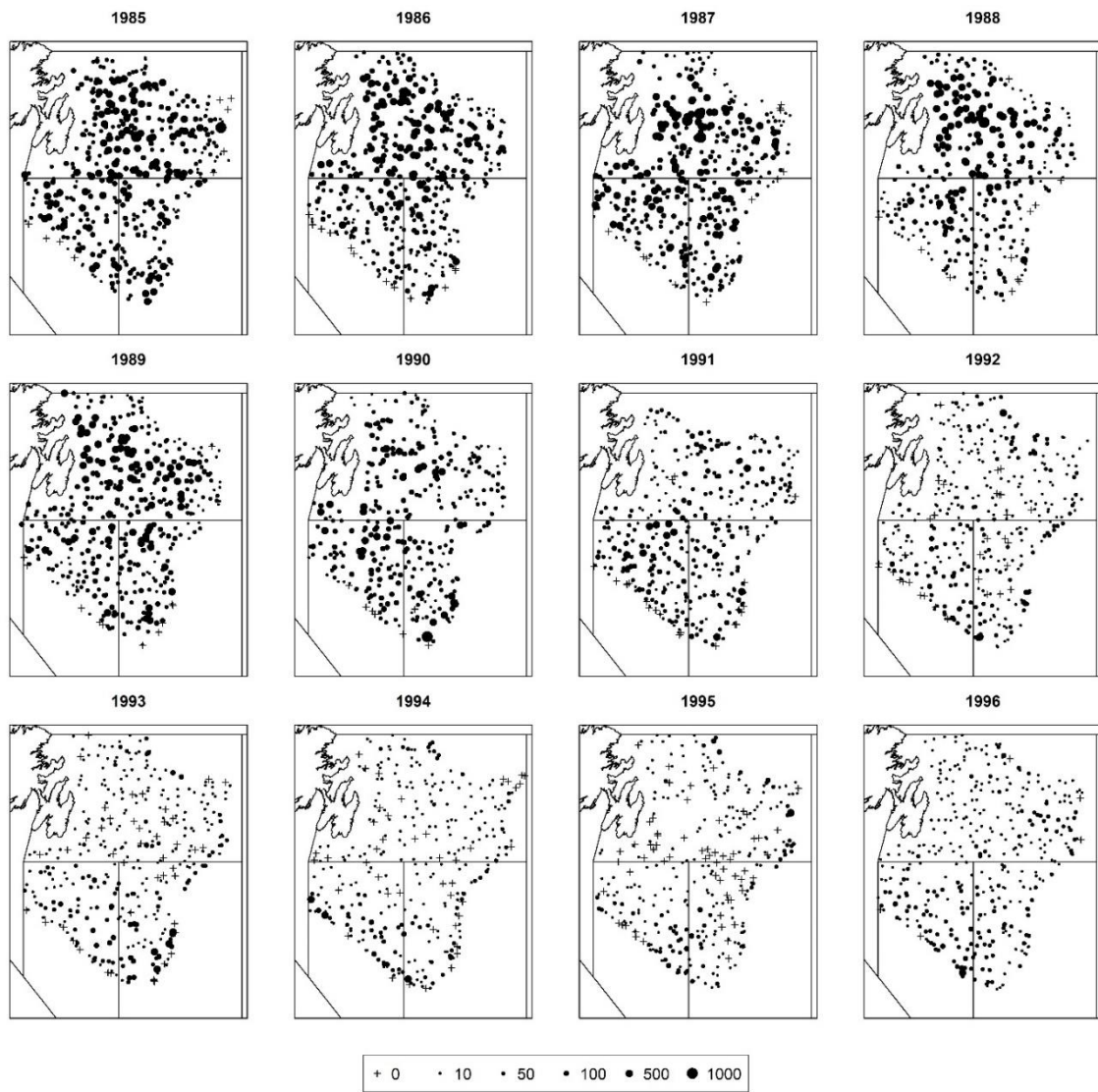


Figure A23. Observed survey catches for American plaice in NAFO divisions 3LNO from 1985 – 1996. No catch is denoted as a plus symbol and positive catches (biomass [kg]) are shown as points that increase in size with increased biomass caught.

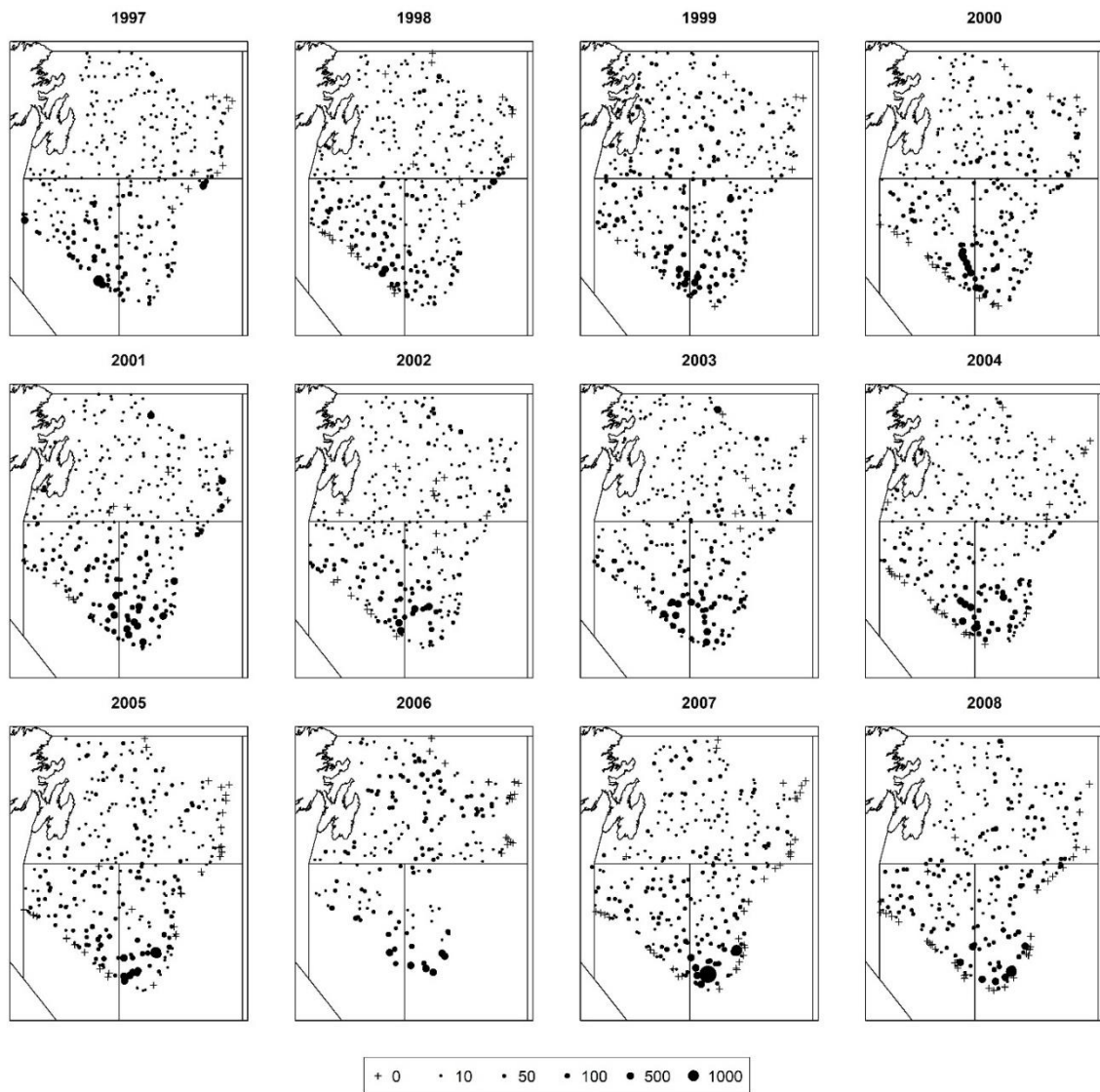


Figure A24. Observed survey catches for American plaice in NAFO divisions 3LNO from 1997 – 2008. No catch is denoted as a plus symbol and positive catches (biomass [kg]) are shown as points that increase in size with increased biomass caught.

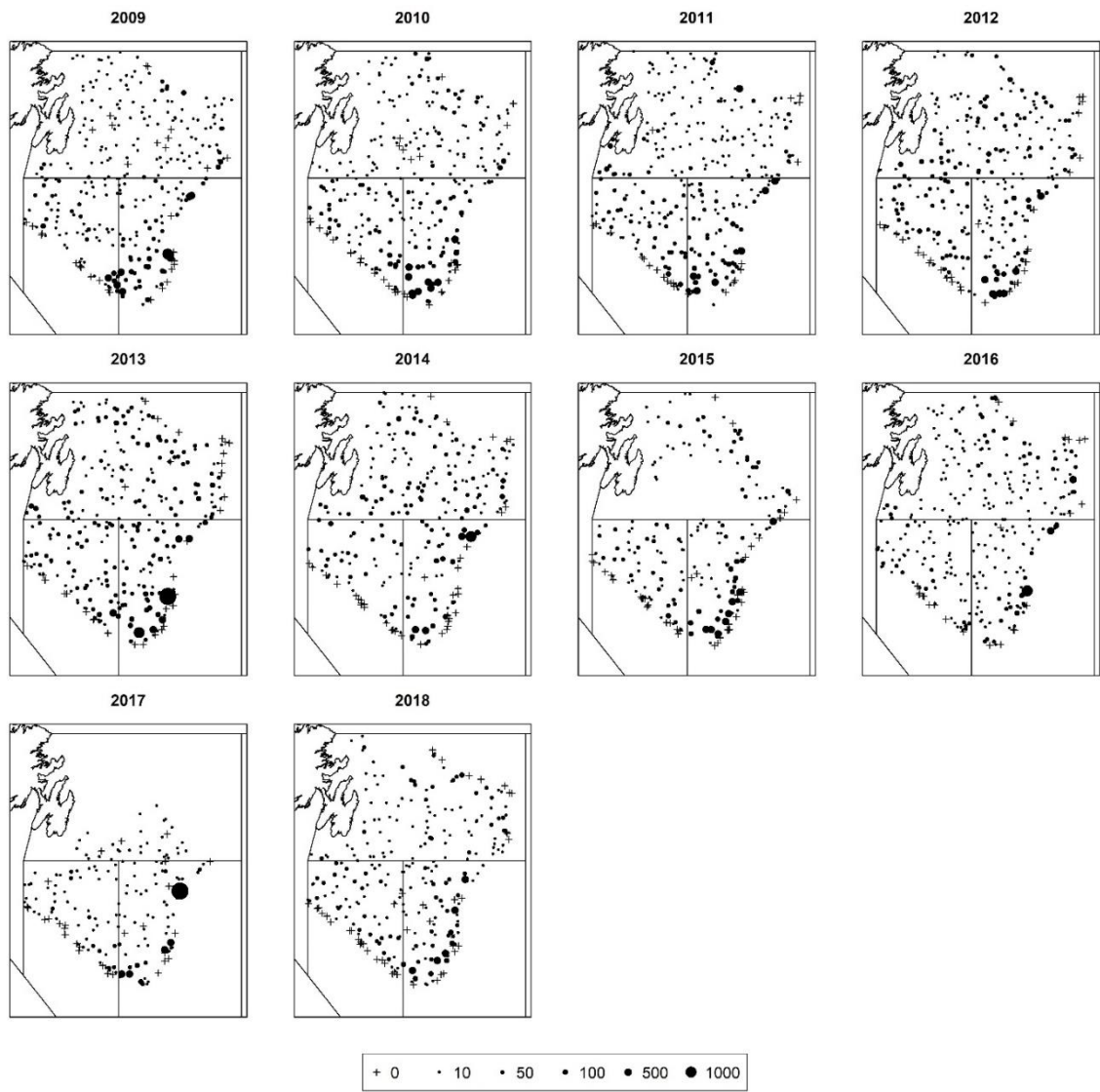


Figure A25. Observed survey catches for American plaice in NAFO divisions 3LNO from 2009 – 2018. No catch is denoted as a plus symbol and positive catches (biomass [kg]) are shown as points that increase in size with increased biomass caught.

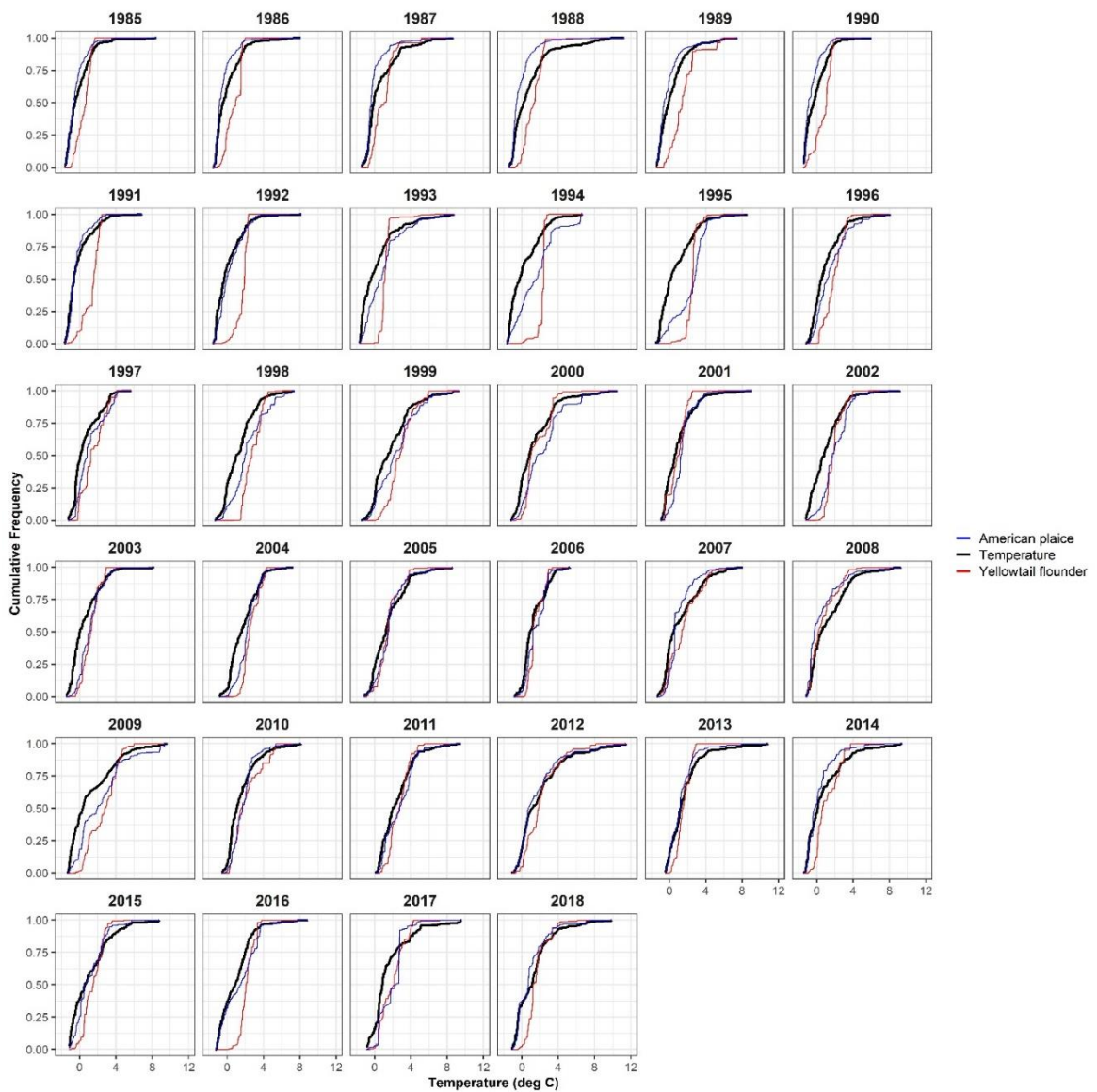


Figure A26. Cumulative distribution functions for the observed (raw data) temperatures (black lines), yellowtail flounder (red lines), and American plaice (blue lines) during surveys on the Grand Banks from 1985 – 2018. The curves were made using the methods described in Perry & Smith (1994).

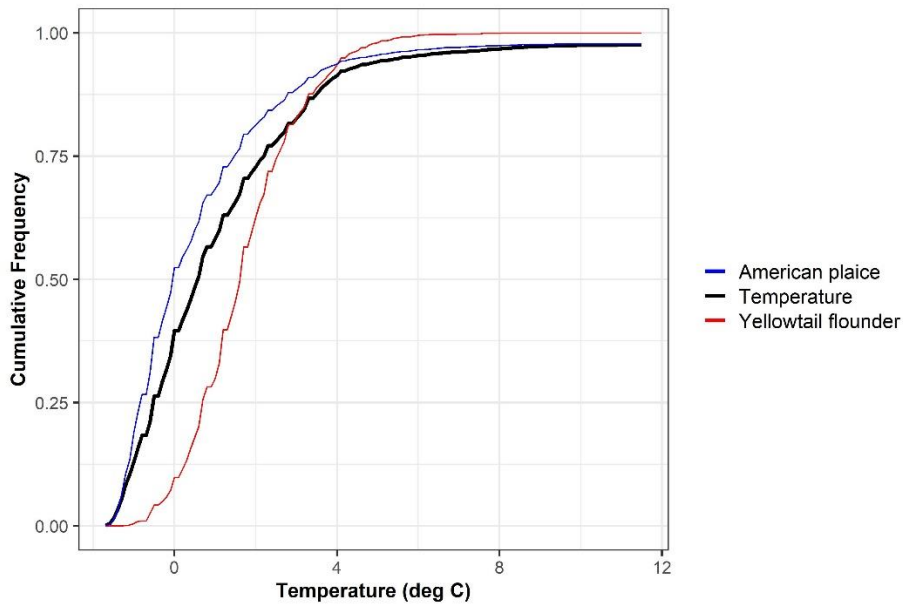


Figure A27. Cumulative distribution functions for the observed (raw data) temperatures (black lines), yellowtail flounder (red lines), and American plaice (blue lines) aggregated across all years (1985 – 2018). Differences in survey design (number of strata/strata sampled) resulted in temperature and American plaice curves not reaching one.

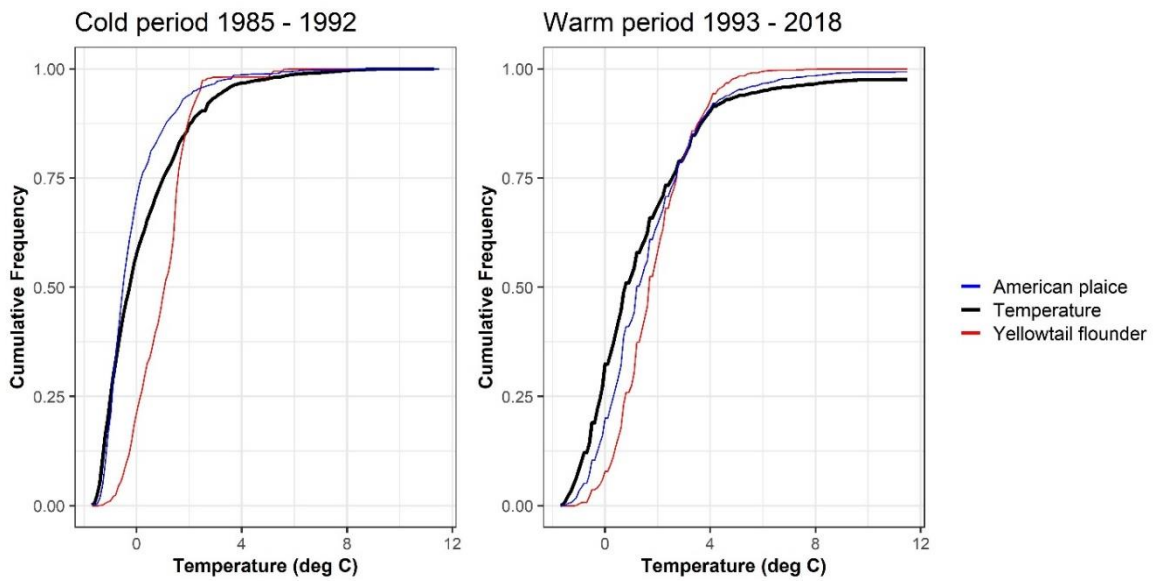


Figure A28. Cumulative distribution functions for the observed (raw data) temperatures (black lines), yellowtail flounder (red lines), and American plaice (blue lines) aggregated from 1985-1992 and 1993-2018 to represent differences in thermal preference before and after the cold period.

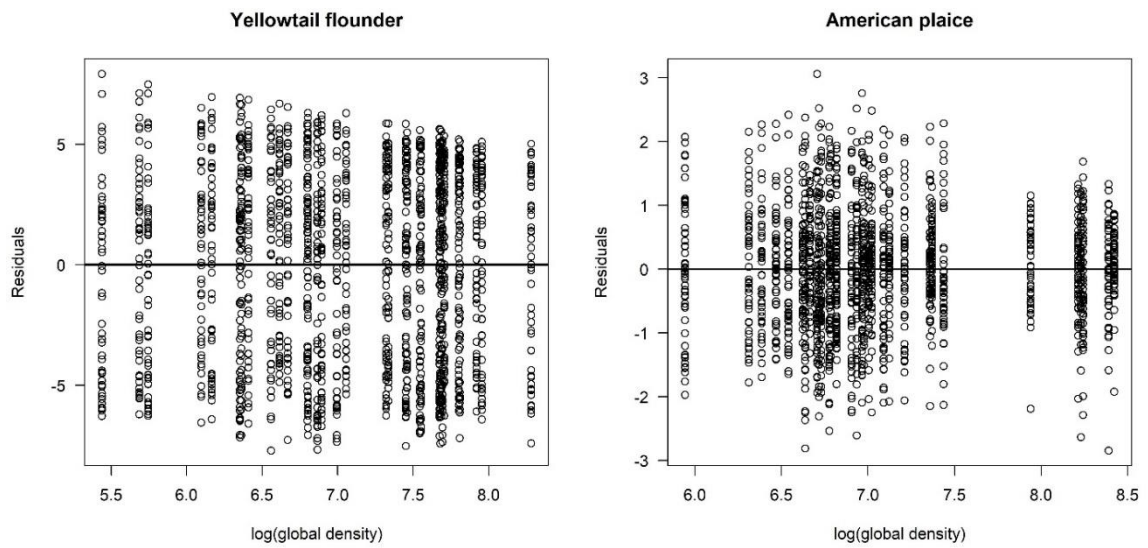


Figure A29. Relationship between the residuals from the linear model and the log of global density for yellowtail flounder and American plaice. The solid black line represents zero.

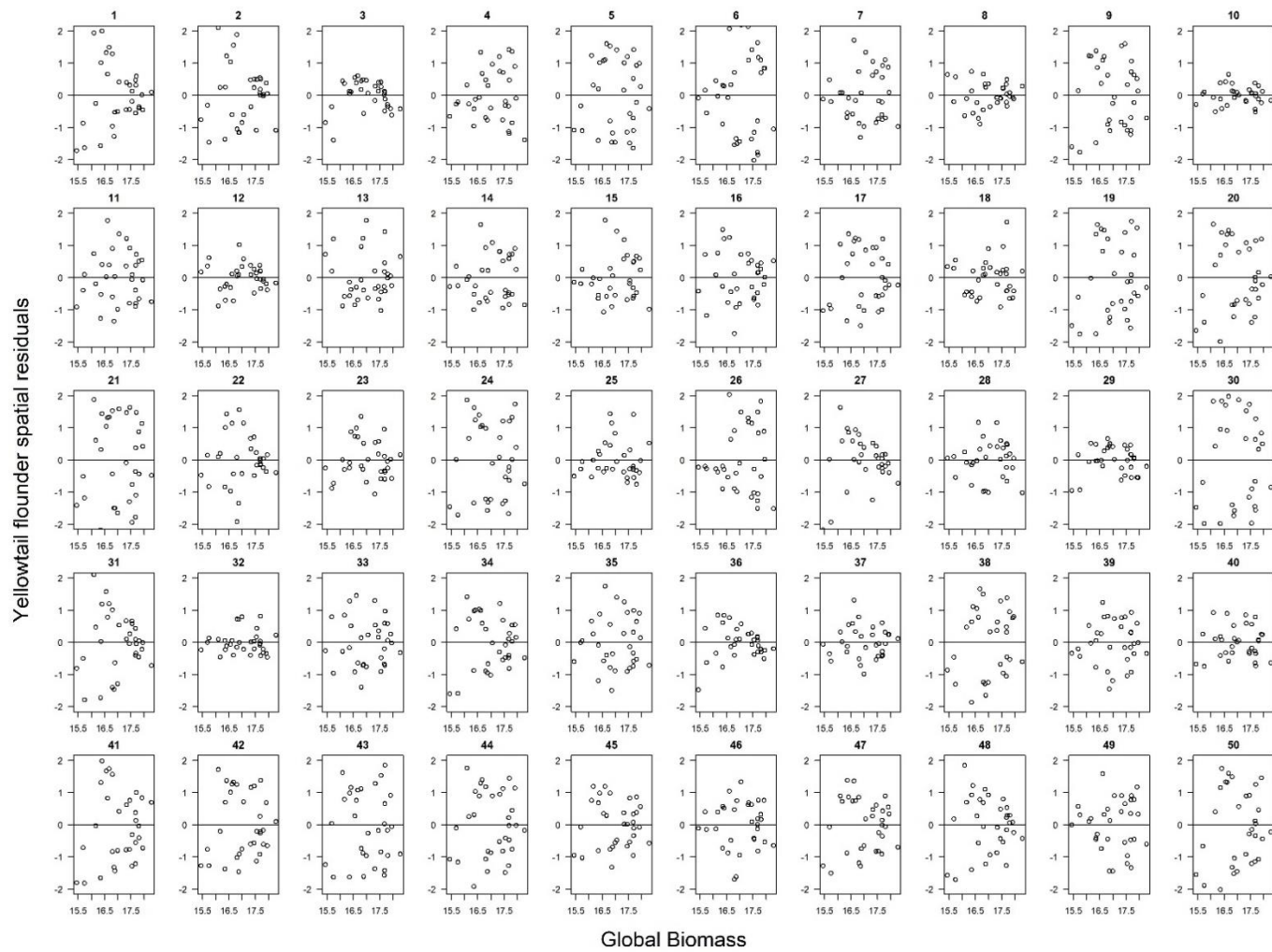


Figure A30. Residuals from the yellowtail flounder mixed-effects model at all 50 knots (panels) compared with the yellowtail flounder global biomass in each year. The solid black line represents zero.

Appendix A Bibliography

Parsons, D. M., Morgan, M., & Rogers, R. (2018). Assessment of yellowtail flounder in NAFO divisions 3LNO using a new stock production model in a Bayesian framework (Issue N6828).

Perry, R. I., & Smith, S. J. (1994). Identifying Habitat Associations of Marine Fishes Using Survey Data: An Application to the Northwest Atlantic. *Canadian Journal of Fisheries and Aquatic Sciences*, **51**(3), 589–602. <https://doi.org/10.1139/f94-061>

Wheeland, L., Dwyer, K., Morgan, J., Rideout, R., & Rogers, R. (2018). Assessment of American Plaice in Div. 3LNO. *NAFO SCS*, **039**, 77.

B. Appendix for Chapter 3

B1. Density value range

I tested a series of simulations with bounded density values to determine how changes in the range of density values would affect model estimates due to the exponential relationship between density and probability of encounter (Eqn 3.1.; Figure B1.1). The ranges tested were (0.5,1.5) and (1,2) since simulations bounded (0,1) are shown within the main text of the manuscript. Each simulation was run 1000 times but only for a type III functional response. This analysis indicates that as density increases, model estimates deviate further from true values (Figure B1.2 & Figure B1.5), have increased bias (Figure B1.3), and decreased difference in AIC between the LFPM and NLFPM (Figure B1.4). However, in all cases the NLFPM outperformed the LFPM and had similar if not slightly better results than the trawl only model. In general, the NLFPM appears to yield very similar results to what is described in the main text of the manuscript when $n_y < 1.5$ and therefore, $pt_y < 0.8$. Furthermore, since the model is designed to be used for poorly sampled forage fish species, I may expect that the main application of the model will be for species that have low density values and should not have much higher density values. However, I would advise caution in interpreting results when $pt_y > 0.8$, especially if this is the case for a majority of the time-series.

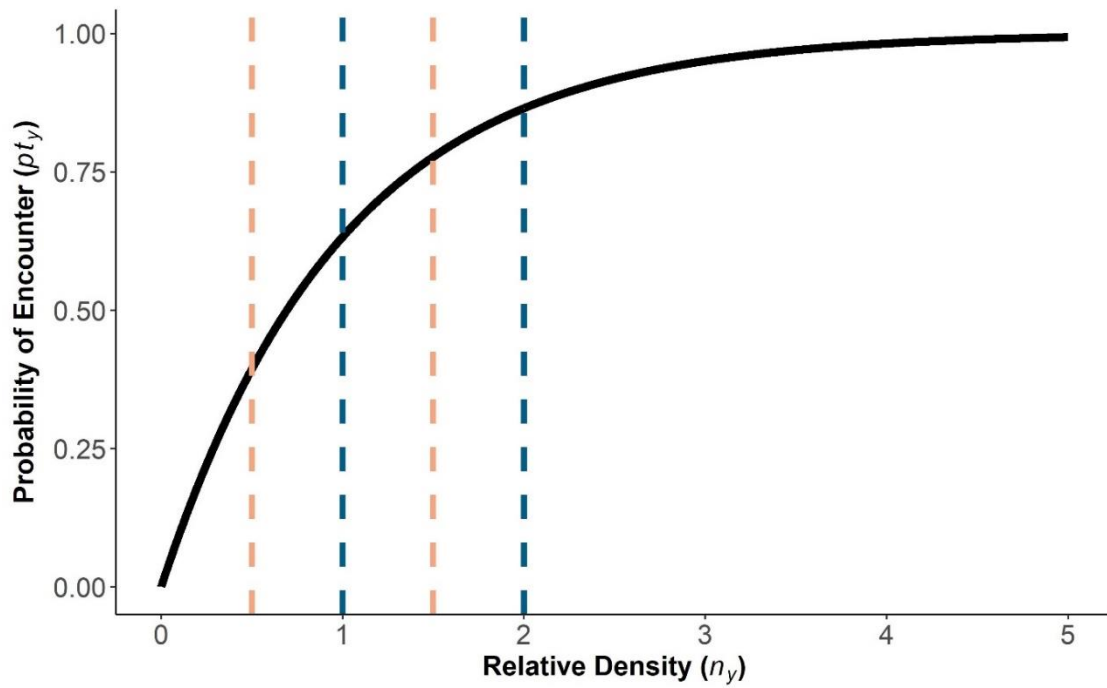


Figure B1.1. Relationship between probability of encounter and density given, $p t_y = 1 - \exp(-n_y)$. Different simulation density ranges are shown by the vertical dashed lines, where the same color lines are used to denote the start and end of the range.

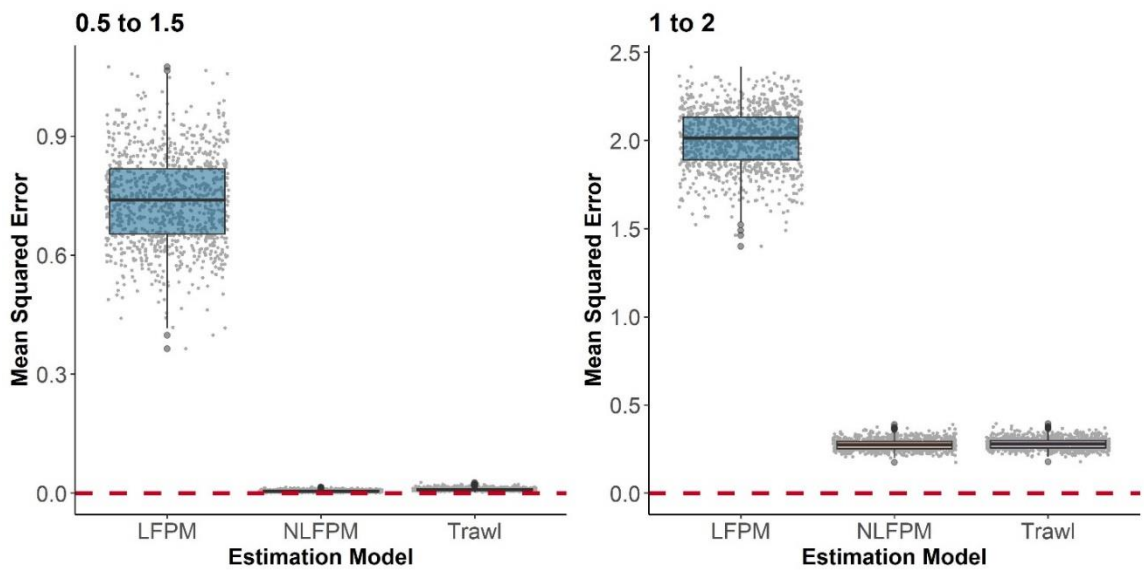


Figure B1.2. Mean squared error (MSE) between estimated prey index of abundance and the scaled true prey abundance from all simulations when density was bounded (0.5, 1.5) and (1,2). Grey points represent the MSE from each simulation and the dashed red line represents zero. The grey points were jittered on the x-axis to improve visualization.

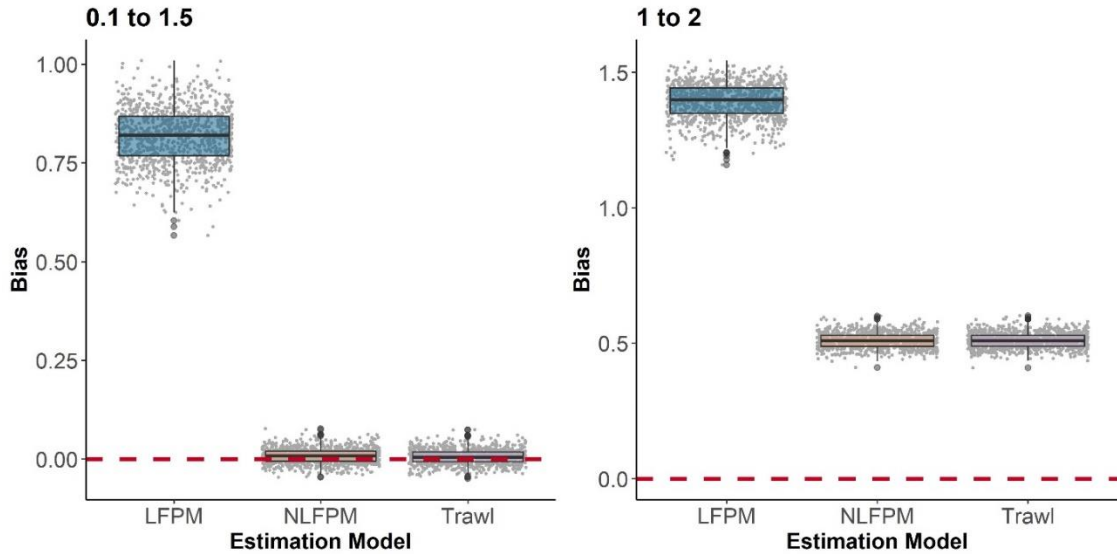


Figure B1.3. Bias between estimated prey index of abundance and the scaled true prey abundance from all simulations when density was bounded (0.5, 1.5) and (1,2). Grey points represent the bias from each simulation and the dashed red line represents zero. The grey points were jittered on the x-axis to improve visualization.

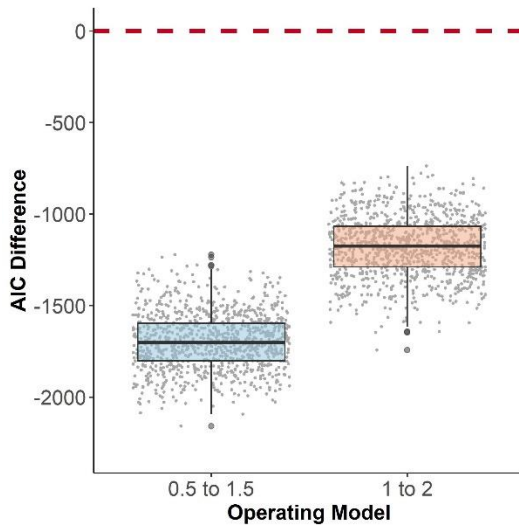


Figure B1.4. Difference in AIC between the NLFPM and LFPM for both operating models. Negative values indicate that the LFPM had a larger AIC than the NLFPM when density was bounded (0.5, 1.5) and (1,2). Grey points represent the difference in AIC

between estimation models from each simulation and the dashed red line represents zero. The grey points were jittered on the the x-axis to improve visualization.

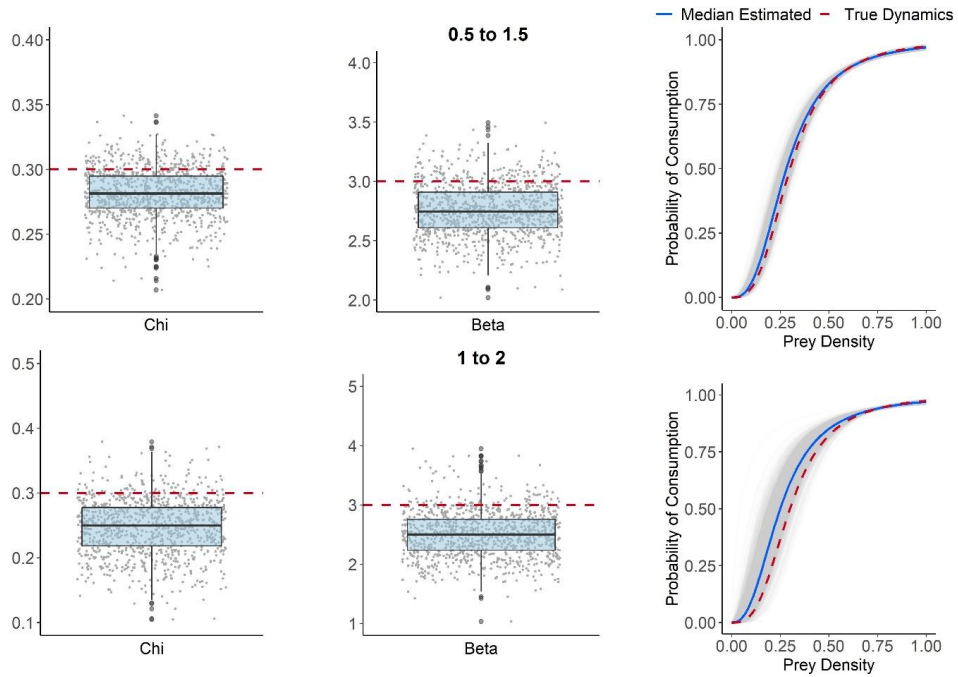


Figure B1.5. Estimates for the shape parameter values in the functional response from the simulation when density was bounded (0.5, 1.5) and (1,2). The dashed red line indicates the true parameter value for each shape. The panels on the far right represent the true shape of the functional response (dashed red lines), the shapes given by all estimated shape parameter values (grey lines), and the median shape parameter values (dark blue lines). The grey points were jittered on the x-axis to improve visualization.

B2. Homogenously distributed sand lance

One of the assumptions of the model is that the prey are homogenously distributed. If this assumption is violated such that samples are taken from areas where prey will never be located, then the absolute value of ps_y and/or pt_y can be negatively biased, which will bias the estimate of the functional response and in turn the estimate of relative prey abundance. Sand lance are known to only be associated with particular bottom types and therefore, may not be caught throughout the Grand Banks. To account for this, I wanted to remove samples from any locations where sand lance were not caught or were so infrequently caught that samples from that location may bias my index of abundance. I identified locations that were unlikely to encounter sand lance by examining the proportion of tows within a grid across the Grand Banks that caught at least one sand lance (Figure B2.1). Using four thresholds (all locations, proportion = 0, proportion <0.05, proportion <0.1), I examined how data removal would modify my model estimates (Table B2.1 and Figures B2.1-B2.9).

Regardless of the occurrence threshold used, my sand lance abundance index did not change substantively. As a result, all analyses shown in the paper will involve the removal of locations where sand lance were never caught. Removing locations where sand lance were never caught should ensure that my assumption is met, however, since removing additional data did not substantively change my conclusions, I would prefer to keep data rather than removing it.

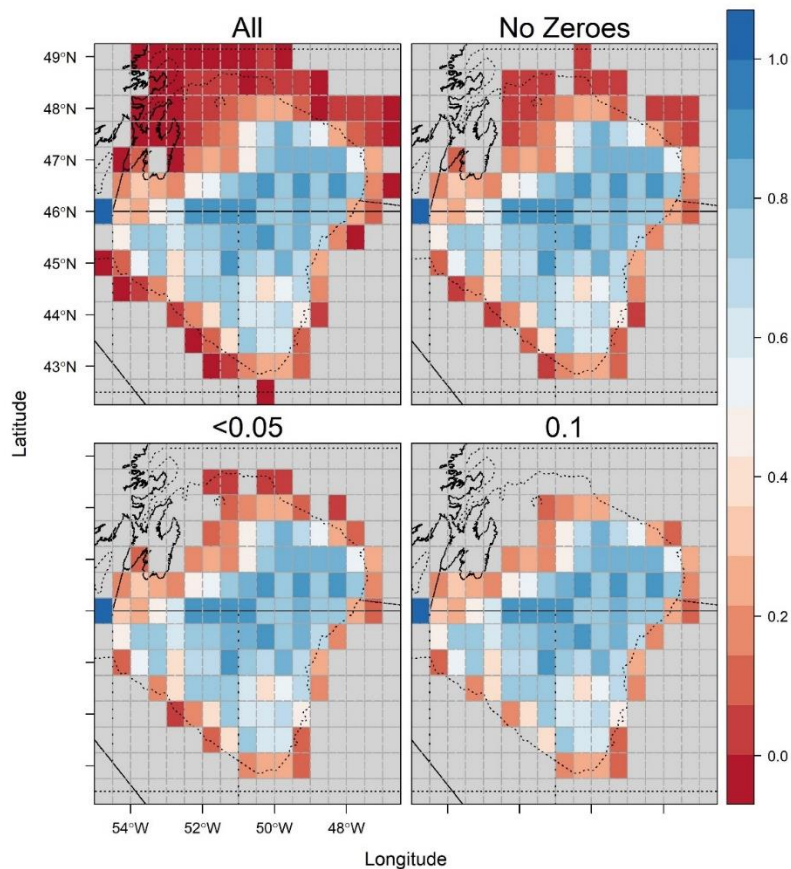


Figure B2.1. Proportion of tows where the spring bottom trawl survey captured at least one sand lance. Each panel represents a different threshold for removing areas: All represents no data removed, No Zeroes represents the removal of cells where sand lance were never caught, <0.05 represents the removal of cells where sand lance were caught in fewer than 5% of tows, and <0.1 represents the removal of cells where sand lance were caught in fewer than 10% of tows. Raster cells are 0.5° x 0.5° (latitude x longitude).

Table B2.1. Number of samples per data type depending on the proportion occurrence threshold cut-off.

Data removed	Trawl	American plaice called	American plaice full	Atlantic cod called	Atlantic cod full
None	6588	22139	4669	10067	4323
Zeroes	6125	21076	3736	8828	3317
<0.05	5512	20083	3518	7724	2908
<0.10	5002	18759	3292	6954	2628

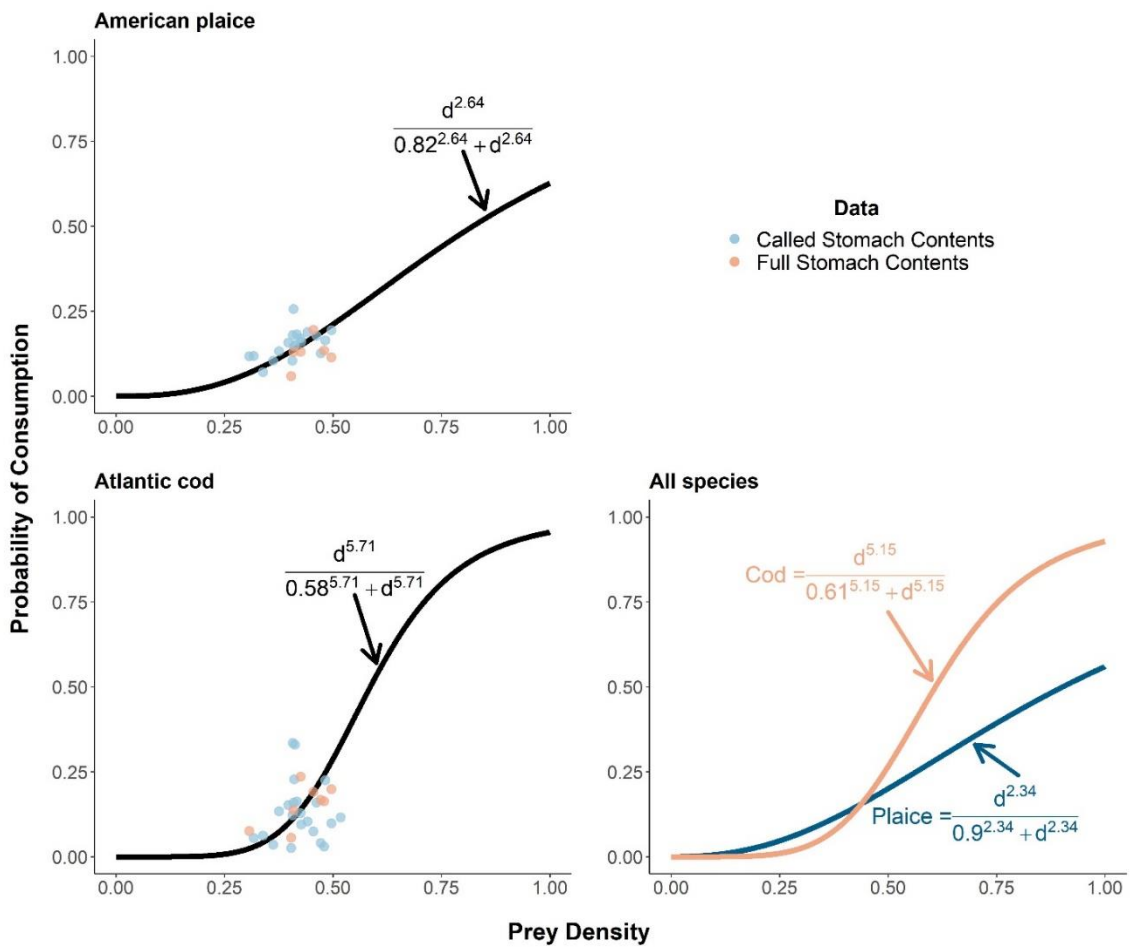


Figure B2.2. Estimated functional response for both predator species when modeled separately and together when no data were removed.

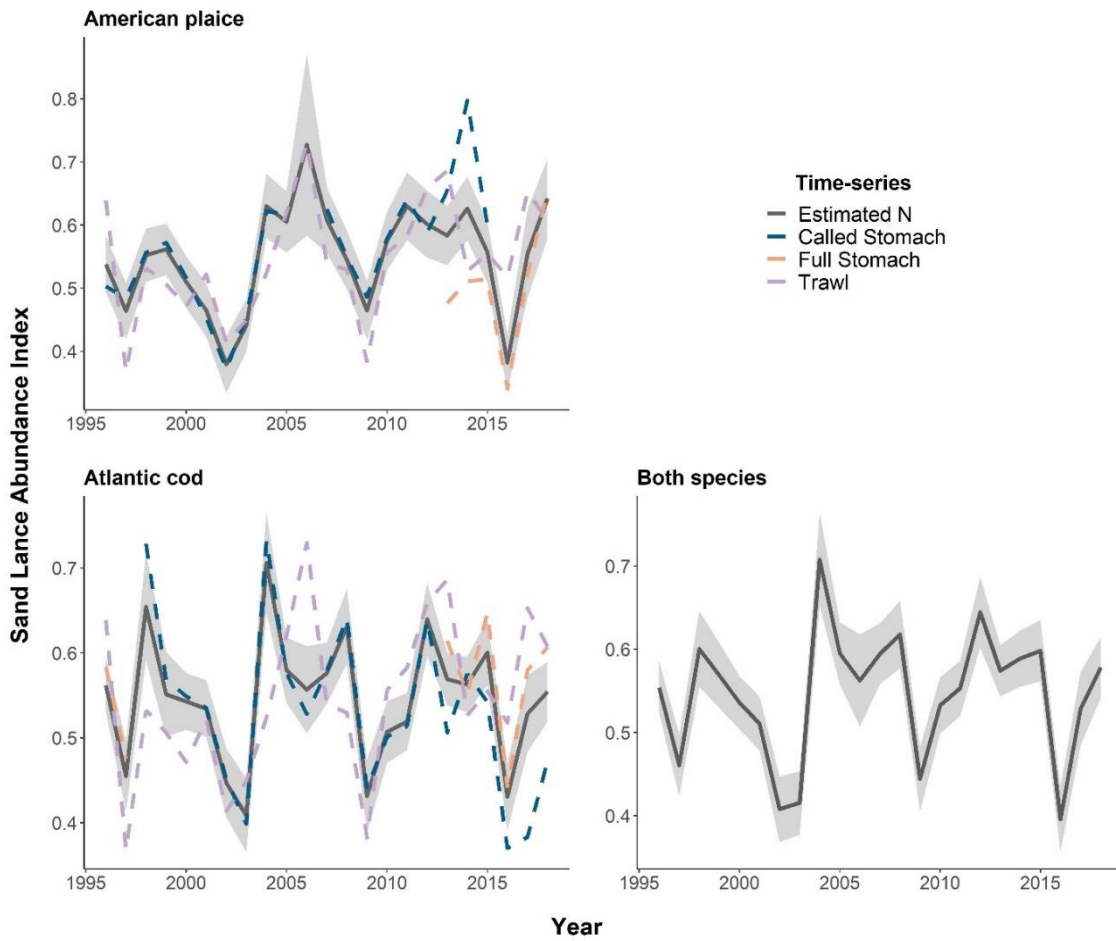


Figure B2.3. Estimated sand lance index of abundance from models that used each predator's data separately and one that modeled American plaice and Atlantic cod data together when no data were removed. The shaded grey area represents the 95% confidence interval around the estimated trend. Dashed lines represent the estimated trends from each data source.

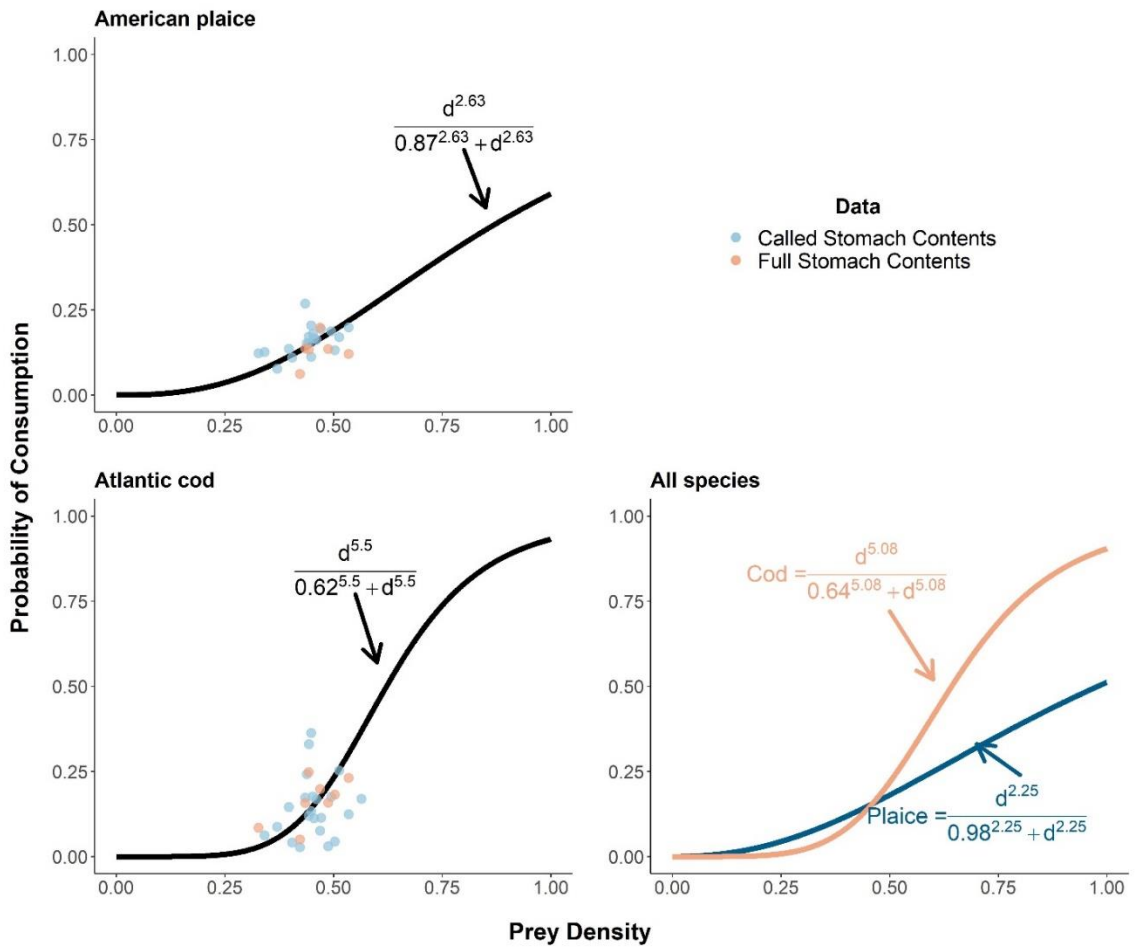


Figure B2.4. Estimated functional response for both predator species when modeled separately and together when raster cells with zeroes were removed.

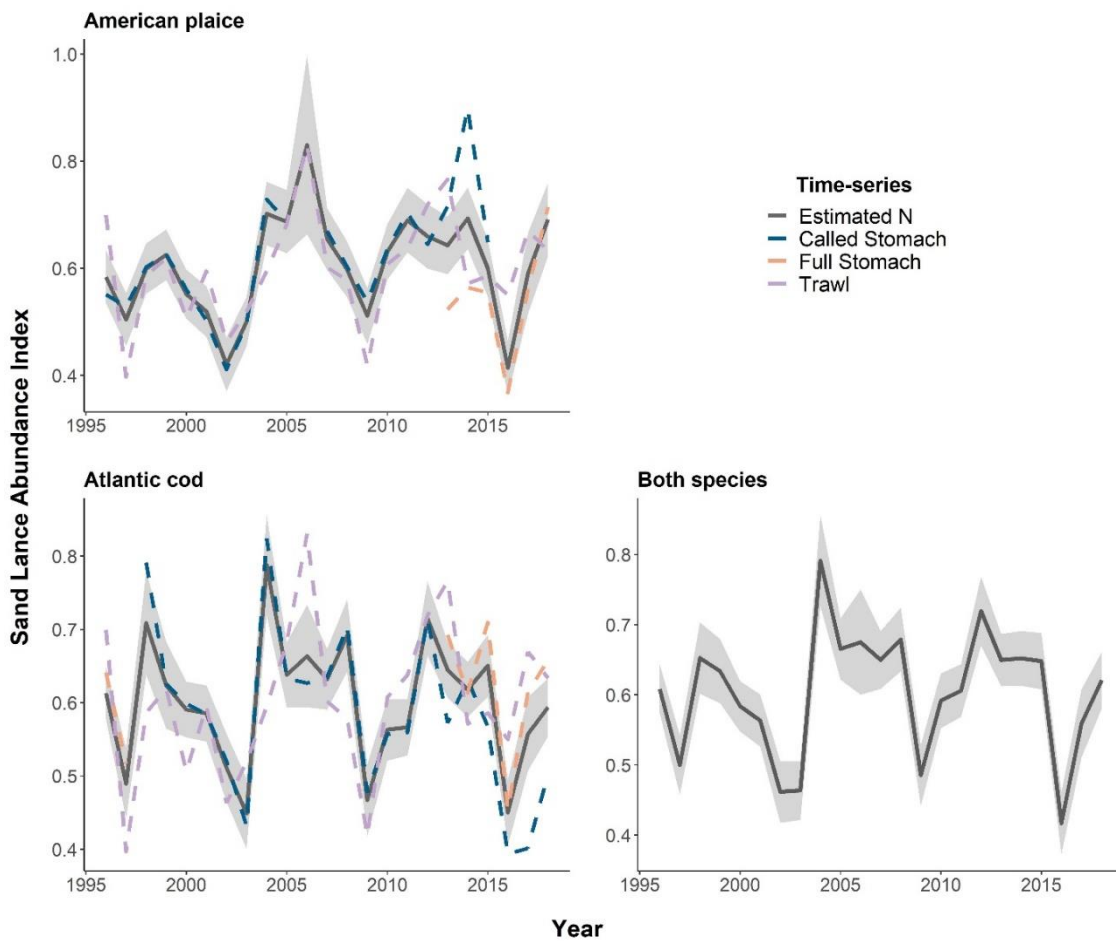


Figure B2.5. Estimated sand lance index of abundance from models that used each predator's data separately and one that modeled American plaice and Atlantic cod data together when raster cells with zeroes were removed. The shaded grey area represents the 95% confidence interval around the estimated trend. Dashed lines represent the estimated trends from each data source.

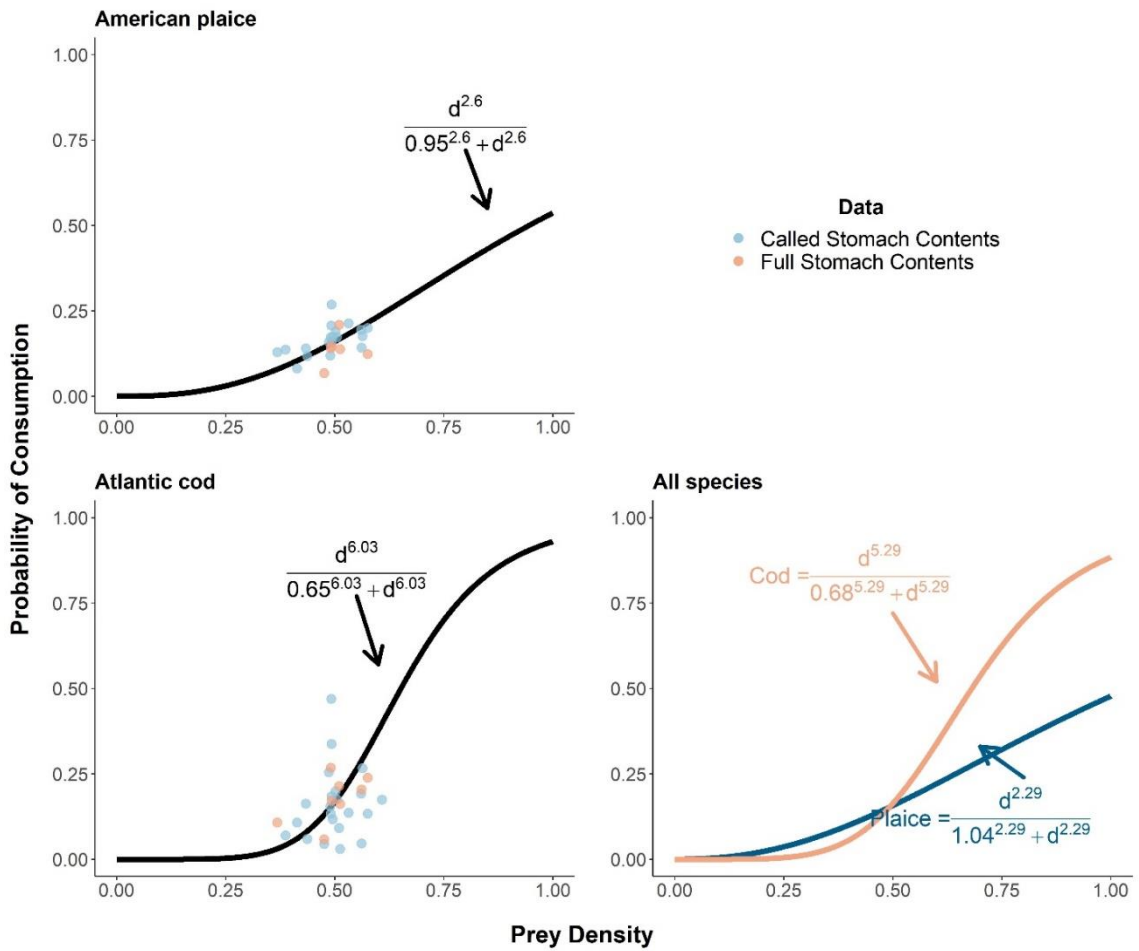


Figure B2.6. Estimated functional response for both predator species when modeled separately and together when raster cells with a proportion of sand lance in tows <0.05 were removed.

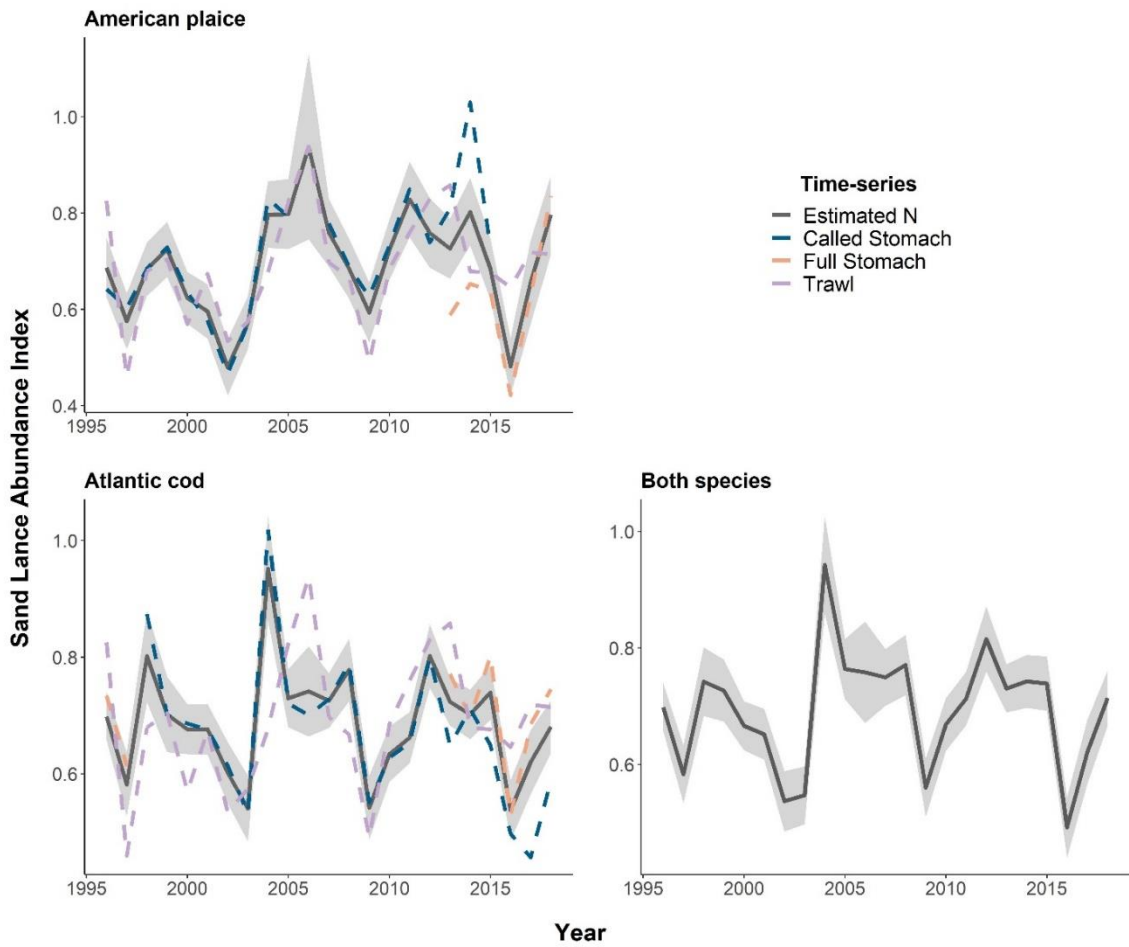


Figure B2.7. Estimated sand lance index of abundance from models that used each predator's data separately and one that modeled American plaice and Atlantic cod data together when raster cells with a proportion of sand lance in tows <0.05 were removed. The shaded grey area represents the 95% confidence interval around the estimated trend. Dashed lines represent the estimated trends from each data source.

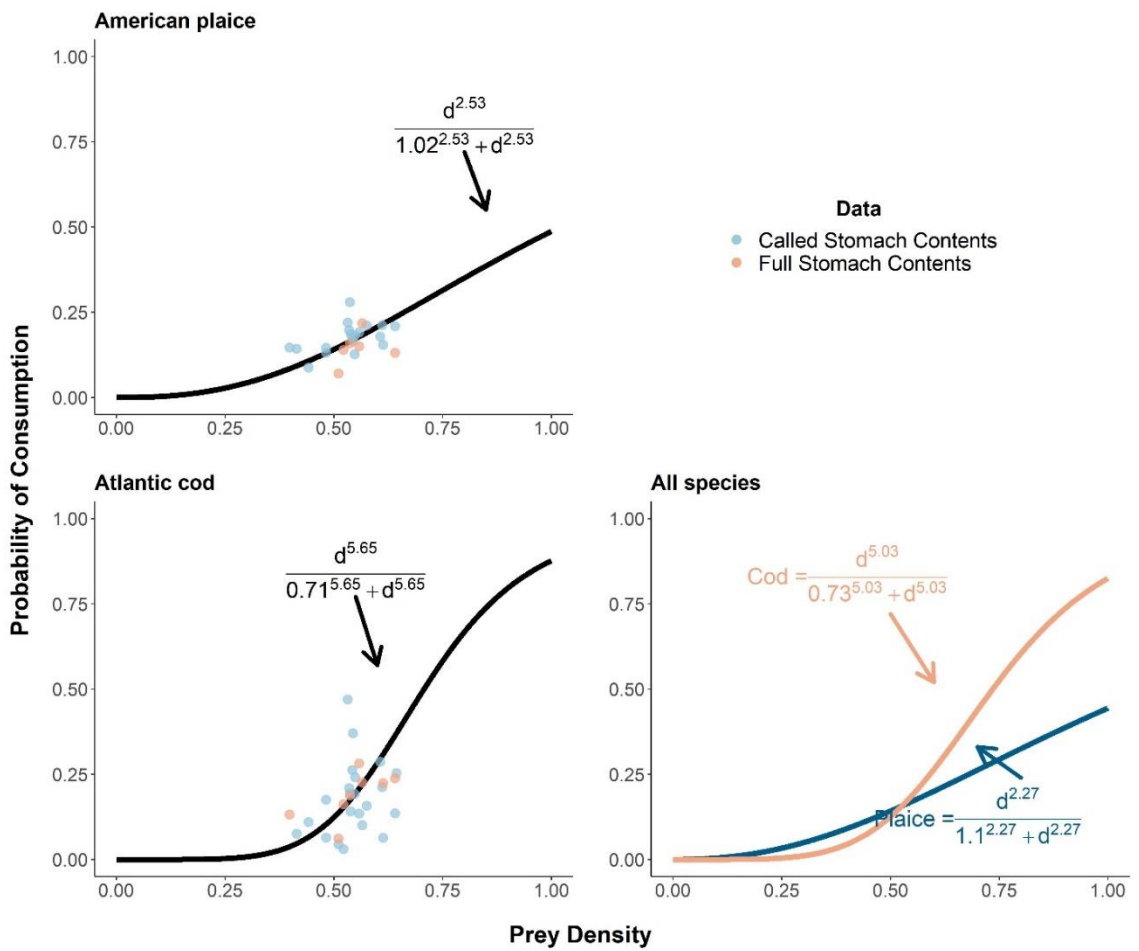


Figure B2.8. Estimated functional response for both predator species when modeled separately and together when raster cells with a proportion of sand lance in tows <0.1 were removed.

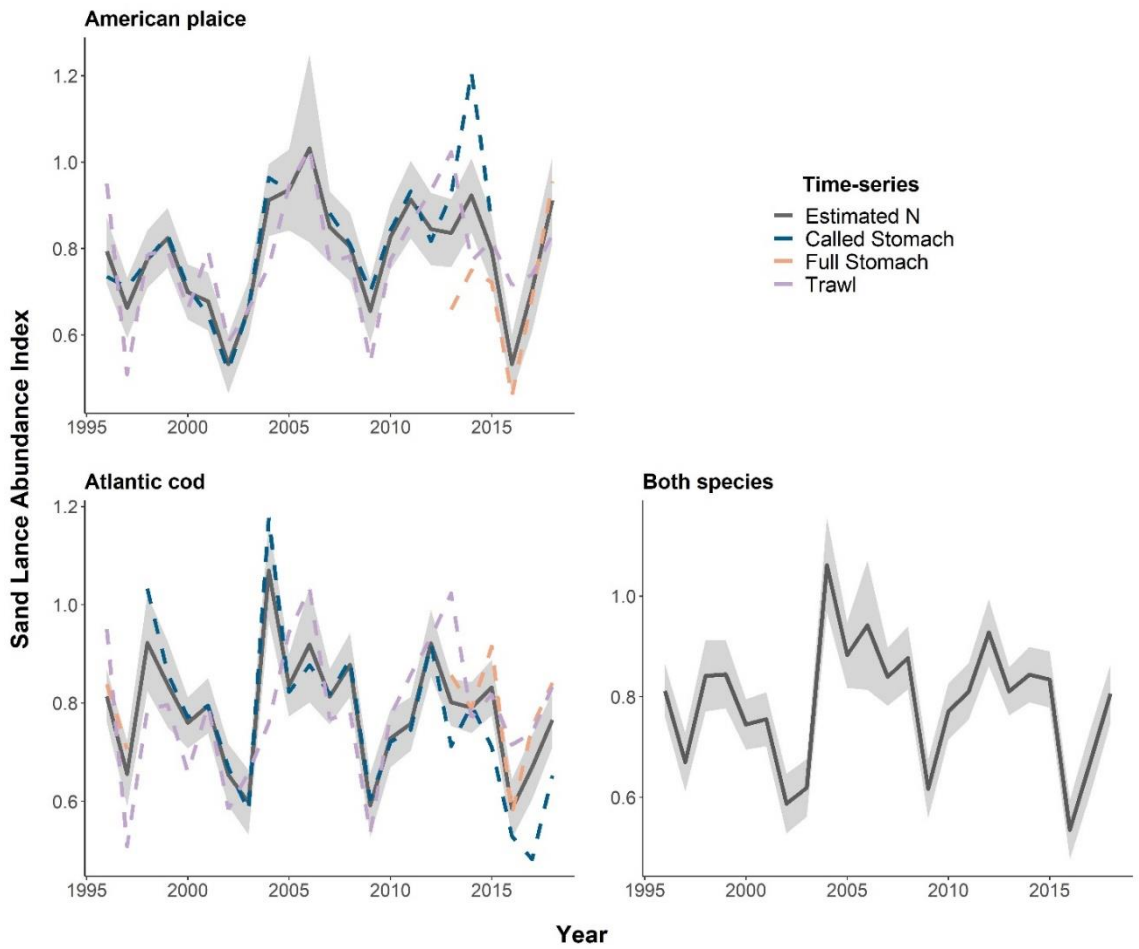


Figure B2.9. Estimated sand lance index of abundance from models that used each predator's data separately and one that modeled American plaice and Atlantic cod data together when raster cells with a proportion of sand lance in tows <0.1 were removed. The shaded grey area represents the 95% confidence interval around the estimated trend. Dashed lines represent the estimated trends from each data source.

B3. Ontogenetic Diet Shift

There is some disagreement between publications about the lengths that Atlantic cod and American plaice begin to regularly consume fishes on the Grand Banks (see Table B3.1). As a result, I examined the frequency of occurrence of sand lance in called and full stomach contents at 5 cm size bins (Figures B3.1 & B3.2). I selected the length at 5% frequency of occurrence in stomachs and removed any data from fish that had lengths below the threshold. This threshold appeared to indicate a small length for fishes that began to regularly consume sand lance and therefore should have only excluded fish that were unlikely to consume sand lance. Fish with larger lengths that had a sand lance frequency of occurrence <5% were kept due to their relatively low sample size. Finally, I compared my results to those from previous studies to determine if the lengths at 5% frequency of occurrence were near previously reported lengths associated with ontogenetic diet shifts on the Grand Banks. This threshold created a cut-off size of 25 cm for American plaice and Atlantic cod. The 25 cm cut-off fell within the range of lengths reported in previous literature (Table B3.1).

Table B3.1. Literature derived minimum length for ontogenetic diet shift to piscivory. FOO in the reference column refers to the frequency of occurrence examined in this paper. Bolded rows indicate the cut-off sizes that were used in the analyses.

Model/data	Size (cm)	Reference
American plaice	>35	Tam and Bundy (2019)
	>30	Pitt (1976)
	>25	>0.05 FOO; Figure A2.3.1
	>20	Gonzalez et al. (2006)
Atlantic cod	>36	Fahrig et al. (1993)
	>25	>0.05 FOO; Figure A2.3.1
	>20	Gonzalez et al. (2006); Sherwood et al. (2007)

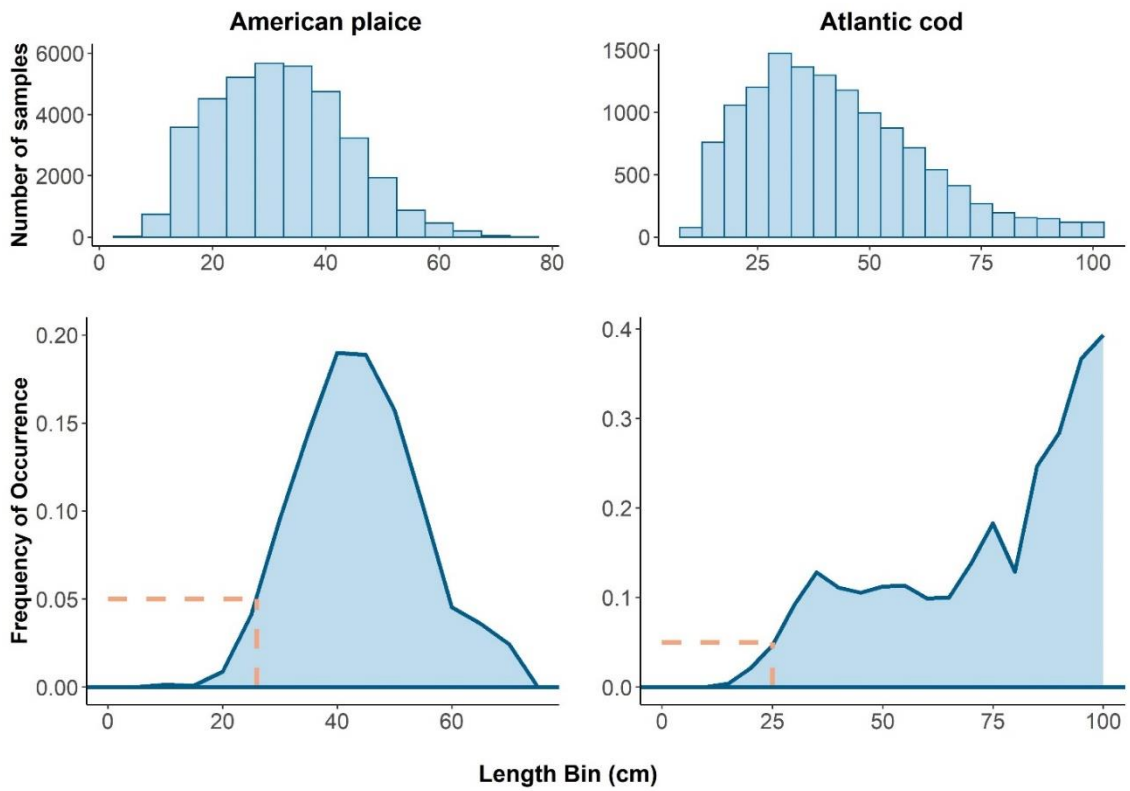


Figure B3.1. Number of called stomachs per 5 cm length bin and the frequency of sand lance occurrence in those stomachs for American plaice and Atlantic cod. Dashed orange lines indicate the length at which frequency of occurrence first reached 0.05. The mean (\pm standard deviation) length above the cut-off threshold was 37 (\pm 8) cm for American plaice and 49 (\pm 19) cm for Atlantic cod.

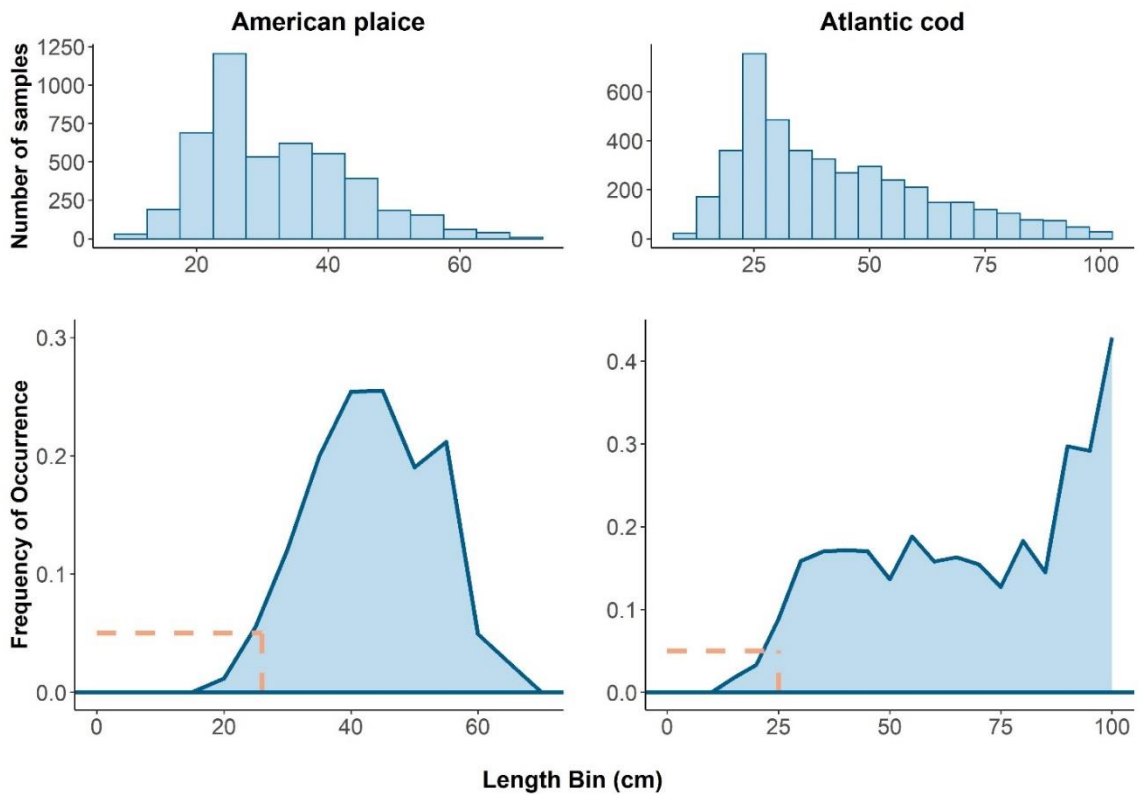


Figure B3.2. Number of full stomach samples per 5 cm length bin and the frequency of sand lance occurrence in those stomachs for American plaice and Atlantic cod. Dashed orange lines indicate the length at which frequency of occurrence first reached 0.05. The mean (\pm standard deviation) length above the cut-off threshold was 30 (\pm 11) cm for American plaice and 41 (\pm 22) cm for Atlantic cod.

B4. Additional supplemental information

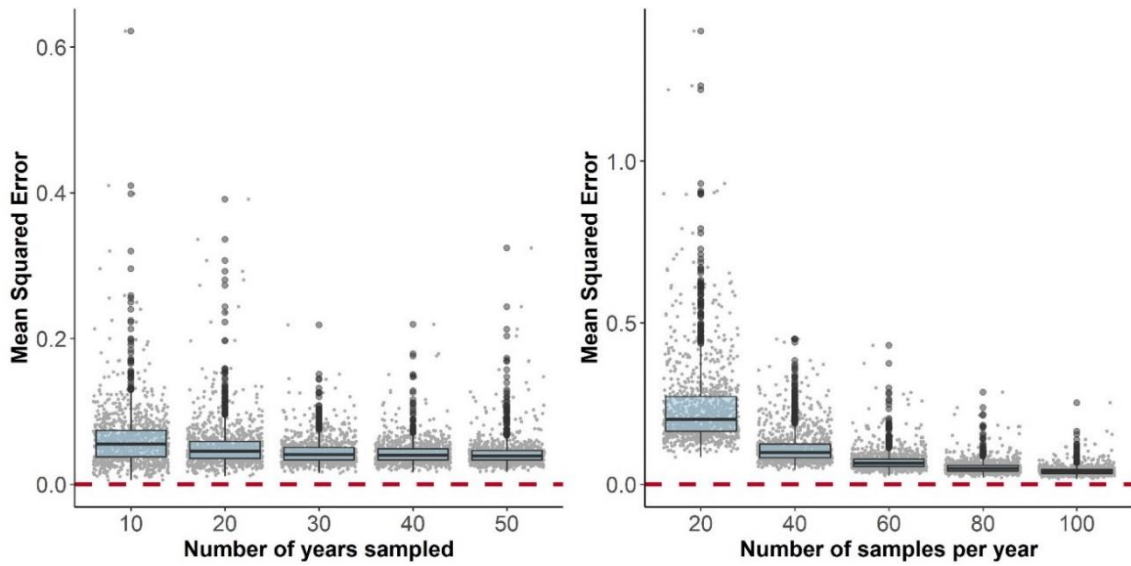


Figure B4.1. Mean squared error (MSE) between estimated prey index of abundance and the true prey abundance from a range of simulations with varying numbers of years sampled and numbers of samples per year. The number of samples per year were always equal between trawls and stomach contents. Grey points represent the MSE from each simulation and the dashed red line represents zero. The grey points were jittered to improve visualization.

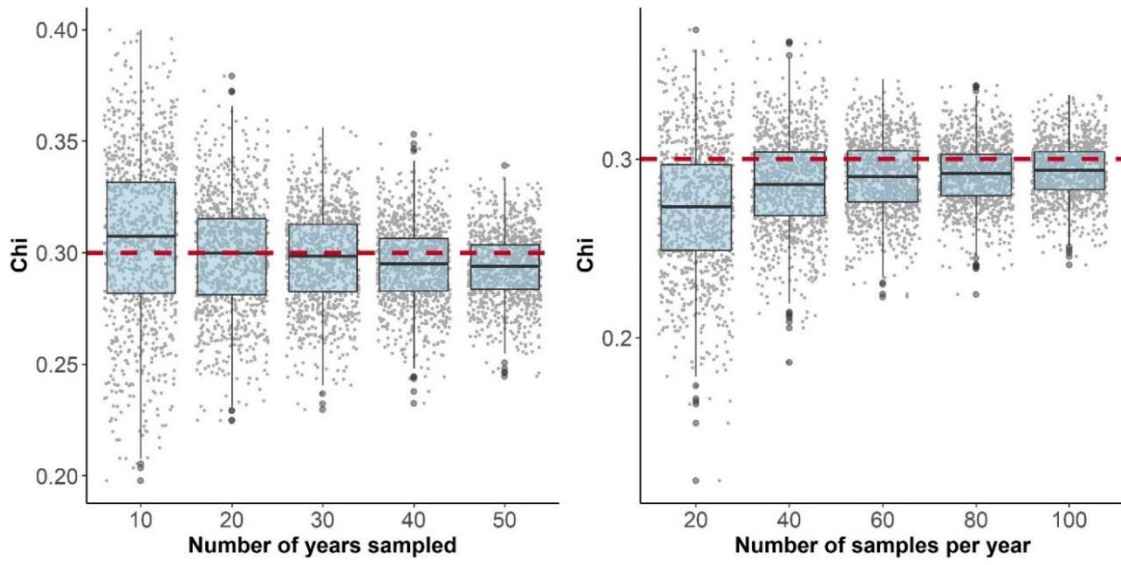


Figure B4.2. Estimates for the chi shape parameter values in the functional response from a range of simulations with varying numbers of years sampled and numbers of samples per year. The number of samples per year were always equal between trawls and stomach contents. The grey points represent the chi estimate from each simulation and the dashed red line indicates the true parameter value for each shape. The grey points were jittered to improve visualization.

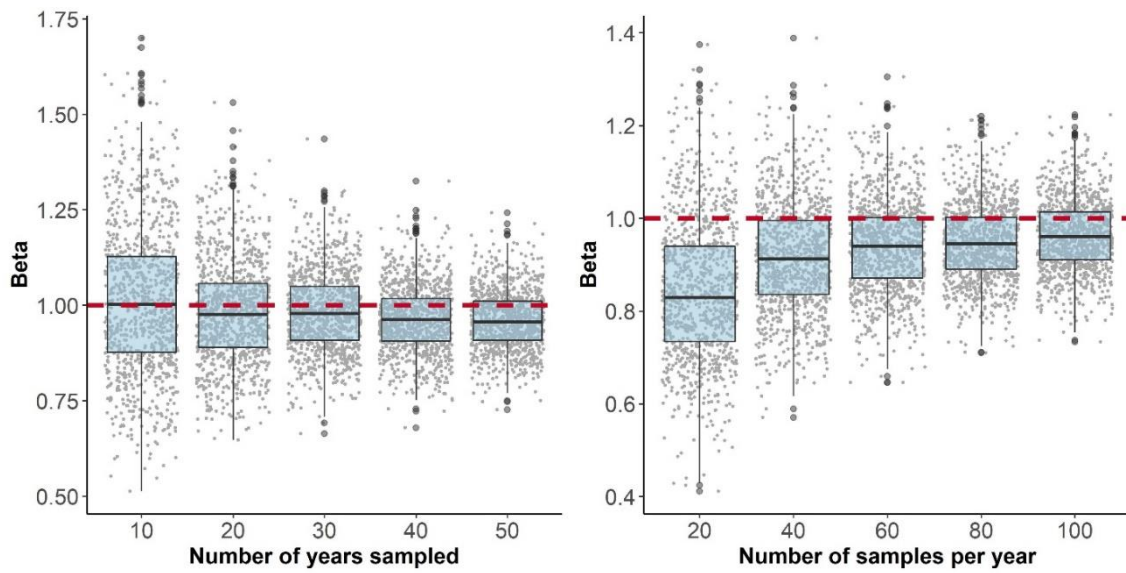


Figure B4.3. Estimates for the beta shape parameter values in the functional response from a range of simulations with varying numbers of years sampled and numbers of samples per year. The number of samples per year were always equal between trawls and stomach contents. The grey points represent the beta estimate from each simulation and the dashed red line indicates the true parameter value for each shape. The grey points were jittered to improve visualization.

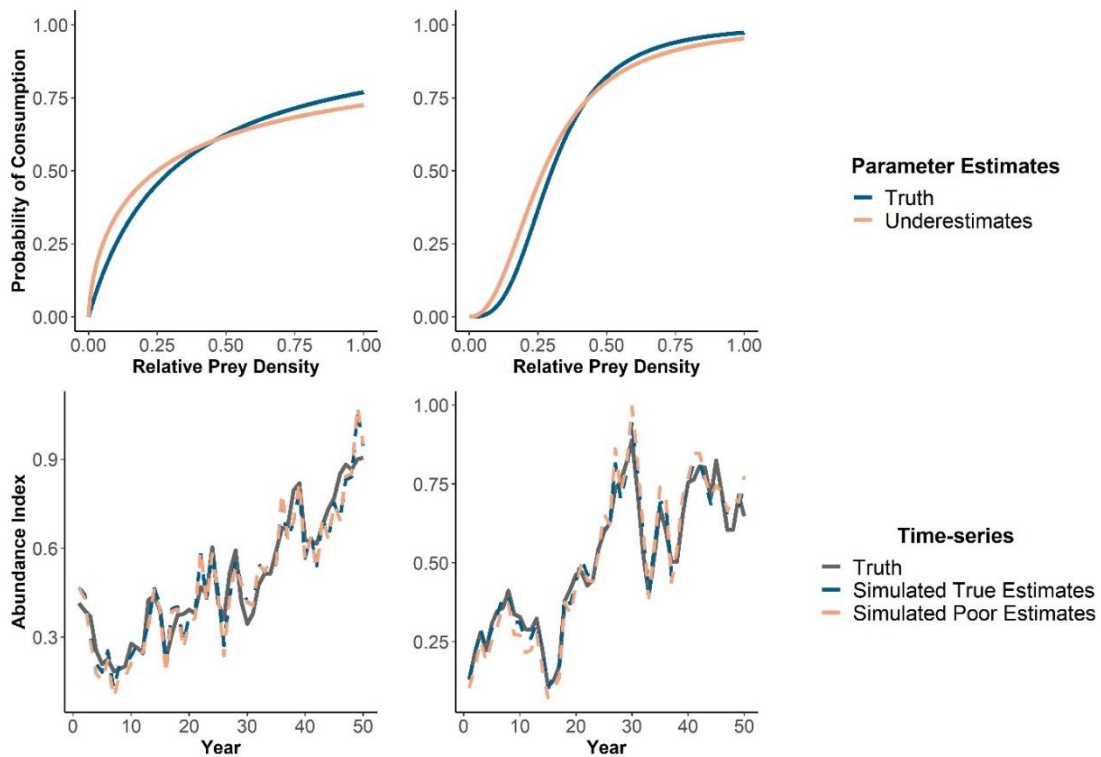


Figure B4.4. Comparison of model estimates when the shape parameters (χ and β) are estimated to match the truth and when they are mis-specified using one simulation. Left panels show comparisons using a Type II operating model and the right panels show comparisons using a Type III operating model. Shape parameters were treated as data and set to equal the largest negative misspecifications from the 1000 simulations.

To determine the influence of stomach content sample size on model estimates I ran 1,000 simulations where I decreased the number of tows that caught predators from 100 to 50 and ran scenarios with decreasing numbers of stomachs sampled per tow (where each scenario had fewer samples than what is shown in the main text): high sample size of 10-20 (~750 stomachs per year), medium sample size of 5-10 (~350 per year), and low sample size of 1-5 (~150 per year). These simulations only examined Type II operating models because there was always a smaller difference between the LFPM and NLFPM for these operating models. Therefore, if modifying the sample size were to

make the NLFPM produce worse estimates than the LFPM it should be apparent first with Type II operating models.

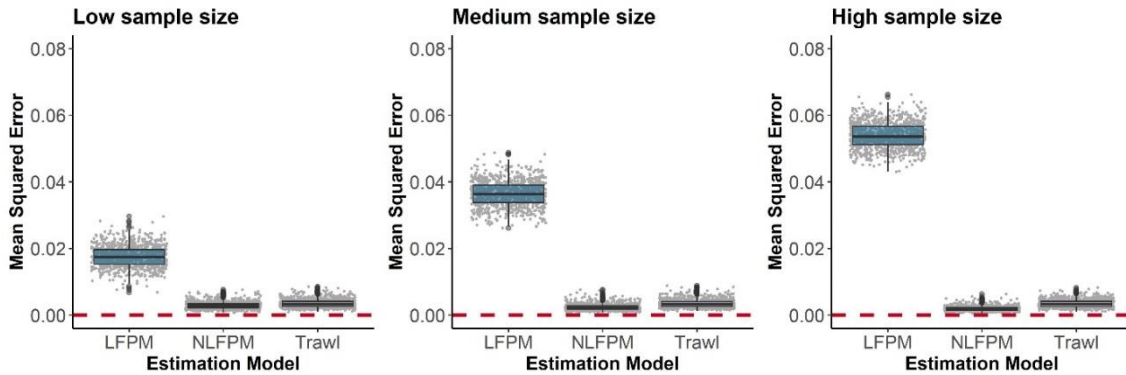


Figure B4.5. Mean squared error (MSE) between estimated relative index of prey abundance and the scaled true prey abundance from simulations with varying stomach content sample sizes. Grey points represent the MSE from each simulation and the dashed red line represents zero. The grey points were jittered on the x-axis to improve visualization.

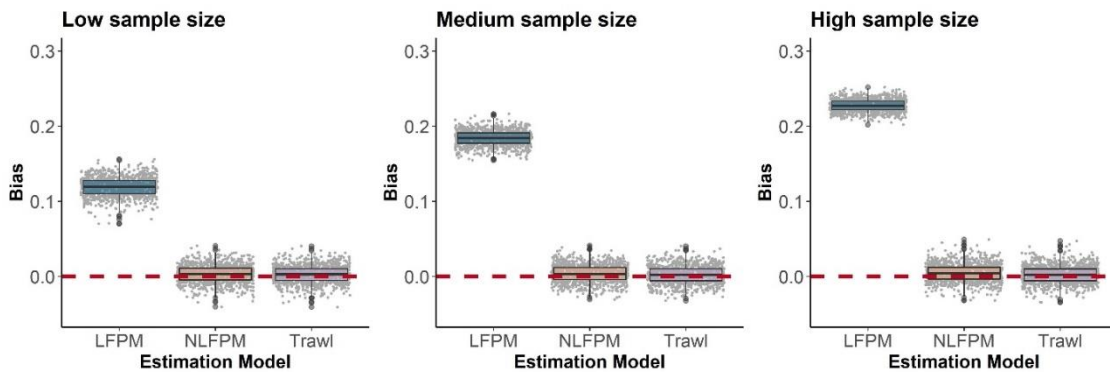


Figure B4.6. Bias between estimated relative index of prey abundance and the scaled true prey abundance from simulations with varying stomach content sample sizes.

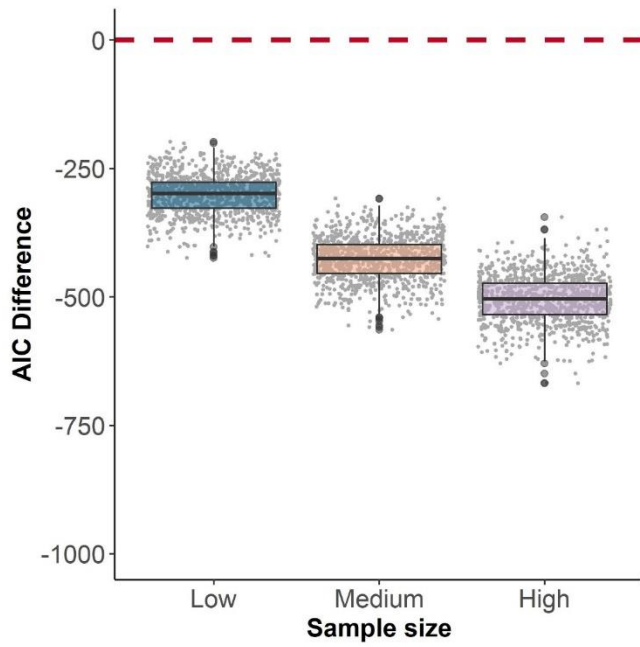


Figure B4.7 Difference in AIC between the NLFPM and LFPM for both operating models from simulations with varying stomach content sample sizes. Negative values indicate that the LFPM had a larger AIC than the NLFPM.

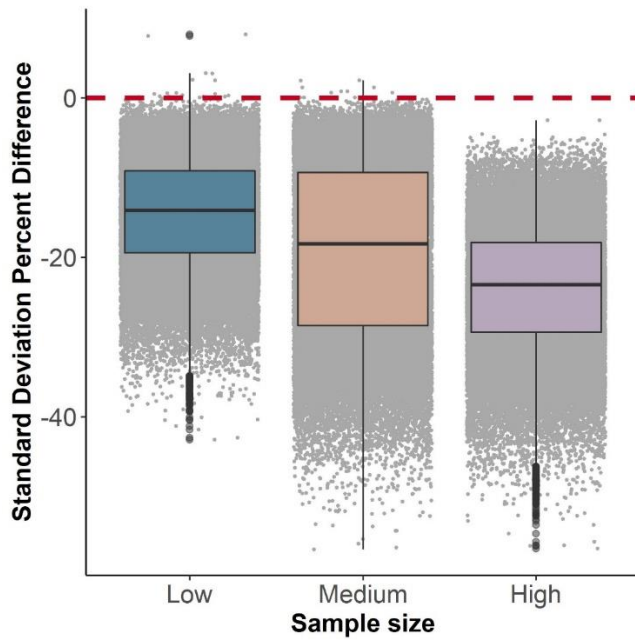


Figure B4.8. Percent difference in annual standard deviation estimates for the prey abundance index between the NLFPM and a model with no stomach contents data for both operating models. Percent was calculated as the difference between standard deviation estimates and the mean of the standard deviation estimates from the model with no stomach contents data. Negative values indicate a smaller standard deviation estimate for a particular year in the NLFPM.

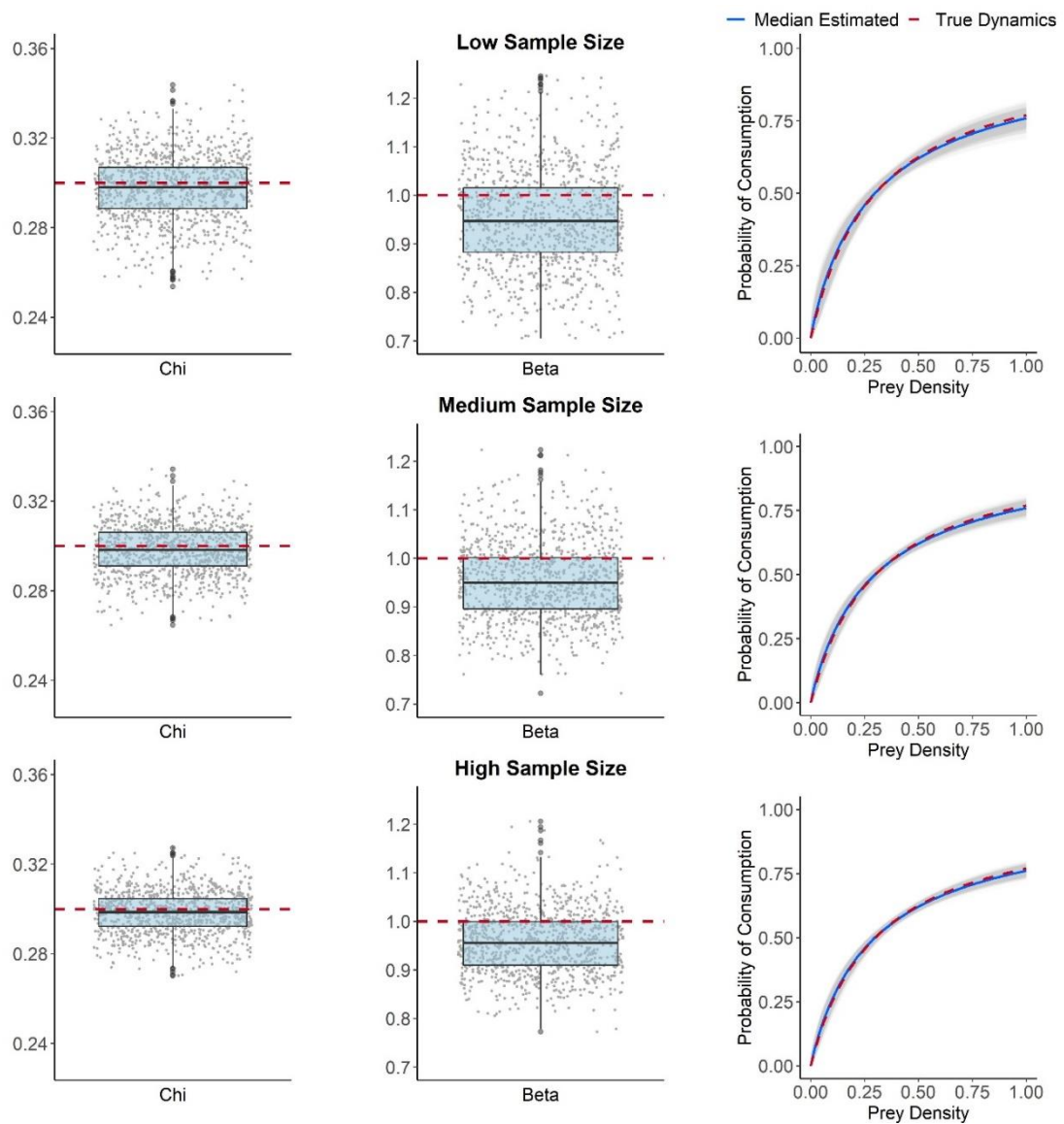


Figure B4.9 Estimates for the shape parameter values in the functional response from simulations with varying stomach content sample sizes. The dashed red line indicates the true parameter value for each shape. The panels on the far right represent the true shape of the functional response (red lines), the shapes given by all estimated shape parameter values (grey lines), and the median shape parameter values (dark blue lines).

To determine whether the range of observed prey density values may influence the model's ability to recover the true estimates I ran 1,000 simulations where I standardized prey density values between 0.25 and 0.5 by using a min/max scaling (see Eqn 3.10). I

chose this range because it approximated the range of observed prey density in my case-study.

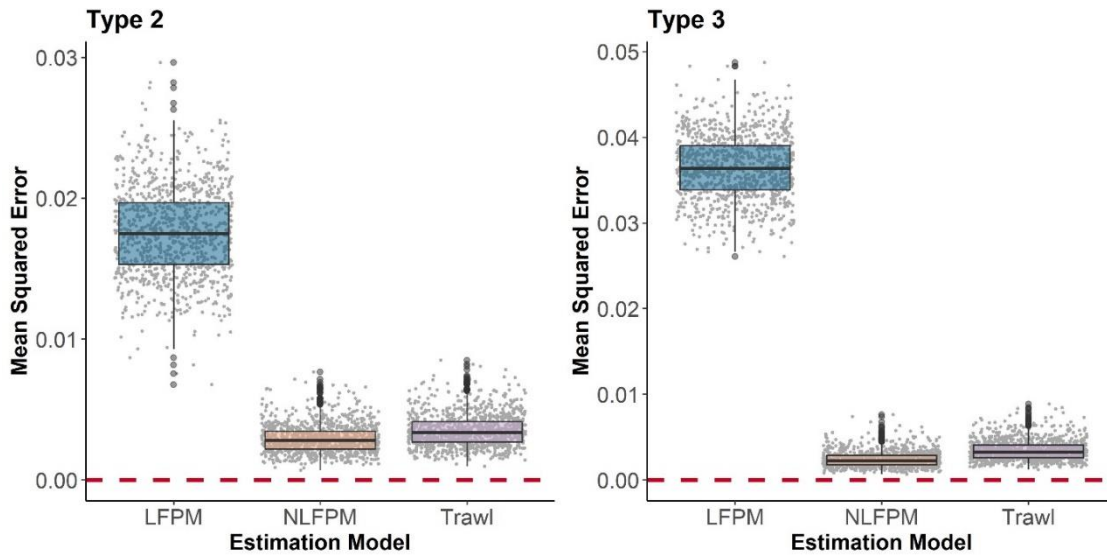


Figure B4.10 Mean squared error (MSE) between estimated relative index of prey abundance and the scaled true prey abundance from simulations with a narrowed range of observed prey density. Grey points represent the MSE from each simulation and the dashed red line represents zero. The grey points were jittered on the x-axis to improve visualization.

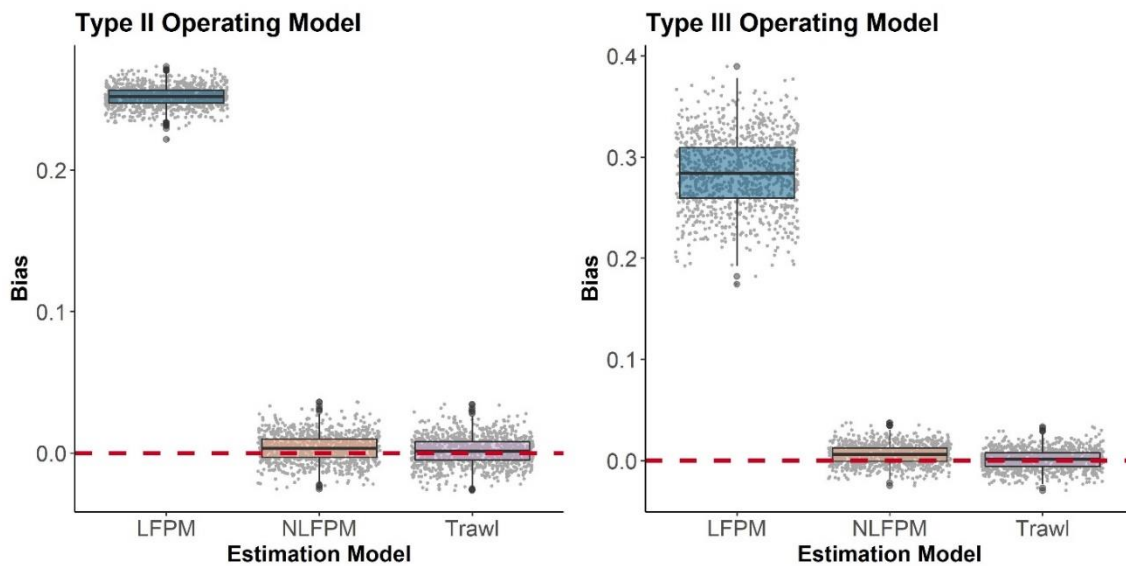


Figure B4.11 Bias between estimated relative index of prey abundance and the scaled true prey abundance from simulations with a narrowed range of observed prey density.

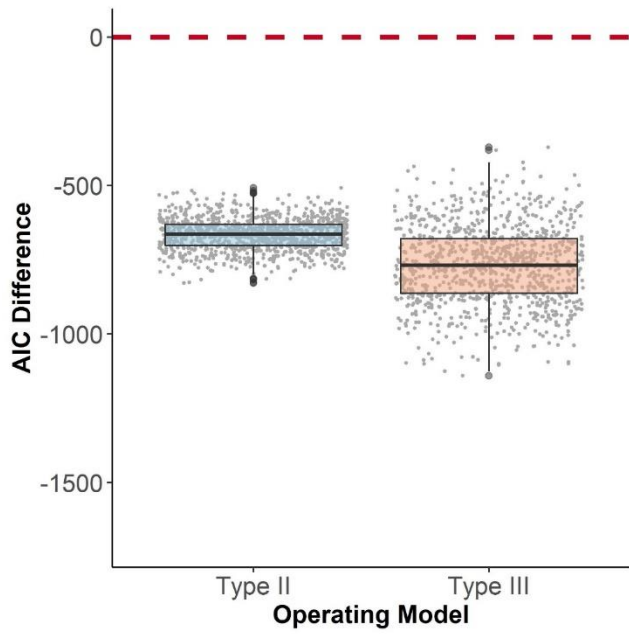


Figure B4.12 Difference in AIC between the NLFPM and LFPM for both operating models from simulations with a narrowed range of observed prey density. Negative values indicate that the LFPM had a larger AIC than the NLFPM.

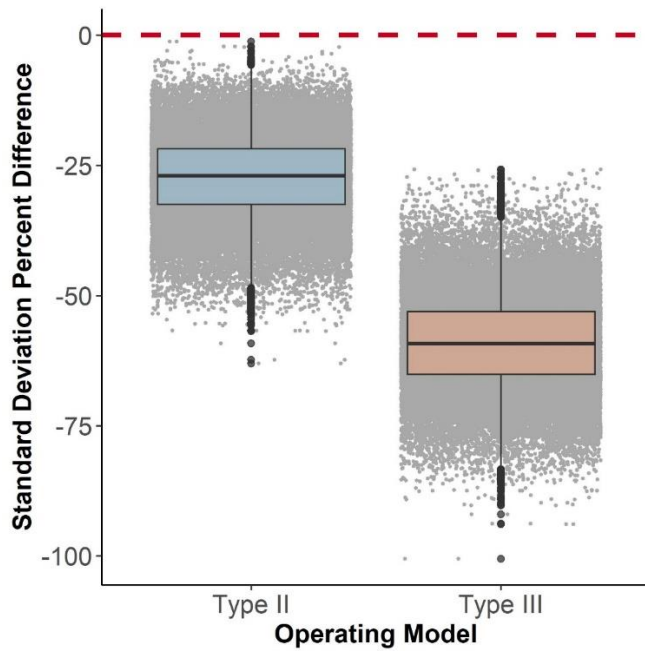


Figure B4.13 Percent difference in annual standard deviation estimates for the prey abundance index between the NLFPM and a model with no stomach contents data for both operating models. Percent was calculated as the difference between standard deviation estimates and the mean of the standard deviation estimates from the model with no stomach contents data. Negative values indicate a smaller standard deviation estimate for a particular year in the NLFPM.

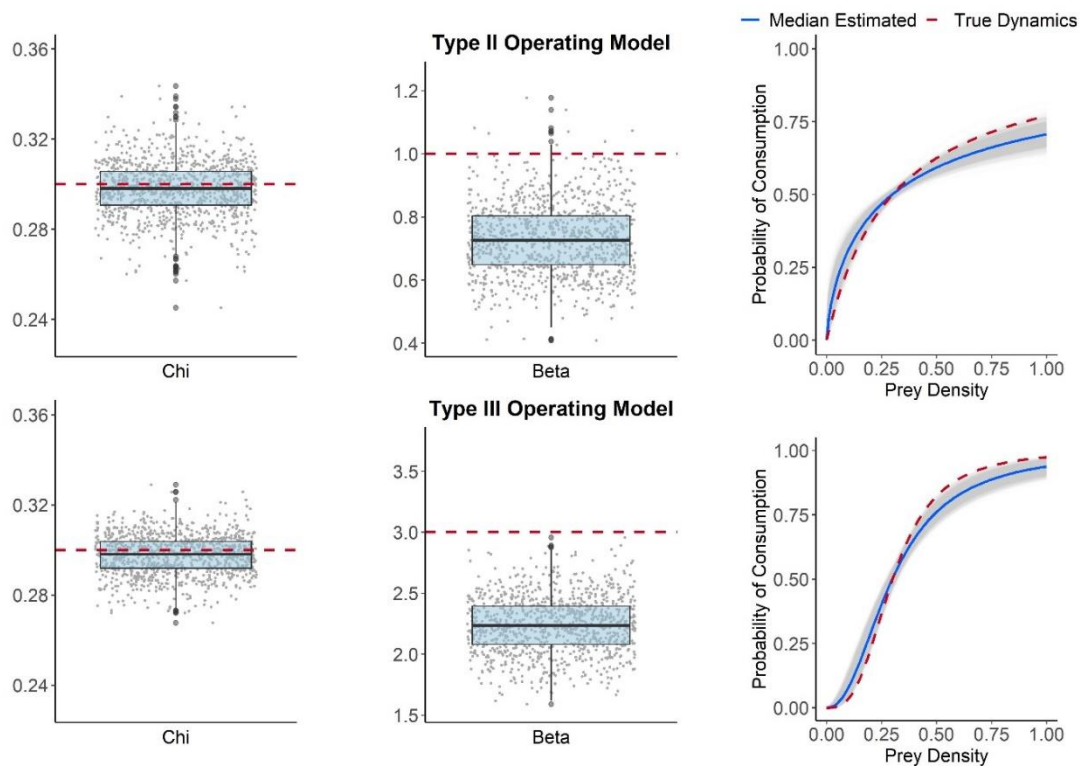


Figure B4.14 Estimates for the shape parameter values in the functional response from simulations with a narrowed range of observed prey density. The dashed red line indicates the true parameter value for each shape. The panels on the far right represent the true shape of the functional response (red lines), the shapes given by all estimated shape parameter values (grey lines), and the median shape parameter values (dark blue lines).

Appendix B Bibliography

- Fahrig, L., Lilly, G. R., & Miller, D. S. (1993). Predator stomachs as sampling tools for prey distribution: Atlantic cod (*Gadus morhua*) and capelin (*Mallotus villosus*). *Canadian Journal of Fisheries and Aquatic Sciences*, **50**(7), 1541-1547.
- Gonzalez, C., Paz, X., Roman, E., and Hermida, M. 2006. Feeding habits of fish species distributed on the Grand Bank (NAFO Divisions 3NO, 2002-2005). *SCR* **06**(31): 22.
- Pitt, T.K. 1976. Food of Yellowtail Flounder on the Grand Bank and a comparison with American Plaice. *ICNAF Res. Bull.* 12: 23–27.
- Sherwood, G.D., Rideout, R.M., Fudge, S.B., and Rose, G.A. 2007. Influence of diet on growth, condition and reproductive capacity in Newfoundland and Labrador cod (*Gadus morhua*): Insights from stable carbon isotopes. *Deep Sea Res. II* **54**: 2794–2809. doi:10.1016/j.dsr2.2007.08.007.
- Tam, J.C., and Bundy, A. 2019. Mass-balance models of the Newfoundland and Labrador shelf ecosystem for 1985-1987 and 2013-2015. *Can. Tech. Rep. Fish. Aquat. Sci.* **3328**: 88. Dartmouth, NS.

C. Appendix for Chapter 4

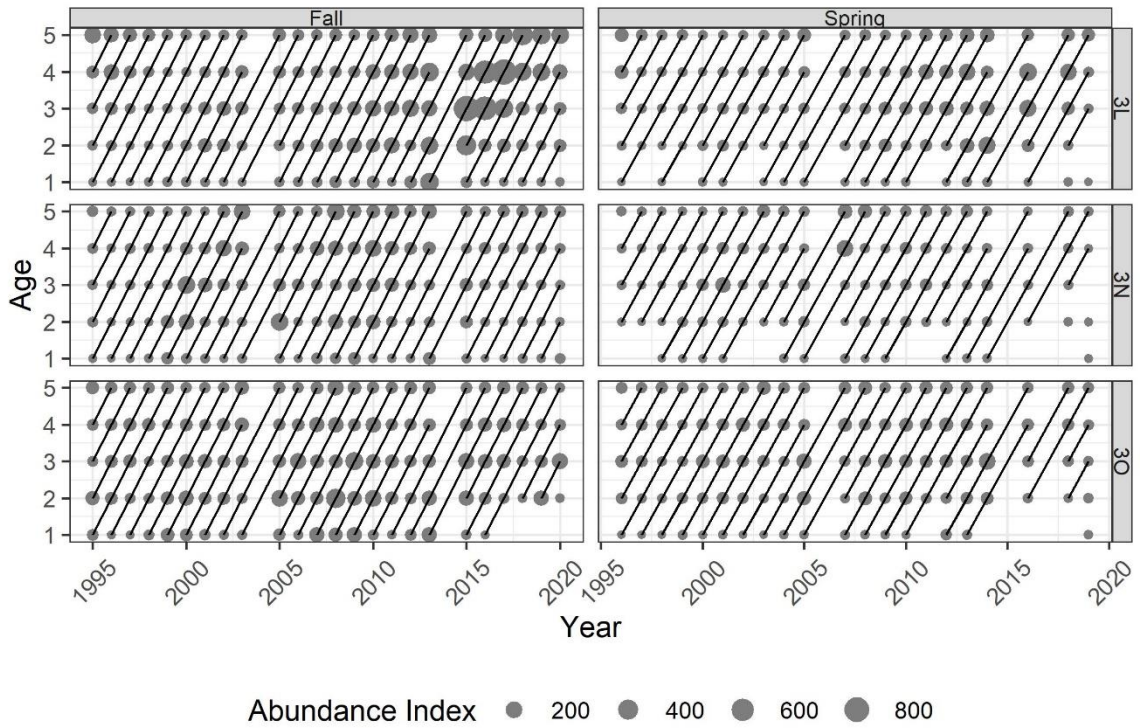


Figure C1. Data used in the metapopulation dynamics process model. The figure shows the spatiotemporal coverage of the survey, where diagonal lines connect cohorts and the size of the bubbles are proportional to the value of the abundance index for a given year and age.

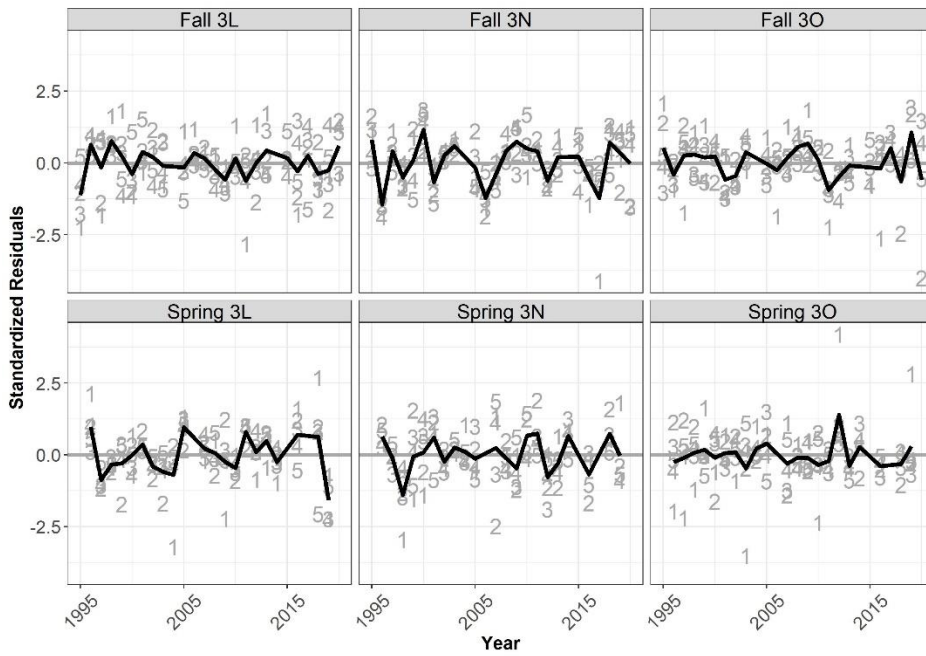


Figure C2. Standardized residuals by survey for model M4. Black lines indicate the mean across ages in a given year, while grey lines indicate zero. Numbers represent the age-class for each residual.

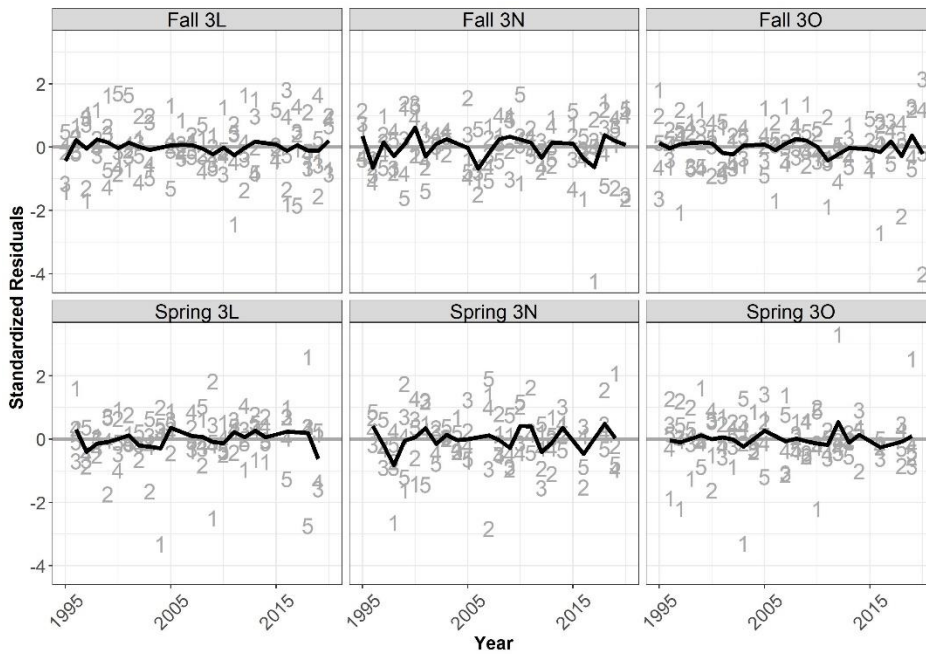


Figure C3. Standardized residuals by survey for model M5. Black lines indicate the mean across ages in a given year, while grey lines indicate zero. Numbers represent the age-class for each residual.

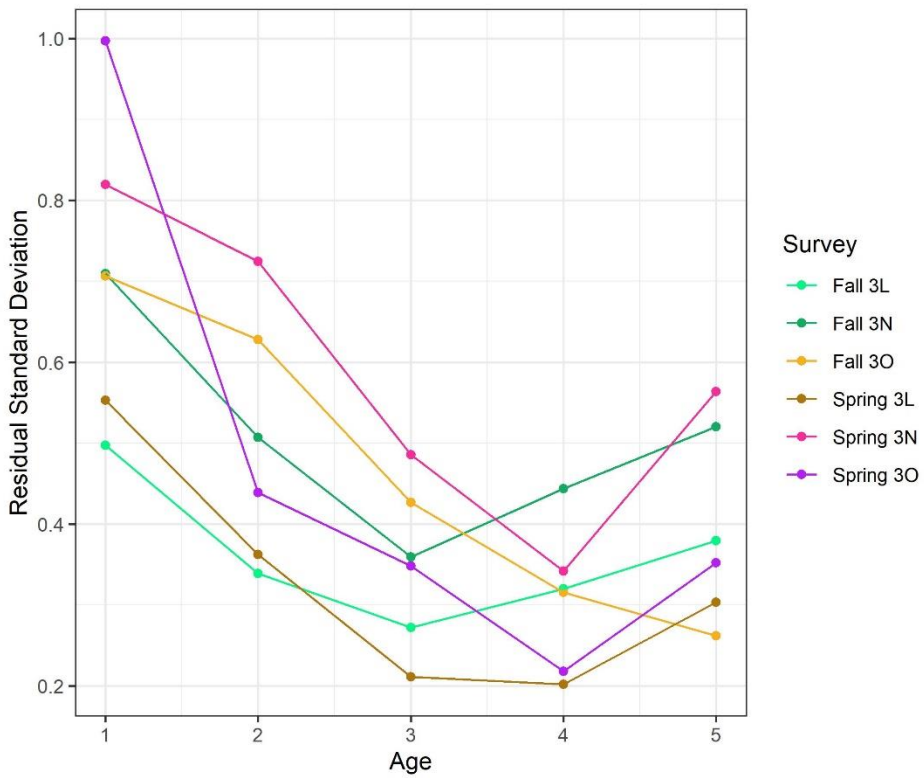


Figure C4. Residual standard deviations by age and survey from model M5.

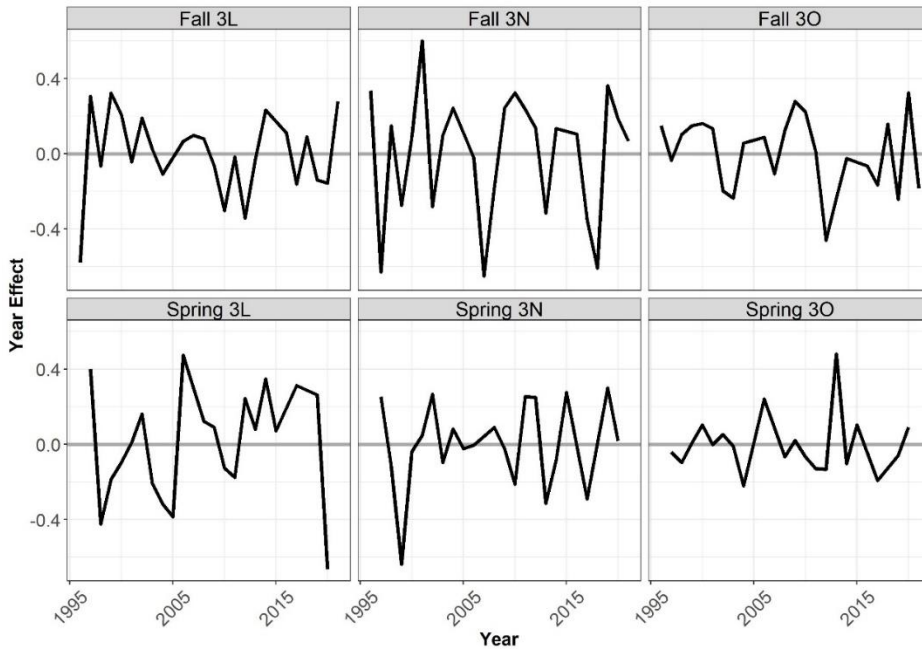


Figure C5. Time-series of survey year-effects estimated for each survey in M5.

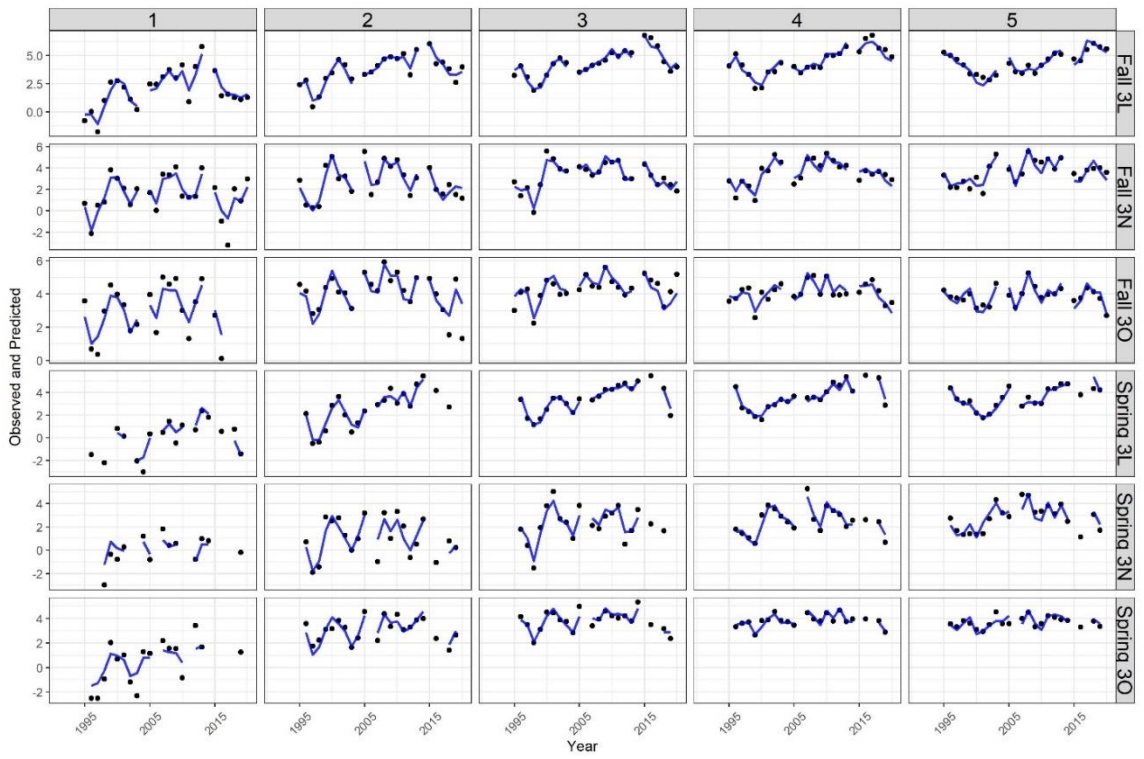


Figure C6. Log-transformed observed and predicted survey trends over time for each survey and age in M5. Black points represent the observed data while blue lines indicate model predictions.

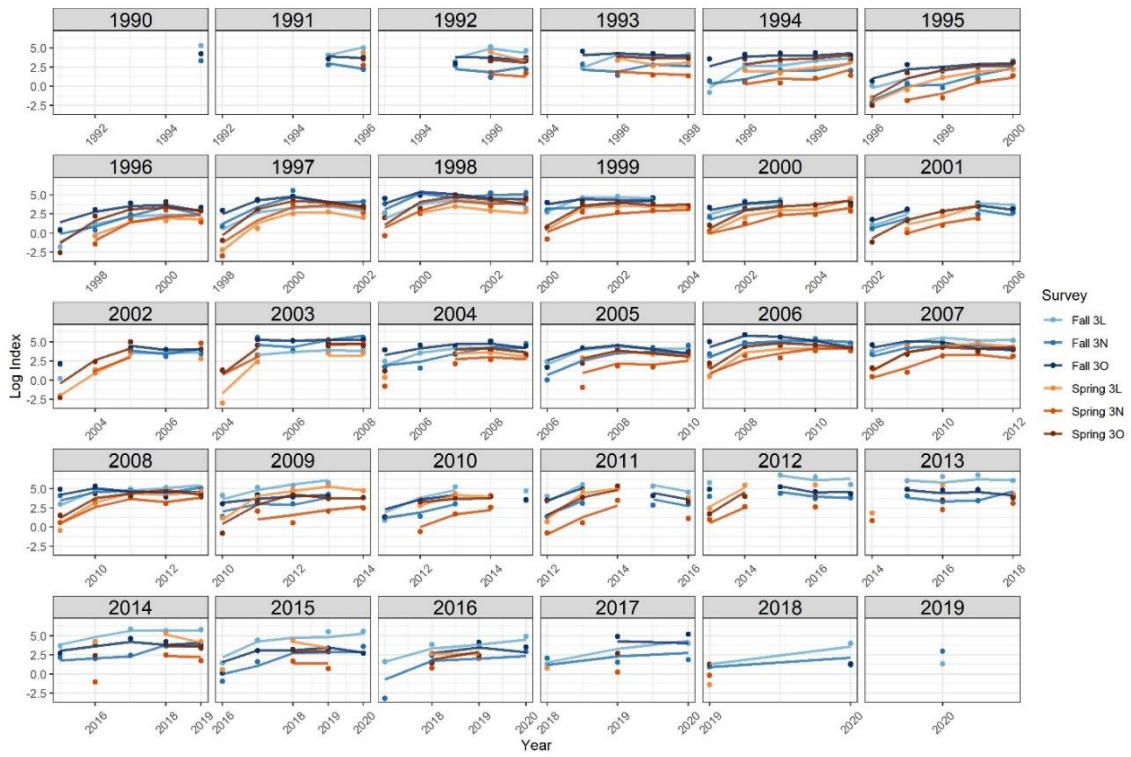


Figure C7. Log-transformed observed and predicted survey trends by cohort for each survey in M5. Points represent the observed data while the lines indicate model predictions.

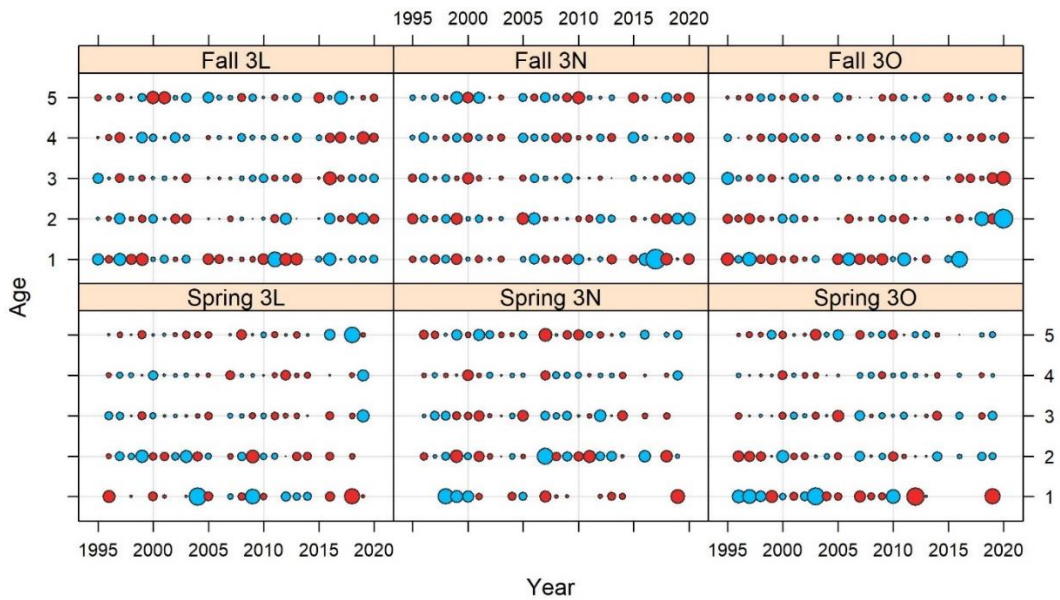


Figure C8. Standardized residual bubble plot for each survey across ages and years from model M5. Symbol sizes are scaled and values greater than average are shown as blue circles, average values are shown as small dots, and less than average values are shown as red circles.

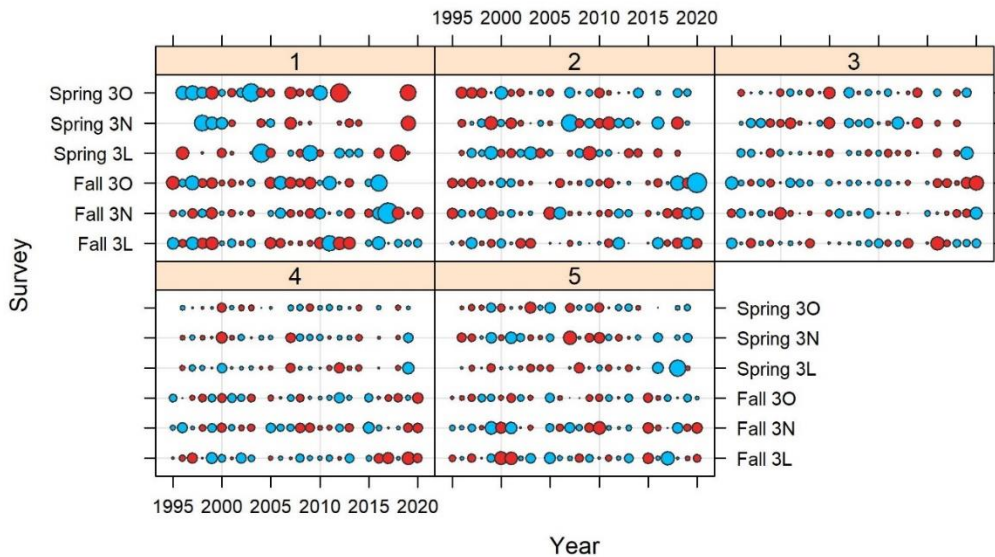


Figure C9. Standardized residual bubble plot for each age across ages and cohorts from model M5. Symbol sizes are scaled and values greater than average are shown as blue circles, average values are shown as small dots, and less than average values are shown as red circles.

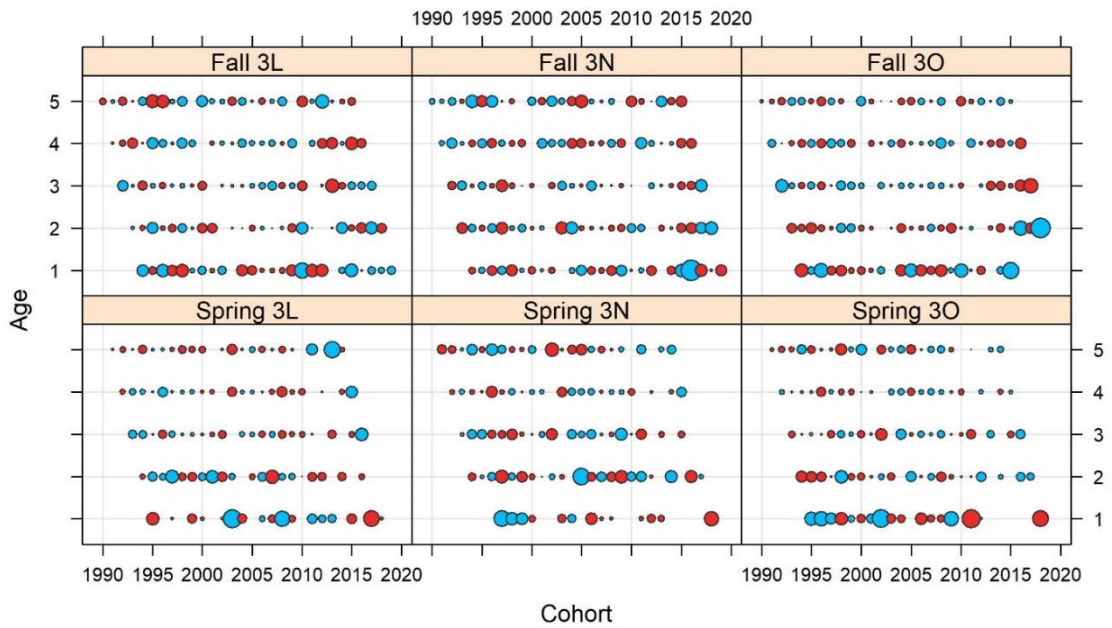


Figure C10. Standardized residual bubble plot for each age across surveys and years from model M5. Symbol sizes are scaled and values greater than average are shown as blue circles, average values are shown as small dots, and less than average values are shown as red circles.

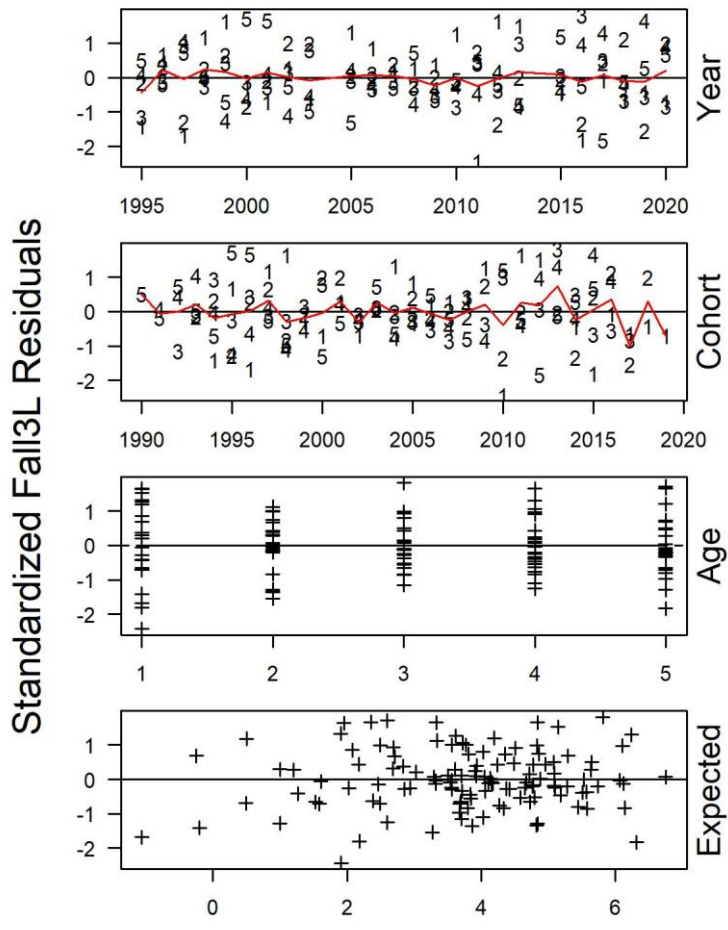


Figure C11. Standardized residual panel plot for the Fall 3L survey from model M5. Numbers represent age, black lines indicate zero, and red lines indicate means.

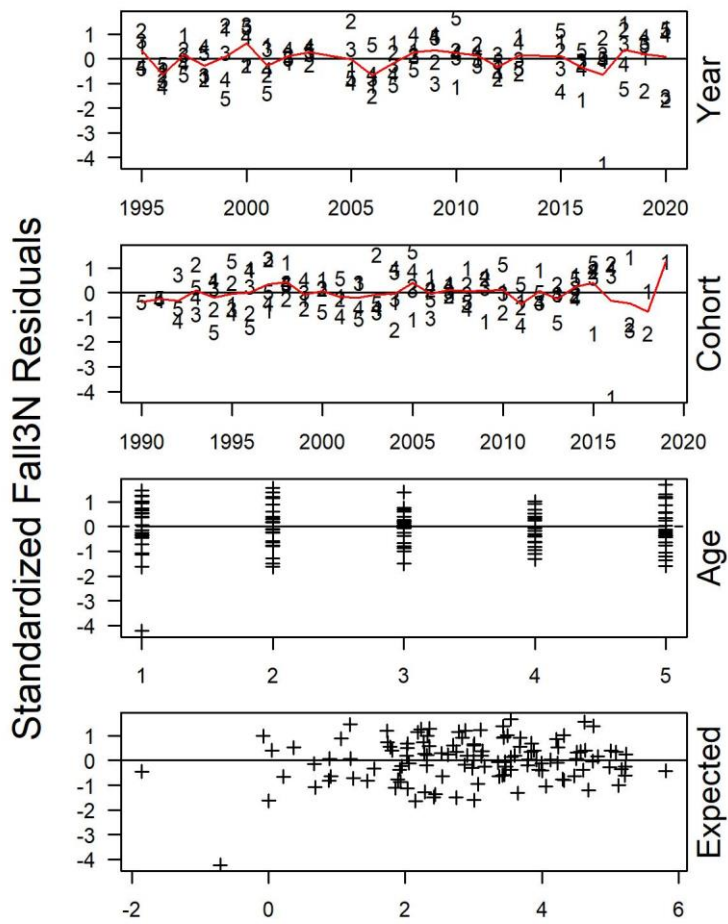


Figure C12. Standardized residual panel plot for the Fall 3N survey from model M5. Numbers represent age, black lines indicate zero, and red lines indicate means.

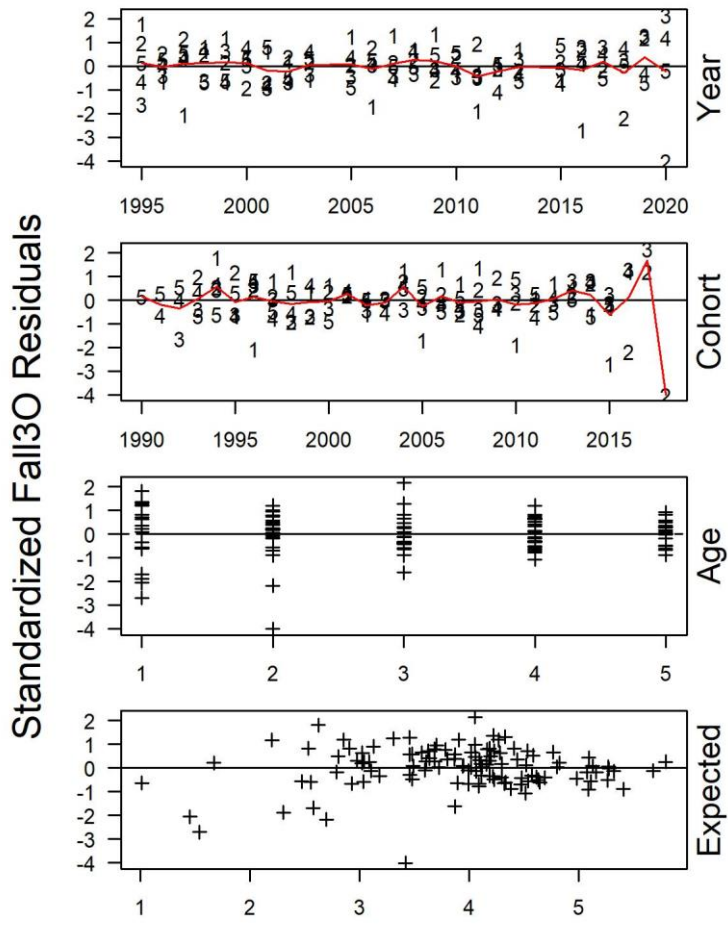


Figure C13. Standardized residual panel plot for the Fall 30 survey from model M5. Numbers represent age, black lines indicate zero, and red lines indicate means.

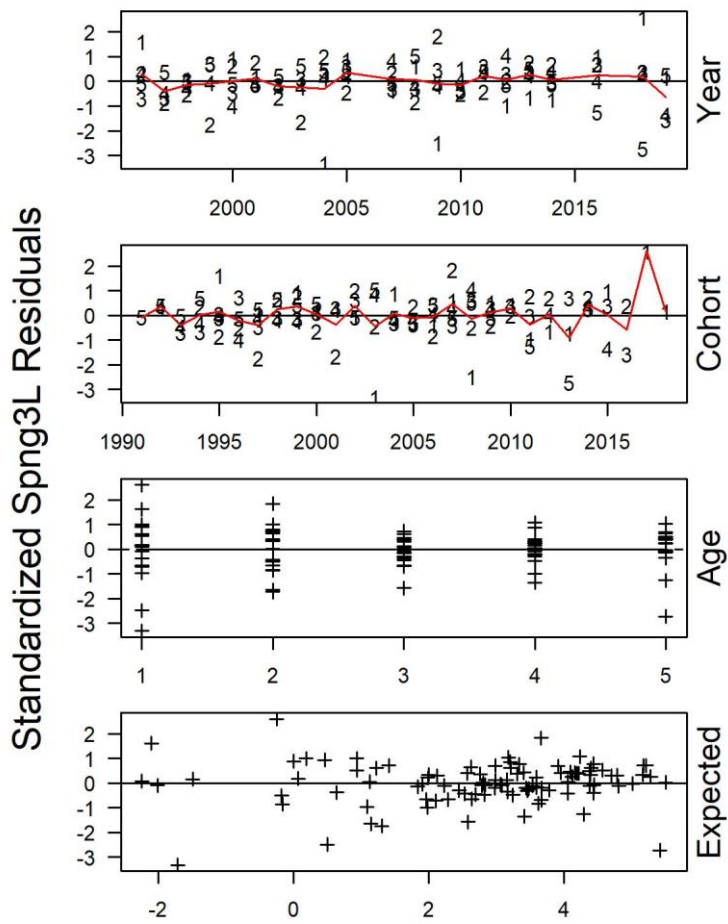


Figure C14. Standardized residual panel plot for the Spring 3L survey from model M5. Numbers represent age, black lines indicate zero, and red lines indicate means.

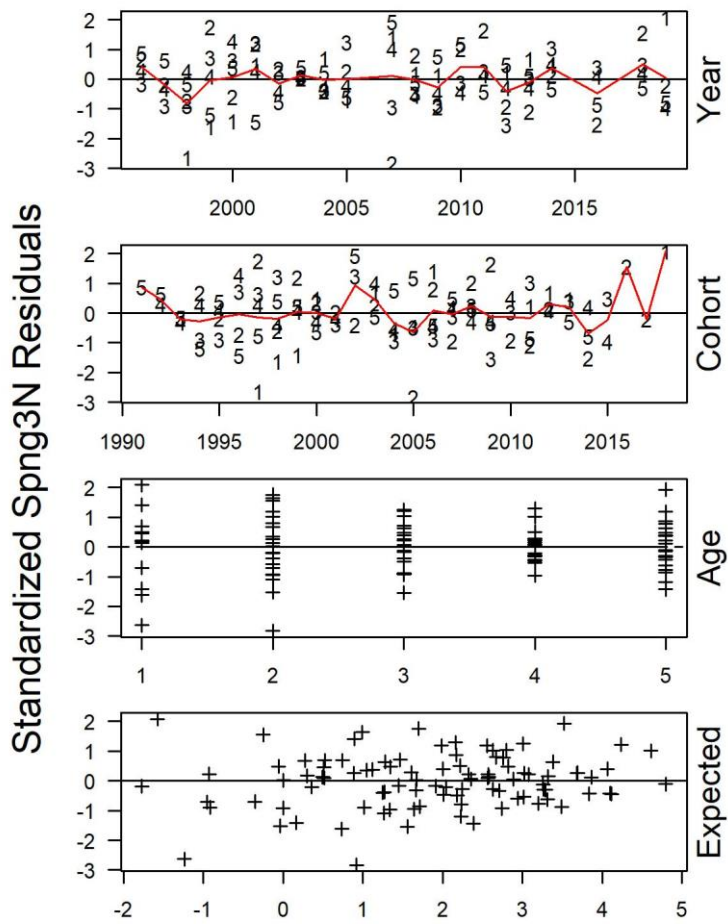


Figure C15. Standardized residual panel plot for the Spring 3N survey from model M5. Numbers represent age, black lines indicate zero, and red lines indicate means.

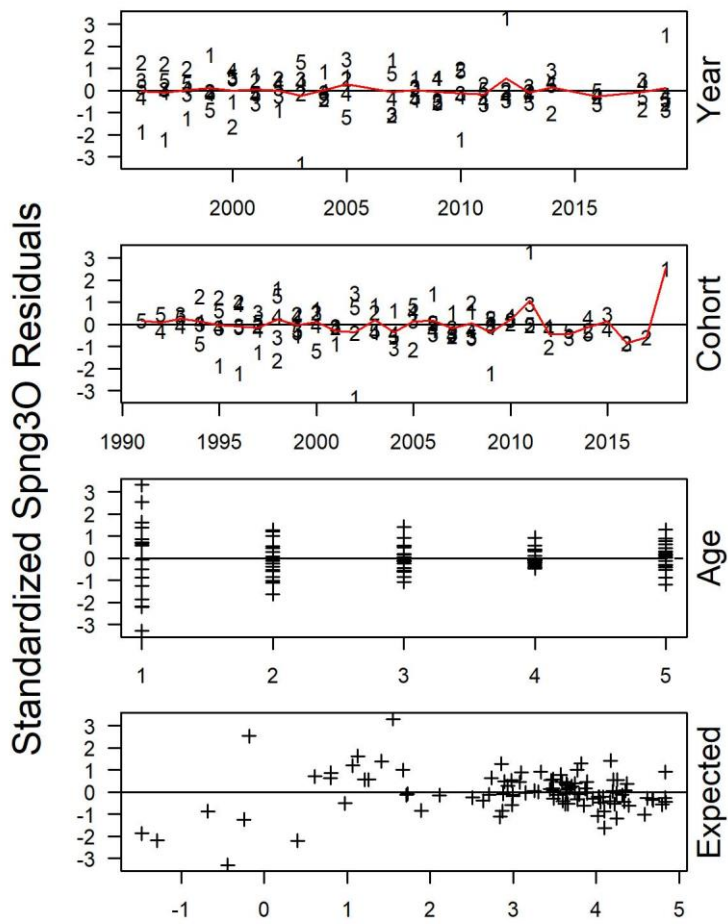


Figure C16. Standardized residual panel plot for the Spring 30 survey from model M5. Numbers represent age, black lines indicate zero, and red lines indicate means.

D. Appendix for Chapter 5

D1. Yellowtail flounder models

D1.1 Model description

We modeled yellowtail flounder population dynamics using a Deriso-Schnute delay-difference model (Deriso 1980; Schnute 1987). There are three primary assumptions for a delay-difference model (Hilborn and Walters 1992a). First, growth in mean body weight is,

$$w_a = \alpha + \rho w_{a-1} \quad (D1)$$

where w_a is weight at age and α and ρ are shape parameter estimates from a Ford-Walford relationship (Thorson et al. 2015a). Second, all fish aged k and older (here $k=5$ years) are equally vulnerable to fishing and third, all fish aged k and older have the same M . We combined weight-at-length data with estimates of length-at-age from Dwyer, Walsh, & Campana (2003) to estimate stock weight-at-age (see Fig. D1.1).

The model is based on a common exponential growth relationship that tracks the number of “mature” fish (considered here as fish aged 5+ years; Walsh & Morgan, 1999) in year y (Tables D1.1 & D1.2). Initial fish numbers were estimated using a separate parameter ($N_0^{y t f l}$) and initial biomass was estimated as $N_0^{y t f l} w_8$ to ensure that biomass was based on weight of a fish of a median age. Models were evaluated with different starting weights, however w_8 yielded results that were most similar to the current stock assessment model. The number of fish born in a year was equal to the number of mature fish in the population ($N_y^{y t f l}$) to create a basic stock recruitment relationship. Recruitment ($R_y^{y t f l}$) was determined based on an annual juvenile survival rate ($S_{juv}^{y t f l}$, here 0.9) for

each year prior to maturity (i.e., $S^{y t f l}_{juv}^5$). Juvenile survival was not time-varying, instead we estimated time-varying recruitment deviations ($\delta_y^{y t f l}$). $\delta_y^{y t f l}$ was multiplicative and bounded between (0,1). This effectively resulted in $S_{juv}^{y t f l}$ being the maximum annual juvenile survival rate, where annual recruitment could only be modified downwards based on $\delta_y^{y t f l}$. Abundance in a given year ($N_y^{y t f l}$) was based on the number of surviving mature individuals from the prior year and recruitment, where survival was based on fishing mortality ($F_y^{y t f l}$) and a stationary estimate of $M^{y t f l}$ (0.2). Meanwhile, the biomass in a given year ($B_y^{y t f l}$) was based on Eqn. D1., the number of fish in the population, and the weight of recruiting fish.

Table D1.1. Base formulation of the state-space delay-difference model for yellowtail flounder, variables and parameters described in Table D1.2.

Process Model		
Recruitment	$R_y^{y\text{tfl}} = N_{y-1}^{y\text{tfl}} S_{juv}^{y\text{tfl}} \frac{\exp(\delta_y^{y\text{tfl}})}{1 + \exp(\delta_y^{y\text{tfl}})} \quad y < 5$ $R_y^{y\text{tfl}} = N_{y-5}^{y\text{tfl}} S_{juv}^{y\text{tfl}5} \frac{\exp(\delta_y^{y\text{tfl}})}{1 + \exp(\delta_y^{y\text{tfl}})} \quad y \geq 5$	$\delta_y^{y\text{tfl}} \sim RW$
Abundance	$N_y^{y\text{tfl}} = N_{y-1}^{y\text{tfl}} S_{y-1}^{y\text{tfl}} + R_y^{y\text{tfl}}$	
Biomass	$B_y^{y\text{tfl}} = (\alpha N_{y-1}^{y\text{tfl}} + \rho B_{y-1}^{y\text{tfl}}) S_{y-1}^{y\text{tfl}} + w_5 R_y^{y\text{tfl}}$	
Survival	$S_y^{y\text{tfl}} = e^{-M^{y\text{tfl}} - F_y^{y\text{tfl}}}$	$\log(F_y^{y\text{tfl}}) \sim \text{AR1}(y)$
Observation Model		
Landings	$EL_y^{y\text{tfl}} = B_y^{y\text{tfl}} \times$ $(1 - e^{-M^{y\text{tfl}} - F_y^{y\text{tfl}}}) \left(\frac{F_y^{y\text{tfl}}}{F_y^{y\text{tfl}} + M^{y\text{tfl}}} \right)$	$\epsilon EL_y^{y\text{tfl}} = \log(L_y^{y\text{tfl}}) - \log(EL_y^{y\text{tfl}})$ $\epsilon EL_y^{y\text{tfl}} \sim N(0, \sigma_L^{y\text{tfl}})$
Survey Indices	$EI_{s,y}^{y\text{tfl}} = \log(q_s^{y\text{tfl}}) +$ $\log(B_y^{y\text{tfl}}) - f_s^{y\text{tfl}} (F_y^{y\text{tfl}} + M^{y\text{tfl}})$	$\epsilon EI_{s,y}^{y\text{tfl}} = \log(I_{s,y}^{y\text{tfl}}) - \log(EI_{s,y}^{y\text{tfl}})$ $\epsilon EI_{s,y}^{y\text{tfl}} \sim N(0, \sigma_{EI,s,y}^{y\text{tfl}})$

Table D1.2. Description of the variables in the yellowtail flounder delay difference model.

Parameter	Description	Input, computed, estimated
w_a	Weight at age a (k describes age at maturity, here 5)	Input
α	Shape parameter for growth in w_a , estimated external to the population dynamics model	Input
ρ	Shape parameter for growth in w_a , estimated external to the population dynamics model	Input
N_0^{yfl}	Number of fish in the population in year 1	Estimated
R_y^{yfl}	Recruitment of fish to mature age in year y	Computed
N_y^{yfl}	Number of mature fish in the population in year y	Computed
S_{juv}^{yfl}	Juvenile survival rate	Input
δ_y^{yfl}	Recruitment deviations in year y	Estimated
S_y^{yfl}	Survival rate of mature fish in year y	Computed
B_y^{yfl}	Biomass of mature fish in the population in year y	Computed
M^{yfl}	Natural mortality rate of mature fish in year y	Input
F_y^{yfl}	Fishing mortality rate of mature fish in year y	Estimated
EL_y^{yfl}	Expected landings of mature fish in year y	Computed
L_y^{yfl}	Landings data in year y	Input
ϵEL_y^{yfl}	Residuals of L_y^{yfl} and EL_y^{yfl}	Computed
σ_L^{yfl}	Standard deviation of the landings likelihood	Input
$EI_{s,y}^{yfl}$	Expected survey index from survey s in year y	Computed
$I_{s,y}^{yfl}$	Survey index data from survey s in year y	Input
q_s^{yfl}	Catchability of a given survey s	Estimated
f_s^{yfl}	Fraction of the year that survey s occurred in	Input
ϵEI_y^{yfl}	Residuals of $I_{s,y}^{yfl}$ and $EI_{s,y}^{yfl}$	Computed
$\sigma_{EI_s}^{yfl}$	Standard deviation for survey s in the survey index likelihood	Estimated

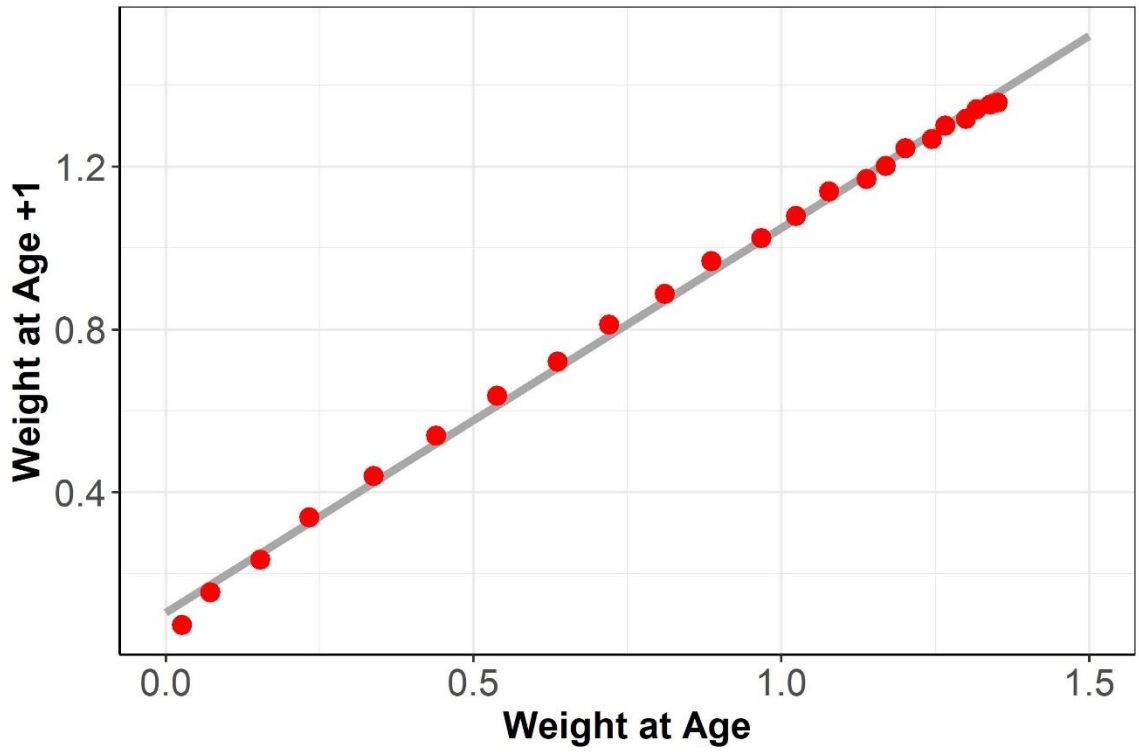


Figure D1.1. Ford-Walford relationship for growth in mean body-weight. Red dots represent the data and the grey line represents the estimated relationship.

D1.2 Model outputs

Residuals and landings estimates from the null model that was used in environmental extended tests (YTFL1; Table 5.1) and the best fitting environment-extended model (YTFL1E1; Table 5.2) are plotted below to allow comparisons.

YTFL1 Model Output

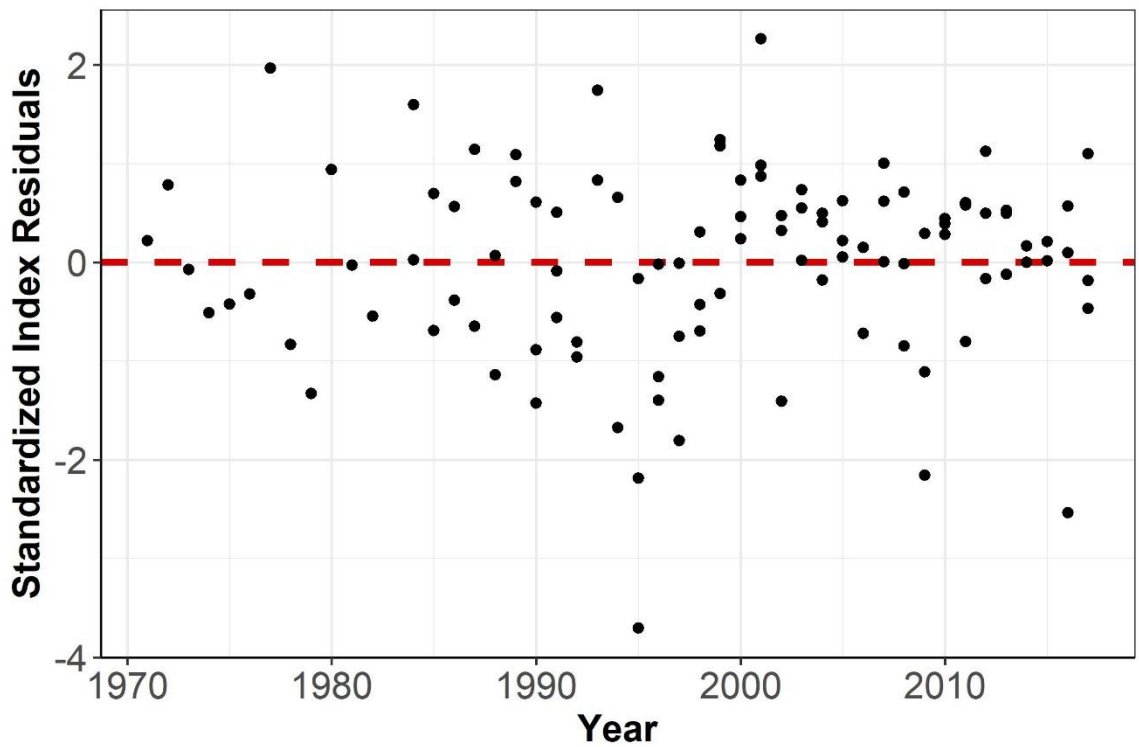


Figure D1.2. Standardized residuals of all survey indices over time from YTFL1. Dashed red line indicates zero.

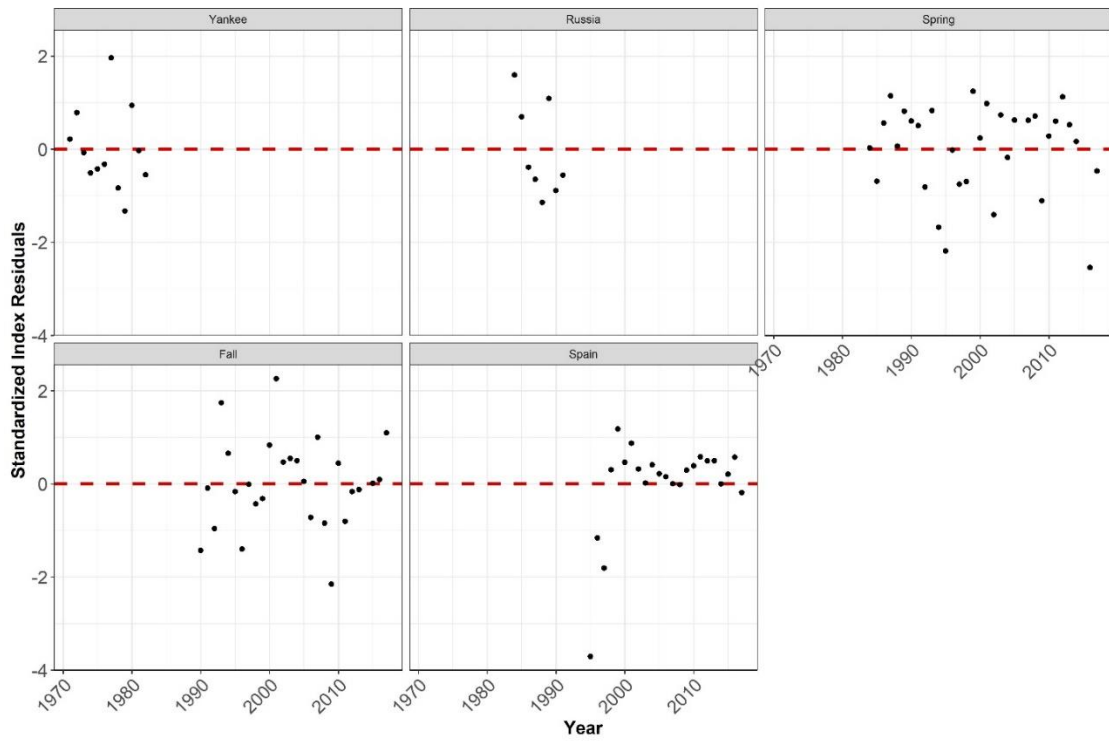


Figure D1.3. Standardized residuals of all survey indices over time and by survey from YTFL1. Dashed red line indicates zero.

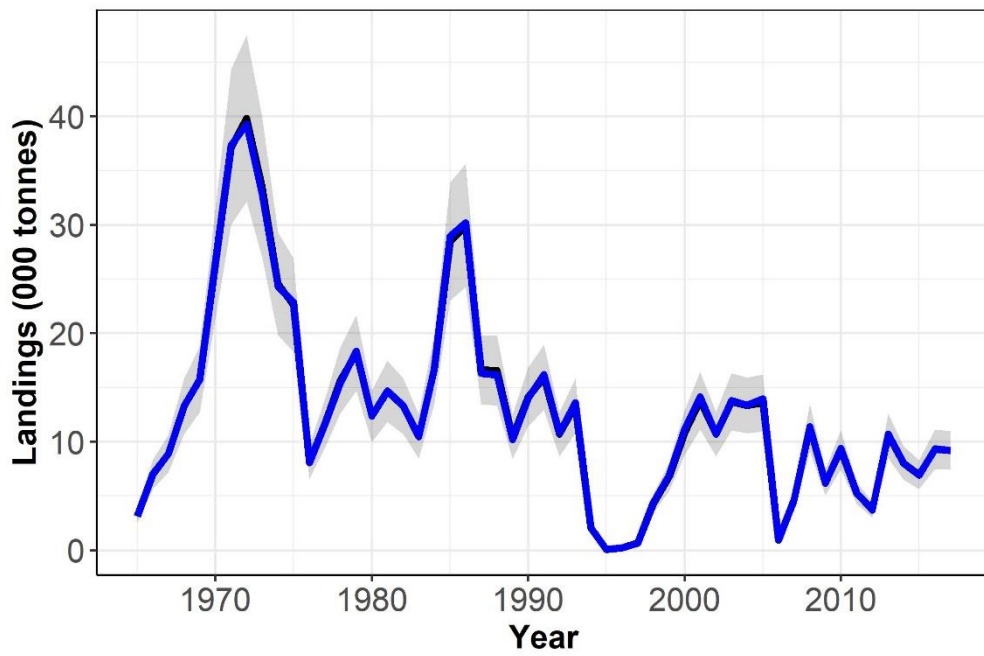


Figure D1.4. Landings estimates (black line) and 95% confidence interval (grey polygon) for YTFL1 compared to landings data.

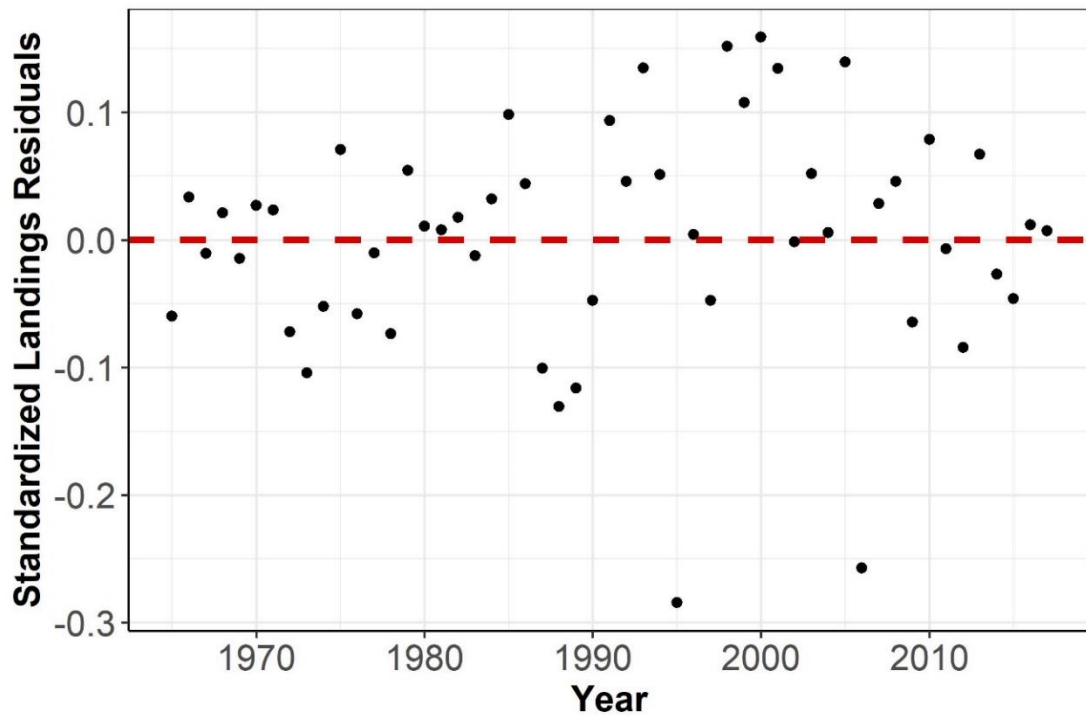


Figure D1.5. Standardized landings residuals over time from YTFL1.

YTFLE1 Model Output

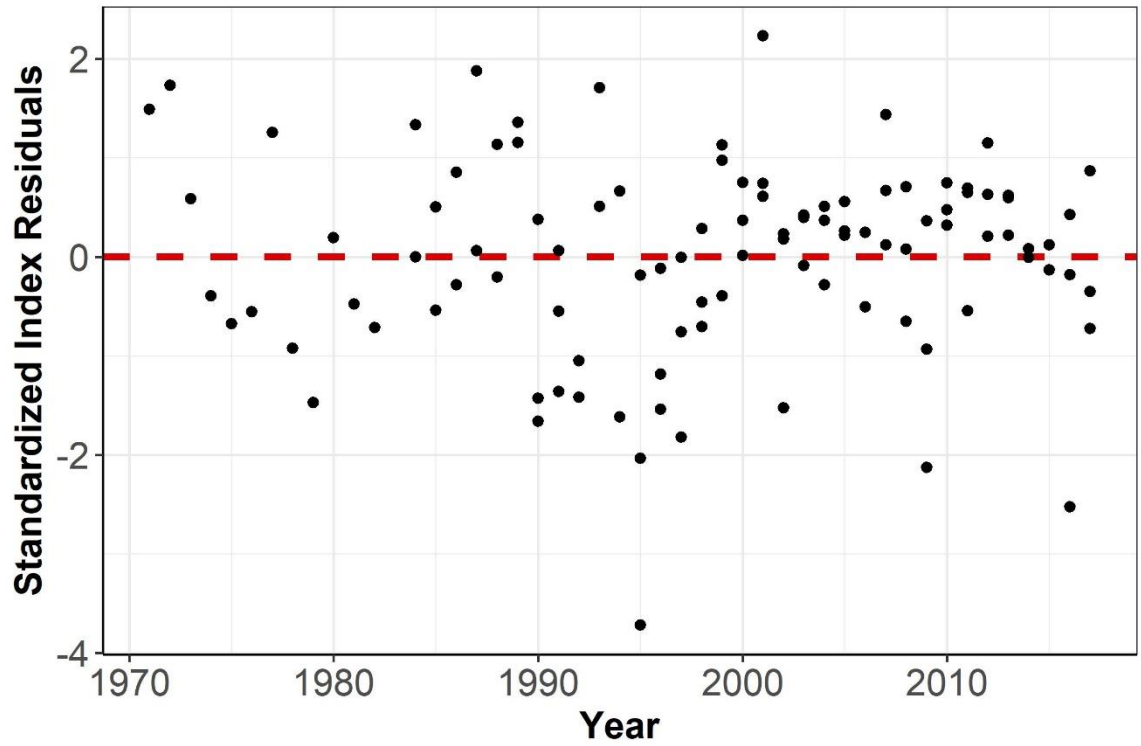


Figure D1.6. Standardized residuals of all survey indices over time from YTFLE1. Dashed red line indicates zero.

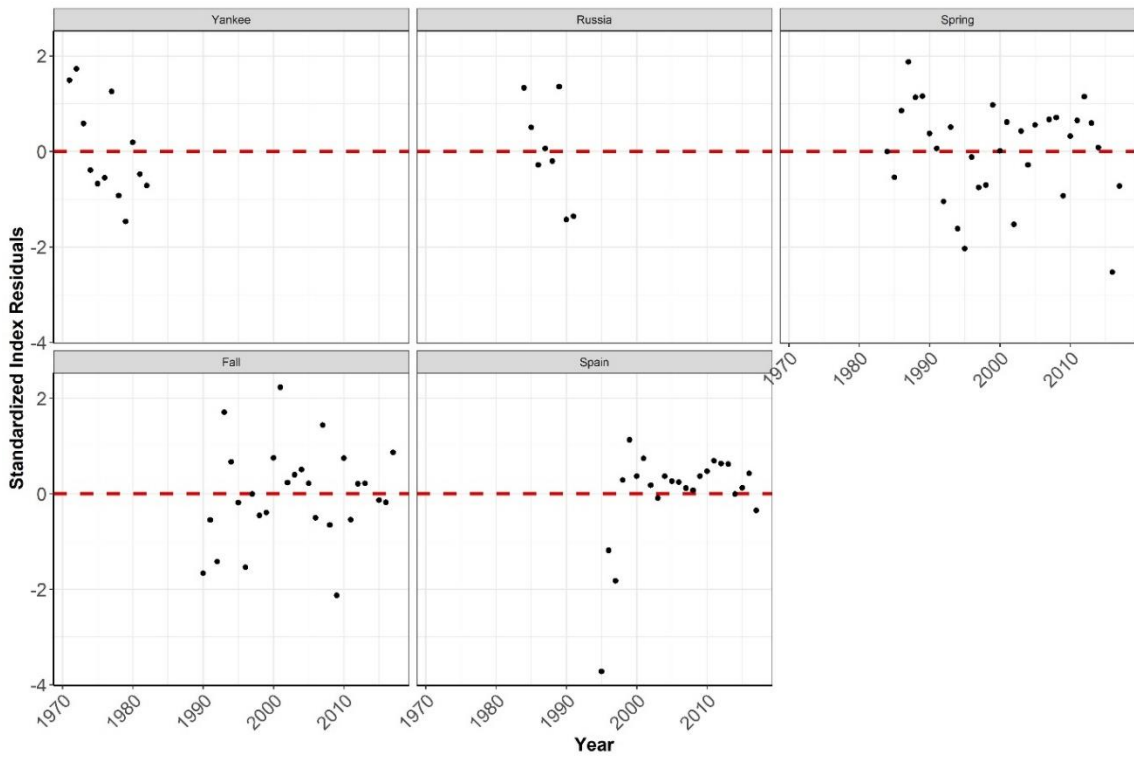


Figure D1.7. Standardized residuals of all survey indices over time and by survey from YTFLE1. Dashed red line indicates zero.

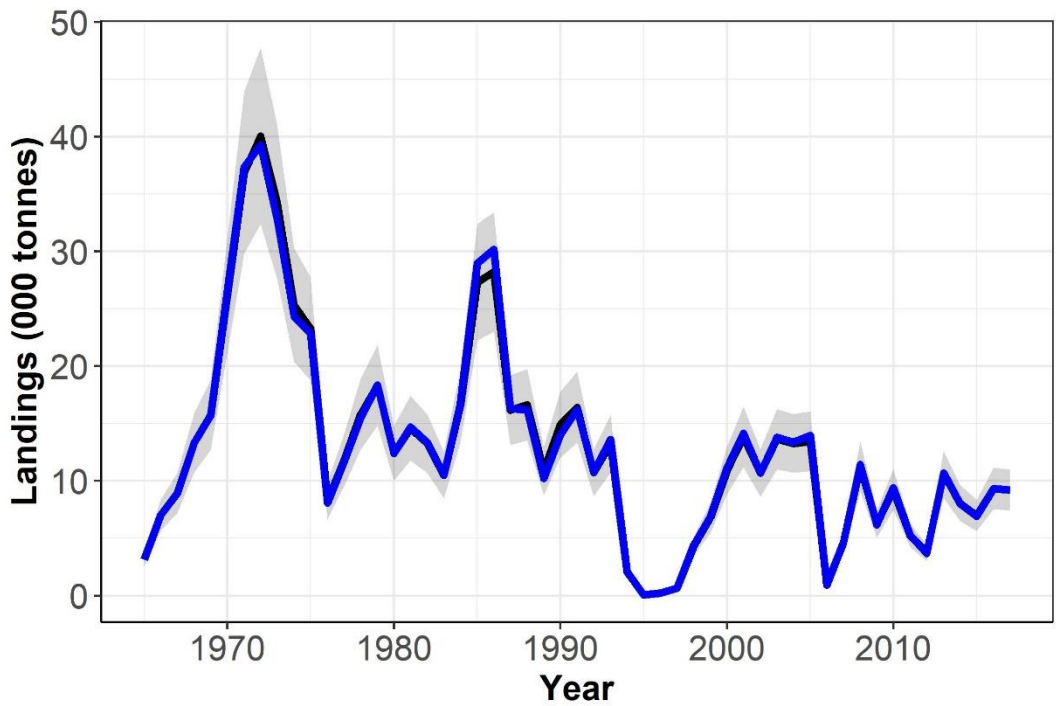


Figure D1.8. Landings estimates (black line) and 95% confidence interval (grey polygon) for YTFLE1 compared to landings data.

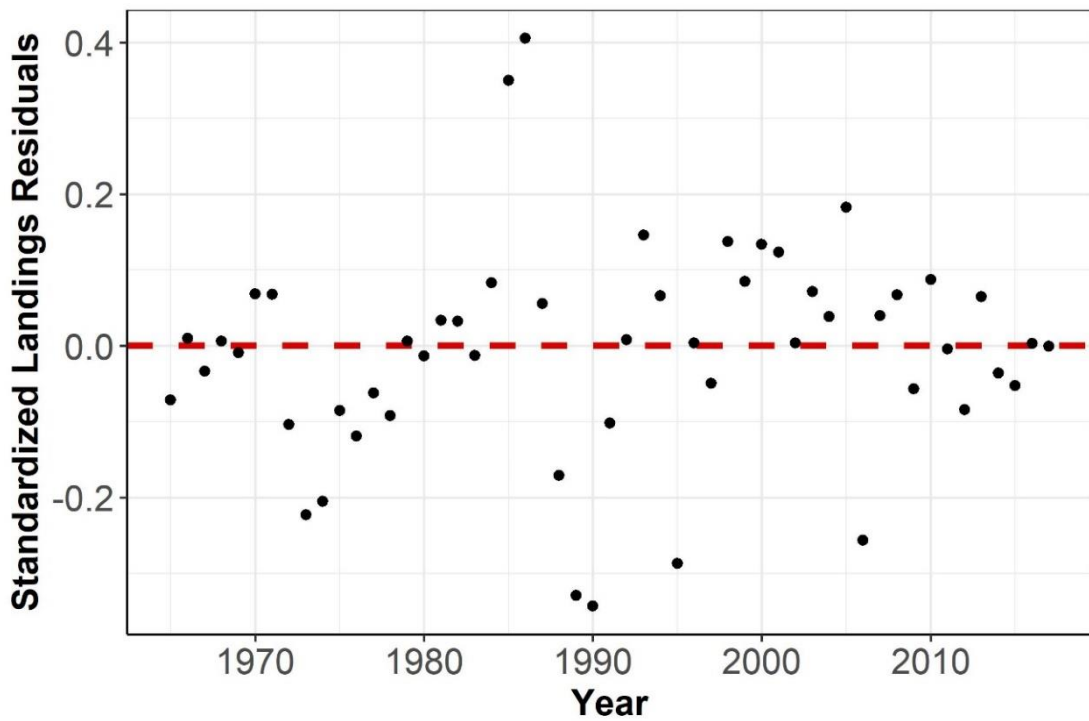


Figure D1.9. Standardized landings residuals over time from YTFLE1.

Appendix D1 Bibliography

- Deriso, R. (1980). Harvesting strategies and parameter estimation for an age-structured model. *Canadian Journal of Fisheries and Aquatic Sciences*, **37**, 268–282.
- Dwyer, K. S., Rideout, R., Ings, D., Power, D., Morgan, J., Brodie, B., & Healey, B. P. (2016). Assessment of American plaice in Div.3LNO. NAFO SCR, **N6573**, 1–19.
- Dwyer, K. S., Walsh, S. J., & Campana, S. (2003). Age determination, validation and growth of Grand Bank yellowtail flounder (*Limanda ferruginea*). *ICES Journal of Marine Science*, **60**, 1123–1138. <https://doi.org/10.1016/S1054>
- Hilborn, R., & Walters, C. (1992). *Quantitative Fisheries Stock Assessment*. Chapman & Hall.
- Perreault, A. M. J., Wheeland, L. J., & Morgan, M. J. (2020). A state-space stock assessment model for American plaice on the Grand Bank of Newfoundland. *Journal of Northwest Atlantic Fishery Science*, **51**, 45–104.
- Pitt, T. K. (1972). Nominal catches of American plaice in Divisions 3L and 3N for the years 1960-1970. *ICNAF Research Bulletin*, **2813**(72/90).
- Schnute, J. (1987). A general fishery model for a size-structured fish population. *Canadian Journal of Fisheries and Aquatic Sciences*, **44**(5), 924–940. <https://doi.org/10.1139/f87-111>
- Thorson, J. T., Ianelli, J. N., Munch, S. B., Ono, K., Spencer, P. D., & Vinbrooke, R. (2015). Spatial delay-difference models for estimating spatiotemporal variation in juvenile production and population abundance. *Canadian Journal of Fisheries and Aquatic Sciences*, **72**(12), 1897–1915. <https://doi.org/10.1139/cjfas-2014-0543>
- Walsh, S. J., & Morgan, M. J. (1999). Variation in maturation of yellowtail flounder (*Pleuronectes ferruginea*) on the Grand Bank. *Journal of Northwest Atlantic Fishery Science*, **25**, 47–59. <https://doi.org/10.2960/J.v25.a5>
- Wheeland, L., Dwyer, K., Kumar, R., Rideout, R., Perreault, A., & Rogers, B. (2021). Assessment of American plaice in Div. 3LNO. NAFO SCR, **21**(035).

D2. American plaice models

D2.1 Model description

We modeled American plaice population dynamics using a modified version of a previously developed state-space age-based model for this stock (Perreault et al. 2020). This model was based on exponential population growth that tracked the numbers and biomass of fish at age a (1 – 15+ years) in year y (Tables A.4.2.1.2 & A4.2.2.2). Initial population numbers at age were freely estimated ($N_{0,a}$). Recruitment was then based on the Beverton-Holt stock recruitment relationship with multiplicative annual recruitment deviations (δ_y^{ampl}). Total mortality was based on a combination of stationary, age-varying natural mortality rates (M_a ; 0.5 for $a < 4$, 0.3 for $a = 4$, 0.2 for $a \geq 5$) and fishing mortality ($F_{y,a}$). Where $F_{y,a}$ was based on the Baranov catch equation. Finally, to account for different survey catchability of small fish between the Engels and Campelen survey gear, we estimated separate survey catchability parameters ($q_{s,a}^{ampl}$) between these surveys for ages 1 – 4.

There are four major differences between our parameterization and the state-space model developed by Perreault et al. (2020): 1) we removed the cohort process error over time and age from the population growth equation to allow the inclusion of natural mortality specific process error. 2) We modeled recruitment using a Beverton-Holt function with deviations rather than using deviations from separate means before and after 1993. The rationale was to account for the stock-recruitment relationship and to have a continuous time-series of deviations. 3) We simplified how fishing mortality was modeled to follow a continuous AR1(y,a), rather than based on AR1(y,a) positive

deviations with a separate mean pre- and post-collapse. This was done to ensure similarities in how fishing mortality was modeled between the two species and to minimize any effects of structural model shifts in fishing mortality on estimates of natural mortality. 4) Finally, we modeled landings using a normal likelihood with a fixed standard deviation rather than a censored likelihood approach to simplify the model and match what was done for the yellowtail flounder model.

Table D2.1. Formulation of the model for American plaice, variables and parameters described in Table D2.2.

Process Model		
Recruitment	$\log(R_y^{ampl}) = \log\left(\frac{\gamma SSB_{y-1}^{ampl}}{1 + \beta SSB_{y-1}^{ampl}}\right) + \delta_{y-1}^{ampl}$	$\delta_y^{ampl} \sim RW$
Abundance	$\log(N_{y,a}^{ampl}) = \log(N_{y-1,a-1}^{ampl}) - Z_{y-1,a-1}^{ampl}$ $\log(N_{y,A^+}^{ampl}) = \log[N_{y-1,A^+-1}^{ampl} \exp^{-Z_{y-1,A^+-1}^{ampl}} + N_{y-1,A^+}^{ampl} \exp^{-Z_{y-1,A^+}^{ampl}}]$	
Mortality	$Z_{y,a}^{ampl} = M_a^{ampl} + F_{y,a}^{ampl}$	$F_{y,a}^{ampl} = 0, \quad a < 4$ $\log(F_{y,a}^{ampl}) \sim AR1(y, a)$
Observation Model		
Landings	$EC_{y,a}^{ampl} = N_{y,a}^{ampl} (1 - e^{-M_a^{ampl} - F_{y,a}^{ampl}}) \left(\frac{F_{y,a}^{ampl}}{F_{y,a}^{ampl} + M_a^{ampl}}\right)$ $ECW_{y,a}^{ampl} = EC_{y,a}^{ampl} W_{y,a}^{ampl}$ $EL_y^{ampl} = \sum_a ECW_{y,a}^{ampl}$	$\epsilon L_y^{ampl} = \log(L_y^{ampl}) - \log(EL_y^{ampl})$ $\epsilon L_y^{ampl} \sim N(0, \sigma_L^{ampl})$
Age composition	$X_{O_{a,y}} = X_{a,y} + C_{y,a}$	$\epsilon_{C_{y,a}} = X_{O_{a,y}} - X_{a,y}$ $\epsilon_{C_{y,a}} \sim AR1(y, a)$
Survey Indices	$EI_{s,y,a}^{ampl} = \log(q_{s,a}^{ampl}) + \log(N_{y,a}^{ampl}) - f_s^{ampl}(Z_{y,a}^{ampl})$ $q_{s,a}^{ampl} = q_{s,a-1}^{ampl} + \delta_{q_{s,a}}^{ampl}$ where $\delta_{q_{s,a}}^{ampl}$ are positive	$\epsilon EI_{s,y,a}^{ampl} = \log(I_{s,y,a}^{ampl}) - \log(EI_{s,y,a}^{ampl})$ $\epsilon EI_{s,y}^{ampl}, a \sim N(0, \sigma_{EI_{s,y}}^{ampl})$

Table D2.2. Description of the variables in the age-based American plaice model

Parameter	Description	Input, computed, estimated
$N_{0,a}$	Initial numbers at age a	Estimated
R_y^{ampl}	Recruitment of fish in year y	Computed
γ	Shape parameter for Beverton-Holt stock recruitment	Estimated
β	Shape parameter for Beverton-Holt stock recruitment	Estimated
SSB_{y-1}^{ampl}	Spawning stock biomass in year $y - 1$	Computed
δ_{y-1}^{ampl}	Recruitment deviations in year $y - 1$	Estimated
$N_{y,a}^{ampl}$	Number of fish at age a in year y	Computed
$Z_{y,a}^{ampl}$	Total mortality rate of fish at age a in year y	Computed
M_a^{ampl}	Natural mortality rate of fish at age a in year y	Input
$F_{y,a}^{ampl}$	Fishing mortality rate of fish at age a in year y	Estimated
$EC_{y,a}^{ampl}$	Expected catch of fish at age a in year y	Computed
$W_{y,a}^{ampl}$	Weight of fish at age a in year y	Input
$ECW_{y,a}^{ampl}$	Expected catch weight of fish at age a in year y	Computed
EL_y^{ampl}	Expected landings of fish in year y	Computed
$CW_{y,a}^{ampl}$	Catch weight data at age a in year y	Input
ϵL_y^{ampl}	Residuals of L_y^{ampl} and EL_y^{ampl}	Computed
L_y^{ampl}	Landings data for year y	Input
σ_L^{ampl}	Standard deviation for landings in the landings likelihood	Input
$X_{0a,y}$	Continuation ratio logit of observed catch proportions-at-age	Computed
$X_{a,y}$	Continuation ratio logit of estimated catch proportions-at-age	Estimated
$\epsilon_{C,y,a}$	Residuals of $X_{0a,y}$ and $X_{a,y}$	Computed
$EI_{s,y,a}^{ampl}$	Expected survey index of survey s for age a in year y	Computed
$q_{s,a}^{ampl}$	Catchability of a given survey s at age a	Computed
f_s^{ampl}	Fraction of the year that survey s occurred in	Input
$\delta_{q_{s,a}}^{ampl}$	Catchability deviations of a given survey s at age a	Estimated
$\epsilon EI_{s,y,a}^{ampl}$	Residuals of $I_{s,y,a}^{ampl}$ and $EI_{s,y,a}^{ampl}$	Computed

$I_{s,y,a}^{ampl}$	Survey index data for survey s at age a in year y	Input
$\sigma_{EI_{s,a}}^{ampl}$	Standard deviation for survey s catch at age a in the survey likelihood	Estimated

D2.2 Model Output

This section shows residual and output plots from the models most discussed in the manuscript. These include the single-species model without time-varying M (AMPL 1; Table 5.1), the single-species model with time-varying M (AMPL2; Table 5.1), and the best performing environmental-extended model with the NL climate index accounting for M deviations (AMPLE6; Table 5.2).

AMPL1 Model Residuals

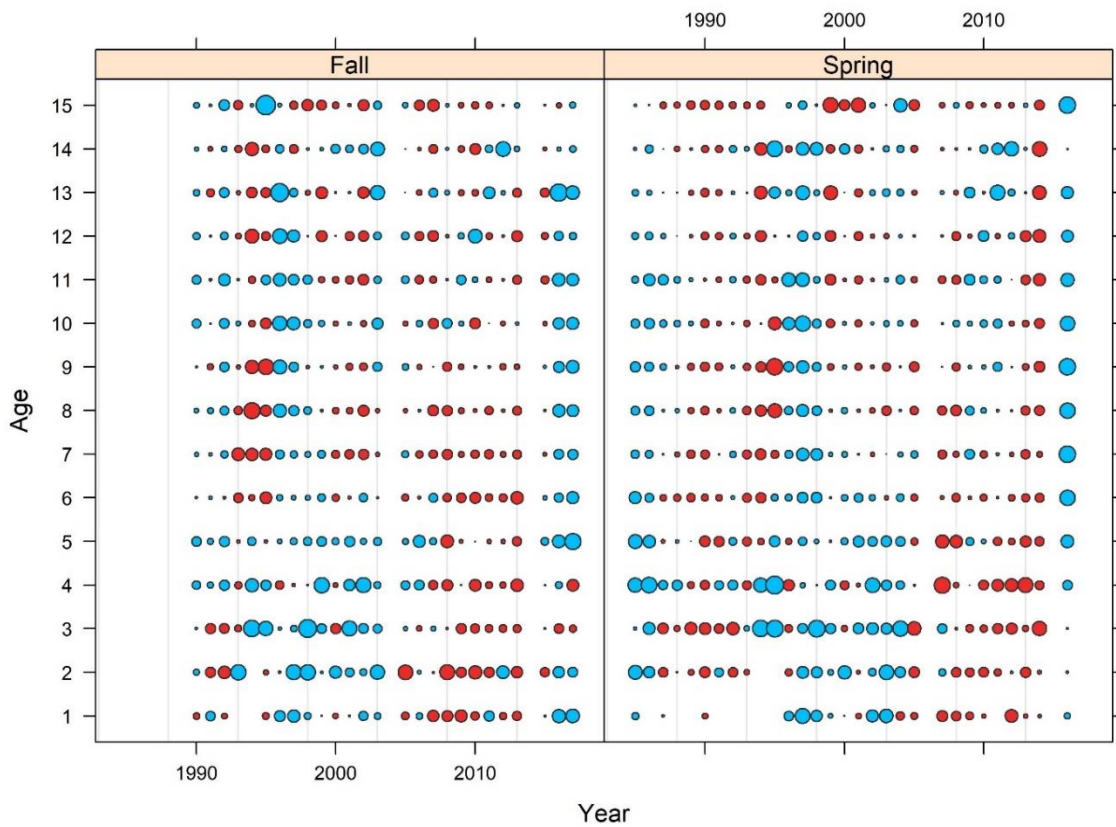


Figure D2.1. Standardized residual bubble plot for each survey across ages and years from AMPL1. Symbol sizes are scaled and values greater than average are shown as blue circles, average values are shown as small dots, and less than average values are shown as red circles.

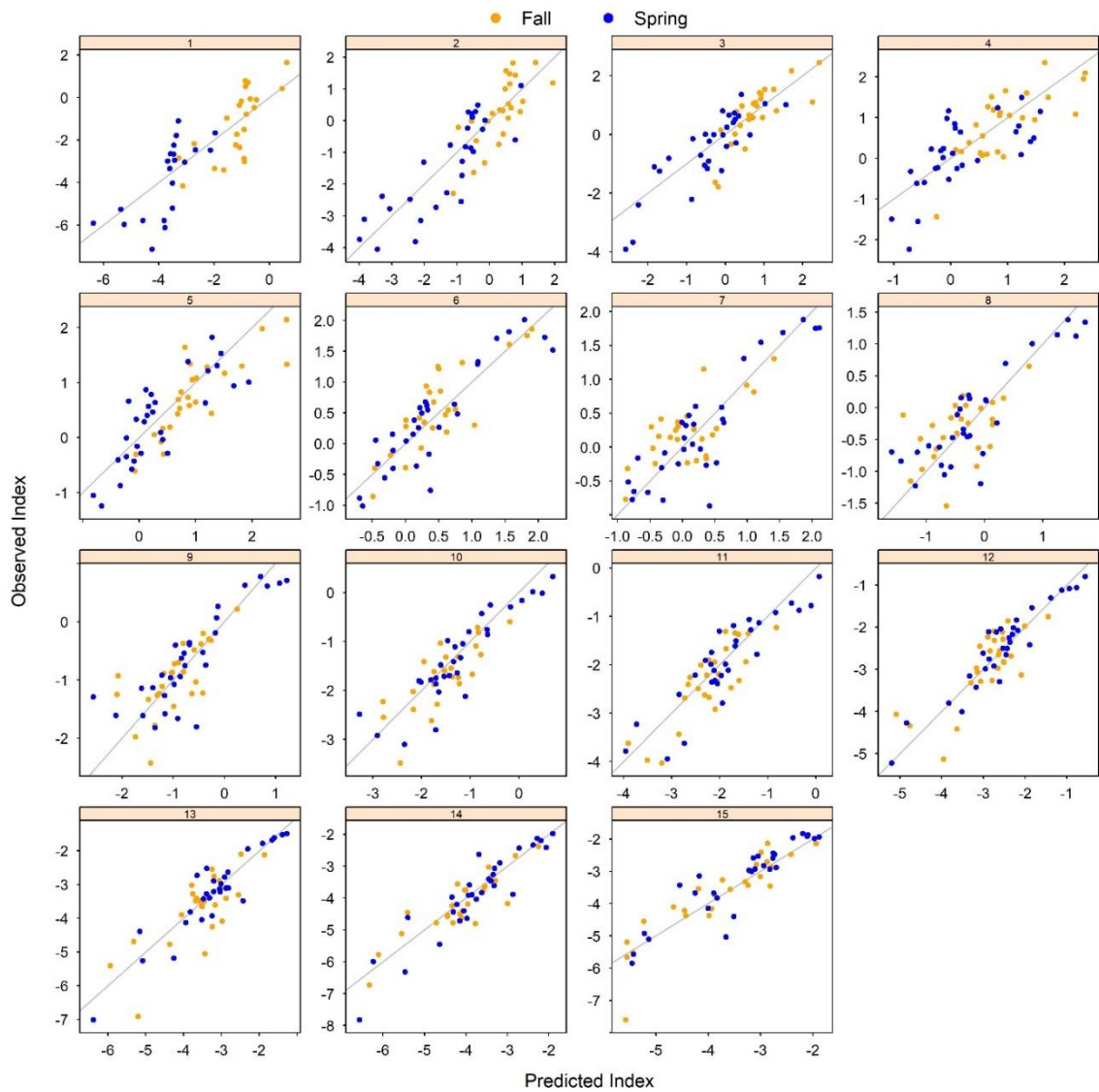


Figure D2.2. Observed vs. predicted survey index residuals at age for AMPL1. Blue dots represent spring while yellow dots represent fall.

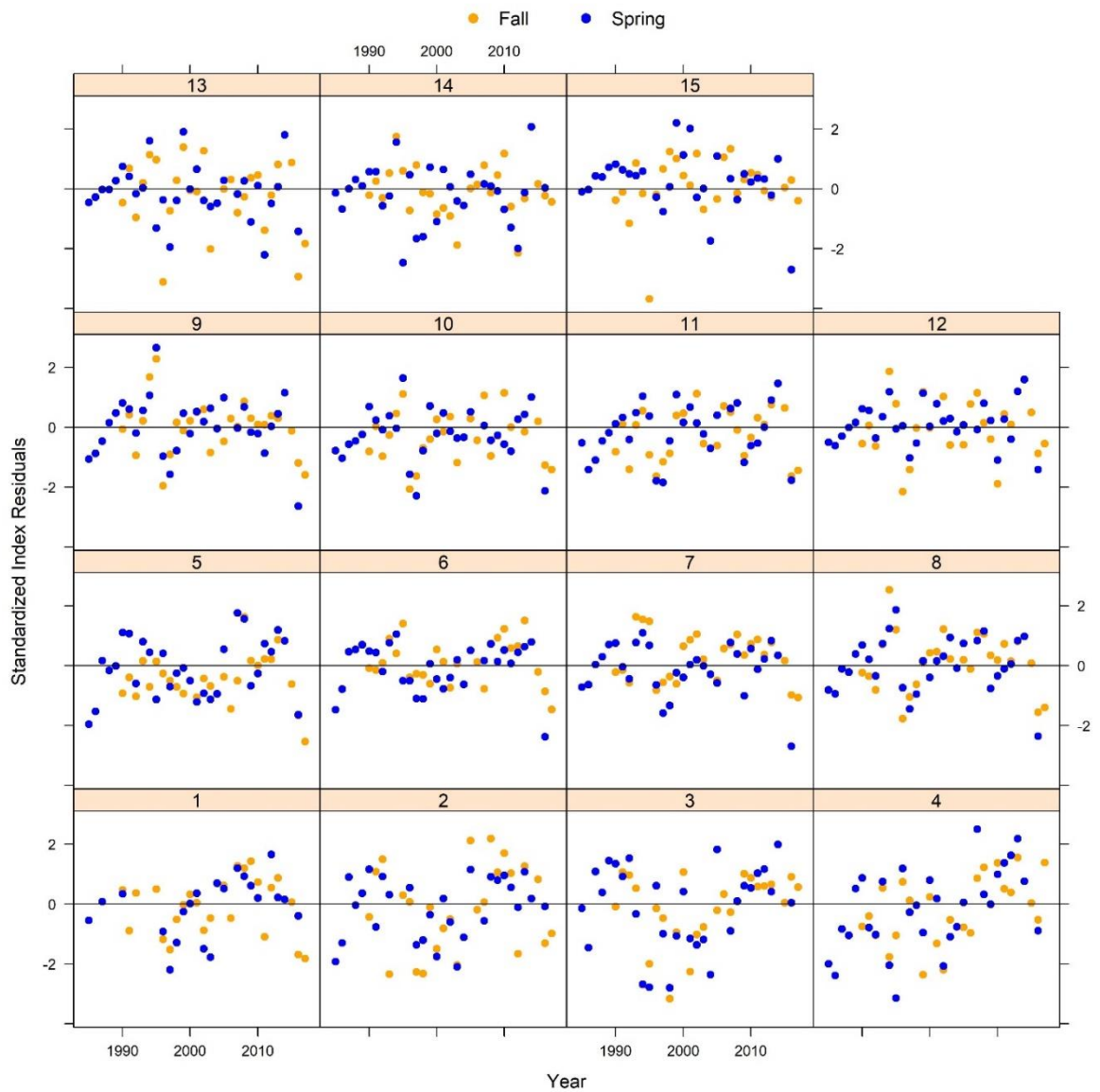


Figure D2.3. Standardized survey index residuals over time for AMPL1. Blue dots represent spring while yellow dots represent fall.

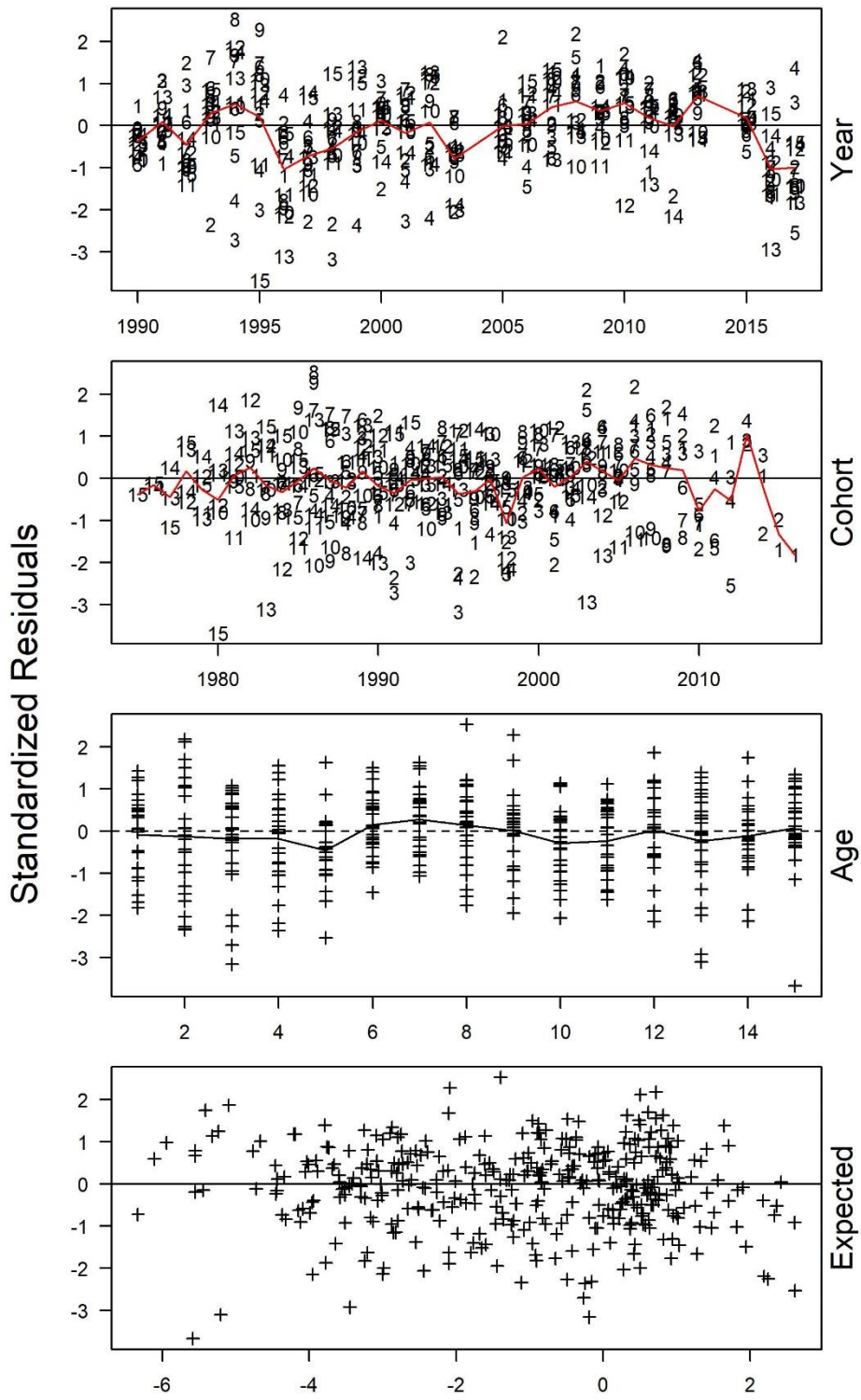


Figure D2.4. Standardized residual panel plot for the spring survey from model AMPL1. Numbers represent age, black lines indicate zero, and red lines indicate means.

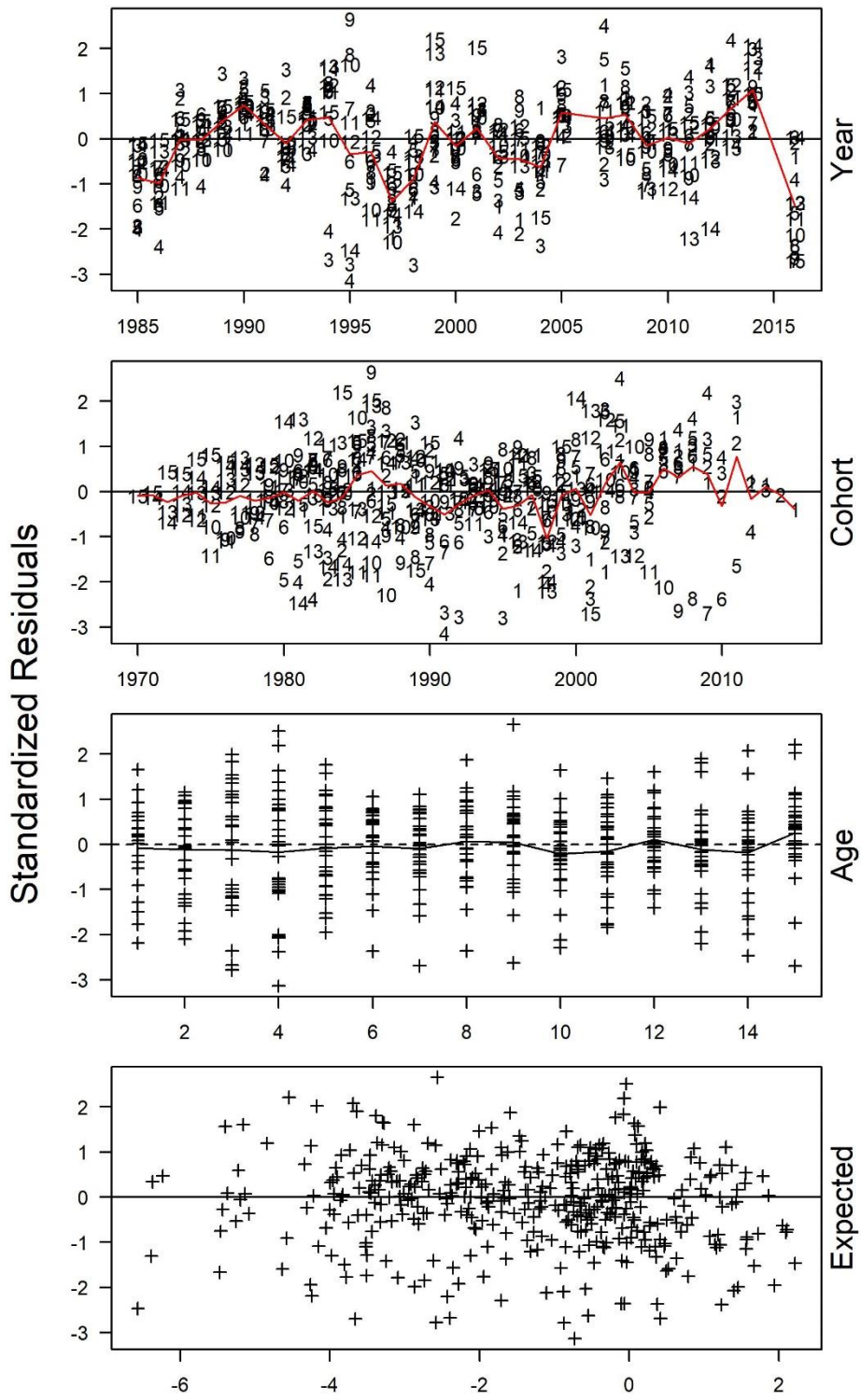


Figure D2.5. Standardized residual panel plot for the fall survey from model AMPL1. Numbers represent age, black lines indicate zero, and red lines indicate means.

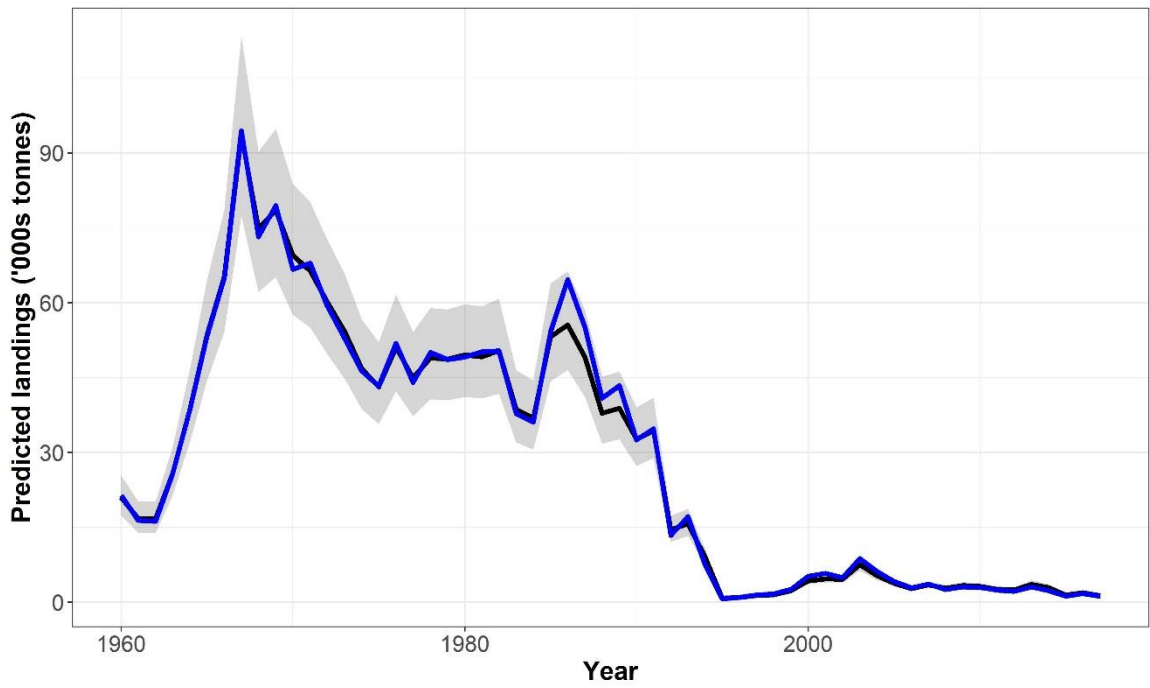


Figure D2.6. Landings estimates (black line) and 95% confidence interval (grey polygon) for AMPL1 compared to landings data.

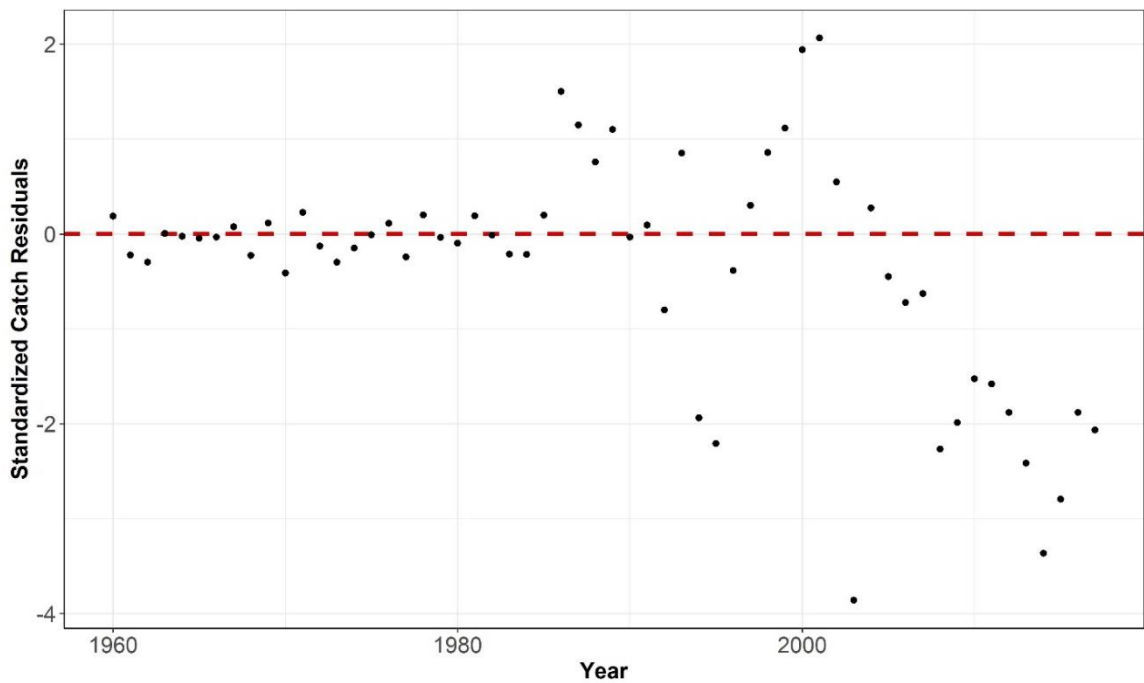


Figure D2.7. Landings residuals over time for AMPL1. Dashed red line indicates zero.

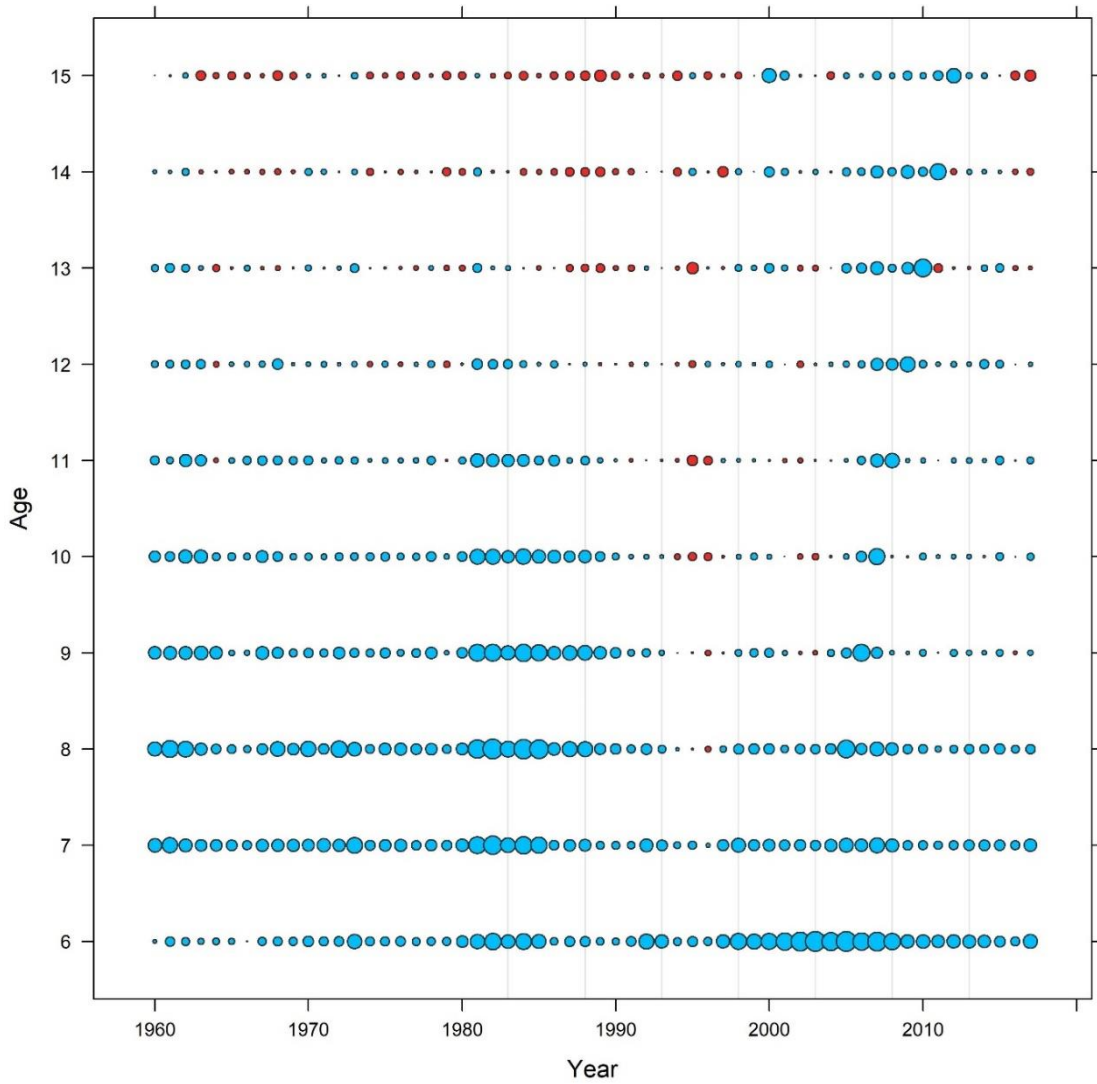


Figure D2.8. Standardized residual bubble plot for the catch proportion-at-age (continuation ratio logits [CRLs]) across ages and years from AMPL1. Symbol sizes are scaled and values greater than average are shown as blue circles, average values are shown as small dots, and less than average values are shown as red circles.

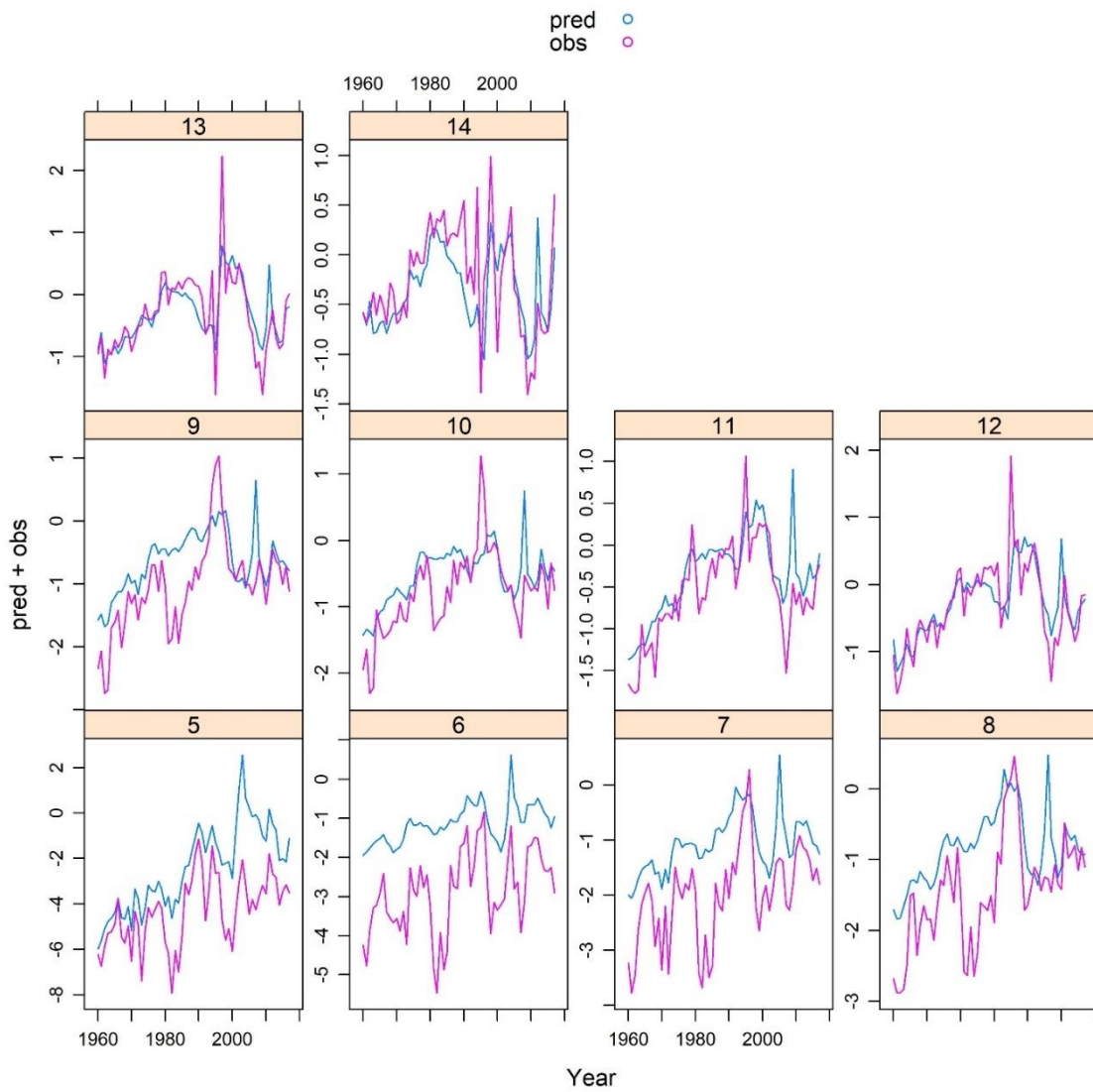


Figure D2.9. Time-series of predicted (blue lines) and observed (pink lines) CRLs by age for AMPL1.

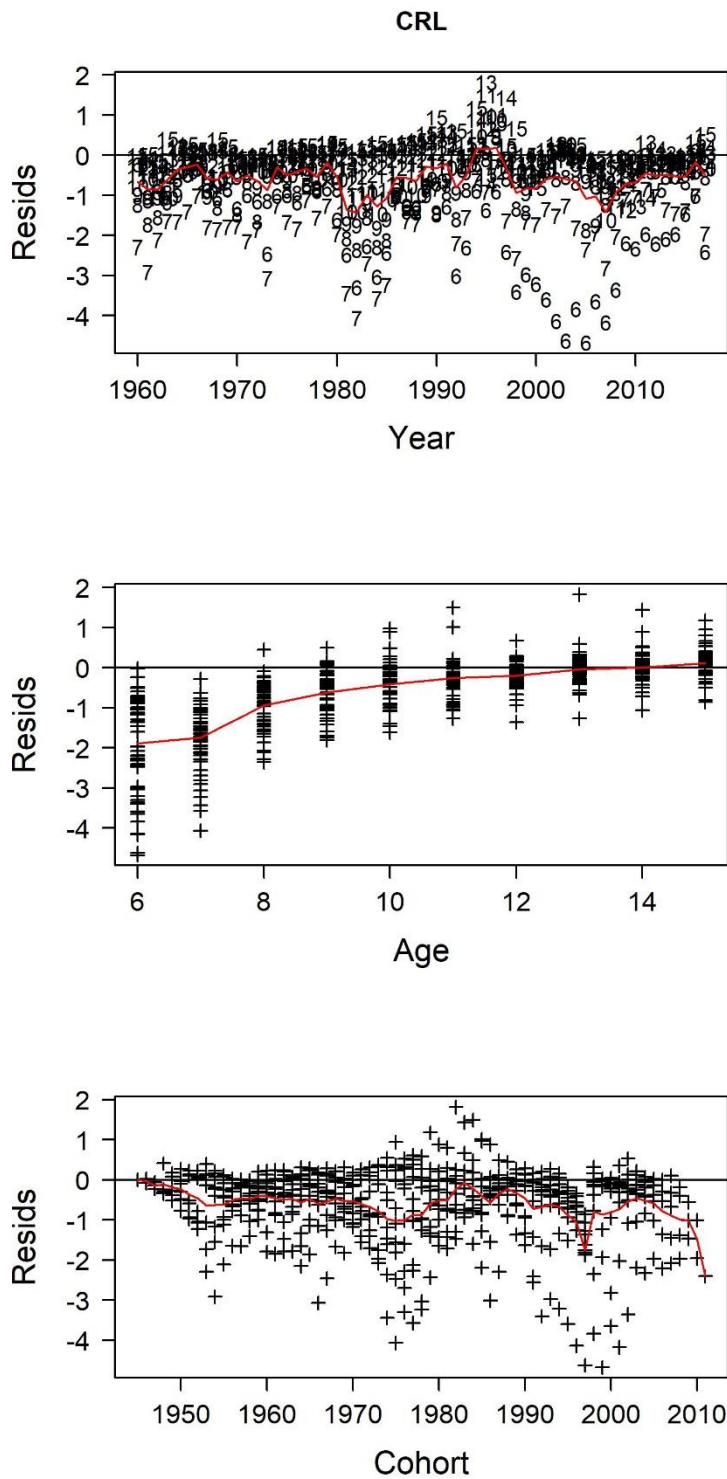


Figure D2.10. Standardized residual panel plot for CRLs from model AMPL1. Numbers represent age, black lines indicate zero, and red lines indicate means.

AMPL2 Model Residuals

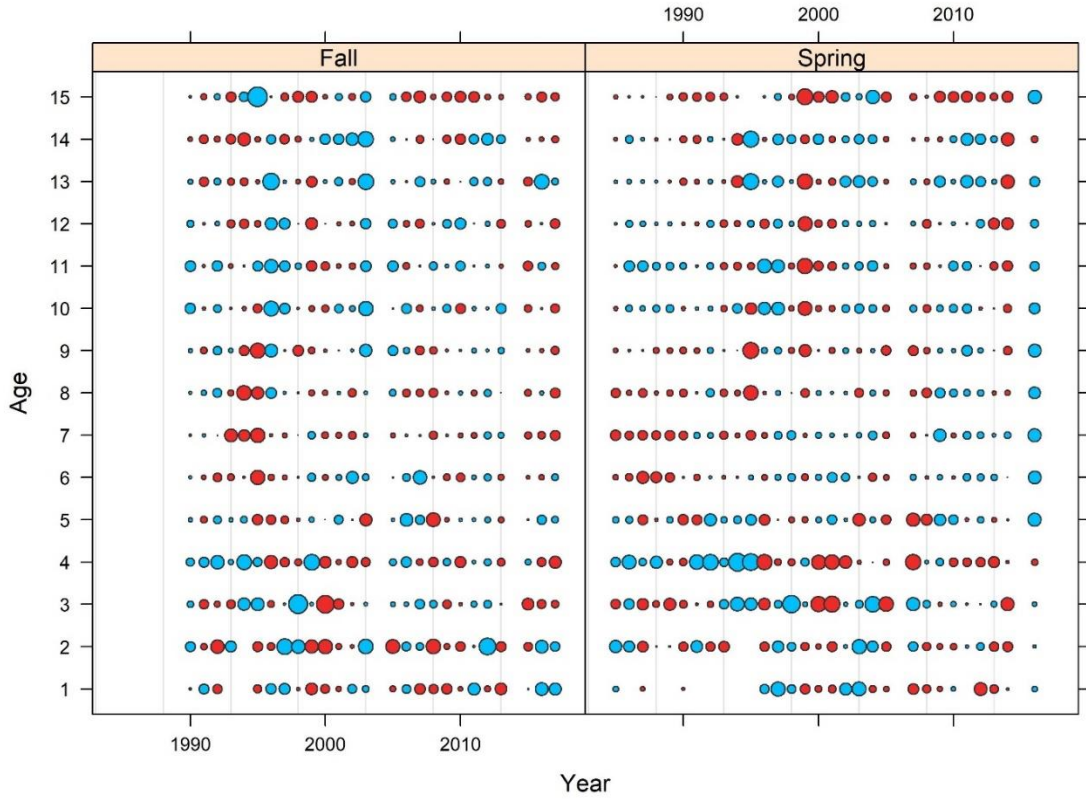


Figure D2.11. Standardized residual bubble plot for each survey across ages and years from AMPL2. Symbol sizes are scaled and values greater than average are shown as blue circles, average values are shown as small dots, and less than average values are shown as red circles.

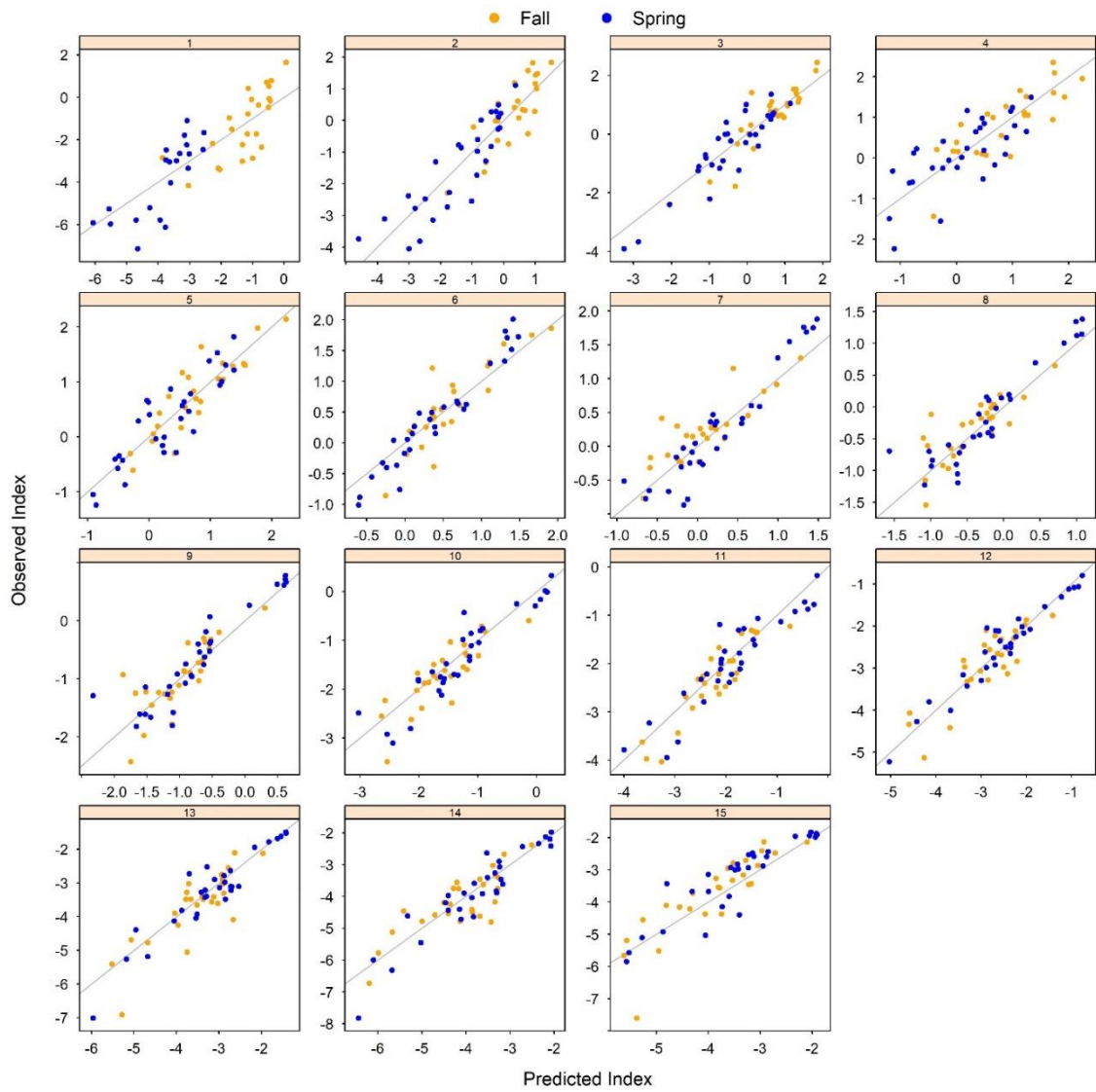


Figure D2.12. Observed vs. predicted survey index residuals at age for AMPL2. Blue dots represent spring while yellow dots represent fall.

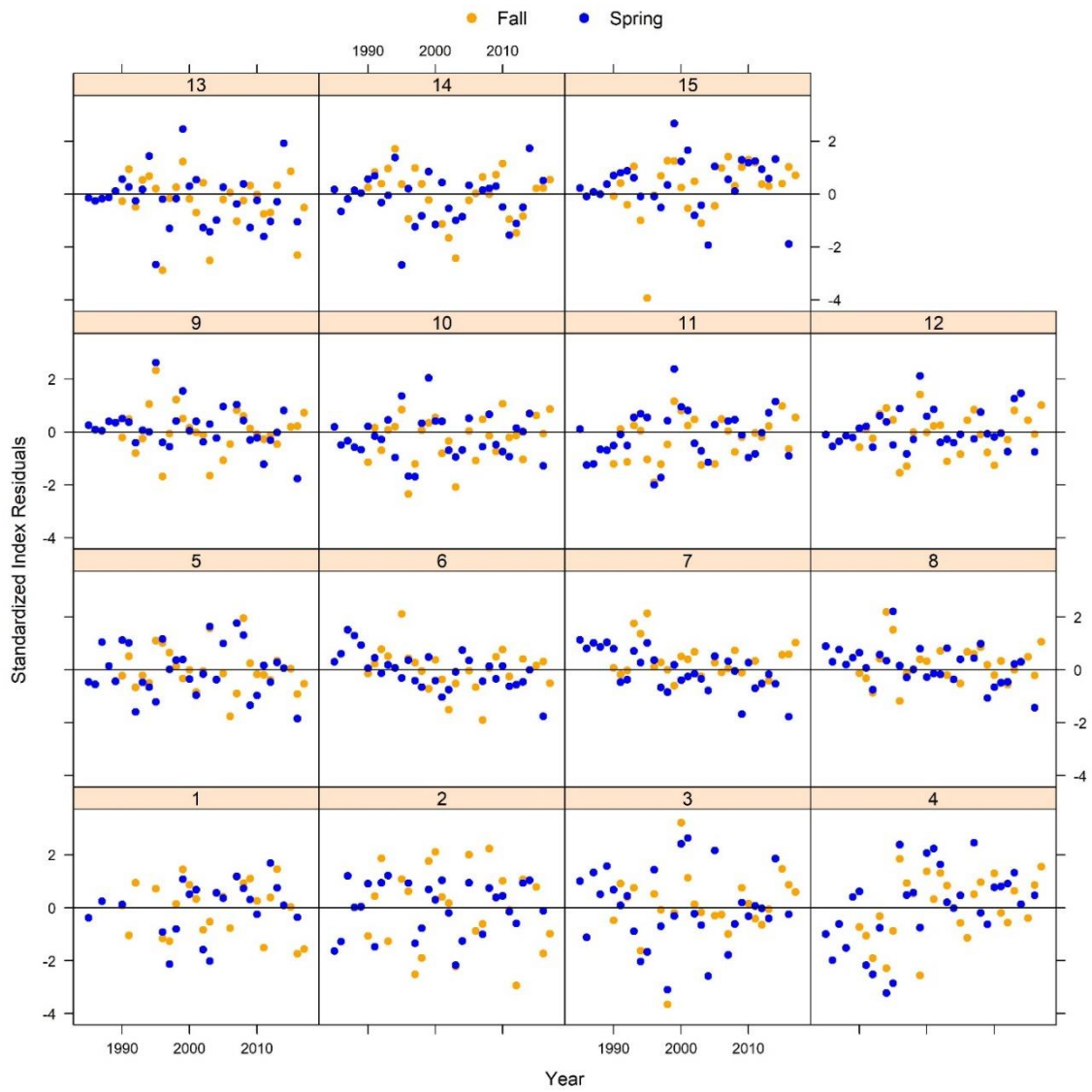


Figure D2.13. Standardized survey index residuals over time for AMPL2. Blue dots represent spring while yellow dots represent fall.

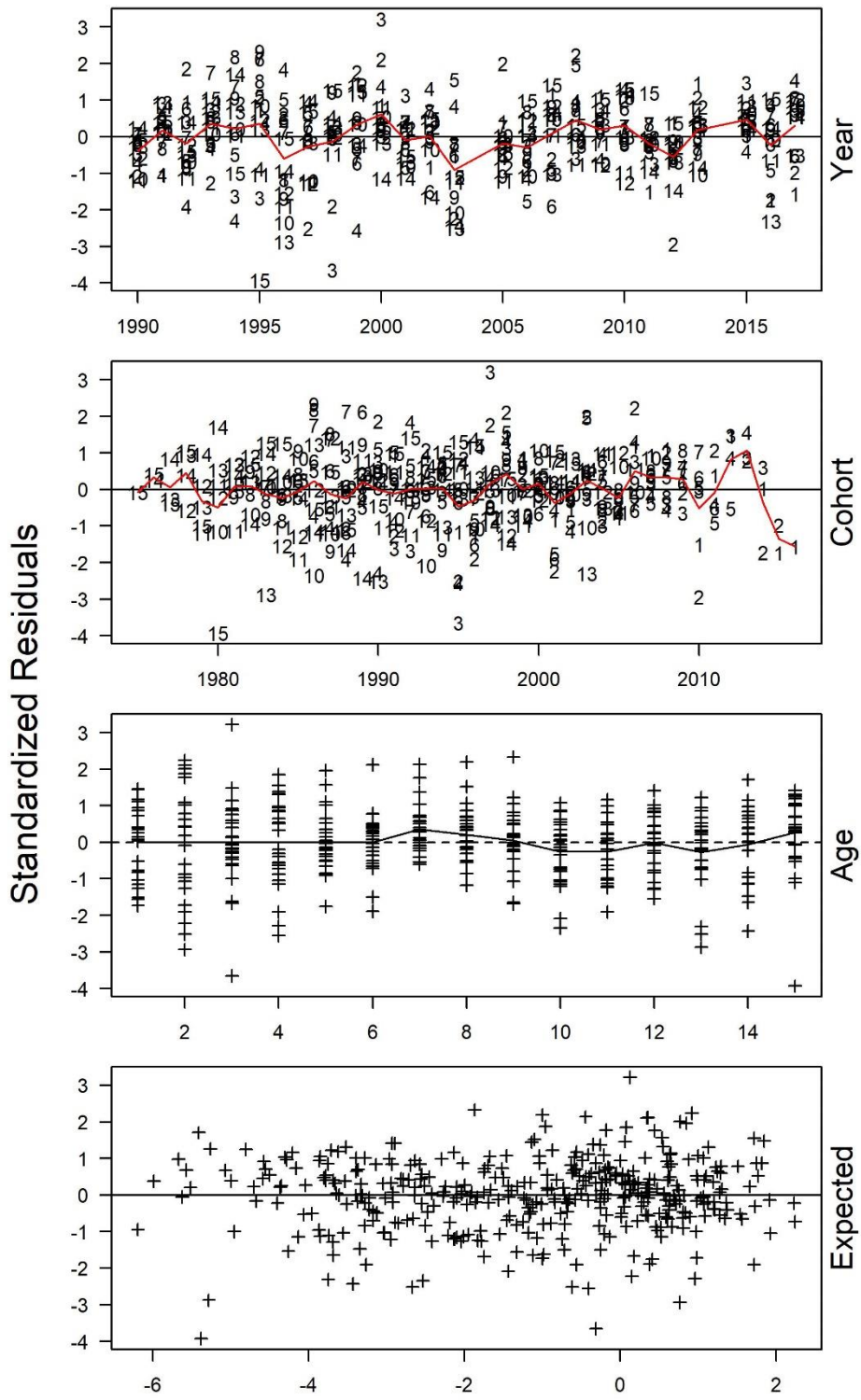


Figure D2.14. Standardized residual panel plot for the spring survey from model AMPL2. Numbers represent age, black lines indicate zero, and red lines indicate means.

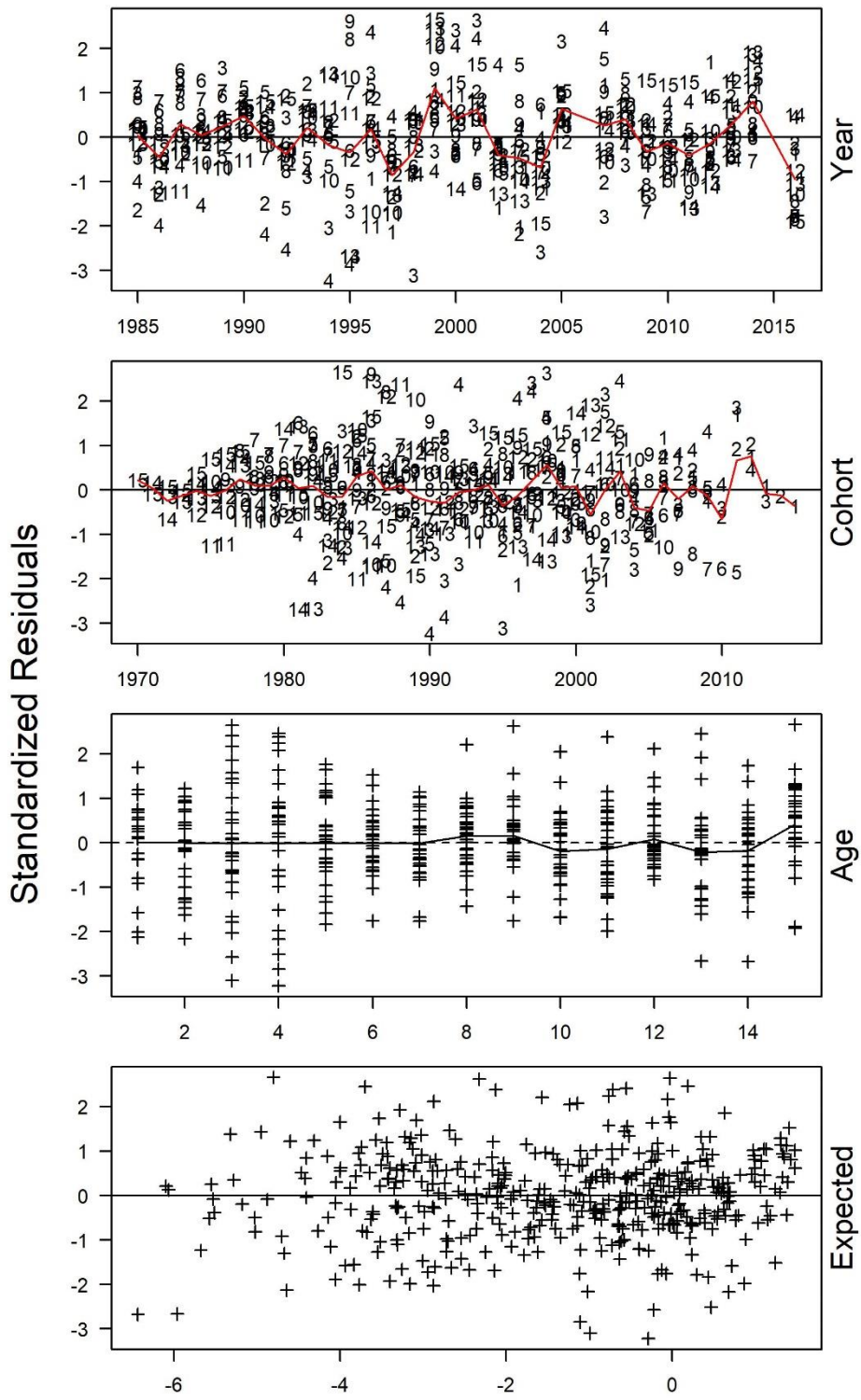


Figure D2.15. Standardized residual panel plot for the fall survey from model AMPL2. Numbers represent age, black lines indicate zero, and red lines indicate means.

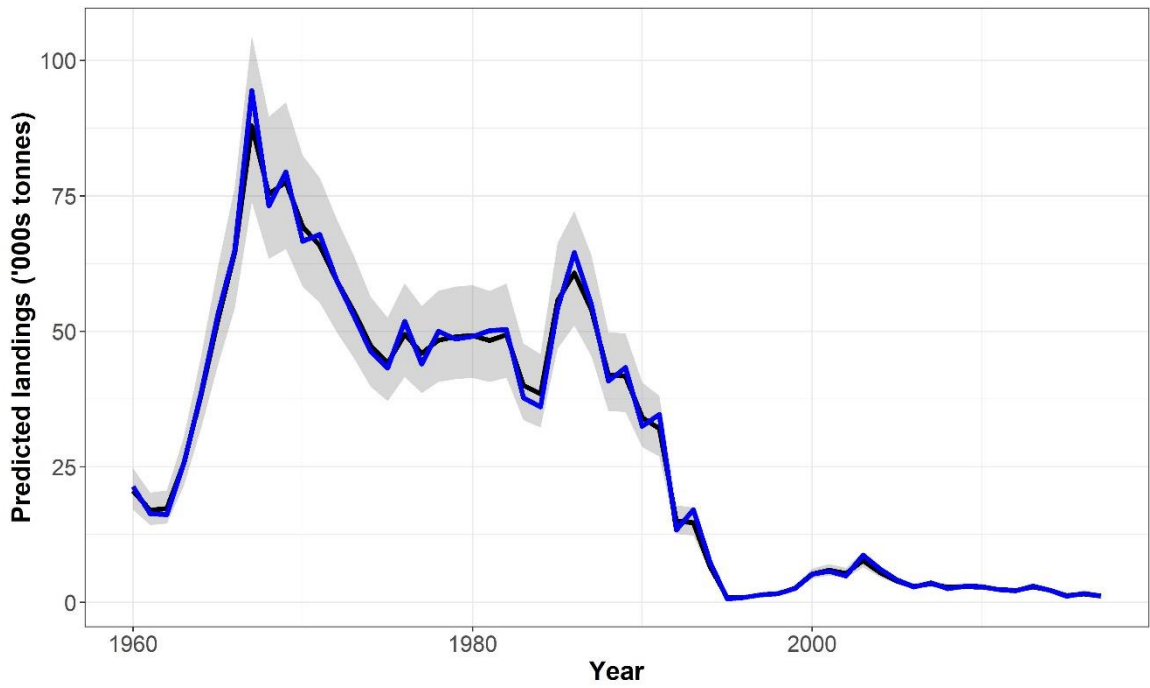


Figure D2.16. Landings estimates (black line) and 95% confidence interval (grey polygon) for AMPL2 compared to landings data.

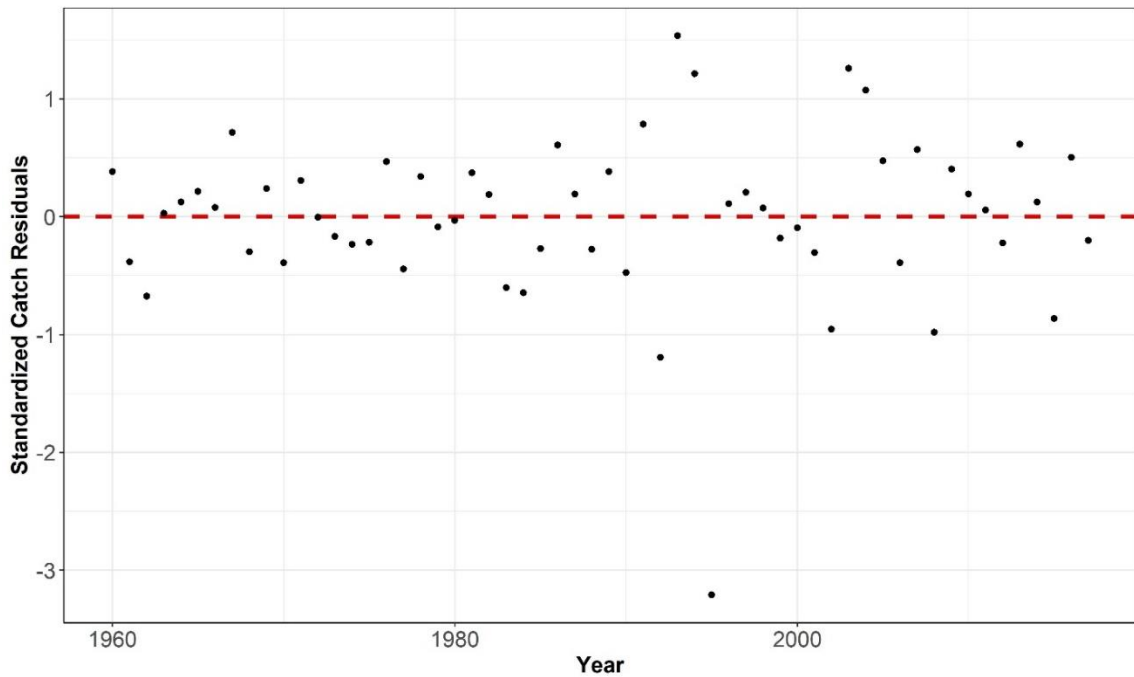


Figure D2.17. Landings residuals over time for AMPL2. Dashed red line indicates zero.

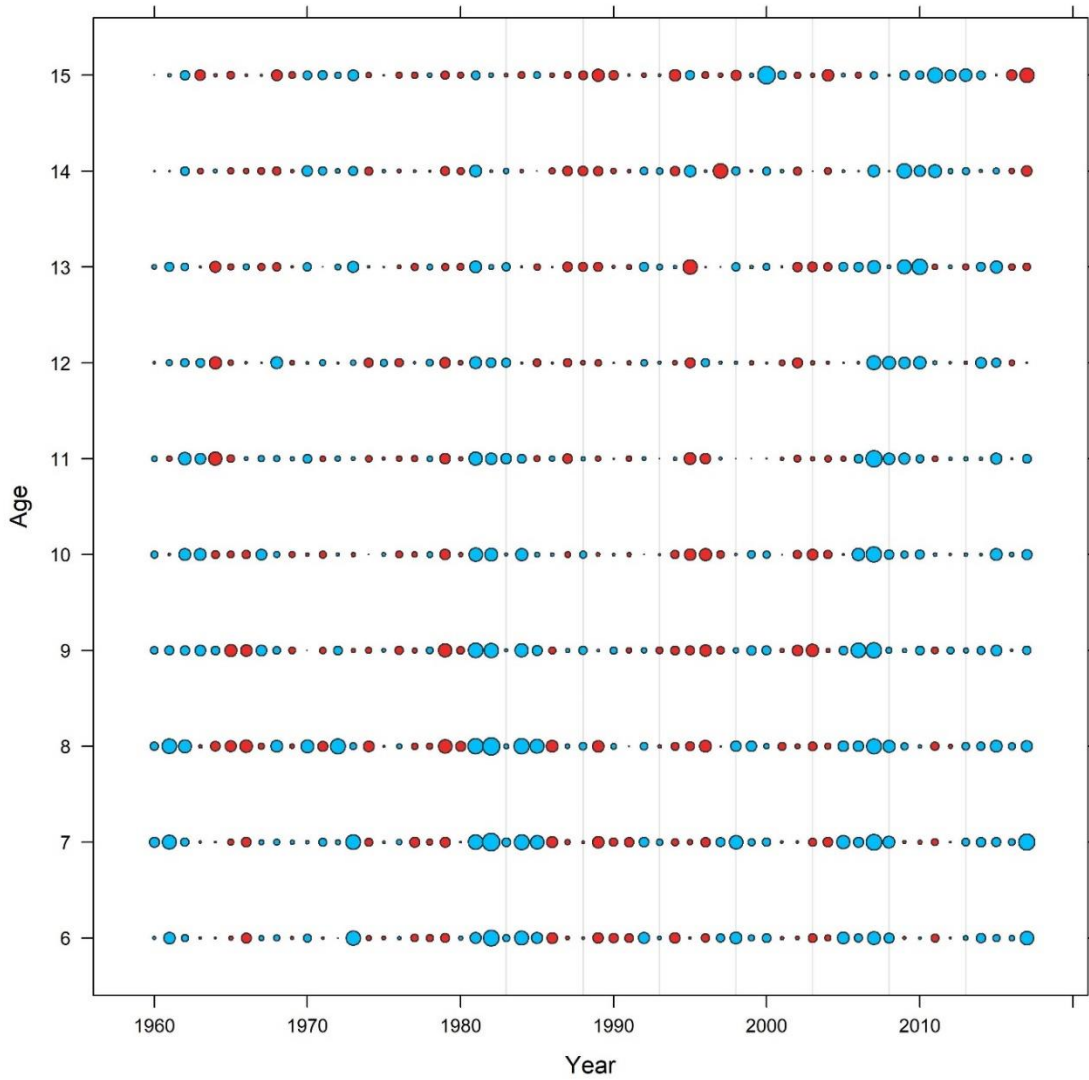


Figure D2.18. Standardized residual bubble plot for the CRLs across ages and years from AMPL2. Symbol sizes are scaled and values greater than average are shown as blue circles, average values are shown as small dots, and less than average values are shown as red circles.

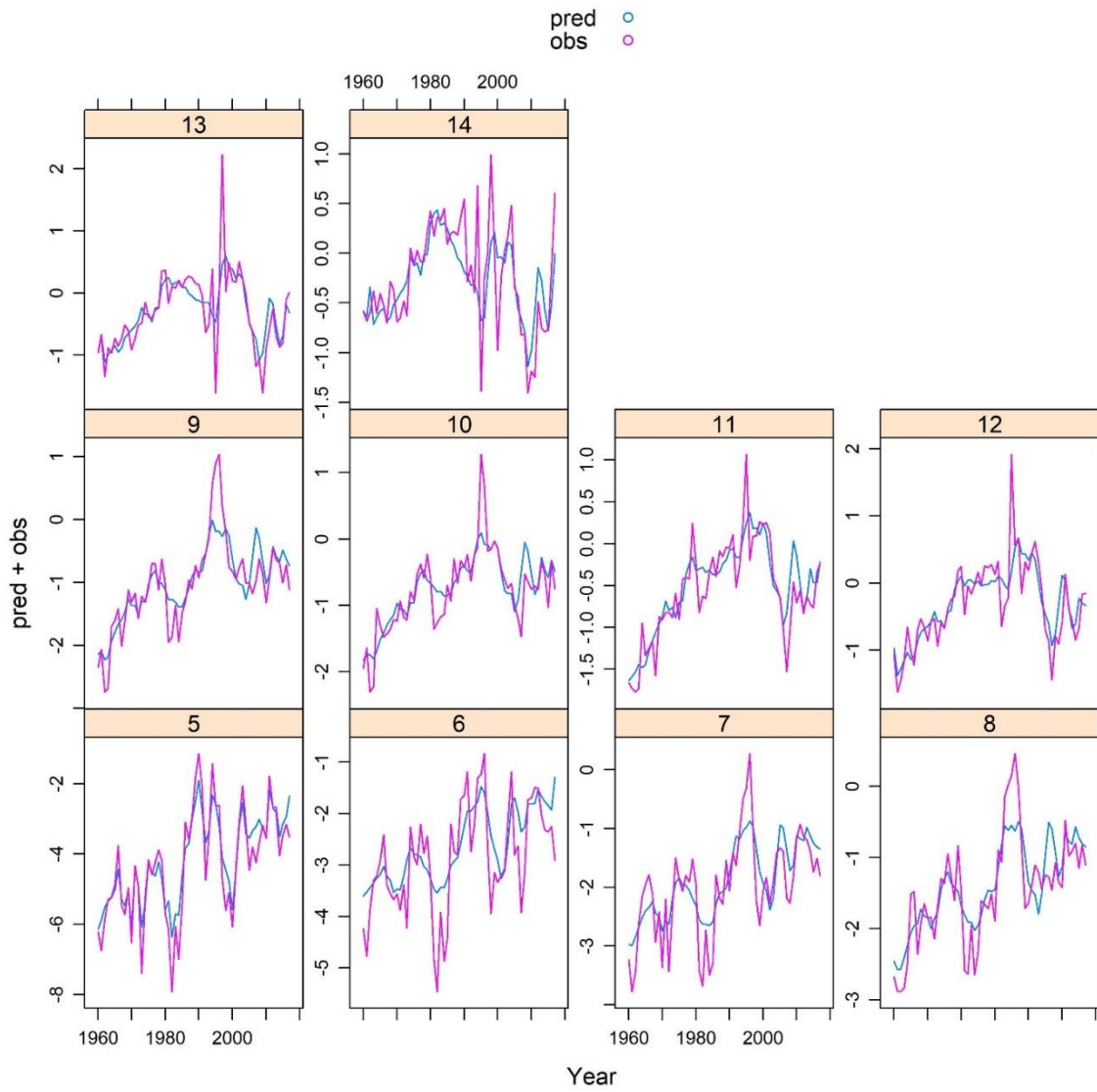


Figure D2.19. Time-series of predicted (blue lines) and observed (pink lines) CRLs by age for AMPL2.

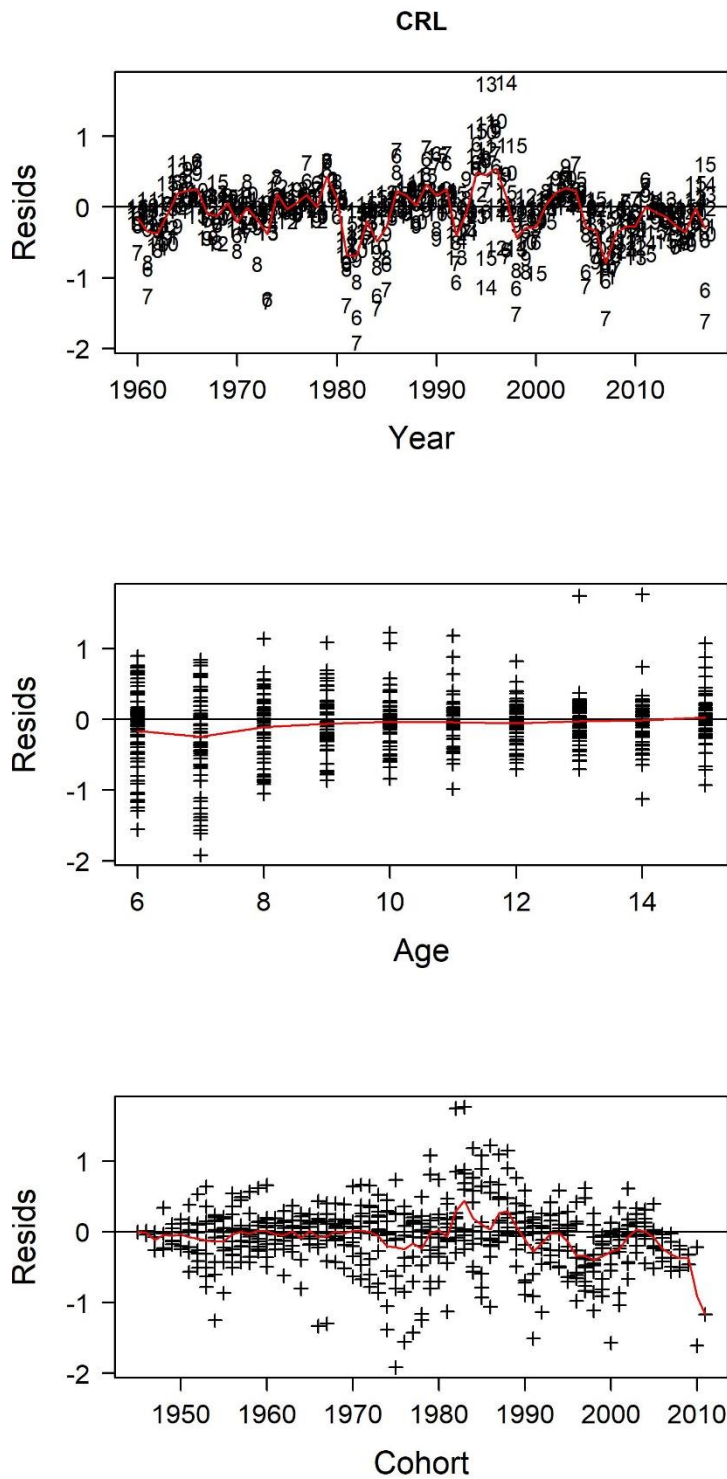


Figure D2.20. Standardized residual panel plot for CRLs from model AMPL2. Numbers represent age, black lines indicate zero, and red lines indicate means.

AMPLE6 Model Output

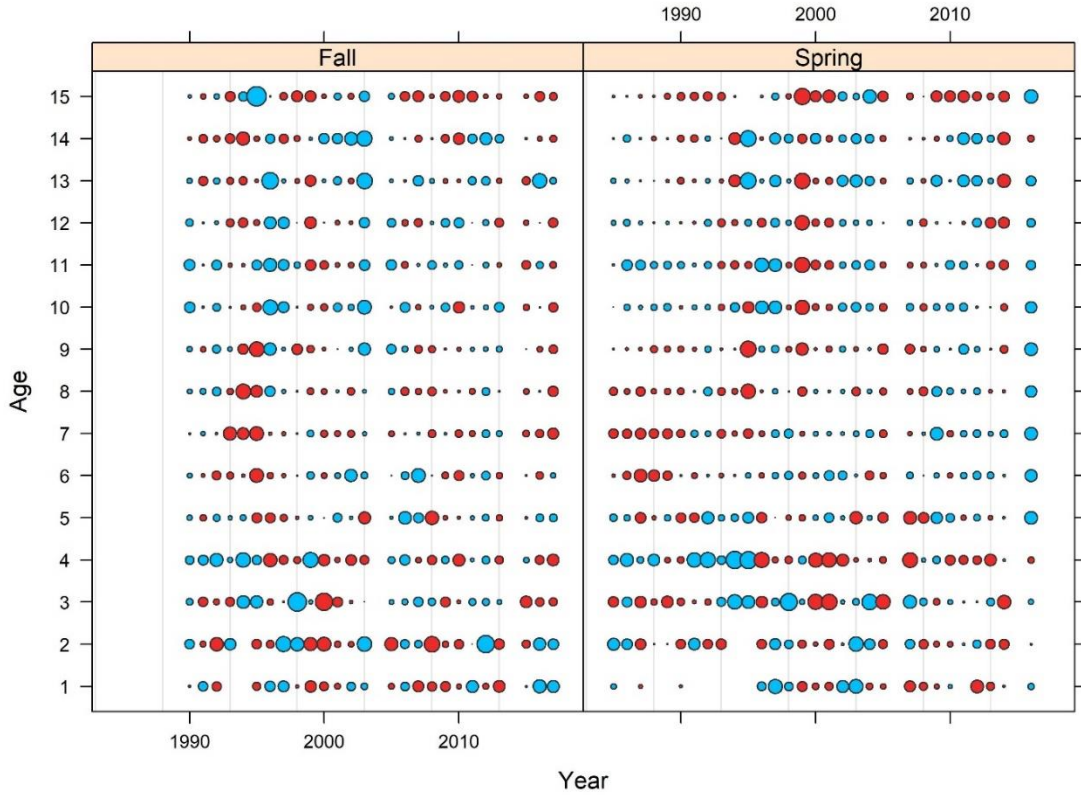


Figure D2.21. Standardized residual bubble plot for each survey across ages and years from AMPLE6. Symbol sizes are scaled and values greater than average are shown as blue circles, average values are shown as small dots, and less than average values are shown as red circles.

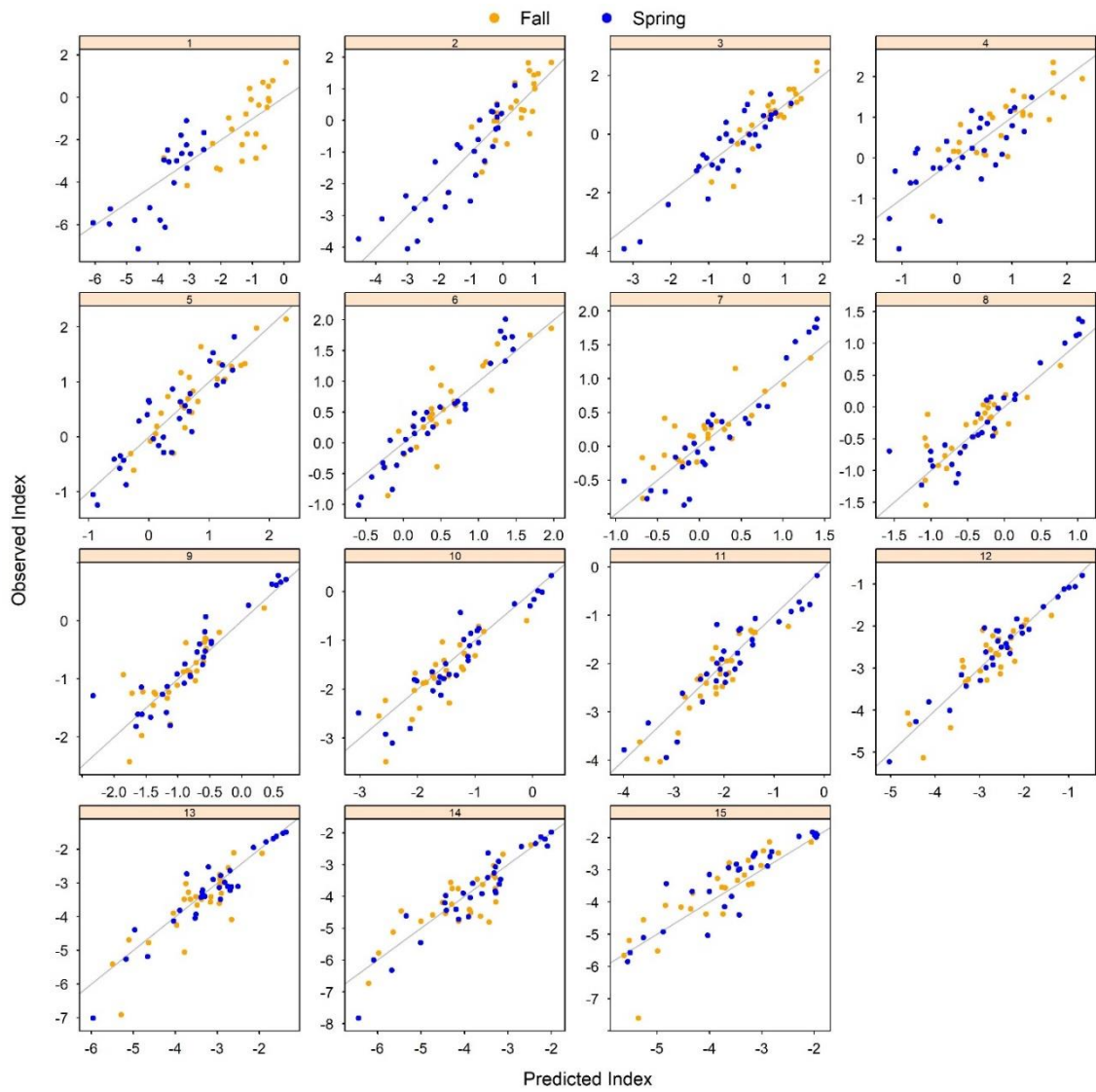


Figure D2.22. Observed vs. predicted survey index residuals at age for AMPLE6. Blue dots represent spring while yellow dots represent fall.

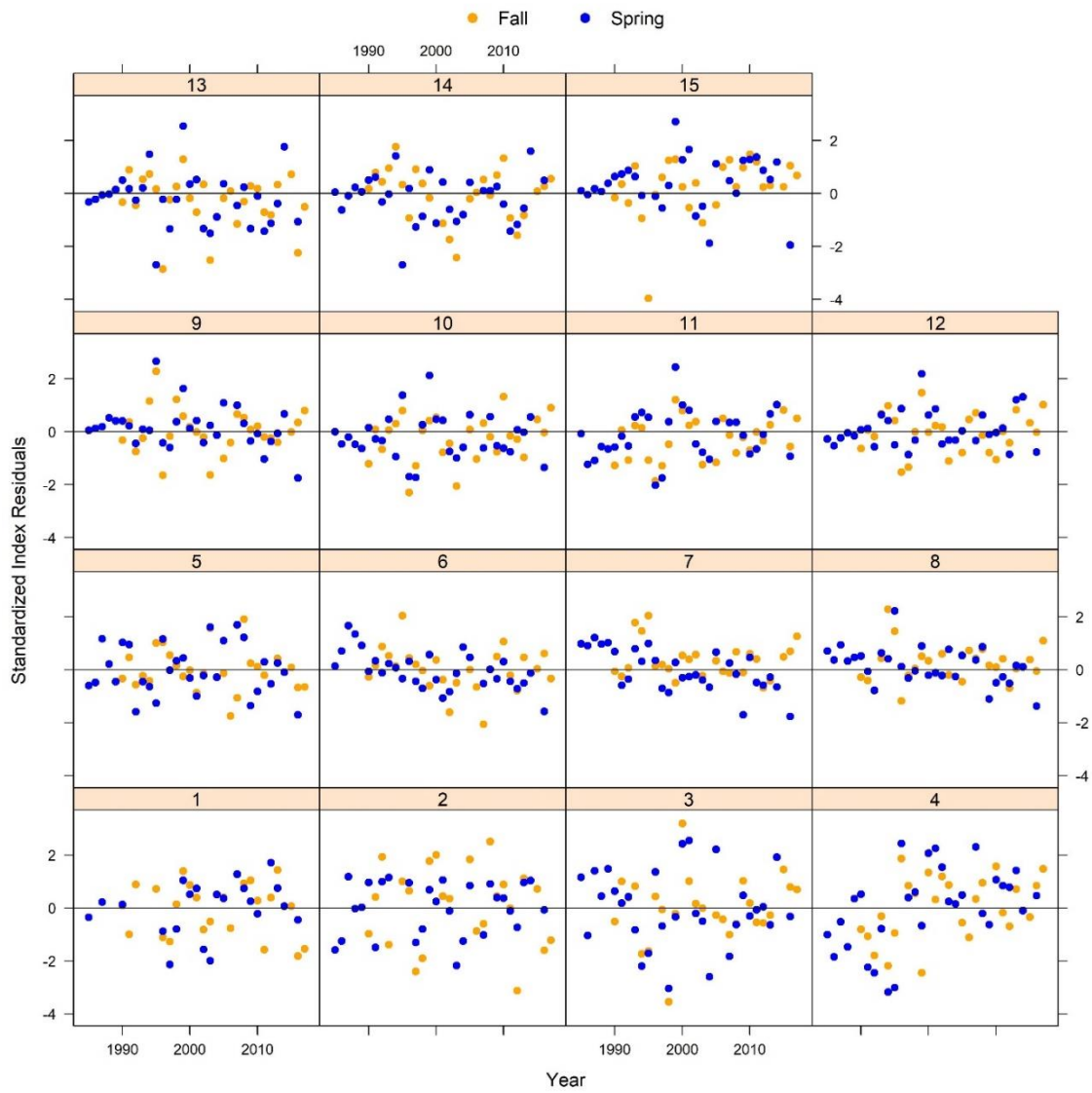


Figure D2.23. Standardized survey index residuals over time for AMPLE6. Blue dots represent spring while yellow dots represent fall.

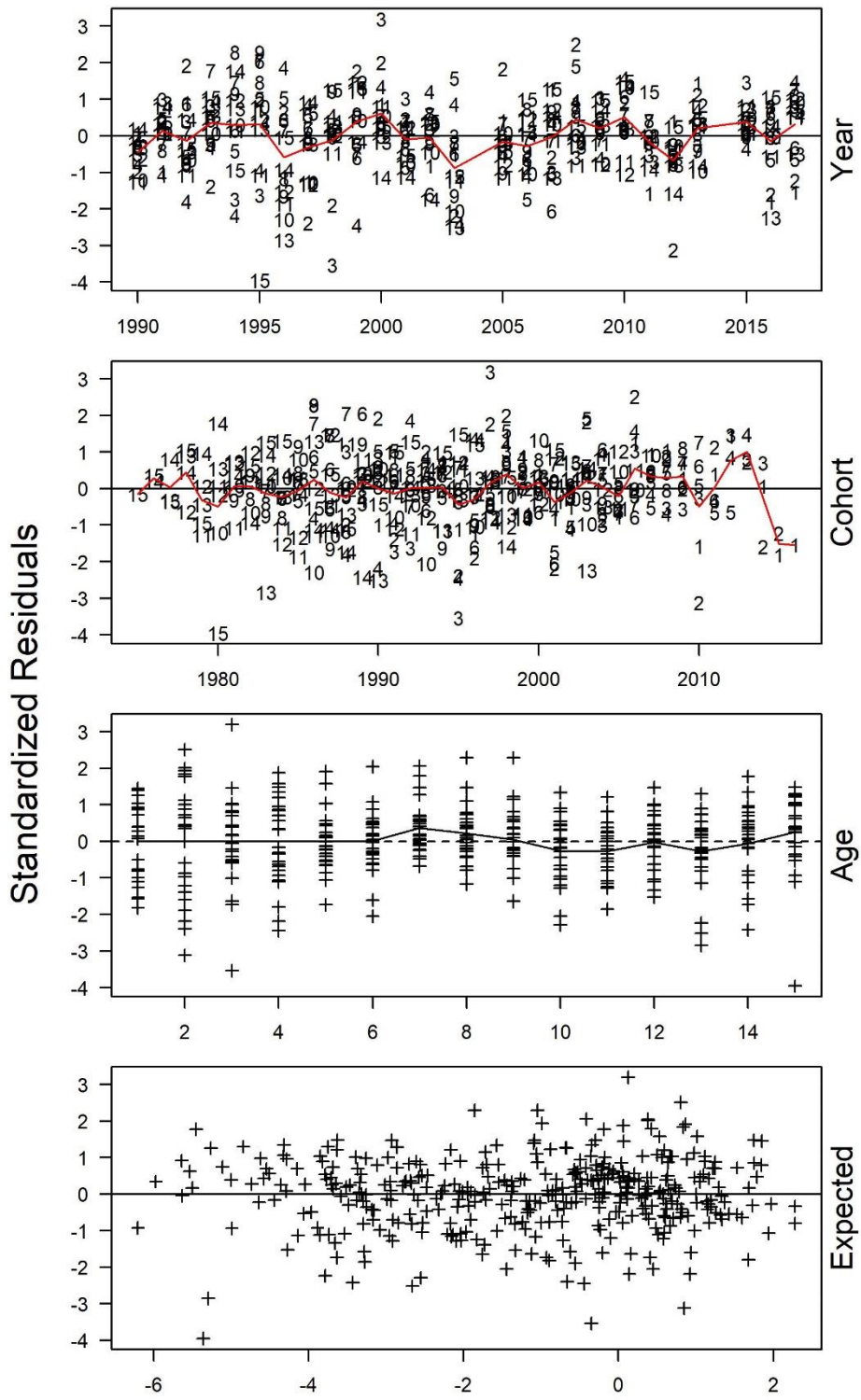


Figure D2.24. Standardized residual panel plot for the spring survey from model AMPLE6. Numbers represent age, black lines indicate zero, and red lines indicate means.

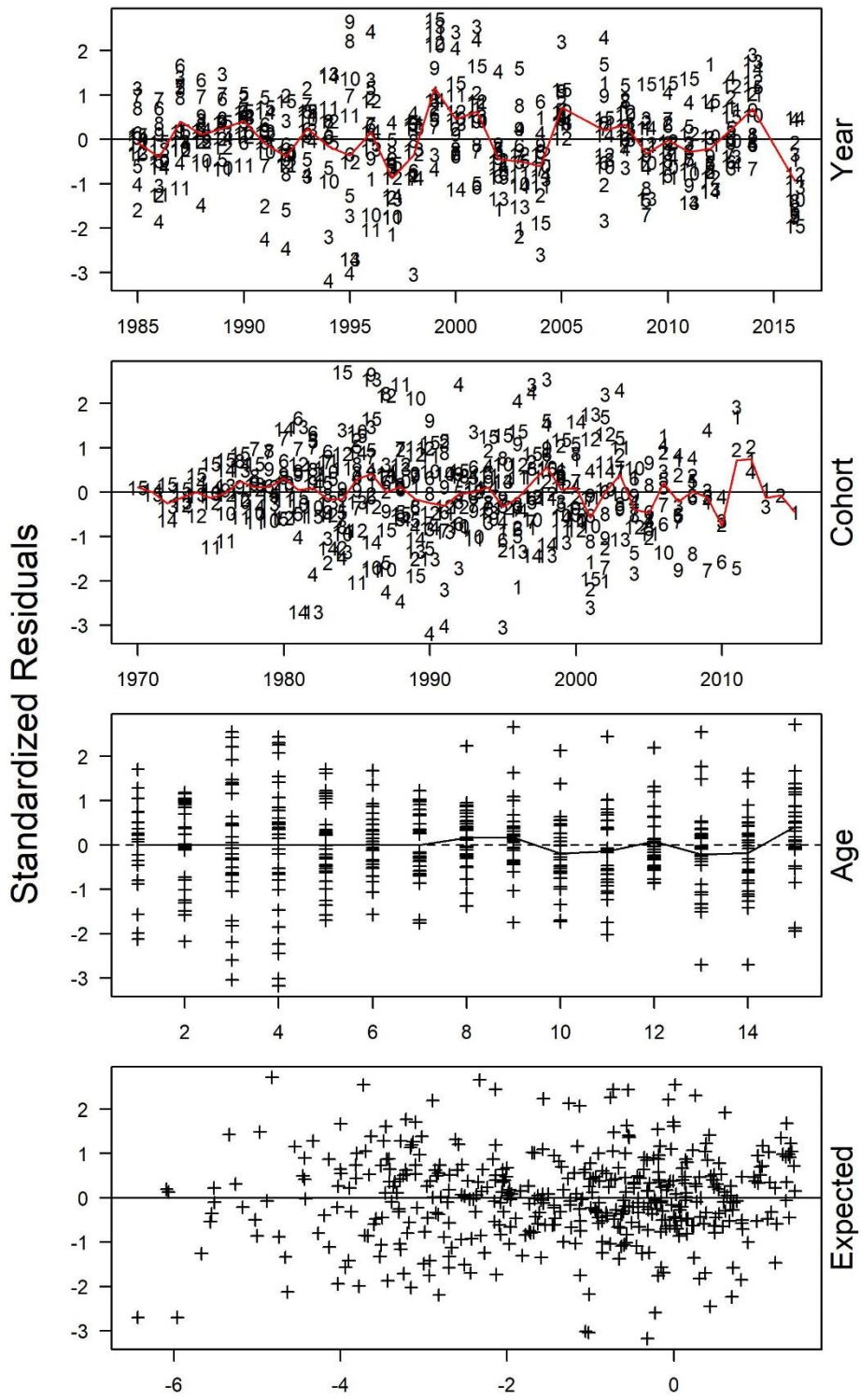


Figure D2.25. Standardized residual panel plot for the fall survey from model AMPLE6. Numbers represent age, black lines indicate zero, and red lines indicate means.

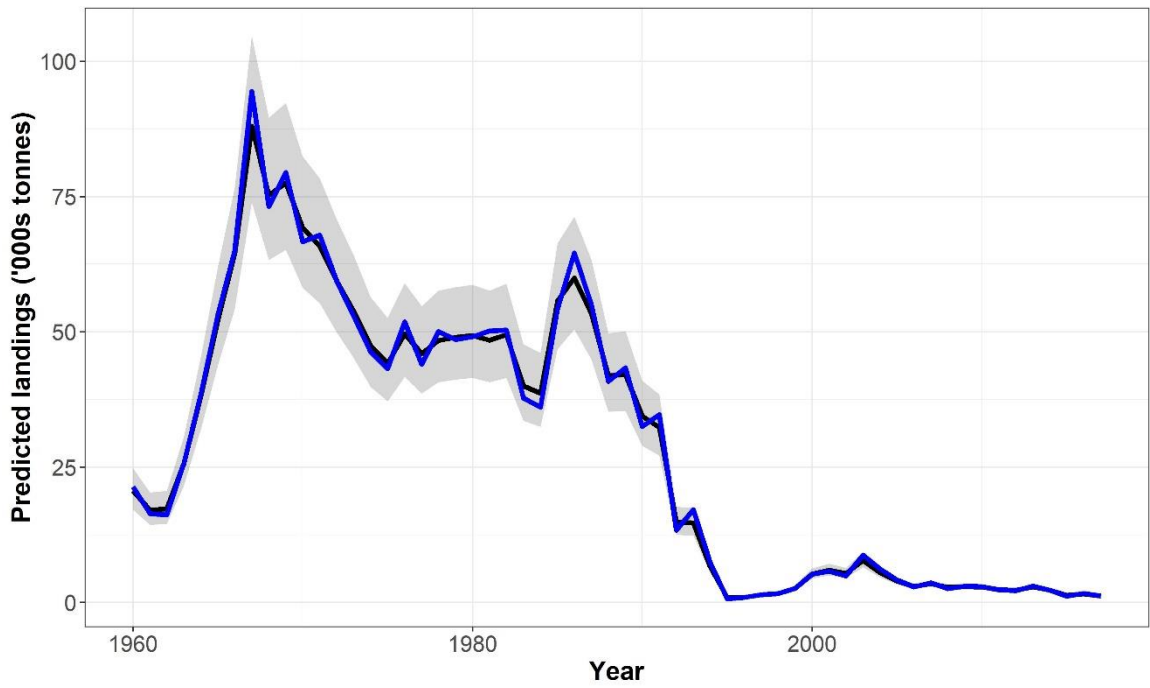


Figure D2.26. Landings estimates (black line) and 95% confidence interval (grey polygon) for AMPLE6 compared to landings data.

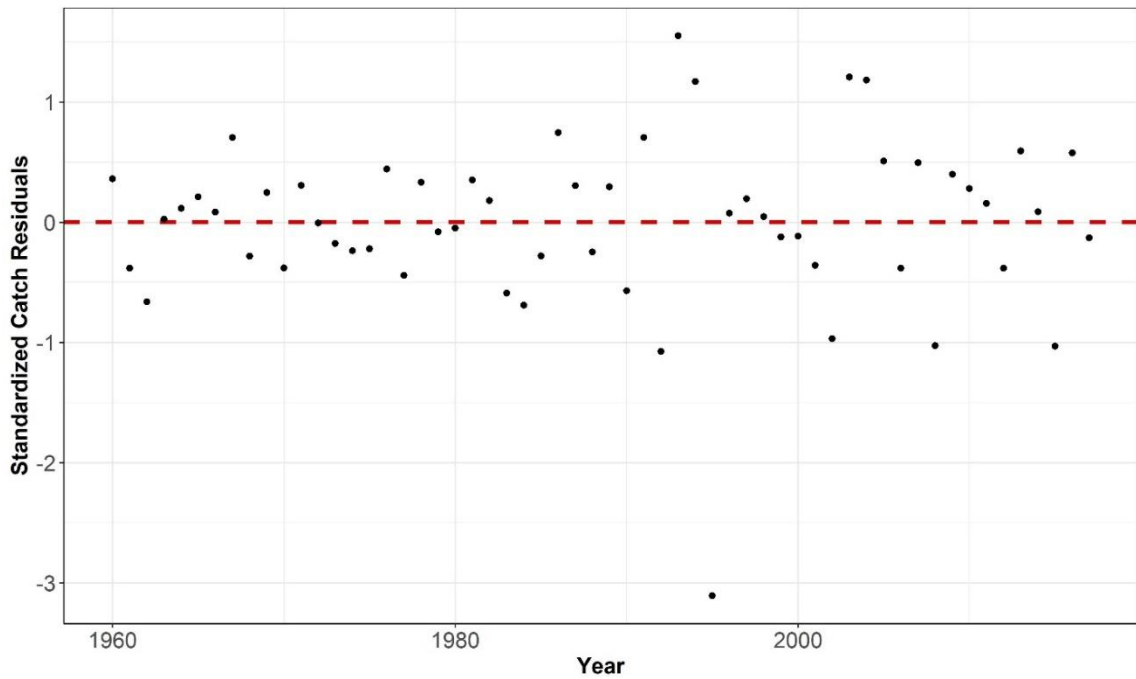


Figure D2.27. Landings residuals over time for AMPLE6. Dashed red line indicates zero.

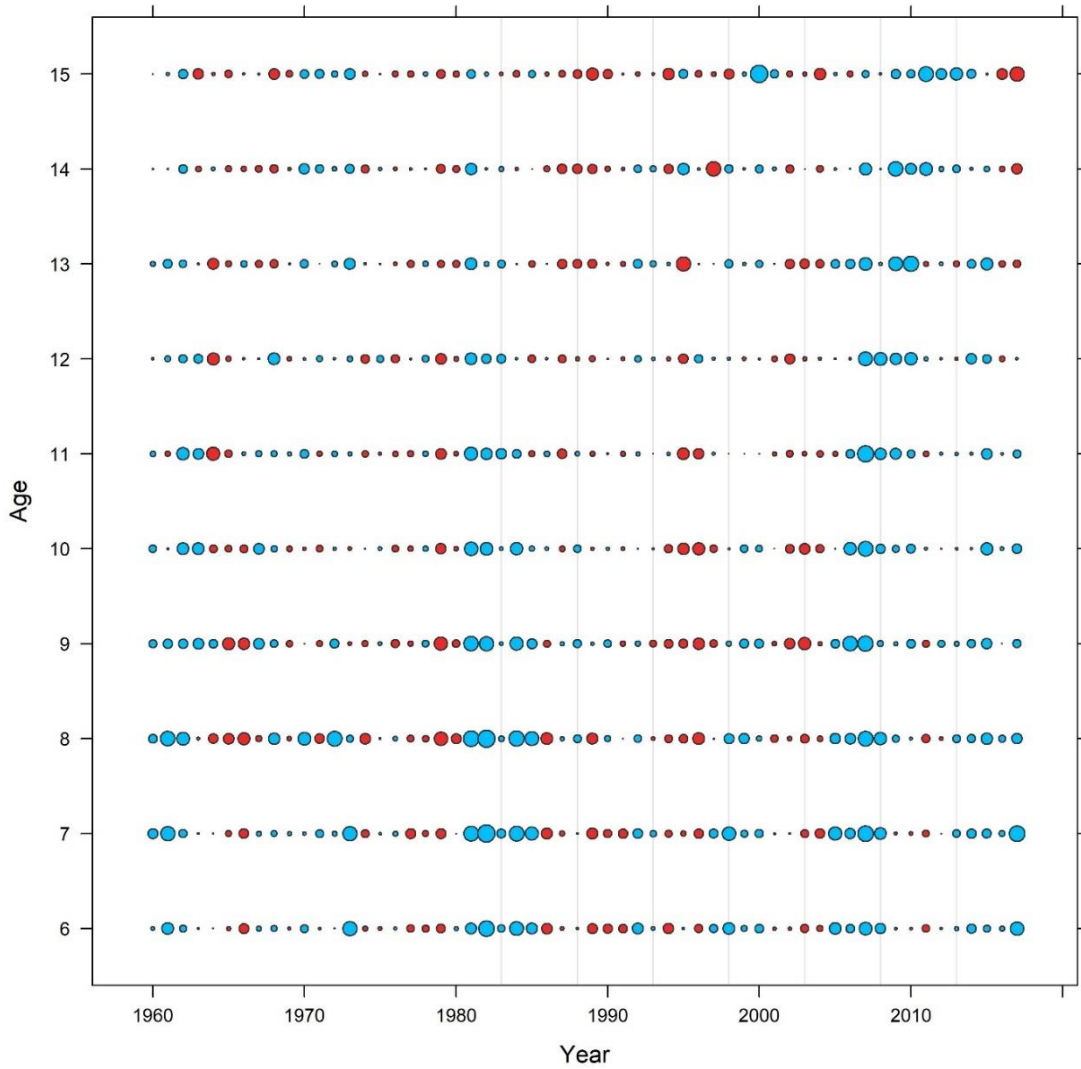


Figure D2.28. Standardized residual bubble plot for the CRLs across ages and years from AMPLE6. Symbol sizes are scaled and values greater than average are shown as blue circles, average values are shown as small dots, and less than average values are shown as red circles.

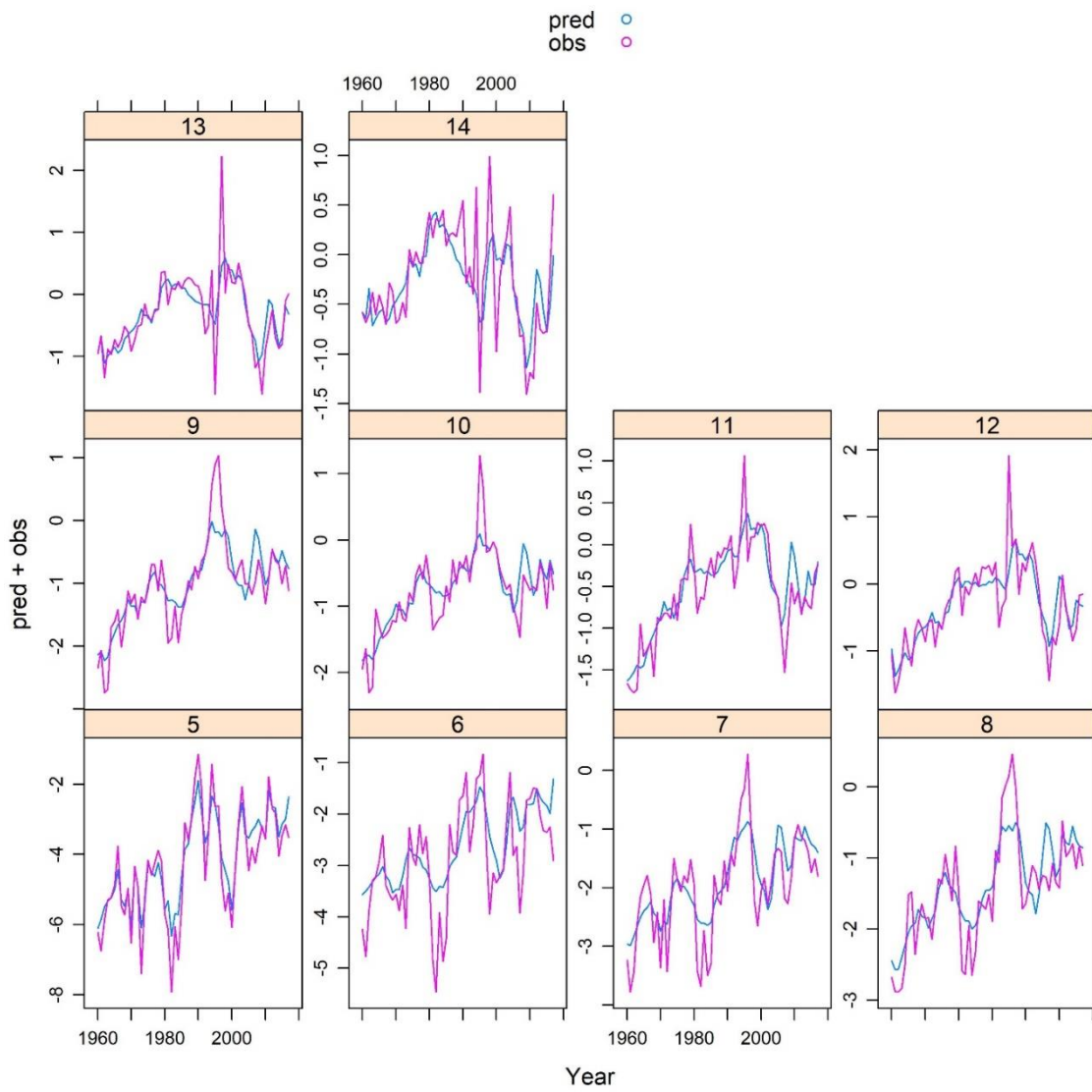


Figure D2.29. Time-series of predicted (blue lines) and observed (pink lines) CRLs by age for AMPLE6.

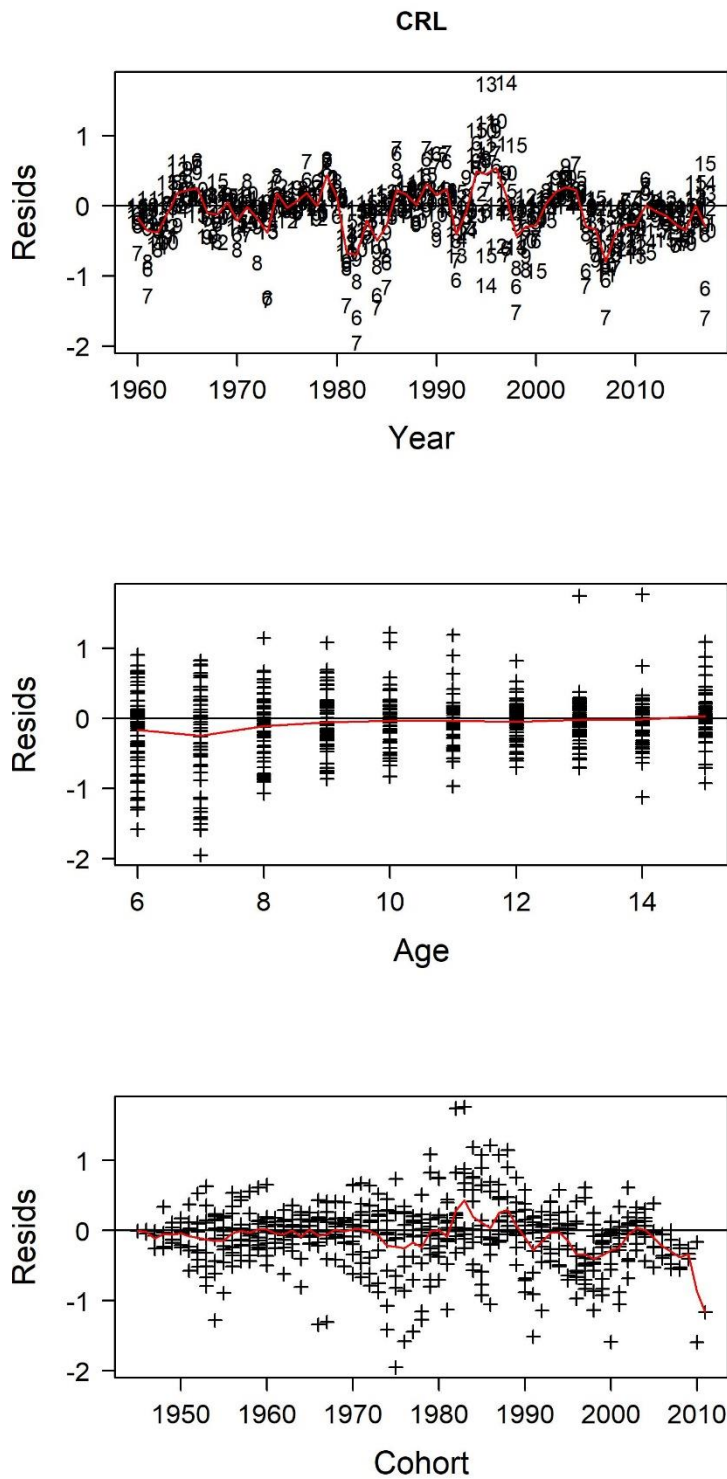


Figure D2.30. Standardized residual panel plot for CRLs from model AMPLE6. Numbers represent age, black lines indicate zero, and red lines indicate means.

Appendix D2 Bibliography

- Dwyer, K. S., Rideout, R., Ings, D., Power, D., Morgan, J., Brodie, B., & Healey, B. P. (2016). Assessment of American plaice in Div.3LNO. NAFO SCR, **N6573**, 1–19.
- Perreault, A. M. J., Wheeland, L. J., & Morgan, M. J. (2020). A state-space stock assessment model for American plaice on the Grand Bank of Newfoundland. *Journal of Northwest Atlantic Fishery Science*, **51**, 45–104.
- Pitt, T. K. (1972). Nominal catches of American plaice in Divisions 3L and 3N for the years 1960-1970. *ICNAF Research Bulletin*, **2813**(72/90).
- Wheeland, L., Dwyer, K., Kumar, R., Rideout, R., Perreault, A., & Rogers, B. (2021). Assessment of American plaice in Div. 3LNO. NAFO SCR, **21**(035).

D3. Ecosystem data

I initially considered including chlorophyll a and zooplankton biomass anomalies on the Grand Banks as a driver based on bottom-up food availability. However, these time-series only began in 1999 and as a result could not be included in a similar model comparison as the other covariates, nor would their signals provide an indication of their roles in the collapse of either flatfish species or the recovery of yellowtail flounder. As a result, I did not include these covariates in the main text but have included them in supplemental figures for context.

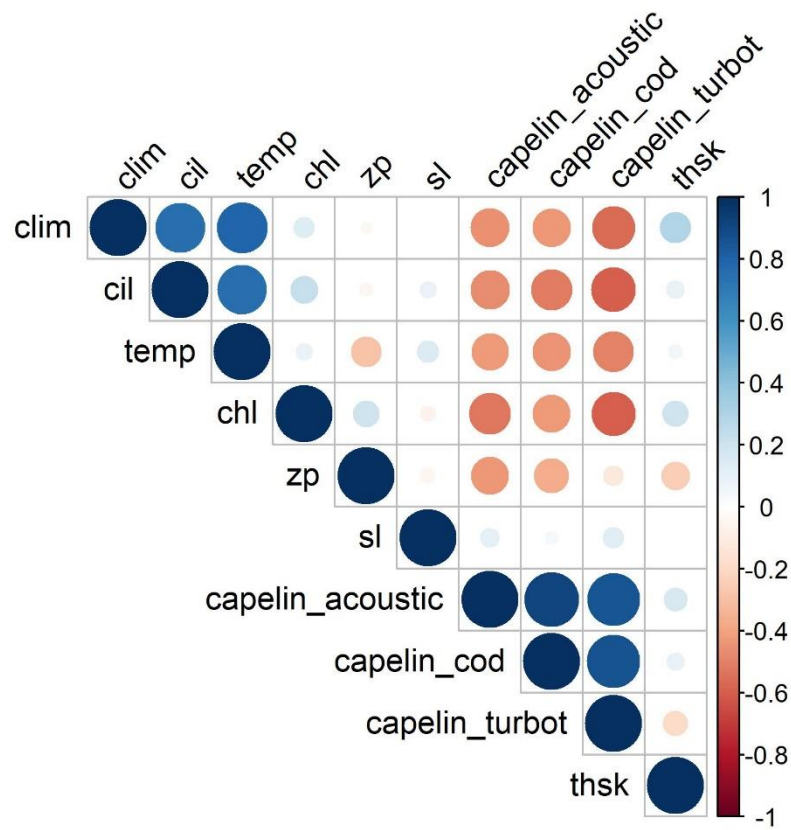


Figure D3.1. Correlation matrix between each of the potential covariate time-series. Clim refers to the Newfoundland climate index, cil refers to the cold-intermediate layer, temp refers to bottom water temperature, chl refers to chlorophyll a anomalies, zp refers to zooplankton biomass, sl refers to North sand lance abundance, capelin_acoustic refers to the acoustic index of abundance for capelin, capelin_cod and capelin_turbot refer to abundance indices derived from the stomach contents of Atlantic cod and Greenland halibut, and thsk refers to the biomass of thorny skate.

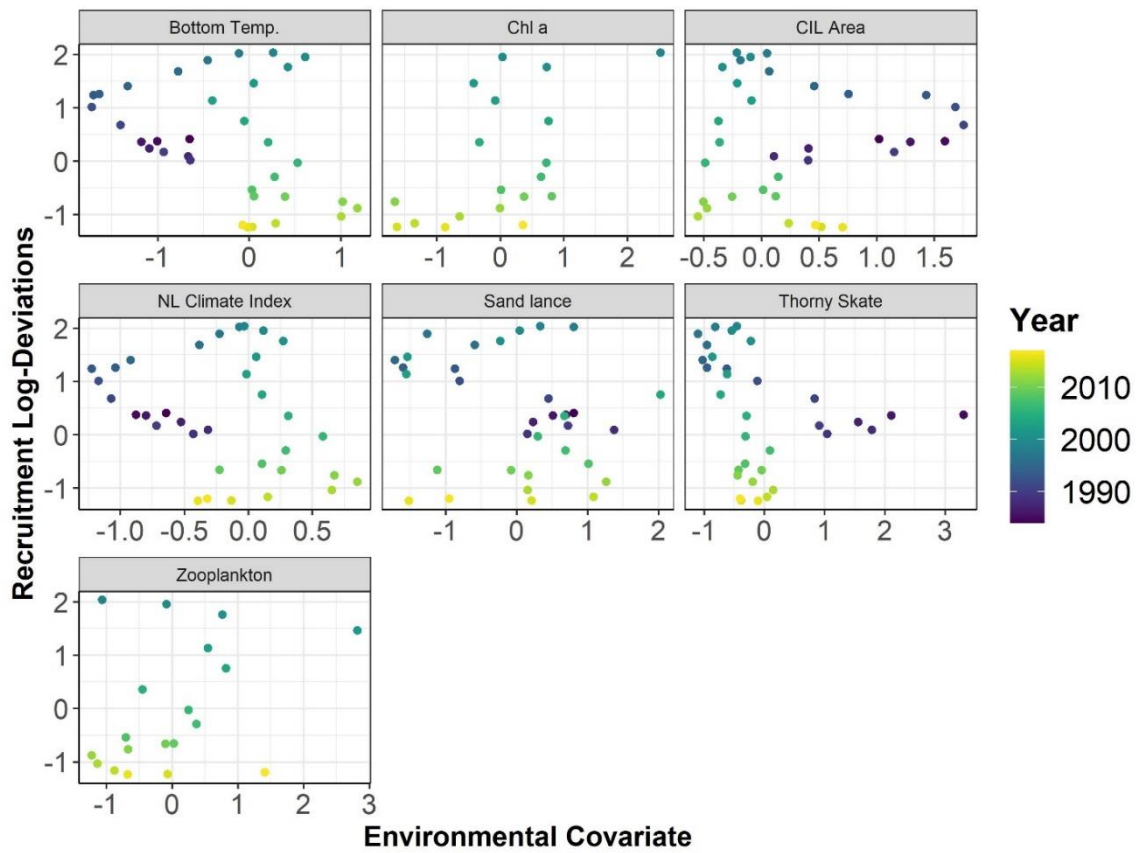


Figure D3.2 Relationship between recruitment log-deviations from YTFL1 with scaled environmental time-series. Bottom temperatures, CIL area, and NL climate index were based on a five-year one-sided moving average. Colors represent the corresponding year for each data point.

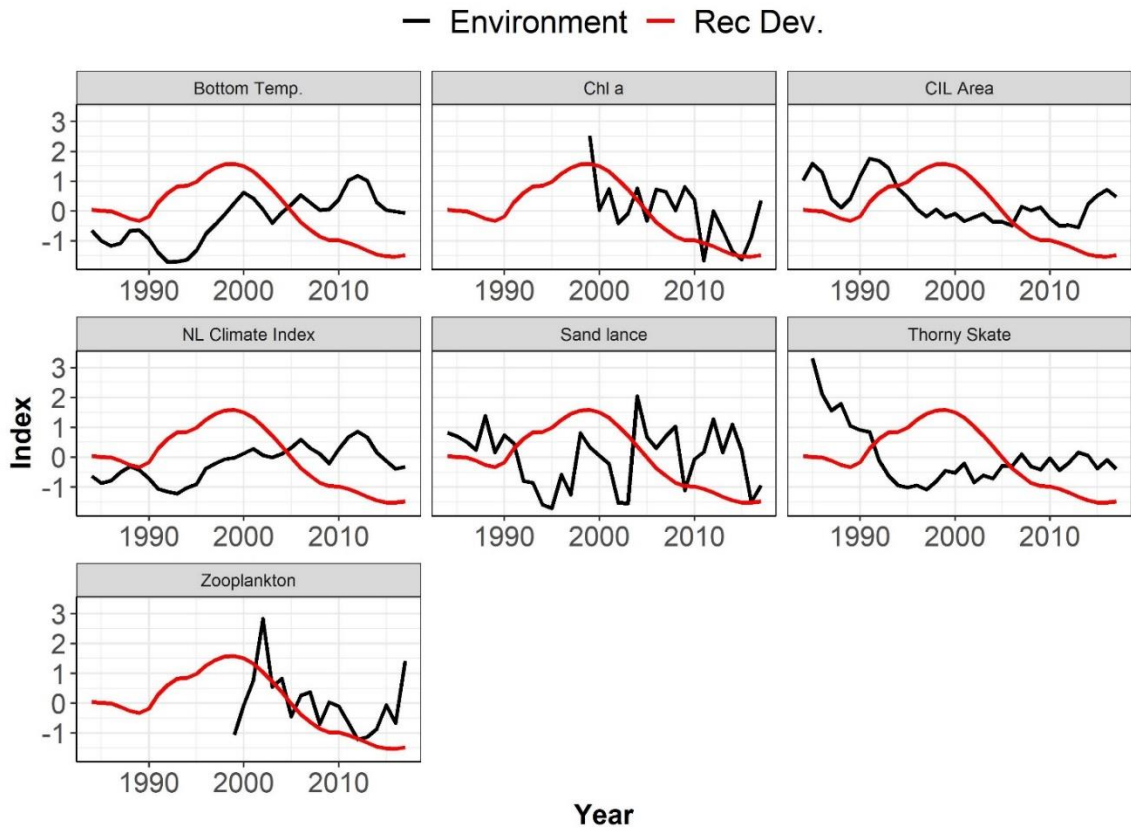


Figure D3.3. Time-series of recruitment log-deviations (Rec Dev.; red lines) from YTFL1 and the scaled environmental time-series (black lines). Bottom temperatures, CIL area, and NL climate index were based on a five-year one-sided moving average.

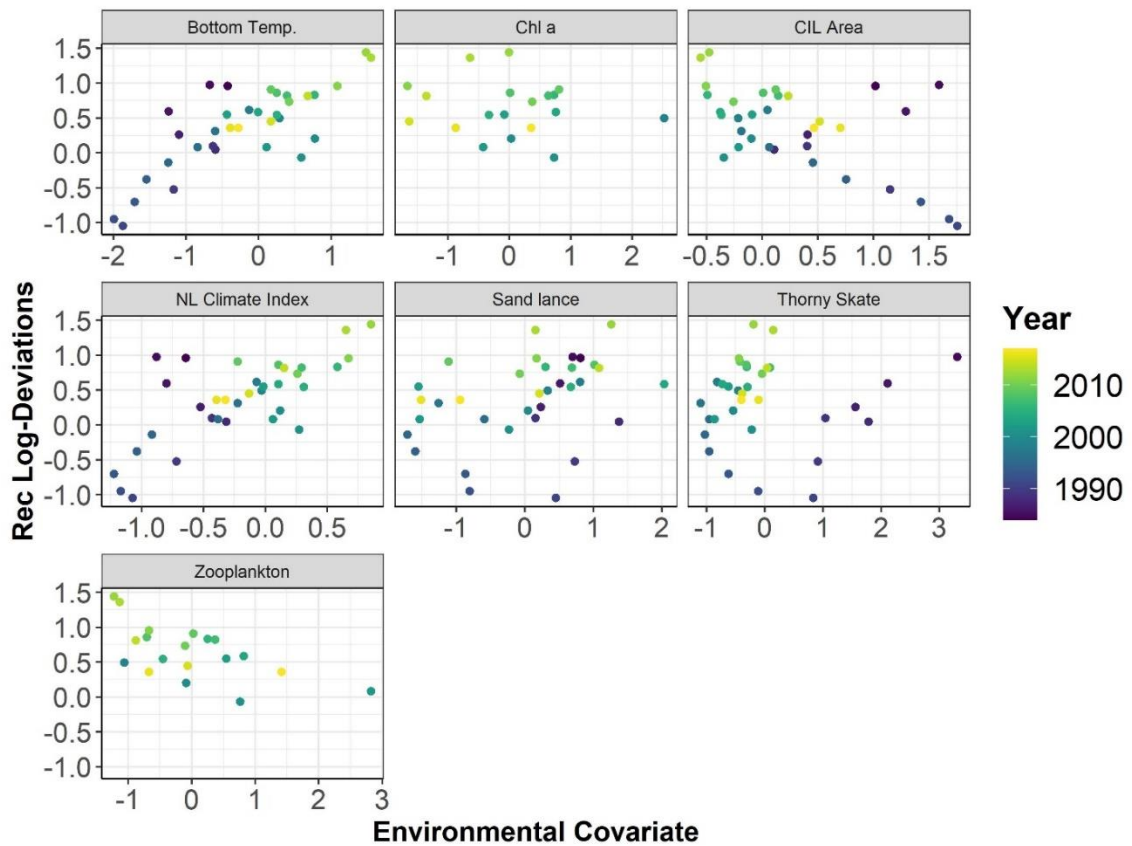


Figure D3.4. Relationship between recruitment log-deviations from AMPL2 with scaled environmental time-series. Bottom temperatures, CIL area, and NL climate index were based on a three-year one-sided moving average. Colors represent the corresponding year for each data point.

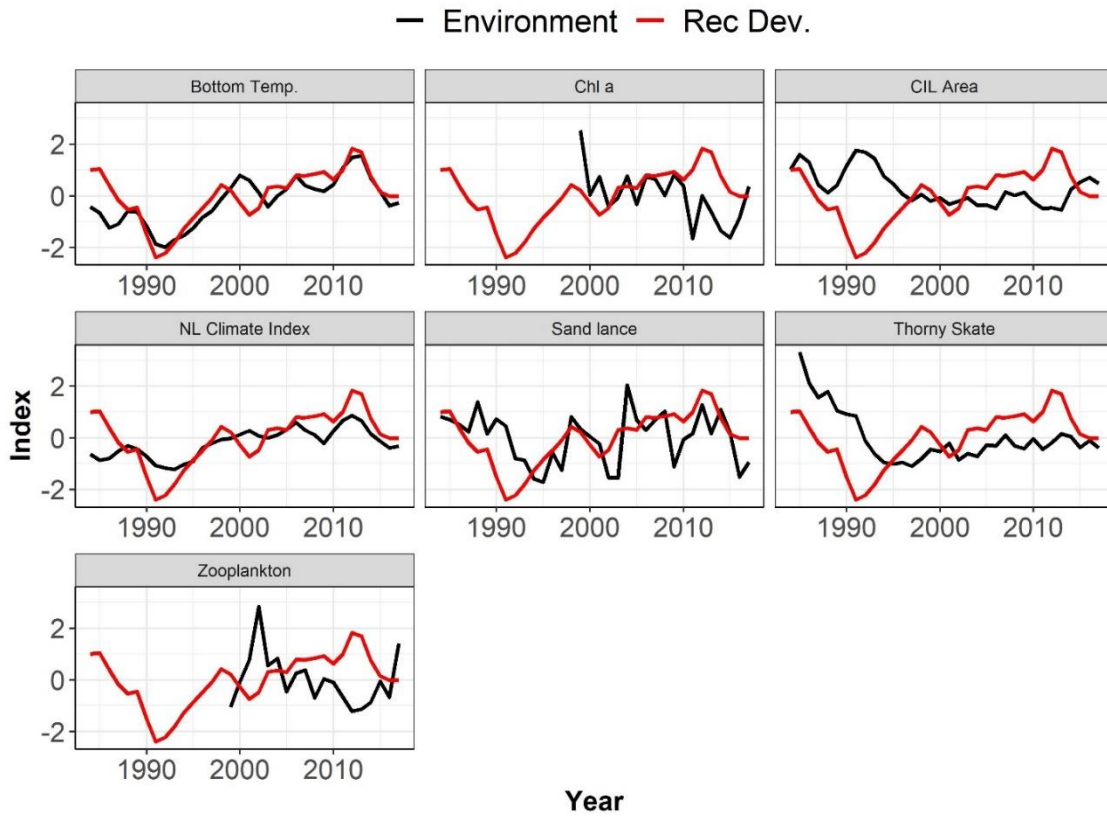


Figure D3.5. Time-series of recruitment log-deviations (Rec Dev.; red lines) from AMPL2 and the scaled environmental time-series (black lines). Bottom temperatures, CIL area, and NL climate index were based on a three-year one-sided moving average.

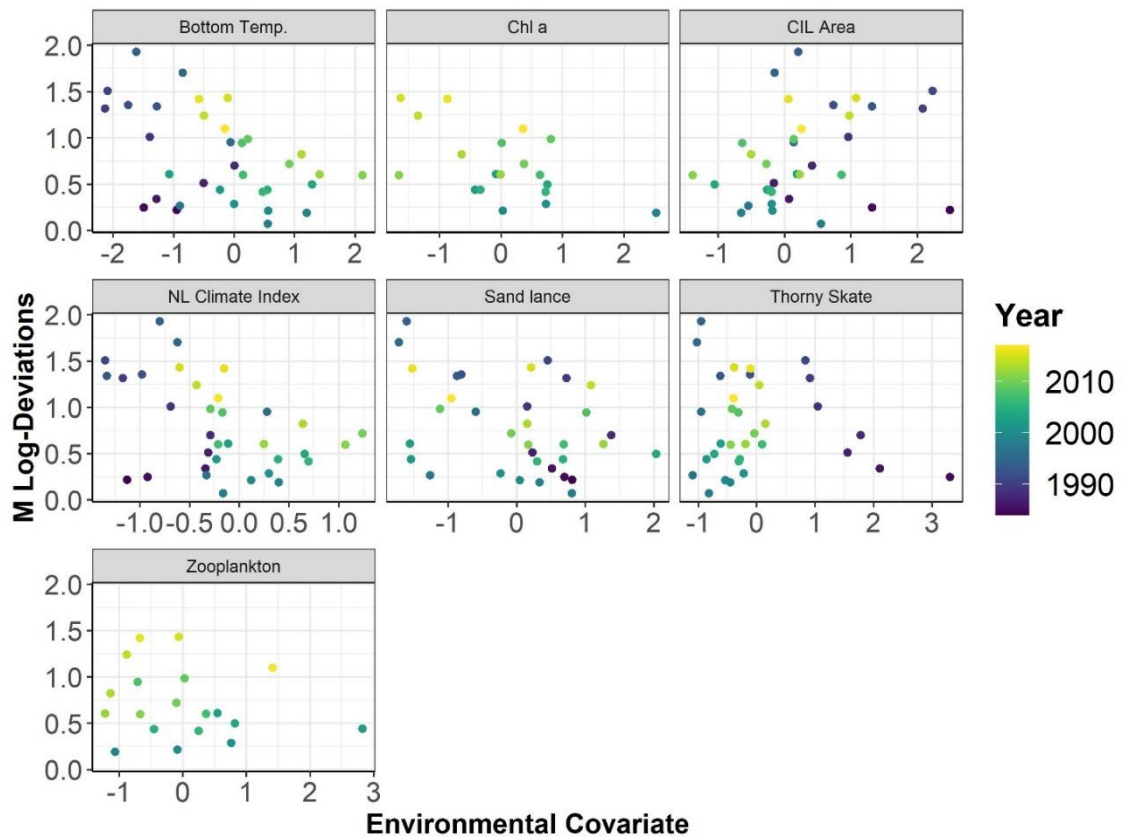


Figure D3.6. Relationship between M log-deviations from AMPL2 with scaled environmental time-series. Colors represent the corresponding year for each data point.

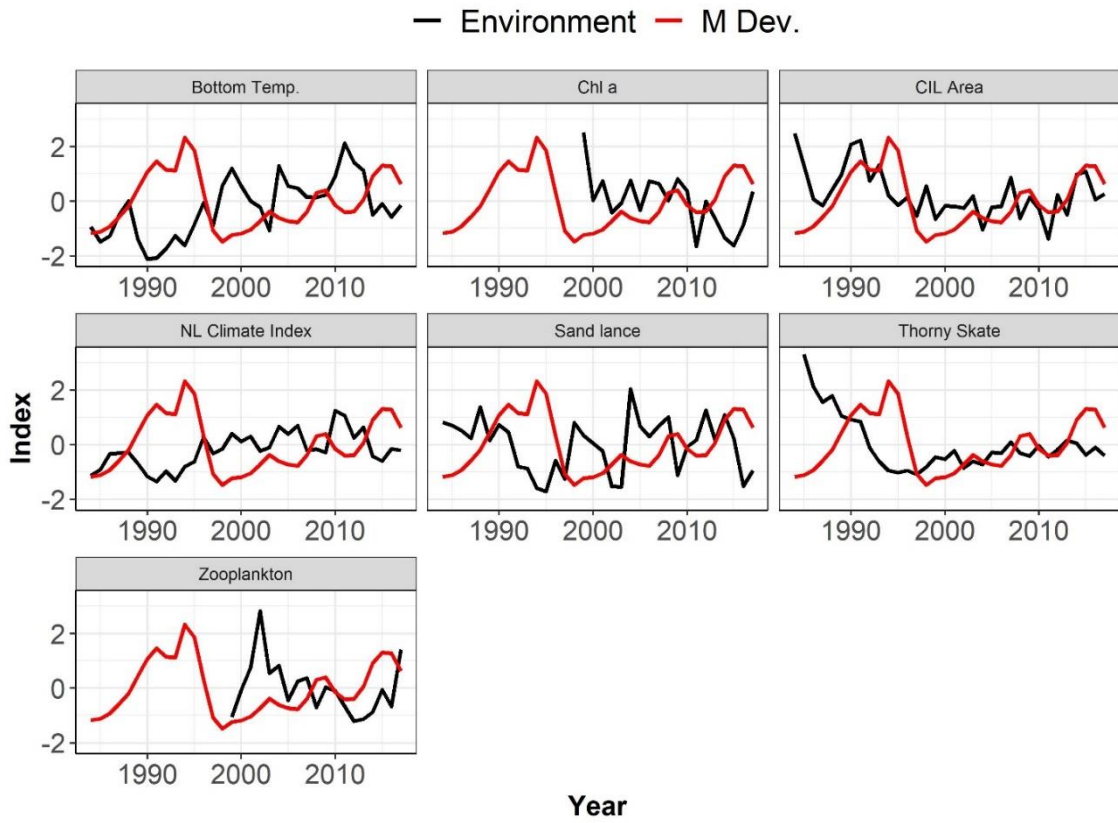


Figure D3.7. Time-series of M log-deviations (M Dev.; red lines) from AMPL2 and the scaled environmental time-series (black lines).

Based on literature and results for yellowtail flounder, I hypothesized that the relationship between the NL climate index and yellowtail flounder recruitment may be driven by the timing of the spring bloom. Therefore, I have included two figures showing the relationship between the start, peak, and end of the spring bloom in NAFO divisions 3NO (where most yellowtail flounder spawning occurs) to provide a preliminary examination of this hypothesis. Spring bloom timing estimates were derived from the SeaWiFS and MODIS satellite sensors. Where estimates from 1998-2003 are from SeaWiFS, 2003 – 2010 represent the mean of estimates from both sensors, and estimates from 2011 – 2017 are from MODIS.

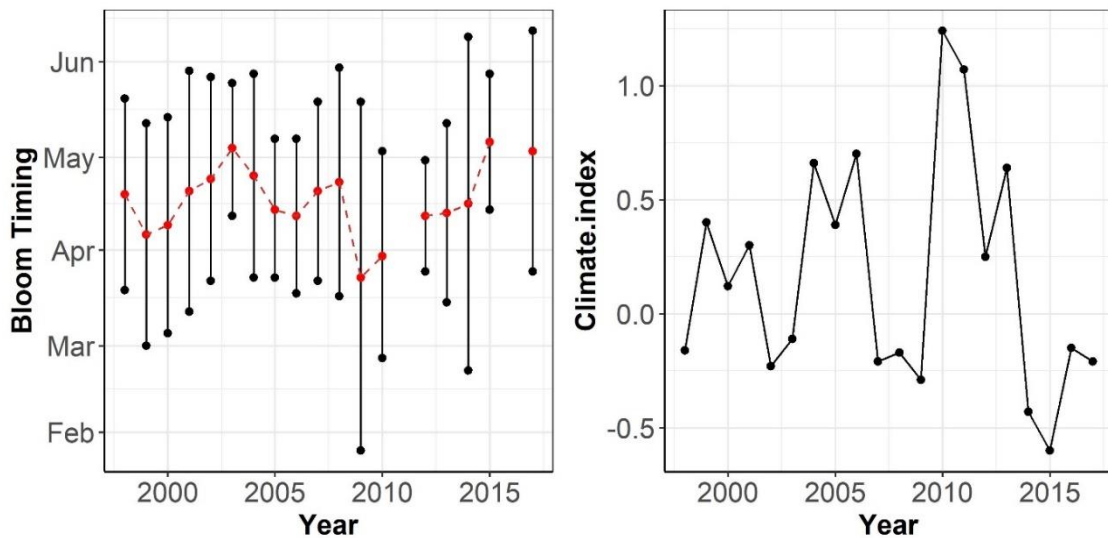


Figure D3.8. Time series of spring bloom timing and the NL climate index from 1998 – 2017. Black dots for the bloom timing figure represent the start and end of the bloom, while the red dots and red dashed line represent the peak timing of the spring bloom.

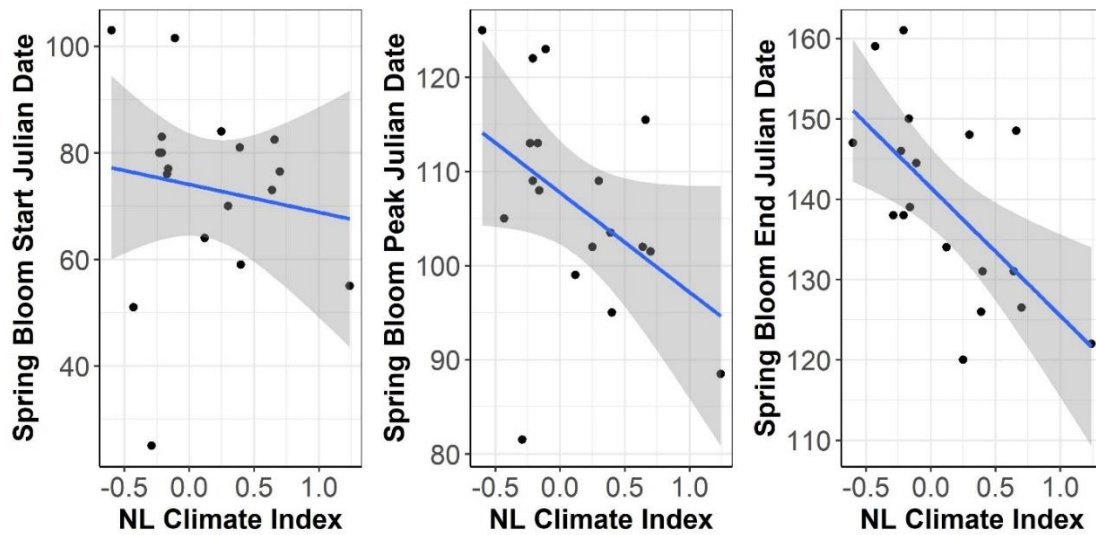


Figure D3.9. Comparison of spring bloom timing with the NL climate index. Panels represent the start, peak, and end Julian dates for the spring bloom. Blue lines represent linear model estimates of the relationship, while grey polygons represent the 95% confidence interval of the estimated relationship from the `geom_smooth()` function in `ggplot2`.